TARGETING SHIKIMATE PATHWAY FOR ANTIMYCOBACTERIAL DRUG DISCOVERY USING TRADITIONALLY USED MEDICINAL PLANTS

Matotoka Mashilo Mash

[redacted]

THESIS

Submitted in fulfilment of the requirements for the degree of

DOCTOR OF PHILOSOPHY

in

MICROBIOLOGY

in the

FACULTY OF SCIENCE AND AGRICULTURE

(School of Molecular and Life Sciences)

at the

UNIVERSITY OF LIMPOPO

Supervisor: Prof P Masoko

Co-supervisor: Dr GTB Mashabela

2022

DECLARATION

I, **Mashilo Mash Matotoka**, declare that **Targeting shikimate pathway for antimycobacterial drug discovery using traditionally used medicinal plants** is my own work in design and execution and has not been previously submitted by me for the degree at this or any other University. All the materials contained therein have been duly acknowledged.

Mashilo Mash Matotoka **Date**

DEDICATION

I dedicate this thesis to my parents; Mahlodi Nelson and Ramadimetja Josephine Matotoka, and to my brothers, Dennis and Ronald Matotoka.

"*If I have seen further than others, it is by standing upon the shoulders of giants*" - Isaac Newton

ACKNOWLEDGEMENTS

I would like to thank God for the provision of life, protection, guidance and courage.

A special thanks to my supervisors, Prof Peter Masoko and Dr Gabriel T. Mashabela for their unwavering support, encouragement and guidance through this journey.

I would like to also thank the Executive Dean of Science and Agriculture, Prof Hlengani J. Siweya for his immense support.

I thank colleagues in the Biochemistry, Microbiology and Biotechnology Department at the University of Limpopo who assisted me during my studies.

I also thank colleagues at the Mycobacterium Metabolism Research Group (MMRG) from Stellenbosch University for assisting me and making my time at the laboratory a memorable experience.

I would like to thank the University of Limpopo and the National Research Foundation (NRF-DAAD In-Country Doctoral Scholarship Programme) for financial support.

"*Just as a plant needs water, in the same way an idea also needs propagation or else both wither and die***" -** Dr BR Ambedkar

TABLE OF CONTENTS

LIST OF ABBREVIATIONS

ATC	Anhydro-tetracycline
BEA	Benzene/ethanol/ammonia hydroxide
BSA	Bovine serum albumin
Cas	CRISPR-associated proteins
CC_{50}	Cytotoxic concentration
CEF	Chloroform/ethyl acetate/formic acid
CRISPR	Clustered regularly interspaced short palindromic repeat
DAHP synthase	3-deoxy-D-arabino-heptulosonate 7-phosphate synthase
DMSO	Dimethyl sulfoxide
DPPH	2,2-di-phenyl-1-picrylhydrazyl
EMW	Ethyl acetate/methanol/ water
FIC	Fractional inhibitory concentration
MBC	Minimum bactericidal concentration
MDR-TB	Multi-drug resistant tuberculosis
MTBC	*Mycobacterium tuberculosis* complex
NADPH	Nicotinamide adenosine dinucleotide phosphate
NSAID	Non-steroidal anti-inflammatory drugs
PAM	Protospacer-adjacent motif
PMA	Phorbol 12-myristate 13-acetate
PPP	Pentose phosphate pathway
pre-crRNA	Pre-CRISPR Ribonucleic acid
ROS	Reactive oxygen species
sgRNA	Single guide RNA
TLC	Thin layer chromatography
UV	Ultraviolet

LIST OF FIGURES

CHAPTER 2

CHAPTER 3

CHAPTER 4

CHAPTER 5

CHAPTER 6

CHAPTER 7

LIST OF TABLES

CHAPTER 3

CHAPTER 4

CHAPTER 5

CHAPTER 6

CHAPTER 7

MANUSCRIPT AND CONFERENCES

Publications

Matotoka, M.M., Mashabela, G.T. and Masoko, P. 2022. Phytochemical content, anti-bacterial activity, anti-inflammatory and cytotoxic effects of traditional medicinal plants against respiratory tract bacterial pathogens. BMC complementary and alternative medicine, (Prepared for publication).

Conference presentations

Matotoka, M.M. and Masoko, P. "Phytochemical content, antioxidant potential and anti-bacterial activity of traditional medicinal plants against respiratory tract bacterial pathogens" 2021: Indigenous Plant Use Forum.

Matotoka, M.M. and Masoko, P. "Phytochemical content, antioxidant potential and anti-bacterial activity of traditional medicinal plants against respiratory tract bacterial pathogens" 2021: University of Limpopo, Faculty of Science and Agriculture Research Day.

Matotoka, M.M. and Masoko, P. "Phytochemical content, antioxidant potential and anti-bacterial activity of traditional medicinal plants against respiratory tract bacterial pathogens" 2021: World Antimicrobial Awareness Week (WAAW) Webinar.

ABSTRACT

Respiratory tract infections (RTIs) are frequent ailments among humans and are a high burden to public health. One strategy for the development of new therapies against pathogenic bacteria such as *Mycobacterium tuberculosis* is to target essential biosynthetic pathways of its metabolism. The aim of this study was to evaluate and target the biosynthesis of aromatic amino acids (shikimate pathway) of Mycobacterial spp using medicinal plant extracts. The selection of the plants in this study was based on their ethnopharmacological use for the treatment of tuberculosis infections and related symptoms. The leaves were dried at ambient temperatures and ground to fine powder. The powdered material was extracted with hexane, dichloromethane, acetone, methanol and water. Phytochemical screening was done using standard protocols that tested for tannins, saponins, terpenoids, alkaloids, flavonoids, steroids, anthraquinones, phlobatannins, quinones, and betacynins. Phytochemical fingerprints were established using thin layer chromatography (TLC) where three mobile phases varying in polarity were used to develop the chromatograms. Total Phenolics, flavonoids, flavonols, tannins, alkaloids and proanthocyanidin contents were quantified using UV/Vis spectrometry. Spectrometric quantification of the free radical (DPPH) scavenging activity and ferric (potassium ferricyanide) reducing power were performed. The heat-dependent bovine serum albumin and egg albumin denaturation assays were used to evaluate anti-inflammatory activity. Antimycobacterial activity was screened using bioautography assay in qualitative analysis. Quantitatively, broth microdilution assay was used to determine the minimal inhibitory concentrations. The Clustered regularly interspaced short palindromic repeats (CRISPR)-Cas9 interference genetic editing technique was used to evaluate and validate the essentiality of the aromatic amino acids in *Mycobacteria* to further determine the vulnerability and draggability of the transketolase (*tkt*) and DAHPs (*aro*G) genes. Plasmid, PLJR962, was used for the CRISPRi/dCas9 gene knockdown experiments. The integrating CRISPRi plasmid expressed both sgRNA with the targeting region (for *tkt* or *aroG*) and the dCas9 handle which is under control of the anhydrotetracycline (ATC) inducible promoters. The spot assay and growth curves were used to for phenotypic characterisation and gene knockdown experiments. RNA microarray (qPCR) was used to evaluate the level of expression inhibition of *tkt* gene . Mechanism of action of plants extracts bioactive components were predicted based on synergy

between gene knockdown, shikimate inhibitors and the plant extracts. To evaluate whether the shikimate intermediates may rescue gene depleted *M. smegmatis* hypomorphs, the cultures were grown in L-tryptophan, L-phenylalanine, L-tyrosine and shikimic acid and growth curves constructed. Cytotoxicity of the extracts was evaluated using the 3-(4,5-dimethylthiazol-2-yl)-2,5-diphenyltetrazolium bromide (MTT) assay on Vero cell lines and phorbol 12-myristate 13-acetate (PMA) differentiated THP-1 macrophages. Phytochemical analysis showed that the various extracts had various polar and non-polar compounds which belonged to phenolics, saponins, steroids, terpenoids, alkaloids, cardiac glycosides and resins. Numerous non-polar compounds from *Gardernia volkensii*, *Senna petersiana*, *Ficus sur* had antimycobacterial activity against *M. smegmatis* in bioautography. Remarkably, acetone extracts from *S. petersiana*, *Acacia senegal*, *Carissa bispinosa*, *P. africanum* and *C. gratissimus* that had moderate to low antimycobacterial activity against wild-type *M. smegmatis* (mc^2 155) demonstrated improved inhibitory activity against the *tkt* PAM1 *M. smegmatis* CRISPRi mutant. Only the acetone *Clerodendrum glabrum*, *Croton gratissimus*, *Peltophorum africanum* and *Gardenia volkensii* demonstrated activity against *M. tuberculosis* H37Rv. These results suggest that the employment of CRISPRi in *M. tuberculosis* to develop screening models may increase changes of obtaining bioactive chemical species because the *tkt* gene knockdown was showed to possess the ability to potentiate the antimycobacterial activity of the plant extracts. An added advantage of the plant extracts is their antioxidant and anti-inflammatory activities which may benefit the host immune system during treatment of infection by reducing free radicals and pro-inflammatory agents that perpetuate the infection. Non-polar compounds were found to generally have higher anti-inflammatory activity than the polar counterpart for all the plant extracts. These results suggest that the non-polar compounds from the tested extracts may not only confer antimycobacterial effects, but also anti-inflammatory activities. *A. senegal*, *G. volkensii*, *F. sur*, *S. petersiana* and *C. glabrum* were found to be toxic to the Vero cell line. However, purification techniques may circumvent their toxic effects. This study demonstrated that the amino acid biosynthesis is a potential antimycobacterial drug target because it was found to be essential, vulnerable and druggable by medicinal plant extracts.

CHAPTER 1

1. INTRODUCTION

1.1 History of tuberculosis

Throughout history, the record of tuberculosis (TB) has resulted in uncountable human mortalities and even currently, this disease still represents a threat to public health (WHO, 2015). The disease is caused by the *Mycobacterium tuberculosis* complex (MTBC), which includes *M. tuberculosis*, *M. bovis*, *M. africanum*, *M. microti* and *M. canetti* (Aro *et al*., 2015; Kaewphinit *et al*., 2014). The most important organism from the MTBC is *M. tuberculosis*, which is the main cause of the common spread of pulmonary TB.

TB is mainly classified as pulmonary or extra pulmonary. Pulmonary TB particularly infects the lungs by the inhalation of aerosols or droplets that are loaded with Mycobacterium cells (Loddenkemper *et al*., 2016). Extra pulmonary TB arises from the dissemination of the tubercle cells from pulmonary lesions in the lung tissue to other sites of the body such as the central nervous system, bones, joints, lymph nodes, abdomen, kidney and bladder via the bloodstream or the lymphatic system (Loddenkemper *et al*., 2016). The first written documents describing TB, dates back to 2300 and 3300 years ago and were found in China and India, respectively (Barberis *et al*., 2017).

Epidemiological studies have indicated that TB infections and associated high mortality rates occur frequently in developing nations among people between the ages of 25 to 54 years (Bhat *et al*., 2018). These are among the most economically fruitful years of human life in developing countries where people between these ages can actively contribute to economic growth. However, the mortality and morbidity imposed by TB infections subsequently results in losses in productivity and therefore adds to the impoverishment of those countries. TB treatment successes in developing nations are considerably below average due to an inconsistent supply of TB drugs and patient commitment to chemotherapy, upsurges in multi-drug resistant TB strains and co-infection with human immunodeficiency virus (HIV) (Bhat *et al*., 2018).

In 2015, there was a renewed commitment towards the containment, suppression and ultimate end of TB infections/mortalities. These renewed efforts were due to the global impact of this disease on the health of millions of people. Under the sustainable development goals, the *End TB Strategy* was proposed to take control of TB infections/mortalities by 2030. Within the proposed target, the objectives were to reduce new TB cases by 80%, reduce 90% of TB deaths and reduce 100% of poverty within TB-affected families (WHO, 2015). Reaching these ambitious targets demands more vigorous responses from researchers to identify new and effective anti-TB drugs to help supplement the already existing chemotherapy.

1.2 Mycobacteria

The *Mycobacterium* genus belongs to the Mycobacteriaceae family and the order Actinomycetales. This genus consists of over 150 known species and has been estimated to have originated more than 150 million years ago (Gutierrez *et al*., 2005). Three million years ago, an early progenitor of *M. tuberculosis* may have infected early hominids in East Africa (Gutierrez *et al*., 2005). The common ancestor of modern strains of *M. tuberculosis* have been proposed to have first emerged 15 000 - 20 000 years ago (Brosch *et al*., 2002; Kapur *et al*., 1994). *Mycobacterium* species have been broadly categorised by their rate of replication, which is due to physiological, phenotypic and phylogenetic differences (Rastogi *et al*., 2001). Although both the fast-growing and slow-growing groups contain pulmonary disease-causing pathogens (particularly in immune-compromised patients), the slowing-growing mycobacterial species such as *M. tuberculosis* are notoriously associated with human pathogenicity (King *et al*., 2017). The unique cell wall components such as peptidoglycan layer, mycolic acids and arabinogalactans are attributed to the success of *M. tuberculosis* as a human pathogen (Kaewphinit *et al*., 2014).

M. tuberculosis cells are obligate human parasites. The infectious life cycle of *M. tuberculosis* is initiated by the primary infection of the lungs by causing lesions; however, the lungs eventually heal due to the host’s immune response. It is common that some of the healed lesions may still contain dormant and/or persister *M. tuberculosis* cells. As such, conventional TB drugs do not exclusively assure the sterilisation of the lesion, being possible that, in spite of the clinical cure, *M. tuberculosis* cells may remain in a latent state inside the lesions (Nair *et al*., 2012).

The dormant and persister tubercle bacilli may re-emerge to develop post-pulmonary TB through endogenous reactivation or exogenous re-infection of the host (Hunter, 2011). The occurrence of post-pulmonary TB leads to the development of lung cavities that allow the proliferation of *M. tuberculosis* cells which can easily be coughed into the environment and transmitted to new hosts (Hunter, 2011).

1.3 Treatment

Tuberculosis chemotherapy is standardised to require the administration of four to five drugs in combination for extended periods (6-9 months) to achieve effective therapy and to prevent the emergence of resistance (Camacho-Corona *et al*., 2008). TB chemotherapy was introduced to pharmaceuticals more than 4 decades ago. It included streptomycin (1943), isoniazid (1952), pyrazinamide (1954), ethambutol (1962) and rifampicin (1963) (Nguta *et al*., 2015). For a typical 6-month treatment, 4 drugs, namely; rifampicin, isoniazid, pyrazinamide and ethambutol are administered under close observation for the first 2 months of treatment. Thereafter, for the remainder of the four months, only a combination of rifampicin and isoniazid is administered (Ghanashyam, 2016).

The mechanisms of action of the first line drugs primarily focus on interfering with protein or ribonucleic acid (RNA) synthesis (Palomino and Martin, 2014; Rahim *et al*., 2012). The increase in MDR-TB strains and persister populations in unsterilised lesions indicate that, through time, *M. tuberculosis* cells develop defence mechanisms against the mode of action of these conventional drugs.

The toxicity of the conventional anti-TB drugs presents side effects such as neuropathy, skin rash, body weakness, headache, gastrointestinal disturbance, psychiatric disorder, arthralgia, hepatitis, peripheral neuropathy, hypothyroidism, epileptic seizures, dermatological effects, ototoxicity and nephrotoxicity (Yang *et al*., 2017; Michael *et al*., 2016). This means that TB patients have to suffer not only from the morbidity of the TB disease, but also the several harsh side effects of the anti-TB drugs as well. This leads to the demand of compounds that can inhibit the growth of *M. tuberculosis* using different and/or novel mechanisms of action. To accomplish this, the identification of suitable and appropriate drug targets in *M. tuberculosis* is required.

1.4 The Pentose phosphate and the shikimate pathway

In vitro studies of the *M. tuberculosis* pentose phosphate pathway (PPP) have demonstrated its essentiality to the survival of the organism. *Mycobacterium leprae* is also an obligate pathogen similar to *M. tuberculosis* and has undergone massive gene mutations and decay over the years. However, evidence of the conservation of a core set of genes (including those of the PPP) that are required for these microorganism's survival in human host have demonstrated the essentiality of the PPP (Fullam *et al*., 2011).

Part of the *M. tuberculosis* pathogenicity and survival lies in its cell wall, which comprises three covalently attached layers (peptidoglycan, arabinogalactan and mycolic acids) that confer low permeability of the cell wall to anti-TB drugs. One of the first committed steps in the production of the arabinogalactan layer of *M. tuberculosis* is the production of D-ribose-5-phosphate which can occur through two processes, either the enzyme ribose-5-phosphate isomerase (Rv2465) can convert ribulose-5-phosphate to D-ribose-5-phosphate (Roos *et al*., 2004) or the transketolase enzyme (Rv1449) can convert sedoheptulose-7-phosphate to D-ribose-5-phosphate (Fullam *et al*., 2011).

The shikimate pathway is an important pathway responsible for the biosynthesis of essential aromatic amino acids from carbohydrate precursors derived from the central carbon metabolism. The shikimate pathway is a seven-step pathway that involves chemical reactions that begin with the condensation of phosphoenolpyruvate from glycolysis and D-erythrose 4-phosphate from the pentose phosphate pathway to produce 3-deoxy-D-arabino-heptulosonate 7-phosphate (DAHP). This first reaction is catalysed by DAHP synthase encoded by the *aroG* gene (Nunes *et al*., 2020).

The end product of the shikimate pathway is chorismate/chorismic acid. Chorismate acts as a branchpoint and further undergoes chemical transformations to produce prephenate (precursor of phenylalanine and tyrosine), anthranilate (precursor of tryptophan), aminodeoxychorismate (precursor of para-aminobenzoic acid—PABA—which, in turn, leads to tetrahydrofolate synthesis), para-hydroxybenzoic acid (precursor of ubiquinone or Coenzyme Q) and isochorismate (common precursor of naphthoquinones, menaquinones and mycobactins) (Nunes *et al*., 2020).

For *M. tuberculosis* pathogenesis, the shikimate pathway allows the tubercle cells to outwit the host's immune system defence. Using a CD4 T-cell-mediated killing mechanism, the host's immune system attempts to isolate and starve the tubercle bacilli of essential amino acids such as tryptophan by recruiting macrophages. However, under stress conditions, *M. tuberculosis* can synthesise its own tryptophan from the chorismite precursor produced from the shikimate pathway. In turn, the starvation killing mechanism of the host's macrophages fails and the tubercle bacilli continue their proliferation and host invasion (Zhang *et al*., 2013).

Every reaction step in both the shikimate pathway and the PPP is enzyme mediated. Accordingly, this study proposes that chemicals structures that can inhibit the activity/expression of enzymes involved in these pathways could decrease the likelihood of survival of the *M. tuberculosis* cells. This may further assist the efficiency of the killing mechanism afforded by the human host (Sivaranjani *et al*., 2019). The shikimate pathway is an attractive target for the development of herbicides and antimicrobial agents because it is essential in plants, bacteria, and apicomplexan parasites but absent in humans. The enzymes of shikimate pathway are conserved among bacteria making it possible that the inhibitors of the shikimate pathway may act on a wide range of pathogens (Nirmal *et al*., 2015).

1.5 Clustered regularly interspaced short palindromic repeat (CRISPR)/Cas system

Clustered regularly interspaced short palindromic repeat (CRISPR)/CRISPR-associated proteins (Cas) is a gene editing approach that exists in a majority of microorganisms such as bacteria and archaea. Microorganisms that have this system use it to acquire resistance and attain immunity against phage attacks and foreign DNA elements by selective cleavage of the nucleic acid backbones (Makarova *et al*., 2011).

With experience and advancement of the CRISPR-cas system as a gene editing tool, the use of the dual RNA system has been circumvented by fusing the crRNA and tracrRNA to produce a chimeric single guide RNA (sgRNA) (Jinek *et al*., 2012). The best-characterised system is the type IIA system from *Streptococcus pyogenes*. The re-purposing of the cas9 endonuclease activity introduced CRISPR interference (CRISPRi) where the cas9 protein endonuclease activity was inactivated by inducing point mutations within HNH and RuvC nuclease domains (Rock *et al*., 2017). Co-expression of the nuclease-dead *S. pyogenes* Cas9 protein (dCas9$_{Spy}$) with an sgRNA designed with 20 nucleotides of complementarity to the target gene simplified silencing of the gene of interest (Rock *et al*., 2017; Choudhary *et al*., 2014).

In CRISPRi/dCas9 system, the dCas9$_{spy}$-sgRNA complex represses the transcription of the target gene by blocking the activity of the RNA polymerase in two main ways, by blocking the RNA polymerase at the target promotor or by causing a steric block to transcription elongation (Rock *et al*., 2017).

1.6 Traditional medicine and medicinal plants

The prevalence of the widespread utilisation of traditional medicine by developing countries has been documented (Peltzer, 2009). Herbal medicine, a prominent form of traditional medicine, serves as a relief for populations in developing countries where health facilities such as hospitals, dispensaries, pharmacies and clinics are underdeveloped and/or expensive for the patients. The use of traditional medicine is further propounded by the trust in the holistic healing of traditional health practitioners. Traditional health practitioners have a strong connection to members of communities because they provide treatment services based on culture, religious background, knowledge, attitudes and beliefs deeply rooted in the community (Hossan *et al*., 2010).

Herbal remedies play an essential role in traditional medicine in rural areas of South Africa, where these are often the therapeutic treatment of choice. The preparation of herbal medicine depends on cultural context. These medicines may be obtained from healers or traders as already prepared plant mixtures, or as raw plant materials (Matotoka and Masoko, 2018).

Natural products, as either pure chemical compounds or standardised plant crude extracts, provide opportunities for new drug leads for the treatment of mycobacterial infections. This is because of the unsurpassed accessibility of chemical diversity from the natural sources (Mariita *et al*., 2010). Plants synthesise active secondary metabolites that have biological activities (Shai *et al*., 2008). These molecules have a potential impact on health effects and their biological significance includes antibacterial, antifungal, antioxidant, anti-inflammatory, anti-cancer, anti-aging and anti-atherosclerotic. However, these phytochemicals need to be researched and tested in order to confirm and determine their therapeutic value (Mulaudzi *et al*., 2012).

The use of medicinal plants appears to be universal in different cultures in the world. However, the plants used for the same diseases and the methods of administration and treatment may vary according to place, culture and ethnicity. Drug discovery is an ongoing mission to obtain safe, efficacious and affordable therapies for tuberculosis. Therefore, multi-disciplinary approaches such as ethnopharmacology and ethnobotany, which involve participatory collaboration with indigenous people, play pivotal roles in retrieving anecdotal information, identification and documentation of medicinal plants used by various demographic groups and cultures to cure disease (Ndhlala *et al*., 2015; Mokgobi, 2014).

Previous studies have demonstrated noteworthy antimycobacterial activity from plant extracts. Some studies have pursued further isolated compounds responsible for the antimycobacterial activity. These findings have therefore stimulated further search towards discovering and developing anti-TB drugs from natural products/medicinal plants.

In this study, the CRISPRi system was implemented in the fast-growing *M. smegmatis*. An *E. coli*–mycobacteria shuttle plasmid was used to achieve expression of gene-specific complementary sequences next to the dCas9-binding region under the control of a tetracycline inducible promoter in the PLJR962 plasmid was constructed. By using this approach, it is possible to efficiently repress diverse sets of genes exhibiting a wide range of native expression levels in *M. smegmatis i.e*., transketolase enzyme from PPP and the DAHP synthase from the shikimate pathway. The unexplored myriad of phytochemicals in the medicinal plant extracts provide probable chances of obtaining hits for active anti-mycobacterial chemical species that may exert novel mechanisms of action. As such, they may have potential to be used to improve the current TB chemotherapy.

1.7 References

Aro, A.O., Dzoyem, J.P., Hlokwe, T.M., Eloff, J.N. and McGaw, L.J. 2015. Some South African Rubiaceae tree leaf extracts have antimycobacterial activity against pathogenic and non-pathogenic *Mycobacterium* species. *Phytotherapy Research*, **29(7)**: Doi:10.1002/ptr.5338.

Bhat, Z.S., Rather, M.A., Maqbool, M. and Ahmad, Z. 2018. Drug targets exploited in *Mycobacterium tuberculosis*: Pitfalls and promises on the horizon. *Biomedicine and Pharmacotherapy*, **103**: 1733–1747.

Brosch, R., Gordon, S.V., Marmiesse, M., Brodin, P., Buchrieser, C., Eiglmeier, K., Garnier, T., Gutierrez, C., Hewinson, G., Kremer, K., *et al*. 2002. A new evolutionary scenario for the *Mycobacterium tuberculosis* complex. *Proceedings of the National Academy of Sciences*, **99(6)**: 3684–3689.

Camacho-Corona M.R., Ramírez-Cabrera, M.A., Santiago, O.G., Garza-González, E., Palacios, I.P. and Luna-Herrera, J. 2008. Activity against drug resistant-tuberculosis strains of plants used in Mexican traditional medicine to treat tuberculosis and other respiratory diseases. *Phytotherapy Research*, **22(1)**: 82–85.

Fullam, E., Pojer, F., Bergfors, T., Jones, T.A. and Cole, S.T. 2011. Structure and function of the transketolase from *Mycobacterium tuberculosis* and comparison with the human enzyme. *Open Biology*, **2**: Doi.10.1098/rsob.110026.

Ghanashyam, B. 2016. Changing the game for multidrug-resistant tuberculosis. *Lancet*, **387(10024)**: 1149–1150.

Gutierrez, M.C., Brisse, S., Brosch, R., Fabre, M., Omaïs, B., Marmiesse, M., Supply, P. and Vincent, V. 2005. Ancient origin and gene mosaicism of the progenitor of *Mycobacterium tuberculosis*. *PLoS Pathogens*, **1(1)**: 5–5.

Hossan, S., Hanif, A., Agarwala, B., Sarwar, S., Karim, M., Taufiq-Ur-ahman, M., Jahan, R. and Rahmatullah, M. 2010. Traditional use of medicinal plants in Bangladesh to treat urinary tract infections and sexually transmitted diseases. *Ethnobotany Research and Applications*, **8**: 61–74.

Hunter, L.R. 2011. Pathology of post primary tuberculosis of the lung: an illustrated critical review. *Tuberculosis*, **91(6)**: 497–509.

Kaewphinit, T., Santiwatanakul, S. and Chansiri, K. 2014. The detection of tuberculosis by loop-mediated isothermal amplification (LAMP) combined with a lateral flow dipstick (in Handbook of Research on Diverse Applications of Nanotechnology in Biomedicine Chapter 13., Chemistry, and Engineering) ed., Shivani, S. The detection of tuberculosis: 269–300.

Kapur, V., Whittam, T.S., Musser, J.M. 1994. Is *Mycobacterium tuberculosis* 15,000 years old? *Journal of Infectious Diseases*, **170(5)**:1348–1349.

King, H.C., Khera-Butler, T., James, P., Oakley, B.B., Erenso, G., Aseffa, A., *et al.* 2017. Environmental reservoirs of pathogenic mycobacteria across the Ethiopian biogeographical landscape. *PLoS one*, **12(3)**: Doi: 10.1371/journal.pone.0173811.

Loddenkemper, R., Lipman, M. and Zumla, A. 2016. Clinical aspects of adult tuberculosis. *Cold Spring Harbor Perspectives in Medicine*, **6(1)**: Doi: 10.1101/cshperspect. a017848.

Mariita, R.M., Okemo, P.O., Orodho, J.A., Kirimuhuzya, C., Otieno, J.N. and Magadula, J.J. 2010. Efficacy of 13 medicinal plants used by indigenous communities around Lake Victoria, Kenya, against tuberculosis, diarrhoea causing bacteria and *Candida albicans. International Journal of Pharmacology and Toxicology*, **2(3)**: 771–91.

Matotoka, M.M. and Masoko, P. 2018. Phytochemical screening and pharmacological evaluation of herbal concoctions sold at Ga Maja, Limpopo Province. *South African Journal of Botany*, **117**: 1–10.

Michael, O. S., Sogaolu, O. M., Fehintola, F. A., Ige, O. M. and Falade, C. O. 2016. Adverse events to first line anti-tuberculosis drugs in patients co-infected with HIV and tuberculosis. *Annals of Ibadan Postgraduate Medicine*, **14(1)**: 21–29.

Mokgobi, M.G. 2014.Understanding traditional African healing. *African Journal for Physical, Health Education, Recreation and Dance*, **20(2)**: 24–34.

Mulaudzi, R.B., Ndhlala, A.R., Kulkarni, M.G. and van Staden, J. 2012. Pharmacological properties and protein binding capacity of phenolic extracts of some

Venda medicinal plants used against cough and fever. *Journal of Ethnopharmacology*, **143**: 185–193.

Nair, J.J., Ndhlala, A.R., Chukwujekwu, J.C. and van Staden, J. 2012. Isolation of di(2-ethylhexyl) phthalate from a commercial South African cognate herbal mixture. *South African Journal of Botany,* **80**: 21–24.

Ndhlala, A.R., Ghebrehiwot, H.M., Ncube, B., Aremu, A.O., Gruz, J., Šubrtová, M. Doležal, K., du Plooy, C.P., Abdelgadir, H.A. and Van Staden, J. 2015. Antimicrobial, anthelmintic activities and characterisation of functional phenolic acids of *Achyranthes aspera* linn.: a medicinal plant used for the treatment of wounds and ringworm in east Africa. *Frontiers in Pharmacology*, **6**: Doi 10.3389/fphar.2015.00274.

Nguta, J.M., Appiah-Opong, R., Nyarko, A.K., Yeboah-Manu, D. and Addo, P.G.A. 2015. Current perspectives in drug discovery against tuberculosis from natural products. *International Journal of Mycobacteriology*, **4**: 165–183.

Nirmal, C.R., Rao, R. and Hopper, W. 2015. Inhibition of 3-deoxy-D-arabino-heptulosonate 7-phosphate synthase from *Mycobacterium tuberculosis*: *In silico* screening and *in vitro* validation. *European Journal of Medicinal Chemistry*, **105**: 182–193.

Nunes, J.E.S., Duque, M.A., de Freitas, T.F., Galina, L., Timmers, L.F.S.M., Bizarro, C.V., Machado, P., Basso, L.A, and Ducati, R.G. 2020. *Mycobacterium tuberculosis* shikimate pathway enzymes as targets for the rational design of anti-tuberculosis drugs. *Molecules*, **25**: Doi:10.3390/molecules25061259

Palomino, J.C. and Martin, A. 2014. Drug Resistance Mechanisms in *Mycobacterium tuberculosis*. *Antibiotics*, **3**: 317–340.

Peltzer, K. 2009. Utilisation and practice of traditional/complementary/alternative medicine (TM/CAM) in South Africa. *African Journal of Traditional, Complementary and Alternative Medicines*, **6(2)**: 175–185.

Rahim, Z., Nakajima, C., Raqib, R., Zaman, K., Endtz, H.P., van der Zanden, AG. and Suzuki, Y. 2012. Molecular mechanism of rifampicin and isoniazid resistance in *Mycobacterium tuberculosis* from Bangladesh. *Tuberculosis*, **92(6)**: 529–534.

Rastogi, N., Legrand, E. and Sola, C. 2001. The *Mycobacteria*: an introduction to nomenclature and pathogenesis. *Revue Scientifique et Technique* (International Office of Epizootics), **20**: 21–54.

Roos, A.K., Andersson, C.E., Bergfors, T., Jacobsson, M., Karlen, A., Unge, T., Jones, T.A. and Mowbray, S.L. 2004. *Mycobacterium tuberculosis* ribose-5-phosphate isomerase has a known fold, but a novel active site. *Journal of Molecular Biology*, **335**: 799–809.

Shai, L.J., McGaw, L.J., Masoko, P. and Eloff, J.N. 2008. Antifungal and anti-bacterial activity of seven traditionally used South African plant species active against *Candida albicans*. *South African Journal of Botany*, **74**: 677–684.

Sivaranjani, P., Naik, V.U., Madhulitha, N.R., Kumar, K.S., Chiranjeevi, P., Alexander, S.P. and Umamaheswari, A. 2019. Design of novel antimycobacterial molecule targeting shikimate pathway of *Mycobacterium tuberculosis*. *Indian Journal of Pharmaceutical Sciences*, **81(3)**:438–447.

World Health Organization. 2015. Post 2015 End-TB Strategy. Global strategy and targets for tuberculosis prevention, care and control after 2015. Geneva.

Yang, T. W., Park, H. O., Jang, H. N., Yang, J. H., Kim, S. H., Moon, S. H., Byun, J. H., Lee, C. E., Kim, J. W. and Kang, D. H. 2017. Side effects associated with the treatment of multidrug-resistant tuberculosis at a tuberculosis referral hospital in South Korea: A retrospective study. *Medicine*, **96(28)**: 74–82.

Zhang, Y.J., Reddy, M.C., Ioerger, T.R., Rothchild, A.C., Dartois, V., Schuster, B.M., Trauner, A., Wallis, D., Galaviz, S., Huttenhower, C., *et al*. 2013. Tryptophan biosynthesis protects mycobacteria from CD4 T-cell-mediated killing. *Cell*, **155**: 1296–1308.

CHAPTER 2

2. LITERATURE REVIEW

2.1 Tuberculosis epidemiology

Tuberculosis (TB) is easily contagious because it can be spread through the air and can infect a subject by the inhalation of aerosols or cough droplets loaded with the tubercle bacilli from an infected host (Tekwu *et al*., 2012). TB is defined by the World Health Organization (WHO) as an infectious disease caused by *M. tuberculosis*, most commonly affecting the lungs, and resulting in symptoms such as fever, night sweats, weight loss, and coughing of sputum and/or blood (WHO, 2015).

Since 1997, WHO has annually published TB reports that consist of various statistics highlighting global TB infections (WHO, 2019). Subsequently, these reports over the past decades, have demonstrated that TB is an epidemic, particularly in developing countries in Africa and south east Asia, which consist of 70% of overall global TB infections (Figure 2.1) (WHO, 2019). In a recent global TB report, South Africa was included among the 30 high TB burdened countries (WHO, 2019). Although the overall incidence of TB in the European region is relatively low, the proportion of TB cases with multi-drug resistant TB in this region was substantially higher than that in all other regions (WHO, 2019).

The global TB report published by WHO for 2019 estimated a total of 235 652 of total new notified TB cases in South Africa. From this estimated number, 89% of the cases were pulmonary TB, 56% were men, 37% were women and 7% were children aged 0-14 years (WHO, 2019). In the Limpopo Province, South Africa, TB was ranked the fourth among the major causes of death (Statistics South Africa, 2018), where the Vhembe District accounted for the highest level of infection (Sukumani *et al*., 2012). Since TB is an airborne disease, the stigma, fear, anxiety, stress, and risk of contracting infection at public healthcare centres largely discourage patients to consult (Ramaliba *et al*., 2017).

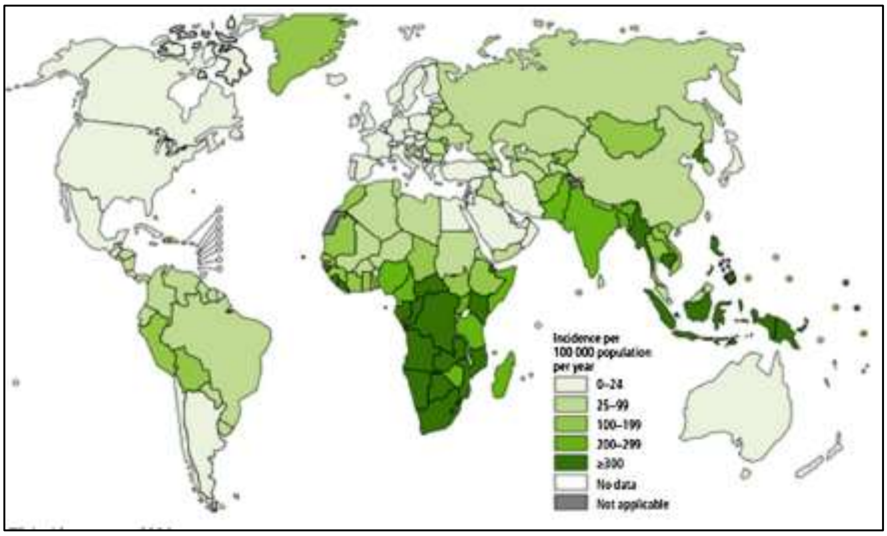

Figure 2. 1: Estimated TB incidence rates (Bhat *et al*., 2018).

2.2 Different types of the tuberculosis disease

2.2.1 Primary pulmonary tuberculosis

Primary pulmonary TB is defined as the TB that infects the lung parenchyma. The parenchyma of the lung is a collection of the functional parts responsible for gaseous exchange, which include the alveoli, alveolar ducts, alveolar walls and respiratory tracheobronchial tree (Suki *et al*., 2011).

A high percentage of this type of TB commonly occurs symptomatic in childhood age or immunodeficient individuals where it can progress to meningitis, disseminated TB or pneumonia. TB can spread as caseating granulomas for a few weeks before immunity is attained by the host (Paige and Bishai, 2010; Davis and Ramakrishnan, 2009). The difficulty is that although immunity against the *M. tuberculosis* may be developed, the lesions created by the microorganism are rarely sterilised and the tubercle cells may still persist in the lung parenchyma (Paige and Bishai, 2010; Davis and Ramakrishnan, 2009).

2.2.2 Post-primary pulmonary tuberculosis

The onset of post-primary pulmonary TB occurs after the initial infection of primary TB and is generally referred to as adult type or secondary TB. Post-primary TB occurs mainly in immunocompetent persons or those who have established immunity to primary TB (Hunter, 2011).

The challenge with post-primary TB in developing countries is that patients who survive the acute infections are prospectively left with lung cavities that contain significant numbers of *M. tuberculosis* cells. These remnant cells may fail to cause disease to the host but can be spewed into the tracheobronchial system and coughed into the environment for over a long period (Hunter, 2011).

2.2.3 Extra-pulmonary tuberculosis

Extra-pulmonary TB (EPTB) refers to the TB that is involved/localised at other sites in the body excluding the lungs e.g., pleura, lymph nodes, abdomen, genitourinary tract, skin, joints and bones, or meninges (Loddenkemper *et al*., 2016). Patients affected by EPTB commonly report symptoms which are related to the involved organ or site (Caws *et al*., 2008). Lifestyle behaviours such as smoking and comorbidities like diabetes and liver dysfunction also promote the risk of EPTB. Genetic factors further attribute to the manifestation of TB (Ayed *et al*., 2018).

2.3 *Mycobacterium tuberculosis*

Actinobacteria is the phylum and class of *M. tuberculosis*. The order of this bacterium is Actinomycetales and belongs to the Mycobacteriaceae family (Gordon and Parish, 2018). The cell size of the *M. tuberculosis* has been estimated to be between 3-5 µm in length and 0.2-0.6 µm in width. The typical cell conformations the bacterium manifests are straight or slightly curved rod shapes (Velayati and Farnia, 2012).

The bacilli cells of *M. tuberculosis* are slow growing with a generation time of 24 hours. The slow growth may be attributed to the presence of single rRNA operon; the complex synthetic requirements of the cell wall; nutrient uptake; and retarded rate of deoxyribonucleic acid replication (Gordon and Parish, 2018). This organism is primarily aerobic, chemoorganotrophic, non-motile and non-sporulating. Optimal growth temperature is 37 °C and may take up to 3 weeks of incubation in laboratory conditions to develop mature rough white, cream or buff-coloured colonies (Figure 2.2) (Gordon and Parish, 2018).

The *M. tuberculosis* is an acid-fast bacteria and therefore, has weak retention of staining dyes using in Gram staining due to their impermeable cell walls. The mycobacteria can be stained using acid-fast methods which entail the use of Ziehl-

Neelsen stain (Figure 2.3). The mycobacterial cell wall core comprises covalently bonded Peptidoglycan layer and the arabinogalactan (AG). This arabinogalactan in turn serves as an attachment site for mycolic acids (MA). Scattered beyond the cell wall core (MA-AG-PG complex), are lipids called phosphatidyl inositol mannosides (PIM), lipomannans (LM) and lipoarabinomannans (LAM) (Figure 2.4) (Maitra *et al*., 2019).

Figure 2. 2: The colony morphology of *Mycobacterium tuberculosis* grown on Löwenstein–Jensen (LJ) medium media (Kaewphinit *et al*., 2014).

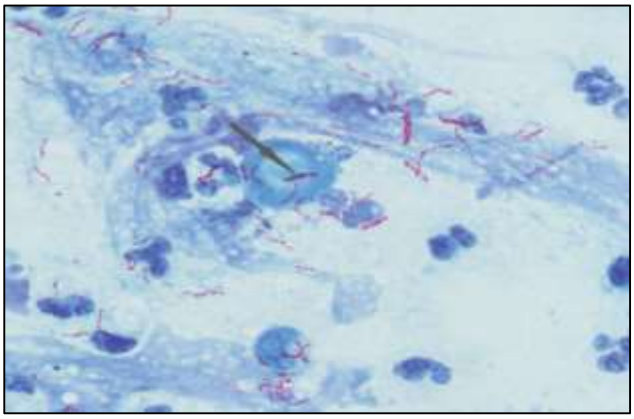

Figure 2. 3: *Mycobacterium tuberculosis* as seen through visualization using the Ziehl–Neelsen stain (red, arrow) (Kaewphinit *et al*., 2014).

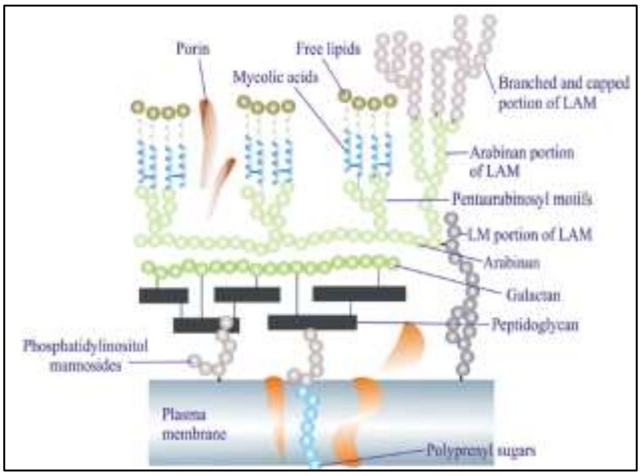

Figure 2. 4: Cell wall of *Mycobacterium tuberculosis* (Kaewphinit *et al*., 2014).

2.4 *Mycobacterium tuberculosis* metabolism

For an obligate pathogen such as *M. tuberculosis* whose life cycle is driven and has evolved in the context of human host infection, metabolism underpins both physiology and pathogenesis (Rhee, 2013). *M. tuberculosis* metabolism has been a focus of intense research towards TB drug discovery (Beste and McFadden, 2010). The genome of the current strains of *M. tuberculosis* are a result of horizontal gene transfer from an early environmental ancestor and coevolution with the human host. Coevolution with its human hosts has been attributed to the difficulties in discovering new TB drugs (Gagneux, 2018). Pathogenic *M. tuberculosis* has managed to exploit, adapt and supplement the metabolic pathways of its ancestral progenitor to improve its ability to persist as an obligate human pathogen (Gagneux, 2018).

Being an prototroph, *M. tuberculosis* possesses its own capacity to biosynthesise essential amino acids, vitamins and cofactors from mineral or organic compounds (Warner, 2015). Furthermore, *M. tuberculosis* possesses an extended complement of genes that encode for enzymes essential in lipid (fatty acid) metabolism, functional citric acid cycle, glycolysis and the pentose phosphate pathway (Warner, 2015).

It has been suggested that *M. tuberculosis* possesses the ability to switch between sugars, host-derived fatty acids, glucose, tricarboxylic acids, amino acids, and cholesterol as sources of nitrogen, carbon, and energy during host infection (Warner, 2015). This ability to switch between different nutrients has been attributed to the

Mycobacterial genome because it possesses genes that encode for enzymes that present a metabolic link between the glycolytic and citric acid pathway (Warner, 2015).

In *M. tuberculosis*, mutants constructed to lack glycolytic potential (glucokinase homologues), Marrero *et al*. (2013) observed deficiency in their persistence in mice models. These findings reinforced the importance of fatty acid (lipid) and carbohydrate metabolism for the long-term survival of *M. tuberculosis in vivo*. Moreover, the ability of this microorganism to co-catabolise different carbon sources demonstrates the importance of carbon metabolism in its life cycle (de Carvalho *et al*., 2010).

Under aerobic conditions, glucose and triacyl glycerides have been postulated to be the primary sources of carbon for *Mycobacterial* bacilli during early replication cycles. Thereafter, under glucose-deficient microenvironments (macrophages), the tubercle bacilli may shift to lipid metabolism as a source of carbon (Boshoff and Barry, 2005).

From a TB drug discovery perspective, the capability for differential catabolism through glycolysis, pentose phosphate pathway and citric acid cycle recommend that during *in vitro* studies, growth media and conditions should be prepared and adjusted appropriately to ensure that relevant physiological metabolic activity is active (Warner, 2015).

2.5 Pathogenesis of *Mycobacterium tuberculosis*

The pathogenesis of *M. tuberculosis* begins when infected aerosol droplets are deposited onto the pulmonary alveolus. The alveoli are delicate respiratory structures that are mainly made up of thin and flat alveolar cells that are stacked firmly together to prevent entry of plasma into the alveolar space (Cardona, 2016).

The distinctive feature of pathogenic mycobacterial species lies in their ability to block normal acidification from host phagosomes. *Mycobacteria* achieve this by preventing phagolysosome fusion. The phagocytosis of viable TB cells by the AMs stimulates the secretion of early secretory antigenic target (ESAT-6) which interrupts phagosome-lysosome union and apoptosis. This eventually permits the entry of tubercle cells into the cytoplasm (Mitchell *et al*., 2016). Following this entry, the tubercle cells replicate inside a single alveolar macrophage by achieving between 5-6 replication cycles resulting in about 32-64 cells (Behar *et al*., 2010). Because the division cycle of the *M.*

tuberculosis cells takes about 24 hrs, this suggests that the process of infecting and causing necrosis on the infected AM may proceed over 5-6 days (Behar *et al*., 2010).

2.6 *Mycobacterium smegmatis*

First discovered in 1884, *Mycobacterium smegmatis* is an obligate aerobic chemo lithotrophic non-motile bacterium that does not form endospores. It can use carbon monoxide and methanol as its inorganic and organic carbon sources, respectively (Park *et al*., 2001). This organism is classified as saprophytic and does not normally inhabit/depend on humans or animals and as such, it is generally deemed as non-pathogenic to humans (Long *et al*., 2012). Infections caused by *M. smegmatis* occur only in rare and extreme cases when compared to other pathogenic species of mycobacteria. It is commonly found on soil, plants and large bodies of water (Etienne *et al*., 2005).

The unique features of the cell wall of this bacterium are similar to those of *M. tuberculosis* in that it consists of a thick peptidoglycan, inner arabinomannan layers and outer waxy layer made up of mycolic acids, which are impermeable to antibiotics (He and De Buck, 2010).

2.7 Tuberculosis treatment

WHO has recommended clinicians not to assume the drug-sensitivity of the *M. tuberculosis* infecting a patient (WHO, 2011). This was due to the increased prevalence of drug-resistant strains of the microorganism (WHO, 2011). Therefore, the therapeutic prescriptions, including combinational therapy given to patients should be based on the evidence of drug-sensitivity of the *M. tuberculosis* strain (WHO, 2011).

Several anti-TB agents were discovered between the 1940s and 1950s where rifampicin was the last to be successfully introduced to the market (Tekwu *et al*., 2012). The primary approach to conventional TB chemotherapy was a directly observed treatment short course (DOT) which covers a period of 6 months. In the first 2 months of treatment, health care workers would give a TB patient 4 drugs, namely; rifampicin, isoniazid, pyrazinamide and ethambutol under close observation. However, on the following 4 months of the chemotherapy, the patients would only continue with the dose consisting of the combination of rifampicin and isoniazid. This 6-month approach to TB infection treatment has been recommended primarily towards pulmonary cases (Millard *et al*., 2015; Chiang *et al*., 2010).

M. tuberculosis represents an anomaly with regard to treatment. Compared to other microbial infection treatments, which may take 14 days of antibiotic treatment, TB chemotherapy is particularly lengthy. Clearly, the challenge in TB treatment lies not in the treatment but in the drugs themselves. Under conventional circumstances, current anti-TB drugs, particularly active against actively growing bacilli cells, lack efficacy on latent or persister populations (Millard *et al*., 2015; Chiang *et al*., 2010).

Multi drug resistant tuberculosis (MDR-TB) generally denotes TB strains that are resistant to first-line treatment drugs, particularly rifampicin and isoniazid. MDR-TB requires extended periods of treatment involving second-line drugs (Lemke, 2013; Iseman, 1993). The use or misuse of anti-mycobacterial agents perpetuated the rise of drug resistant tubercular bacilli strains. The natural tendency for patients to discontinue treatment when they feel better, inconsistent access and supply of medication and the adverse side effects, discourage patients from taking the full course of the chemotherapy. In such conditions, the tubercle cells have the opportunity to recover and recognise the used anti-tubercular agents (Gemechu *et al*., 2013).

In 1902, the first TB vaccine was developed from *Mycobacterium bovis* that infected a cow with TB. It took 13 years with subsequent culturing to generate a mutant strain that possessed high immunogenicity and low virulence. The vaccine was called the Bacillus Calmette–Guérin (BCG), partly named after its inventors, Albert Calmette and Camille Guérin (Hawgood, 2007). The vaccine has been in use for human vaccination since 1921, and has been recommended by WHO for infant immunisation since 1974. Subsequently, the BCG vaccine has been adopted into national vaccination programmes as of 2018 in 180 countries, including Asia, Africa, Europe and America (Li *et al*., 2021). However, prior exposure to certain mycobacteria, including members of the *Mycobacterium avium* complex, have been implicated in the reduction of Bacille Calmette-Guerin (BCG) vaccine efficacy against adult pulmonary TB in humans (King *et al*., 2017). Moreover, it provides unsatisfactory results towards preventing the reactivation of latent infection in adults because it is unable to establish a population of central memory T-cells. The vaccine establishes immunity represented by effector memory T-cells; these distribute in the lungs and may protect humans for 10-15 years but are gradually lost. With no central memory response to compensate, the individual loses any further resistance to TB (Orme, 2010).

2.8 Tuberculosis drugs

Based on the type of *M. tuberculosis* infection, either first line or second line drugs may be administered for the intended cure of the disease (Table 2.1).

2.8.1 First-line drugs

First-line drugs are the first choice for treating TB because they are considered a very effective treatment of the disease with minimal side effects (Table 2.1) (Jnawali and Ryoo, 2013).

2.8.1.1 Rifampicin

Introduced into the market in 1972, rifampicin (RIF) is still one of the primary constituents used in the multi-drug treatment therapy for TB (Palomino and Martin, 2014). Patients commonly experience side effects such as gastrointestinal upset and hepatotoxicity (Jnawali and Ryoo, 2013). The inhibition of the mycobacterial bacilli is a result of the interference of transcription, where rifampicin binds to the β-subunit of the ribose nucleic acid (RNA) polymerase, thus inhibiting the elongation of the messenger RNA (Bhat *et al*., 2018).

2.8.1.2 Isoniazid

Known also as isonicotinic acid hydraziden, isoniazid (INH) together with rifampicin form the basis of the TB chemotherapy regimen. Common side effects of isonaizd include hepatotoxicity and neurotoxicity (Jhamb *et al*., 2014; Jnawali and Ryoo, 2013). The mechanism of action involves the inhibition of the mycolic acid synthesis pathway through the NADH-dependent enoyl-acyl carrier protein (ACP)-reductase, encoded by *inh*A gene (Bhat *et al*., 2018).

2.8.1.3 Ethambutol

Ethambutol (EMB) [dextro-2,2’-(ethylenediimino)di-1-butanol], is proposed to inhibit the activity of the arabinosyl-transferase enzyme in *M. tuberculosis* (Bhat *et al*., 2018). Typical side effects associated with the administration of ethambutol include dizziness, blurred vision, colour blindness, nausea, vomiting, stomach pain, loss of appetite, headache, rash, itching, breathlessness, swelling of the face, lips or eyes, numbness or tingling in the fingers or toes (Jnawali and Ryoo, 2013).

2.8.1.4 Pyrazinamide

Similar to isoniazid, pyrazinamide is a pro-drug that requires prior transformation to its activated form first before it can exert its effects (Jnawali and Ryoo, 2013). The conversion of pyrazinamide to its active form, pyrazinoic acid is mediated by pyrazinamidase/nicotinamidase (PZase) (Jnawali and Ryoo, 2013). Side effects of administration include hypersensitivity and gastrointestinal toxicities (Jnawali and Ryoo, 2013).

2.8.1.5 Streptomycin

Streptomycin is an antimycobacterial agent in the class of aminocyclitol glycosides (Jhamb *et al*., 2014). Side effects associated with streptomycin involve toxicities to the vestibular and renal systems (Jnawali and Ryoo, 2013). The proposed mode of action of streptomycin is its binding to the 16S rRNA, which then restricts proofreading during translation and therefore leads to the inhibition of protein synthesis (Jnawali and Ryoo, 2013).

2.8.2 Second-line drugs against tuberculosis

Secondary-line drugs are prescribed for conditions where the first-line drugs were ineffective towards treatment and cure of the TB infection (Sileshi *et al*., 2020). Numerous factors such as HIV infection, diabetes mellitus, low body weight, cavitation on chest x-ray, high bacterial burden, drug resistance, positive culture after two months of treatment, and socio-demographic factors like drug abuse, alcoholism, smoking, and poor treatment adherence may lead to the failure of treatment by the first-line drugs (Sileshi *et al*., 2020).

2.8.2.1 Fluoroquinolones

Fluoroquinolones inhibit the growth of *M. tuberculosis* by targeting and halting the deoxyribose nucleic acid (DNA) gyrase activity. The inhibition of this enzyme leads to disruption of DNA replication (Chang *et al*., 2010). Common side effects include gastrointestinal intolerance, rashes, dizziness, and headache, which have been based on short-term administration (Jnawali and Ryoo, 2013).

2.8.2.2 Aminoglycosides

Kanamycin and amikacin are aminoglycosides prescribed as second-line injectable anti-mycobacterial drugs against multi-drug resistant (MDR) *M. tuberculosis* infections (Palomino and Martin, 2014). Their mode of action stems from the inhibition of protein synthesis by modifications at the 16S rRNA level. A common side effect of aminoglycosides is mainly renal toxicity (Jnawali and Ryoo, 2013).

2.8.2.3 Ethionamide

Ethionamide (ETH, 2-ethylisonicotinamide) is a derivative of isonicotinic acid and like isoniazid, involved in inhibiting the mycolic acid synthesis pathway (Banerjee *et al*., 1994). Side effects associated with the administration of ETH include gastrointestinal side effects, such as abdominal pain, nausea, vomiting and anorexia. It can cause hypothyroidism, particularly if it is used with *para*-aminosalicyclic acid (Jnawali and Ryoo, 2013).

2.8.2.4 Para-Amino salicylic acid

Now classified as a second-line drug, *p*-Amino salicylic acid (PAS) used to be a first-line antimycobacterial drug administered together with isoniazid and streptomycin. PAS is now administered for the treatment of multi-drug resistant (MDR) and extensively drug-resistant *M. tuberculosis* although its use and benefit are restricted due to its extreme toxicity (Rengarajan *et al*., 2004).

2.8.2.5 Cycloserine

Cycloserine is a D-alanine analog used as a second-line antimycobacterial drug against MDR-TB. Although a fully elucidated mechanism of cycloserine has not been reported, several studies have proposed that this drug prevents the biosynthesis of the peptidoglycan proteins which are essential for the bacterial wall (Bruning *et al*., 2011). The neurological effects associated with the administration of this drug have limited its use (Li *et al*., 2019).

2.8.3 New antimycobacterial agents for the treatment of TB

2.8.3.1 Bedaquiline

Research towards the discovery of new anti-TB drugs have identified bedaquiline as a potential source to treat MDR-TB. The chemical name of bedaquiline is 1-(6-bromo-2methoxy-quinolin-3-yl)-4-dimethylamino-2-naphtalen-1-yl-1-phenyl-butan-2-ol; it belongs to the diarylquinoline class (Field, 2015). The proposed mechanism of action of this compound is the interference of the action of mycobacterial adenosine triphosphate (ATP) synthase activity by disrupting the proton transfer chain (de Jonge *et al*., 2007).

2.8.3.2 Delamanid

Research into delamanid, a derivative of nitro-dihydro-imidazooxazole, has been reported to inhibit methoxy- and Keto-mycolic acids (Matsumoto *et al*., 2006).

2.9 Potential antimycobacterial targets used in this study

The elucidation and publication of the complete genome of *M. tuberculosis* provided new opportunities in TB drug screening studies that are focused on the identification of low molecular chemical species that can inhibit the activity of target enzymes (Yuan and Sampson, 2018).

Gene products encoded by the *Mycobacterial* genome for the function and control of cell wall synthesis, DNA replication, RNA synthesis, protein synthesis, energy metabolism and folate metabolism have been integral potential targets that have been exploited in TB drug discovery (Bhat *et al*., 2018). In this study, the pentose phosphate pathway and the shikimate pathway were selected and investigated as targets of potential antimycobacterial agents.

2.9.1 Pentose phosphate pathway in *Mycobacterium tuberculosis*

The pentose phosphate pathway (PPP) is focused on the production of nicotinamide adenosine dinucleotide phosphate (NADPH) and pentoses (five-carbon sugars) that are derived from glucose, a six-carbon sugar. NADPH is a cofactor that is an essential electron donor that is primarily used in anabolic reactions such cholesterol synthesis, steroid synthesis, ascorbic acid synthesis, xylitol synthesis, cytosolic fatty acid synthesis and microsomal fatty acid chain elongation (Rodwell, 2015). NADPH is the reduced form of $NADP^+$ and differs from NAD^+ by carrying an additional phosphate group esterified at the 2' position on the ribose moiety carrying the adenine group (Vasudevan *et al*., 2011).

In vitro studies of the *M. tuberculosis* PPP have demonstrated its essentiality to the survival of the organism. *Mycobacterium leprae* is also an obligate pathogen similar to *M. tuberculosis* and has undergone massive gene mutations and decay over the years. However, evidence of the conservation of the core set of genes that are involved in the PPP demonstrated the essentiality of this pathway towards the viability of *M. tuberculosis* cells (Fullam *et al*., 2011).

The pentose phosphate pathway has two major kinds of reactions (Figure 2.5). The first reaction involves the oxidative reactions that lead to the production of a ribulose 5-phosphate and NADPH. Glucose-6-phosphate, which is an intermediate of glycolysis, is oxidised to 6-phosphogluconate by the help of glucose-6-phsphate dehydrogenase (*Vasudevan et al*., 2011). Through oxidative decarboxylation, the 6-phosphogluconate loses its carboxyl group in the form of carbon dioxide to produce ribulose 5-phosphate.

Ribulose 5-phosphate can enter either one of the two isomerisation reactions, one produces xylulose-5-phosphate and the other isomerisation reaction produces ribose-5-phosphate (Vasudevan *et al*., 2011). Two molecules of xylulose-5-phosphate and one molecule of ribose-5-phosphate undergo a rearrangement of the carbon skeletons to give two molecules of fructose-6-phosphate and one molecule of glyceraldehyde-3-phosphate (Vasudevan *et al*., 2011). The former and the latter are intermediates of glycolysis; hence, they further demonstrate the link between the PPP and the glycolytic pathway.

Apart from the phosphopentose-3-epimerase and phosphopentose isomerase that are involved in the nonoxidative reactions of the PPP, two important enzymes, namely, transketolase and transaldolase, are responsible for the rearrangement of the carbon atoms of xylulose-5-phosphate and ribose-5-phosphate (Vasudevan *et al*., 2011).

First, transketolase transfers 2 carbons from xylulose 5-phosphate to ribose 5-phosphate, thereby producing the 7-carbon sugar sedoheptulose 7-phosphate plus glyceraldehyde 3-phosphate. Second, transaldolase transfers 3 carbons back from sedoheptulase 7-phosphate to glyceraldehyde 3-phosphate, producing fructose 6-phosphate and erythrose 4-phosphate. Finally, transketolase transfers 2 carbons to the erythrose 4-phosphate from another molecule of xylulose 5-phosphate, producing fructose 6-phosphate and glyceraldehyde 3-phosphate (Vasudevan *et al*., 2011) (Figure 2.5).

One of the important intermediates produced by the PPP is 4-carbon sugar erythrose-4-phosphate. The nonoxidative reactions operate independently of the oxidative reactions and are highly conserved because of their crucial role in supplying erythrose 4-phosphate (Tzin and Galili, 2010). This intermediate is one of the important precursors for the biosynthesis of essential aromatic amino acids such as tyrosine, phenylalanine, and tryptophan. Erythrose-4-phosphate (E4P), from the PPP together with Phosphoenolpyruvate (PEP) from the glycolytic pathway, are involved in the first reaction step towards the production of chorismate through the shikimate pathway that is responsible for the production of the essential amino acids (Tzin and Galili, 2010).

2.9.2 Shikimate pathway in *M. tuberculosis*

The shikimate pathway is the only metabolic route for the synthesis of aromatic compounds in the living world, and it operates only in bacteria, fungi, plants, and apicomplexans. The aromatic compounds such as aromatic amino acids, vitamin K and ubiquinone are important prerequisites and essential nutritional supplements for the metabolism of an organism. However, higher eukaryotes such as mammals (including humans) cannot synthesise their own essential ammino acids and are dependent on diet to acquire these compounds (Neetu *et al*., 2020).

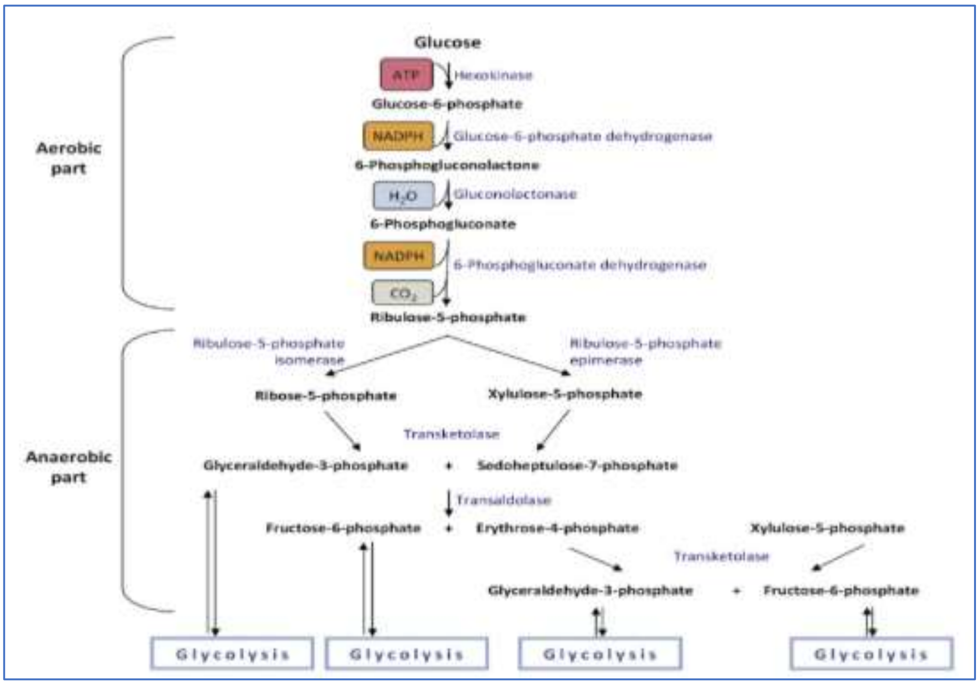

Figure 2. 5: The pentose phosphate pathway (Werner *et al*., 2016).

The shikimate pathway is a seven-step pathway catalysed by seven separate monofunctional enzymes that are encoded by separate genes (Figure 2.6). Although the pathway operates identically in the above-mentioned living systems, sometimes there exist variations in the primary structural organisation of its component enzymes in different organisms (Neetu *et al*., 2020).

The first step of the shikimate pathway begins with substrates that are intermediates of the carbon metabolism of the organism. The erythrose 4-phosphate provided by the pentose phosphate pathway and the phosphoenolpyruvate provided by the glycolytic pathway undergo a stereospecific aldol-like condensation reaction to produce 3-deoxy- D-arabino-heptulosonate 7-phosphate (DAHP) and an inorganic phosphate group. Encoded by the *aro*G gene, the DAHP synthase catalyses this first reaction (Tzin and Galili, 2010). The conversion of DAHP to DHQ encompasses the formation of a carbo-cyclic ring which is a precursor benzene ring in aromatic amino acids, folic acids and numerous secondary metabolites (in the case of plants) (Tzin and Galili, 2010; Kapnick and Zhang, 2008).

The DHQ dehydratase is formerly known as the 3-dehydroshikimate enzyme. In this third step, DHQ is converted to 3-Dehydroshikimate (DHS). The fourth step of this pathway is a NADPH-dependent reduction of DHS to form shikimate, from which the pathway derives its name (Ducati *et al*., 2007). This fourth step is reversible and is catalysed by the shikimate dehydrogenase enzyme encoded by the *aro*E gene. The involvement of NADPH in this fourth step further highlights the importance of the pentose phosphate pathway to the shikimate pathway. This fourth step marks the end of the first half of the shikimate pathway (Ducati *et al*., 2007).

The second half of the shikimate pathway begins with the fifth step, where the shikimate and adenosine triphosphate (ATP) are co-substrates to the Shikimate kinase (SK) encoded by the aroK gene (Kapnick and Zhang, 2008). The phosphate group from ATP is transferred to the 3-hydroxyl group of the shikimate molecule to produce shikimate-3-phosphate, the product of the fifth step (Tzin and Galili, 2010; Pereira *et al*., 2007). In the sixth step, through 5-Enolpyruvylshikimate 3-phosphate synthase (*aro*A encoded), Shikimate-3-phosphate undergoes condensation to yield 5-Enolpyruvylshikimate 3-phosphate and an inorganic phosphate group. For the seventh and final step of the shikimate pathway, the chorismate end product is produced when the second double bond in the aromatic ring is added by catalytic activity of the aroF encoded chorismate synthase enzyme (Tzin and Galili, 2010; Kapnick and Zhang, 2008).

The mycobacterial shikimate pathway leads to the biosynthesis of chorismic acid, which is converted by distinct enzymes to prephenate (precursor of phenylalanine and tyrosine), anthranilate (precursor of tryptophan), amino deoxy-chorismate (precursor of para-aminobenzoic acid—PABA—which, in turn, leads to tetrahydrofolate synthesis), para-hydroxybenzoic acid (precursor of ubiquinone or Coenzyme Q) and isochorismate (common precursor of naphthoquinones, menaquinones and mycobactins) (Figure 2.7) (Nunes *et al*., 2020).

All seven enzyme homologs of the shikimate pathway have been identified in the *M. tuberculosis* genome (Kapnick and Zhang, 2008). Enzymes that participate in the shikimate pathway are important as they represent potential molecular targets for the development of antimicrobial drugs. Studies of gene disruption have shown that the shikimate pathway is essential for the growth of *M. tuberculosis* (Parish and Stoker, 2002). Genetic manipulation techniques that were used to disrupt the *aro*K gene, which is responsible for the translation of the shikimate kinase enzyme, demonstrated the essentiality of the shikimate pathway towards *M. tuberculosis* growth (Mehta *et al*., 2015). Importantly, shikimate kinase represents one of two non-constitutively produced enzymes in the shikimate pathway, the latter being the DAHP synthase enzyme that facilitates the first step in the pathway (Ducati *et al*., 2007).

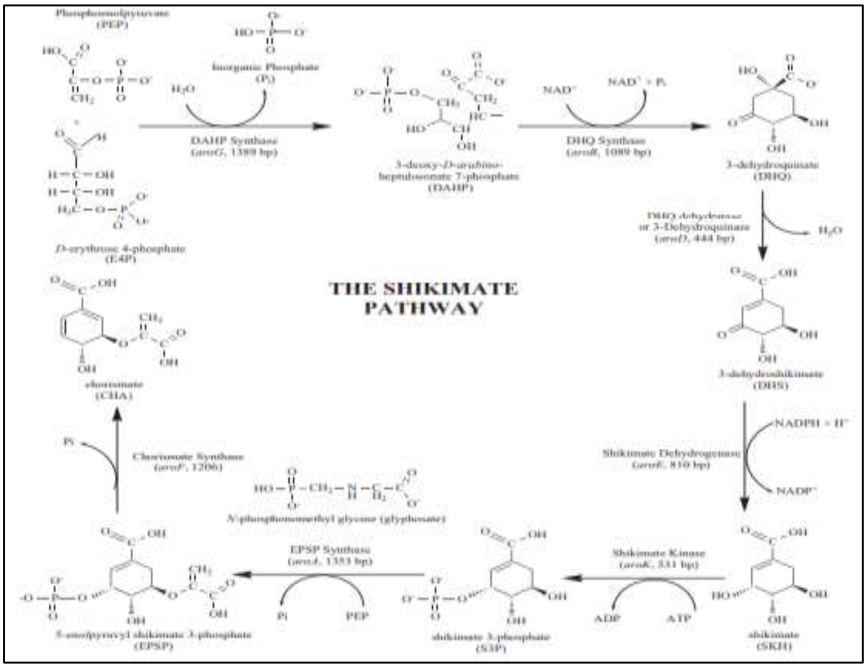

Figure 2. 6: The shikimate pathway (main trunk) (Ducati *et al*., 2007).

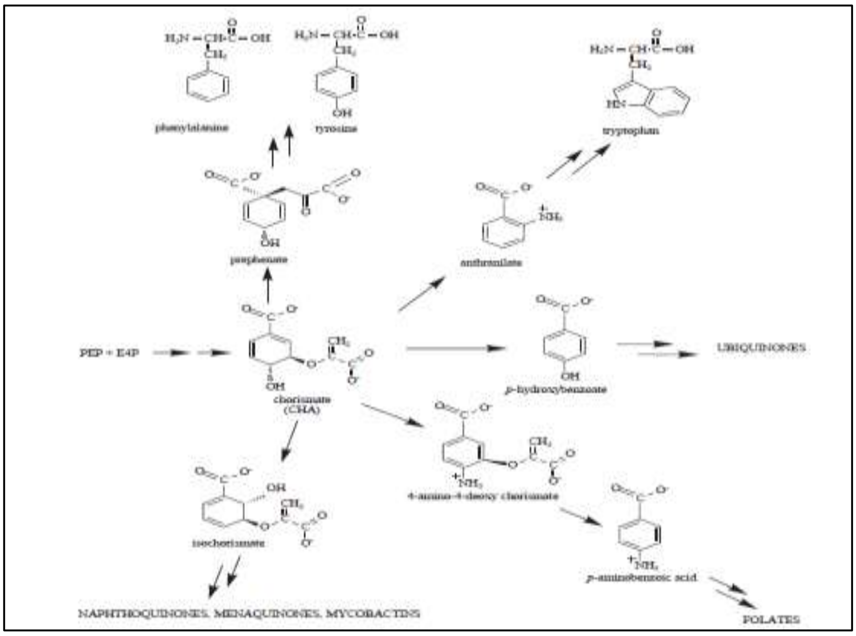

Figure 2. 7: Chorismate is a key precursor of mycobacterial biosynthesis of aromatic amino acids ubiquinones, folates, naphthoquinones, menaquinones and mycobactins (Ducati *et al*., 2007).

2.9.3 Transketolase enzymes

The transketolases are encoded by the *tkt* gene and are involved in the non-oxidative portion of the pentose phosphate pathway (PPP). *In vivo*, these enzymes are involved in the stereospecific carbon-carbon bond formation at two important points in the PPP. The first catalytic reaction the transketolase enzyme facilitate is the transfer of a two-carbon ketol from D-xylulose-5-phosphate to D-ribose-5-phosphate, producing D-sedoheptulose-7-phosphate. The second reaction involving the transketolase enzymes is another transfer of a two-carbon ketol from D-xylulose-5-phosphate to D-erythrose-4-phosphate producing fructose-6-phosphate (Fullam *et al*., 2011).

Functional *tkt* gene and its subsequent transketolase enzymes have also been identified in *M. tuberculosis* by the use of a number of proteomic studies and two-dimensional liquid chromatography–mass spectrometry studies (Fullam *et al*., 2011; Malen *et al*., 2007). The *tkt* (rv1449c) is the only gene in the genome encoding a putative transketolase in *M. tuberculosis*. The overall structure of each *M. tuberculosis* transketolase monomer consists of three domains interconnected by flexible linker regions (Figure 2.8) (Fullam *et al.*, 2011). Although there are some similarities in the 3D structure of the transketolase enzymes of *M. tuberculosis* and humans, key differences still ensure selectivity of inhibitors (Fullam *et al*., 2011). The essentiality of the transketolase enzymes in *M. tuberculosis* was demonstrated by Kolly *et al*. (2014) using RNA silencing and the protein degradation (RSPD) system to show that the depletion of the *tkt* arrested the microorganism's intracellular growth and reduced its virulence.

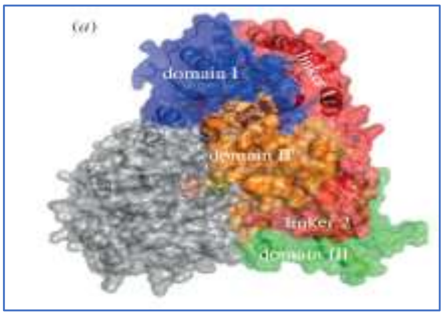

Figure 2. 8: Surface representation of *M. tuberculosis* transketolase dimer with bound cofactor (pink) with one monomer in grey and the second monomer coloured by domains (blue, domain I; orange, domain II; green, domain III; red, linkers 1, 2) (Fullam *et al*., 2011).

2.9.4 3-Deoxy-D-Arabino-Heptulosonate-7-Phosphate Synthase (DAHPS)

The 3-Deoxy-D-Arabino-Heptulosonate-7-Phosphate Synthase (DAHPS) is the first enzyme involved in the shikimate pathway. Correspondingly, it catalyses the first committed step of the pathway towards the synthesis of aromatic compounds bacteria, fungi and plants (Blackmore *et al*., 2013). It catalyses the stereo-specific aldol-like condensation of E4P and PEP to produce a seven-carbon keto acid called 3-deoxy-D-arabino-heptulosonate-7-phosphate (DAHP) and release of inorganic phosphate (Pi) (Blackmore *et al*., 2013).

In other microorganisms such as *Escherichia coli*, three structural genes, *aro*F, *aro*G and *aro*H, were revealed to code for three feedback inhibitor-sensitive DAHPS isoenzymes. However, sequence homology studies in *M. tuberculosis* exposed that only a single open reading frame (ORF), the *aro*G gene consisting of 1389 base-pairs was responsible for coding the type II DAHPS enzyme, commonly denoted as MtDAHPS (Figure 2.9) (Nunes *et al*., 2020).

The inhibition of the DAHPs activities *in vivo* and is a major regulatory mechanism of this pathway because it represents the principal means by which metabolite flow into aromatic compound synthesis is regulated. The structure-based approach and E-pharmacophore based virtual screening identified 3-pyridine carboxyaldehyde, α-tocopherol and rutin as lead compounds to inhibit MtDAHPS (Nirmal *et al*., 2015). However, further efforts are needed to show whether these chemical compounds reach and inhibit MtDAHPS in the intracellular context and target engagement results in the arrested growth of bacilli (Nirmal *et al*., 2015).

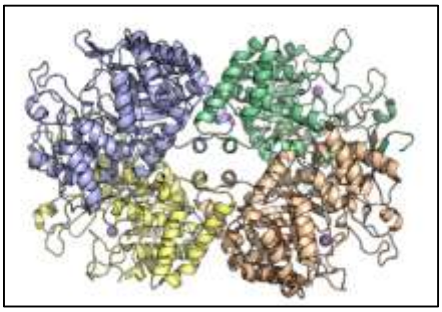

Figure 2. 9: The Structure of the MtDAPHS tetramer showing monomeric units. Mn2+ ions at the MtDAHPS active site are shown as purple spheres (Nunes *et al*., 2020).

2.10 The use of molecular biology in drug discovery

A central requirement for the identification of new drug targets is the genetic tools to investigate gene essentiality, target vulnerability and compound mode of action (McNeil and Cook, 2019).

2.10.1 The use of genome-editing tools in TB drug discovery

Over the past decades, the use of molecular biology and the development of genetic technology techniques such as gene editing have provided researchers unique opportunities to manipulate the genome of a variety of cell types and microorganisms (Norouzi-Barough *et al*., 2018).

The existing techniques that evaluate the functionality of genes primarily rely on introducing genomic deletions by homologous recombination. These techniques may implement non-replicating vectors, long linear DNA fragments, incompatible plasmids, counter-selectable marker SacB6, specialised transducing mycobacteriophage carrying the allelic exchange substrate and overexpression of mycobacteriophage-encoded recombination proteins (Choudhary *et al*., 2015). Unfortunately, these techniques are not particularly appropriate for targeting essential genes and generating specific chromosomal mutations in the mycobacterial genome (Choudhary *et al*., 2015).

The knowledge of inducible promoters in gene expression in microorganisms allowed for the development of various gene expression technologies that can assist in the identification and characterisation of essential genes that regulate vital cellular metabolism (Ehrt and Schnappinger, 2006).

New strategies that bypass the major drawbacks of some techniques such as the inability to provide the native expression level of a target gene in conditional mutant strain under permissive conditions have been developed. These approaches include systems such as RNA interference, expression of engineered transcription activator-like effector nucleases (TALENs), zinc-finger nucleases (ZFNs) and most recently, interference by clustered regularly interspaced short palindromic repeat (CRISPR) sequences (Norouzi-Barough *et al*., 2018; Choudhary *et al*., 2015). The CRISPR interference (CRISPRi) approach is more advantageous compared to RNA interference, TALENs and ZFNs due its cost effectiveness, simplicity and applicability to a majority of microorganisms for targeted gene regulation (Barrangou *et al*., 2007). In addition, since the synthesis of RNA and its entry into the cell is easier than protein domains (TALENs and ZFNs), designing and reprogramming CRISPR/Cas9 are further simplified (Torres-Ruiz and Rodriguez-Perales, 2015).

2.10.2 Clustered regularly interspaced short palindromic repeat (CRISPR)/Cas system

Clustered regularly interspaced short palindromic repeat (CRISPR)/ CRISPR-associated proteins (Cas) is a gene editing approach that exists in a majority of microorganisms such as bacteria and archaea (Koonin and Makarova, 2019).

CRISPR-Cas confers adaptive immune system because it stores the memory of previous encounters with foreign DNA molecules by inserting unique spacer sequences derived from those invading DNA molecules into the CRISPR arrays (Choudhary *et al*., 2014). The entire CRISPR-cas locus therefore consists of the CRISPR array, which is often palindromic, and repeats about 25-40 bp separated by the unique spacers (typically 30–40 bp each) (Koonin and Makarova, 2019). The CRISPR array and the spacers are commonly adjacent to a cluster of multiple cas genes which are organised in one or more operons encoding both the adaptation and the effector modules, often along with accessory genes (Koonin and Makarova, 2019). To inactivate or destroy the invading DNA fragments, the transcripts of the unique CRISPR spacers recognise the cognate invading DNA sequences and employ the Cas enzymes. The employed Cas enzymes are directed to their unique target site sequences onto which they use their nuclease activity to break the backbone of the foreign DNA, thus inactivating it (Koonin and Makarova, 2019).

2.10.2.1 Different phases involved in CRISPR-cas system

There are three pivotal and intertwined steps involved in the CRISPR-cas system for a microorganism to acquire immunity to invasive foreign DNA, mainly adaptation, pre-crRNA (pre-CRISPR RNA) expression and processing and the interference step, respectively (Koonin and Makarova, 2019; Choudhary *et al*., 2014).

The adaptation stage involves the integration of invasive DNA fragments into the host genome. The highly conserved cas enzymes, particularly cas1 and cas2 are recruited to bind to a target DNA fragment and introduce double-stranded breaks into this DNA. Commonly, during this adaptation phase, cas1 and cas2 proteins form a complex where, cas1 becomes the enzymatically active subunit that cleaves to both the source (protospacer-containing DNA) and the CRISPR array. Cas2 in this complex performs as the structural scaffold (Amitai and Sorek, 2016).

A fragment of the DNA is then released from the invading DNA fragment, now called the protospacer, and is inserted between two repeats in the CRISPR array (Amitai and Sorek, 2016). Most frequently, the insertion of the fragment would be into the proximal repeat unit that immediately follows the leader sequence, so that it becomes a spacer. Selection of spacer precursors (proto-spacers) from the invading nucleic acids is achieved by encountering short (2–4 bp) motif known as Protospacer-Adjacent Motif (PAM) (Mojica *et al*., 2009). Some microorganisms utilise an alternative route of adaptation to acquire spacer sequences by using RNA transcripts transcribed by the genomic DNA of mobile genetic elements. A reverse transcriptase encoded by the CRISPR-cas locus and commonly fused to cas1 protein, reverse transcribes the sequence embedded in the RNA prior to integration into its own genome. Once the spacer sequences are integrated into the microorganism’s genome, the CRISPR array is then repaired by the cellular repair machinery (Ivancic-Bace *et al*., 2015).

The second stage of the CRISPR-cas system is the expression of the pre-CRISPR RNA (pre-crRNA) transcript followed by its processing. The pre-crRNA transcript is expressed from the CRISPR locus and is initially expressed as a single long RNA sequence which is consequently processed into a mature RNA transcript (Choudhary *et al*., 2014). The processing is achieved by either a single endonuclease (such as Cas6 in *Pyrococcus furiosus*), by multi-protein complex such as CRISPR-associated complex for antiviral defence (cascade) in *Escherichia coli* or external RNase enzymes (Hochstrasser and Doudna, 2015).

In the third and final stage, the mature crRNA is recruited as a guide (gRNA) to direct respective complexes of Cas proteins. The gRNA recognises the protospacer or a closely similar sequence in the genome of a virus or a plasmid adjacent to the respective PAM sequences. Consequently, the Cas proteins bind to the PAM sequences which leads to the cleavage of the targeted invading DNA sequences (Figure 2.10) (Nishimasu and Nureki, 2017).

2.10.2.2 CRISPR interference

The CRISPR-cas system has three main classifications, and of these, the more popular and commonly used is the type IIA CRISPR from *Streptococcus pyogenes* because of its simplicity. This system involves an endonuclease Cas9 and two RNAs, a mature crRNA and a partially complementary transacting RNA, for the RNA-guided repression of foreign DNAs (Rock *et al*., 2017). With experience and advancement of the CRISPR-cas system as a gene editing tool, the use of the dual RNA system has been circumvented by fusing the crRNA and tracrRNA to produce a chimeric single guide RNA (sgRNA) (Jinek *et al*., 2012). This sgRNA possesses both required motifs for holding the cas9 endonuclease and simultaneous hybridisation with the target DNA sequence (Jinek *et al*., 2012).

The re-purposing of the cas9 endonuclease activity introduced CRISPR interference (CRISPRi), which is effectively used for gene silencing by transcription repression of target genes. CRISPRi has been efficiently developed and extensively characterised in *E. coli* and *bacillus subtilis*. In CRISPRi, the cas9 protein endonuclease activity was inactivated by inducing point mutations within HNH and RuvC nuclease domains (Rock *et al*., 2017). The consequence of the inactivation of the nuclease deficient cas9 (denoted as dcas9) is the inability of the enzyme to produce double stranded cuts onto the target DNA. Instead, Co-expression of the nuclease-dead *S. pyogenes* Cas9 protein (dCas9*Spy*) with an sgRNA designed with 20 nucleotides of complementarity to the target gene juxtaposed to an appropriate PAM yields specific silencing of the gene of interest (Rock *et al*., 2017; Choudhary *et al*., 2014).

The modified CRISPR system was termed as CRISPRi due to the ability of the dCas9 to interfere with DNA transcription which may repress as many gene expressions as by a thousand-fold (Qi *et al*., 2013). In CRISPRi, the $dcas9_{spy}$-sgRNA complex represses the transcription of the target gene by blocking the activity of the RNA polymerase in two main ways: by blocking the RNA polymerase at the target promotor or by causing a steric block to transcription elongation (Figure 2.11) (Rock *et al*., 2017).

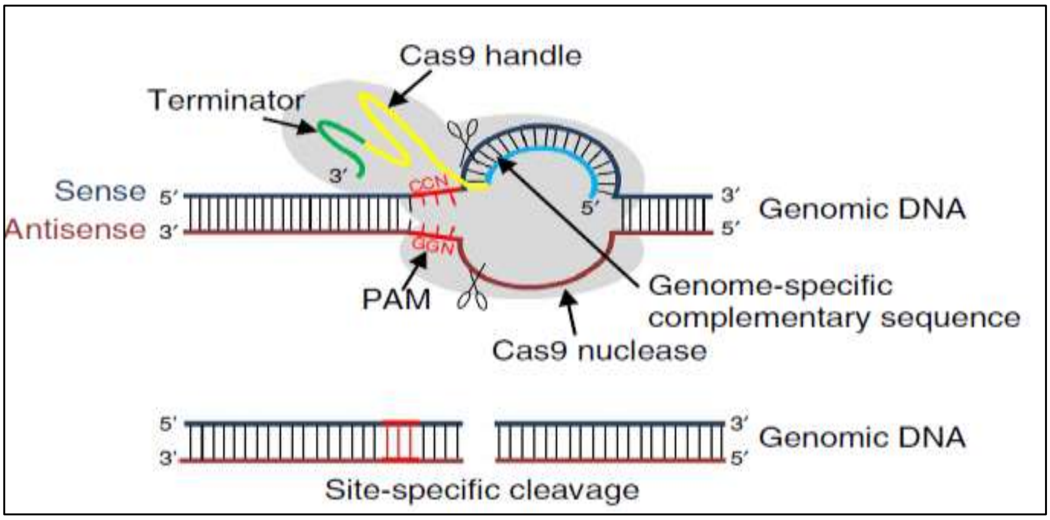

Figure 2. 10: Cartoon representation of CRISPR-mediated regulation of gene expression

Key: The sgRNAs comprises three regions, a 20 nt complementary sequence (cyan), followed by 42 nt Cas9 handle (yellow) and a 40 nt transcription terminator (green), derived from *S. pyogenes*. The wild-type Cas9 protein binds to the sgRNA and forms a protein–RNA complex

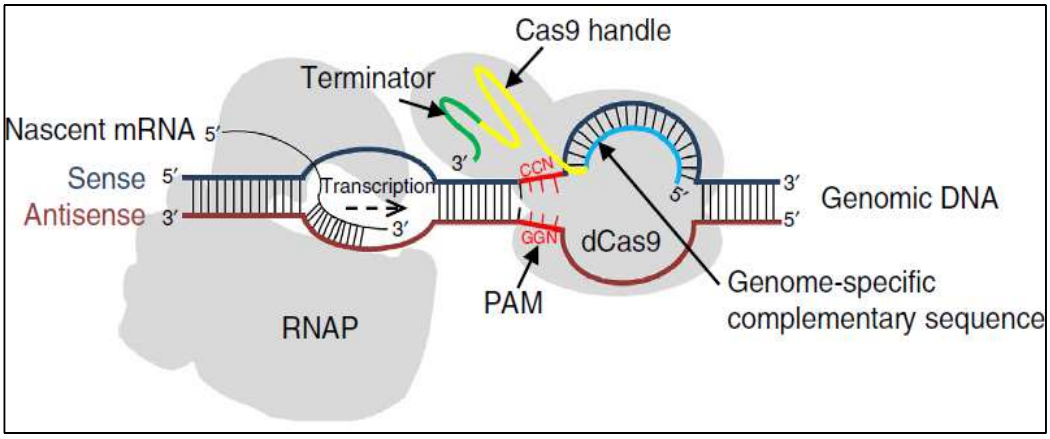

Figure 2. 11: Cartoon depicting the regulation of gene expression by CRISPRi due to the interference of RNAP transcription by nuclease-deficient dCas9.

2.11 Traditional medicine

Indigenous knowledge systems (IKS) are defined as local knowledge that is unique to a given culture or society. It is the knowledge by which food security, animal and human health and sustainability are achieved. In this sense, this knowledge is the local people's capital (Dan *et al*., 2010). The vast knowledge of such plants is now beginning to be acknowledged by the rest of the world and so is the role played by indigenous people as custodians of the traditional medicine (Idu and Onyibe, 2007).

There have been multiple successes in developing therapeutics for treatment and cure of various diseases by allopathic medicine which can be commonly accessed through pharmacies. In spite of the availability of the allopathic medicine, people still opt and prefer the use of traditional medicine. Traditional medicines have records of being used for the treatment of respiratory diseases. Semenya and Maroyi (2019) reported that 184 plant species from 77 botanical families were used as TB treatment and its opportunistic remedies against infections in the Limpopo Province, South Africa. Tabuti *et al*. (2010) reported 88 plant species used to treat TB in Uganda. Kandel *et al*. (2008) reported that reasons involved in patients defaulting their treatments include change of residence, adverse reactions to the quadruple drugs, lack of adequate information about the treatment course and bodily disabilities. The extent of progress of the disease is exacerbated by being too sick or too old to collect treatment because the public healthcare centres are too far and inconsistent availability of drugs in the clinics. This highlighted the importance and prevalent use of medicinal plants towards the management of TB and its related symptoms (Kandel *et al*., 2008).

Common signs and symptoms that traditional health practitioners use to diagnose TB include cough spanning over two months, weight loss, difficulty in breathing, wheezing cough, standing body hair, slimy sputum, bloody cough, chronic fever, cough with vomiting, dry cough, sweating and dehydration (Tabuti *et al*., 2010). The popular form of administration of medicine is an oral dosage of 1-2 teaspoons/tablespoons of a decoction of selected medicinal plants, taken 3 times in a day and this treatment is carried out until the patient becomes asymptomatic or recovers. Due to a lack of preservative components, traditional health practitioners prepare their decoctions when required by the patient to ensure active medicine (Tabuti *et al*., 2010). With the increased reporting and documentation of the ethnopharmacological use of medicinal plants for the treatment of TB and accompanying symptoms, these pharmacological effects still need to be validated and the safety of the therapies has to be established.

2.12 Medicinal plants

Ever since ancient times, humans depended on nature and its biodiversity to meet their needs of food, shelter and therapy towards diseases. Medicinal plants have been the cornerstone of herbal medicine, where infusions, macerations, tinctures and decoctions of plant parts such as leaves, roots, stem bark, stem, flowers and fruits have been used to treat diseases (Cano and Volpato, 2004). In those early times, knowledge and information about the causes of illness or the choice of the plant species to be used as cure was insufficient. Thus, the selection and use of certain plants for their curative effects was mainly due to intuition, experimentation and the experience gained and possessed by elders in a community (Mokgobi, 2014).

Sub-Saharan Africa boasts an estimated 45 000 plant species (Linder, 2014), where 45.5% (20 456) are indigenous plant taxa spread across the republic of South Africa. Only 10% (≈2062 plant species) of total flora of South Africa has been recorded to be used in traditional medicine (Williams *et al*., 2013). Ross (2010) suggested that eight in ten black South Africans have used herbal remedies either alone or coupled with modern medicine at some period. In the Limpopo Province, Bapedi traditional healers, whose medicines primarily consists of medicinal plants, are primarily dispersed in the Capricorn, Sekhukhune and Waterberg districts, which jointly comprise more than 17 municipalities (Semenya and Potgieter, 2015). With such a widespread and popular use, the huge market for herbal medicine due to high demands is understandable.

Medicinal plants produce chemicals classified as primary and secondary metabolites. Primary metabolites are produced for the growth and development of the plants and these include proteins, carbohydrates, amino acids and chlorophyll. Secondary metabolites, commonly known as phytochemicals, include chemical species such as phlobatannins, anthocyanin, betacynin, flavonoids, tannins, phenolics, alkaloids, glycosides flavonoids, steroids, saponins and terpenoids (Tripathi and Mishra, 2015). These chemicals are not explicitly required for the growth of the plant but are synthesised for the survival of the plant against pathogen infection (bacteria, fungi, viruses), herbivores, insects (or pests) and harsh environmental conditions such as unfavourable climate, insufficient nutrient supply (Kennedy and Wightman, 2015; Tripathi and Mishra, 2015).

2.13 Phytochemicals from medicinal plants

The types of phytochemicals and their amounts produced may vary considerably from genus and species of plants. Phytochemicals are abundant, chemically diverse and unique and are easily accessible. They are found in the different parts of the plants including flowers, nuts, fruits, leaves, bark and seeds. As such, they are cost effective to study. In spite of the knowledge of the occurrence of these chemicals, many more chemicals are yet to be isolated and characterised (Tomás-Barberán and Andrés-Lacueva, 2012).

Phytochemicals have been reported to have biological activities such as Antioxidant, antiulcer, antidiabetic, anticancer, anti-hyperlipidaemic, anti-inflammatory, antimicrobial, anti-spermatogenic, anti-cancer effects, atherosclerosis, neuro-degradation, obesity, articular rheumatism, skin aging and diabetes (Song *et al*., 2012).

When ingested, some of phytochemicals may improve the retention and absorption of nutrients and particular growth factors. Phytochemicals may participate in biological pathways as Co-factors, inhibitors, catalysers or ligands in enzymic reactions. Phytochemicals may also antagonise cell surface/ intracellular receptors. In the intestine, these chemicals have the ability to act as sequestrants to remove undesirable substances or reduction of harmful gastrointestinal bacteria (Tripathi and Mishra, 2015). A single plant species can synthesise a myriad of bioactive secondary metabolites, where they may share similar bioactivities, each can have its own activity and mechanism of action due to multiple stereoisomers.

2.14 Plants used in this study

The plants used in this study were chosen for screening based on their traditional uses for the treatment of TB.

2.14.1 *Peltophorum africanum* Sond

Peltophorum africanum is one of the widely known members from the Fabaceae family. A common name for this tree is Weeping wattle (English) and *Mosetlha* (Sepedi) (Figure 2.12) (Mongalo, 2013). Mazimba (2014) reported the ethnobotanical applications of the root and bark decoctions to include treatment of eye infections, joints and back pains, toothache, ascites and abdominal disorders, diarrhea, dysentery, infertility, skin, rashes and blisters, venereal diseases, depression, anthelmintic, coughs and gargled to treat sore throat (Mazimba, 2014; Mongalo, 2013). Its pharmacological activities include α-Glucosidase inhibition antibacterial, antioxidant, anthelmintic, antifungal and anti-HIV (Mazimba, 2014; Mongalo, 2013).

Figure 2. 12: *Peltophorum africanum* (Mongalo, 2013).

2.14.2 *Gardenia volkensii* k. Schum

Gardenia volkensii belongs to the Rubiaceae family, which has common names such as bushveld gardenia, sand veld gardenia, savanna gardenia, Transvaal gardenia and Morala (Sepedi) (Maroyi, 2020) (Figure 2.13). The fruits and roots as parts of this plant are widely used in ethnomedicine for the treatment of asthma, infertility, earache, sore eyes, epilepsy and headache (Juma and Majinda, 2007), respiratory infections (asthma, chest complaints, colds and pneumonia, sore throat and TB (Maroyi, 2020). The nutritional value of the fruits of this plant is indicated by their consumption by various animals such as elephants, kudu, velvet monkeys and baboons (Juma and Majinda, 2007).

Figure 2. 13: *Gardenia volkensii* leaves used in this study.

2.14.3 *Senna petersiana* (Bolle) Lock

Senna petersiana Bolle Lock. belongs to the Caesalpiniaceae (Fabaceae) family (Figure 2.14) (Foden and Potter, 2005)*. petersiana* is primarily distributed in KwaZulu-Natal, Limpopo, Mpumalanga provinces of South Africa. In English, it is commonly known as Dwarf Cassia, Eared Cassia, Eared Senna, Monkey Pod, Monkey Senna. It is called Bohlôko (Northern Sotho), Apiespeul (Afrikaans), Munembenembe (Venḓa), Uhwabile (Zulu) and Umnembenembe (Zulu) in various South African languages and tribes (Foden and Potter, 2005). Several studies have isolated bioactive compounds from *S. peterisana*. Tshikalange *et al*. (2005) isolated and reported the antimicrobial and antiviral activities of luteolin from *S. petersiana*.

Figure 2. 14: *Senna petersiana* leaves (Foden and Potter, 2005).

2.14.4 *Carissa bispinosa* (L.) Desf. Ex Brenan

Carissa bispinosa (Figure 2.15) belongs to the Apocynaceae family of evergreen shrubs that grow to heights between 2-10 m. Common names of *C. bispinosa* are *forest num-num* in English, and *isibethankunzi* and *isabetha* in isiZulu (Maroyi, 2013). The roots of *C. bispinosa* are extracted and drunk as cough and diarrhoea medicine (Maroyi, 2013). Local people in KwaZulu Natal, South Africa depend on the sale of the fruits from the carissa spp. These fruits would usually be sold in the summer months. The popularity of the fruits is attributed to their nutritional content such as Vitamin C, calcium, magnesium and phosphorus (Patel, 2013). Although Gwatidzo *et al*. (2018) reported the antioxidant activity of flavonoids from the fruit of *C. bispinosa*, there is little to no scientific documentation of the biological activities of the leaves of this plants.

Figure 2. 15: *Carissa bispinosa* (Hyde *et al*., 2021)..

2.14.*5 Clerodendrum glabrum* E. Mey. var. *glabrum*

Clerodenrum glabrum belongs to the Lamiaceae family (Figure 2.16). Its common names include glorybower, bagflower and bleeding-heart (Fouad *et al*., 2013). The roots and the bark are usually dried, pulverised and then boiled to treat ailments such as oral ulcers, diarrhoea, coughs (Masevhe *et al*., 2015). Phyto-constituents isolated and identified from *C. glabrum* include monoterpene and its derivatives, sesquiterpene, diterpenoids, triterpenoids, flavonoid and flavonoid glycosides (Wang *et al*., 2017).

Figure 2. 16: *Clerodendrum glabrum* (Teclegeorgish *et al*., 2020).

2.14.6 *Acacia senegal* (L.) Willd.

Acacia senegal (L.) Willd. (Figure 2.17) belongs to the Fabaceae family and is one of the most important tree species in Africa, and the species distribution area occupies more than 50 % of the sub-Saharian regions in Africa (Odee *et al*., 2015).

The species is famous for its gum arabic, a dried exudate rich in soluble fibers, which emerges from slits made in the bark of the stems and branches and tapped by the local populations (Odee *et al*., 2015). The paste of the tree is used in the treatement of a cold, cough, diarrhoea, dysentery, expectorant, gonorrhoea, sore throat and the disorders of the urinary tract (Agrawal, 2018). Antimicrobial compounds isolated and identified from *A. senegal* include Eicosanoic acid, Tetracosanol, Docosanoic acid, 3α-Hydroxyeuph-25-ene, α-Amyrin, Stigmasterol, ßSitosterol, Betulin3-O-stearate, Eicosanyl 3-Oferuloyl-quinate and ßSitosterol-ß-Dglucoside, D-Pinitol (Jain *et al*.,

Figure 2. 17: *Acacia senegal* (Odee *et al*., 2015).

2012).

2.14.7 *Ficus sur* Forssk

In South Africa, *Ficus sur* is mainly distributed in Eastern Cape, KwaZulu-Natal, Western Cape, Limpopo, and Mpumalanga usually alongside rivers and waterways, riverine forests and drier woodlands (Burrows and Burrows, 2003) (Figure 2.18). Various parts of this plant are used traditionally to treat various ailments which mainly pertain to the respiratory system. The milky white latex from the bark, root and bark decoctions have been used to treat pulmonary TB, influenza and skin infections (Olufisayo, 2017).

The chemical profile of the plant is not well characterised as only a few compounds have been isolated from the prepared extracts. Two pentacyclic triterpenoids have been isolated from the latex of the *Ficus sur*, namely; acetate-α-amyrin and acetate-β-amyrin of ursene and oleanane structures, respectively (Feleke and Brehane, 2005). Two pharmacologically active triterpenoids (lupeol and β-sitosterol), one pheaophytin

(pheaophytin a) and one flavonoid (epicatechin) were isolated from the fruits and leaves (Olufisayo, 2017).

Figure 2. 18: *Ficus sur* leaves (Hankey, 2003) and fruits (Olufisayo, 2017).

2.14.8 *Croton gratissimus* var. *gratissimus* Burch.

The *Croton* genus is a diverse group of plants that encompass herbs, shrubs and trees. This genus belongs to the Euphorbiaceae family and the Croton species is widely distributed in different parts of the world with varying ethnobotanical uses including the treatment of cancer, constipation, diabetes, digestive problems, dysentery, external wounds, intestinal worms, pain, ulcers and weight loss (Salatino *et al*., 2007).

Native tropical, central and sub-Saharan Africa, *Croton gratissimus* Burch. (Figure 2.19) commonly known as lavender Croton or lavender fever berry, is used to treat fever, dysentery and convulsions. In Benin, the leaf decoction is used as anti-hypertensive, anti-microbial (against urinary infections) and to treat malaria-linked fever (Block *et al*., 2002). Essential oil hydrodistilled from the leaves of *Croton gratissimus* was found to be mainly composed by sabinene (14.6%), α-phellandrene (12.3%), β-phellandrene (10.7%), α-pinene (6.05%), and germacrene D (5.9%) (Lawal *et al*., 2017).

Figure 2. 19: *Croton gratissimus* var. *gratissimus* (Naidoo, 2018).

2.15 Purpose of the study

2.15.1 Aim

The aim of this study is to evaluate antimycobacterial activity of eight traditionally used medicinal plants by targeting the shikimate pathway of *Mycobacterium tuberculosis*.

2.15.2 Objectives

The objectives of this study include:

i. phytochemical profiling of the plants extracts using thin layer chromatography;
ii. screening and quantification of different phyto-constituents in the plants extracts using standard tests;
iii. evaluation of antioxidant activity of the plants extracts;
iv. determination of anti-inflammatory activity of the different plants extracts;
v. determination of antimycobacterial activities of the plants extracts;
vi. determination of the combinational effects of bioactive plants extracts;
vii. toxicological evaluation of bioactive extracts;
viii. phenotypic characterisation of the *crispri* hypomorphs;
ix. determination of probable mechanisms of action of bioactive antimycobacterial crude extracts.

2.16 Hypothesis

The use of traditional medicinal plant extracts to target and inhibit the activity of 3-deoxy-D-arabino-heptulosonate 7-phosphate synthase and transketolase from the shikimate pathway will result in improved antimycobacterial activity.

2.17 References

Agrawal, T. 2018. Ethnobotany of the *Acacia senegal*. *World Journal of Pharmaceutical Research*, **7(3)**: 384–388.

Akintola, A.O., Kehinde, A.O., Adebiyi, O.E. and Ademowo, O.G. 2013. Anti-tuberculosis activities of the crude methanolic extract and purified fractions of the bulb of *Crinum jagus*. *Nigerian Journal of Physiological Sciences*, **28**: 135–140.

Amitai, G and Sorek, R. 2016. CRISPR-Cas adaptation: insights into the mechanism of action. *Nature Reviews Microbiology*, **14**: 67–76.

Ayed, H.B., Koubaa, M., Marrakchi, C., Rekik, K. and Hammami, F., *et al*. 2018. Extrapulmonary Tuberculosis: update on the epidemiology, risk factors and prevention strategies. *International Journal of Tropical diseases*, **1(6)**: Doi.10.23937/ijtd-2017/1710006.

Banerjee, A., Dubnau, E., Quemard, A., Balasubramanian, V., Um, K.S., Wilson, T., Collins, D., De Lisle, G. and Jacobs jr, W.R. 1994. inhA, a gene encoding a target for isoniazid and ethionamide in *Mycobacterium tuberculosis*. *Science*, **263(5144)**: 227-30.

Behar, S.M., Divangahi, M. and Remold, H.G. 2010. Evasion of innate immunity by *Mycobacterium tuberculosis*: is death an exit strategy? *Nature Reviews Microbiology*, **8**: 668–674.

Beste, D.J, and McFadden, J. 2010. System-level strategies for studying the metabolism of *Mycobacterium tuberculosis*. *Molecular BioSystems*, **6**: 2363–2372.

Bhat, Z.S., Rather, M.A., Maqbool, M. and Ahmad, Z. 2018. Drug targets exploited in Mycobacterium tuberculosis: pitfalls and promises on the horizon. *Biomedicine and Pharmacotherapy*, **103**: 1733–1747.

Blackmore, N.J., Reichau, S., Jiao, W., Hutton, R.D., Baker, E.N., Jameson, G.B. and Parker, E.J. 2013. Three sites and you are out: ternary synergistic allostery controls aromatic amino acid biosynthesis in *Mycobacterium tuberculosis*. *Journal of Molecular Biology*, **425**: 1582–1592.

Block, S., Stevigny, C., De Pauw-Gillet, M.C., de Hoffmann, E., Llabres, G., Adjakidje, V. and Quetin-Leclercq, J. 2002. Ent-trachyloban-3beta-ol, a new cytotoxic diterpene from *Croton zambesicus*. *Planta Medica*, **68(7)**: 647–649.

Boshoff, H.I. and Barry, C.E. 2005. Tuberculosis–Metabolism and respiration in the absence of growth. *Nature Reviews Microbiology*, **3**: 70–80.

Burrows, J.E. and Burrows, S.M. 2003. Figs of southern and south-central Africa. Umdaus Press Hatfield, South Africa.

Cano, J.H. and Volpato, G. 2004. Herbal mixtures in the traditional medicine of eastern Cuba. *Journal of Ethnopharmacology*, **90**: 293–316.

Cardona, P.J. 2016. The progress of therapeutic vaccination with regard to tuberculosis. *Frontiers in Microbiology*, **7(1536)**: Doi.10.3389/fmicb.2016.01536.

Caws, M., Thwaites, G., Dunstan, S., Hawn, T.R., Lan, N.T., Thuong, N.T., Stepniewska, K., Huyen, M.N., Bang, N.D., Loc, T.H., *et al*. 2008. The influence of host and bacterial genotype on the development of disseminated disease with *Mycobacterium tuberculosis*. *PLoS Pathogens*, **4**: e1000034.

Chang, K.C., Yew, W.W. and Chan, R.C.Y. 2010. Rapid assays for fluoroquinolone resistance in *Mycobacterium tuberculosis*: a systematic review and meta-analysis. *Journal of Antimicrobial Chemotherapy*, **65(8)**: 1551-1561.

Chiang, C.Y., Centis, R. and Migliori, G.B. 2010. Drug-resistant tuberculosis: past, present, future. *Respirology*, **15(3)**: 413–432.

Choudhary, E., Thakur, P., Pareek, M. and Agarwal, N. 2015. Gene silencing by CRISPR interference in Mycobacteria. *Nature Communications,* **6**: 6267. Doi: 10.1038/ncomms7267.

Dan, V., Mchombu, K. and Mosimane, A. 2010. Indigenous medicinal knowledge of the San people: The case of Farm Six, Northern Namibia. *Information Development*, **26**: 129–140.

Davis, J.M. and Ramakrishnan, L. 2009. The role of the granuloma in expansion and dissemination of early tuberculous infection. *Cell*, **136**: 37–49.

de Carvalho, L.P., Fischer, S.M., Marrero, J., Nathan, C., Ehrt, S. and Rhee, KY. 2010. Metabolomics of *Mycobacterium tuberculosis* reveals compartmentalized co-catabolism of carbon substrates. *Chemistry and Biology*, **17**: 1122–1131.

de Jonge, M., Koymans L., Guillemont J., Koul A., Andries K. 2007. A computational model of the inhibition of Mycobacterium tuberculosis ATPase by a new drug candidate R207910. *Proteins*, **67**: 971–980

Ducati, R., Basso, L. and Santos, D. 2007. *Mycobacterial* shikimate pathway enzymes as targets for drug design. *Current Drug Targets*, **8**(3): 423–435.

Ehrt, S. and Schnappinger, D. 2006. Controlling gene expression in *Mycobacteria*. Future. *Microbiology*, **1**: 177–184.

Etienne, G., Laval, F., Villeneuve, C., Dinadayala, P., Abouwarda, A., Zerbib, D., Galamba, A. and Daffe, M. 2005. The cell envelope structure and properties of Mycobacterium smegmatis mc^2 155: is there a clue for the unique transformability of the strain? *Microbiology*, **151**: 2075–2086.

Feleke, S. and Brehane, A. 2005. Triterpene compounds from the latex of Ficus sur i. *Bulletin of the Chemical Society of Ethiopia*, **19(2)**: 307–310.

Field, S.K. 2015. Bedaquiline for the treatment of multidrug-resistant tuberculosis: great promise or disappointment? *Therapeutic Advances in Chronic Disease*, **6(4)**: 170–184.

Foden, W. and Potter, L. 2005. *Senna petersiana* (Bolle) Lock. National assessment: red list of South African plants version 2020(1). http://redlist.sanbi.org/species.php?species=388-12. Accessed on 2021/01/09.

Fouad, M.A., Wanas, A.S. and Khalil, H.E. 2013. Phytochemical and biological studies of *Clerodendrum glabrum* leaves. *International Journal of Pharmacognosy and Phytochemistry*, **28(2)**:1164–1168.

Fullam, E., Pojer, F., Bergfors, T., Jones, T.A. and Cole, S.T. 2011. Structure and function of the transketolase from *Mycobacterium tuberculosis* and comparison with the human enzyme. *Open Biology*, **2**: Doi.10.1098/rsob.110026.

Gagneux, S. 2018. Ecology and evolution of *Mycobacterium tuberculosis*. *Nature Reviews Microbiology*, **16**: 202–213.

Gemechu, A., Giday, M., Worku, A. and Ameni, G. 2013. Open Access In vitro Anti-mycobacterial activity of selected medicinal plants against *Mycobacterium tuberculosis* and *Mycobacterium bovis* Strains. *BMC Complementary and Alternative Medicine*, **13**: 291.

Gordon, S.V. and Parish, T. 2018. Microbe profile: *Mycobacterium tuberculosis*: humanity's deadly microbial foe. *Microbiology*, **164**: 437–439.

Gwatidzo, L.; Dzomba, P. and Mangena, M. 2018. TLC separation and antioxidant activity of flavonoids from *Carissa bispinosa*, *Ficus sycomorus* and *Grewia bicolar* fruits. *Nutrire*, **43**: 1–3.

Hankey, A. 2003. *Ficus sur* Forssk. Walter Sisulu National Botanical Garden, http://www.pza.sanbi.org/ficus-sur.

Hawgood, B.J. 2007. Albert Calmette (1863-1933) and Camille Guérin (1872-1961): the C and G of BCG vaccine. *Journal of Medical Biography*, **15(3)**: 139–146.

He, Z. and De Buck, J. 2010. Cell wall proteome analysis of *Mycobacterium smegmatis* strain MC2 155. *BMC Microbiology*, **10(121)**: Doi. 10.1186/1471-2180-10-121.

Hochstrasser, M.L. and Doudna, J.A. 2015. Cutting it close: CRISPR-associated endoribonuclease structure and function. *Trends in Biochemical Sciences*, **40**: 58–66.

Hunter, L.R. 2011. pathology of post primary tuberculosis of the lung: an illustrated critical review. *Tuberculosis*, **91(6)**: 497–509.

Hyde, M.A., Wursten, B.T., Ballings, P. and Coates Palgrave, M. 2021. Flora of Zimbabwe: species information: individual images: *Carissa bispinosa*.

https://www.zimbabweflora.co.zw/speciesdata/image-display.php?species_id=144930&image_id=2. Accessed: 9 January 2021.

Idu, M. and Onyibe, H.I. 2007. Medicinal plants of Edo state, Nigeria. *Research Journal of Medicinal Plant*, **1**: 32–41.

Iseman, M. 1993. Treatment of multidrug-resistant tuberculosis. *New England Journal of Medicine,* **329**: 784–794.

Ivancic-Bace, I., Cass, S.D., Wearne, S.J. and Bolt, E.L. 2015. Different genome stability proteins underpin primed and naive adaptation in *E. coli* CRISPR-Cas immunity. *Nucleic Acids Research*, **43**: 10821–10830.

Jain, R., Sharma, P., Bhagchandani T. and Jain, S. 2012. Phytochemical investigation and antimicrobial activity of *Acacia senegal* root heartwood. *Journal of Pharmacy Research*, **5**: 4934–4938.

Jhamb, S.S., Goyal, A. and Singh, P.P. 2014. Determination of the activity of standard anti-tuberculosis drugs against intramacrophage *Mycobacterium tuberculosis*, *in vitro*: MGIT 960 as a viable alternative for BACTEC 460. *The Brazilian Journal of Infectious Diseases*, **18(3)**: 336–340.

Jinek, M., Chylinski, K., Fonfara, I., Hauer, M., Doudna. And Charpentier, E. 2012. A programmable dual-RNA-guided DNA endonuclease in adaptive bacterial immunity. *Science*, **337**: 816–821.

Jnawali, H.N. and Ryoo, S. 2013. First– and second–Line drugs and drug resistance. *Tuberculosis - Current Issues in Diagnosis and Management*: Doi.10.5772/54960.

Juma, B. F. and Majinda, R. R. T. 2007. Constituents of *Gardenia volkensii*: their brine shrimp lethality and DPPH radical scavenging properties. *Natural Product Research*, **21(2)**: 121–125.

Kaewphinit, T., Santiwatanakul, S. and Chansiri, K. 2014. The detection of tuberculosis by loop-mediated isothermal amplification (LAMP) combined with a lateral flow dipstick (in Handbook of Research on Diverse Applications of Nanotechnology in

Biomedicine Chapter 13., Chemistry, and Engineering) ed., Shivani, S. *The detection of tuberculosis*: 269–300.

Kandel, T.R., Mfenyana, K., Chandia, J. and Yogeswaran, P. 2008. The prevalence of and reasons for interruption of antituberculosis treatment by patients at Mbekweni Health Centre in the King Sabata Dalidyebo (KSD) district in the Eastern Cape Province. *South African Family Practice*, **50**: 47–50.

Kapnick, S.M. and Zhang, Y. 2008. New tuberculosis drug development: targeting the shikimate pathway. *Expert Opinion on Drug Discovery*, **3(5)**: 565–577.

Kennedy, D.O. and Wightman, E.L. 2015. Herbal extracts and phytochemicals: plant secondary metabolites and enhancement of human brain function. *Advances in Nutrition*, **2**: 32–50.

King, H.C., Khera-Butler, T., James, P., Oakley, B.B., Erenso, G., Aseffa, A., *et al.* 2017. Environmental reservoirs of pathogenic mycobacteria across the Ethiopian biogeographical landscape. *PLoS one*, **12(3)**: Doi: 10.1371/journal.pone.0173811.

Kolly, G.S., Sala, C., Vocat, A., Cole, S.T. 2014. Assessing essentiality of transketolase in *Mycobacterium tuberculosis* using an inducible protein degradation system, *FEMS Microbiology Letters*, **358(1)**: 30–35.

Koonin, E.V. and Makarova, K.S. 2019. Origins and evolution of CRISPR-Cas systems. *Philosophical Transactions of the Royal Society B*, **374**: Doi.10.1098/rstb.2018.0087.

Lawal, O.A., Ogunwande, I.A., Osunsanmi, F.O., Opoku, A.R. and Oyedeji, A.O. 2017. *Croton gratissimus* leaf essential oil composition, antibacterial, antiplatelet aggregation, and cytotoxic activities. *Journal of Herbs Spices and Medicinal Plants*, **23(1)**: 77–87.

Lemke, T.L. 2013. Anti-mycobacterial Agents. In: Lemke, T.L., Williams,. D..A, editors. *Foye's principles of medicinal chemistry. 7th edition*. Lippincott, Williams and Wilkins. Philadelphia.

Li, J., Zhan, L. and Qin, C. 2021. The double-sided effects of *Mycobacterium Bovis* bacillus Calmette–Guérin vaccine. *npj Vaccines*, **6(14)**: Doi.10.1038/s41541-020-00278-0.

Li, Y., Wang, F., Wu, L., Zhu, M., He, G., Chen, X., Sun, F., Liu, Q., Wang, X. and Zhang, W. 2019. Cycloserine for treatment of multidrug-resistant tuberculosis: a retrospective cohort study in China. *Infection and Drug Resistance*, **12**: 721–731.

Linder, H.P. 2014. The evolution of African plant diversity. *Frontiers in ecology and evolution*, **2**: Doi.10.3389/fevo.2014.00038.

Loddenkemper, R., Lipman, M. and Zumla, A. 2016. Clinical aspects of adult tuberculosis. *Cold Spring Harbor Perspectives in Medicine*, **6(1)**: Doi. 10.1101/cshperspect.a017848.

Long, Q., Zhou, Q., Ji, L., Wu, J., Wang, W. and Xie, J. 2012. *Mycobacterium smegmatis* genomic characteristics associated with its saprophyte lifestyle. *Journal of Cellular Biochemistry*, **113**: 3051–3055.

Maitra, A., Munshi, T., Healy, J., Martin, L.T., Vollmer, W., Keep, N.H. and Bhakta, S. 2019. Cell wall peptidoglycan in *Mycobacterium tuberculosis*: An Achilles' heel for the TB-causing pathogen. *FEMS Microbiology Reviews*, **43(5)**: 548–575.

Malen, H., Berven, F.S., Fladmark, K.E. and Wiker, H.G. 2007. Comprehensive analysis of exported proteins from *Mycobacterium tuberculosis* H37Rv. *Proteomics*, **7**: 1702–1718.

Maroyi, A. 2013. Traditional use of medicinal plants in south-central Zimbabwe: review and perspectives. *Journal of Ethnobiology and Ethnomedicine*, **9(31)**: Doi:10.1186/1746-4269-9-31

Maroyi, A. 2020. *Gardenia volkensii* K. Schum. (Rubiaceae): review of medicinal uses, Phytochemistry and biological activities. *Journal of Pharmacy and Nutrition Sciences*, **10**: 175–181.

Marrero, J., Trujillo, C., Rhee, K.Y. and Ehrt, S. 2013. Glucose phosphorylation is required for *Mycobacterium tuberculosis* persistence in mice. *Public Library of Science Pathogens*, **9**: Doi: 10.1371/journal.ppat.1003116.

Masevhe, N.A., McGaw, L.J. and Eloff, J.N. 2015. The traditional use of plants to manage candidiasis and related infections in Venda, South Africa. *Journal of Ethnopharmacology*, **168**: 364–372.

Matsumoto, M.; Hashizume, H.; Tomishige, T.; Kawasaki, M.; Tsubouchi, H.; Sasaki, H.; Shimokawa, Y.; Komatsu, M. 2006. OPC-67683, a nitro-dihydro-imidazooxazole derivative with promising action against tuberculosis *in vitro* and in mice. *PLoS Medicine*, **3**: Doi.10.1371/journal.pmed.0030466.

Mazimba, O. 2014. Pharmacology and phytochemistry studies in *Peltophorum africanum*. *Bulletin of Faculty Pharmacy, Cairo University*, **52(1)**: 145–153.

McNeil, M.B. and Cook, G.M. 2019. Utilization of CRISPR interference to validate MmpL3 as a drug target in *Mycobacterium tuberculosis*. *Antimicrobial Agents and Chemotherapy*, **63**: Doi: 10.1128/AAC.00629-19.

Mehta, S., Mehta, S.S., Thokchom, S.K., Patyal, P. and Bhatnagar, S. 2015. A critical insight into shikimate kinase pathway. *International Journal of Current Pharmaceutical Research*, **7(4)**: 111–113.

Millard, J., Ugarte-Gil, C. and Moore, D.A., 2015. Multidrug resistant tuberculosis. *British Medical Journal*, **350**: Doi. 10.1136/bmj.h882.

Mitchell, G., Chen, C. and Portnoy, D.A. 2016. Strategies used by bacteria to grow in macrophages. *Microbiology Spectrum*, **4**: Doi: 10.1128/microbiolspec.MCHD-0012-2015.

Mojica, F. J., Diez-Villasenor, C., Garcia-Martinez, J. and Almendros, C. 2009. Short motif sequences determine the targets of the prokaryotic CRISPR defence system. *Microbiology*, **155**: 733–740.

Mokgobi, M.G. 2014. Understanding traditional African healing. *African Journal for Physical, Health Education, Recreation and Dance*, **20(2)**: 24–34.

Mongalo, N.I. 2013. *Peltophorum africanum* Sond [Mosetlha]: a review of its ethnomedicinal uses, toxicology, phytochemistry and pharmacological activities. *Journal of Medicinal Plants Research*, **7(48)**: 3484–3491.

Naidoo, D. 2018. Secretory Structures of *Croton gratissimus* Burch. var. *gratissimus* (Euphorbiaceae): micromorphology and histo–phytochemistry. Master of Science in Biological Sciences, University of KwaZulu-Natal, Westville, South Africa, p. 5.

Neetu, N., Katiki, M., Dev, A., Gaur, S., Tomar, S. and Kumar, P. 2020. Structural and biochemical analyses reveal that chlorogenic acid inhibits the shikimate pathway. *Journal of Bacteriology*, **202(18)**: Doi: 10.1128/JB.00248-20.

Nirmal, C.R., Rao, R., Hopper, W. 2015. Inhibition of 3-deoxy-D-arabino-heptulosonate 7-phosphate synthase from *Mycobacterium tuberculosis*: In silico screening and in vitro validation. *European Journal of Medicinal Chemistry*, **105**: 182–193.

Nishimasu, H. and Nureki, O. 2017. Structures and mechanisms of CRISPR RNA-guided effector nucleases. *Current Opinion in Structural Biology*, **43**: 68–78.

Norouzi-Barough, L., Sarookhani, M.R., Salehi, R., Sharifi, M.R. and Moghbelinejad, S. 2018. CRISPR/Cas9, a new approach to successful knockdown of ABCB1/P-glycoprotein and reversal of chemosensitivity in human epithelial ovarian cancer cell line. *Iranian Journal of Basic Medical Sciences,* **21**:181–187.

Nunes, J.E.S., Duque, M.A., de Freitas, T.F., Galina, L., Timmers, L.F.S.M., Bizarro, C.V., Machado, P., Basso, L.A. and Ducati, R.G. 2020. *Mycobacterium tuberculosis* shikimate pathway enzymes as targets for the rational design of anti-tuberculosis drugs. *Molecules*, **25**: Doi.10.3390/molecules25061259.

Odee, D.W., Wilson, J., Omondi, S., Perry, A. and Cavers, S. 2015. Rangewide ploidy variation and evolution in *Acacia senegal*: a north–south divide?. *Journal for Plant Sciences*, **7**: Doi.10.1093/aobpla/plv011.

Olufisayo, O.O. 2017. Phytochemical, elemental and biological studies of three Ficus species (Moraceae) found in KwaZulu-Natal, South Africa. PhD thesis, school of Chemistry and Physics, College of Agriculture, Engineering and Science, University of KwaZulu-Natal, Westville.

Orme, L.M. 2010. The Achilles heel of BCG. *Tuberculosis*, **90**: 329–332

Paige, C. and Bishai, W.R. 2010. Penitentiary or penthouse condo: the tuberculous granuloma from the microbe's point of view. *Cellular Microbiology*, **12**: 301–309.

Palomino, J.C. and Martin, A. 2013. Tuberculosis clinical trial update and the current anti-tuberculosis drug portfolio. *Current Medicinal Chemistry*, **20**: 3785–3796.

Palomino, J.C. and Martin, A. 2014. Drug resistance mechanisms in *Mycobacterium tuberculosis*. *Antibiotics*, **3**: 317–340.

Parish, T. and Stoker, N.G. 2002. The common aromatic amino acid biosynthesis pathway is essential in *Mycobacterium tuberculosis*. *Microbiology*, **48**: 3069–3077.

Park, S. Hwang, E., Park, H., Kim, J., Heo, J., Lee, K., Song, T., Kim, E., Ro, T., Kim, S., Kim, Y. 2001. Growth of Mycobacteria on carbon monoxide and methanol. *Journal of Bacteriology*, **185**:142–147.

Pereira, J.H., Vasconcelos, I.B., Oliveira, J.S., *et al*. 2007. Shikimate kinase: a potential target for development of novel antitubercular agents. *Current Drug Targets*, **8(3)**: 459–468.

Qi, L. S. *et al*. 2013. Repurposing CRISPR as an RNA-guided platform for sequence-specific control of gene expression. *Cell*, **152**: 1173–1183.

Ramaliba, T.M., Tshitangano, T.G., Akinsola, H.A. and Thendele. 2017. Tuberculosis risk factors in Lephalale local municipality of Limpopo province, South Africa. *South African Family Practice*, **59(5)**: 182–187.

Rhee, K. 2013. Minding the gaps: metabolomics mends functional genomics. *European Molecular Biology Organization Reports*, **14**: 949–950.

Rock, J. M., Hopkins, F.F., Chavez, A., Diallo, M., Chase, M.R., Gerrick, E.R., Pritchard, J.R., Church, G.M., Rubin, E.J., *et al*. 2017. Programmable transcriptional repression in mycobacteria using an orthogonal CRISPR interference platform. *Nature Microbiology*, **2**: Doi. 10.1038/nmicrobiol.2016.274.

Rodwell, V. 2015. Harper's illustrated Biochemistry, 30th edition. USA: McGraw Hill. pp. 123–124, 166, 200–20.

Roos, A.K., Andersson, C.E., Bergfors, T., Jacobsson, M., Karlen, A., Unge, T., Jones, T.A. and Mowbray, S.L. 2004. *Mycobacterium tuberculosis* ribose-5-phosphate isomerase has a known fold, but a novel active site. *Journal of Molecular Biology*, **335**: 799–809.

Ross, E. 2010. Inaugural lecture: African spirituality, ethics and traditional healing implications for indigenous South African social work education and practice. *South African Journal of Bioethics and Law,* **3(1)**: 44–51.

Salatino, A., Salatino, M.L.F. and Negri, G. 2007. Traditional uses, chemistry and pharmacology of Croton species (Euphorbiaceae). *Journal of the Brazilian Chemical Society*, **18(1)**:11–33.

Semenya, S.S. and Maroyi, A. 2019. Ethnobotanical survey of plants used by Bapedi traditional healers to treat tuberculosis and its opportunistic infections in the Limpopo Province, South Africa. *South African Journal of Botany*, **122**: 401–421.

Semenya, S.S. and Potgieter, M.J. 2015. *Kirkia wilmsii*: a Bapedi treatment for hypertension. *South African Journal of Botany*, **100**: 228–232.

Shi, L., Sohaskey, C.D., Kana, B.D., Dawes, S., North, R.J., Mizrahi, V. and Gennaro, M.L. 2005. Changes in energy metabolism of *Mycobacterium tuberculosis* in mouse lung and under *in vitro* conditions affecting aerobic respiration. *Proceedings of the National Academy of Sciences of the United States of America,* **102(43)**: 15629–15634.

Sileshi, T., Tadesse, E., Makonnen, E. and Aklillu, E. 2020. The impact of first-line anti-tubercular drugs' pharmacokinetics on treatment outcome: a systematic review. *Clinical Pharmacology: Advances and Applications*, **2021(13):** 1–12.

Song, N.R., Lee, K.W. and Lee, H.J. 2012. Molecular targets of dietary phytochemicals for human chronic diseases: cancer, obesity and alzheimer's diseases. *Journal of Food and Drug Analysis*, **20**: 342–345.

Statistics South Africa. 2018. Mortality and causes of death in South Africa: findings from death notification; Statistics South Africa: Pretoria, South Africa.

Suki, B., Stamenovic, D. and Hubmayr, R. 2011. Lung parenchymal mechanics. *Comprehensive Physiology*, **1(3)**: 1317–1351.

Sukumani, J.T. Lebese, R.T., Khoza, L.B. and Risenga, P.R. 2012. Experiences of family members caring for tuberculosis patients at home at Vhembe district of the Limpopo Province. *Curationis*, **35**: 1–8.

Tabuti, J.R.S., Kukunda, C.B. and Waako, P.J. 2010. Medicinal plants used by traditional medicine practitioners in the treatment of tuberculosis and related ailments in Uganda. *Journal of Ethnopharmacology***, 127**: 130–136.

Teclegeorgish, Z.W., Mokgalaka, N.S., Vukea, N., de la Mare, J-A. and Tembu, V.J. 2020. Cytotoxicity of triterpenoids from *Clerodendrum glabrum* against triple negative breast cancer cells *in vitro*. *South African Journal of Botany*, **133**: 144–150.

Tekwu, E.M., Askun, T., Kuete, V., Nkengfack, A.E., Nyasse, B., Etoa, F-X. and Beng, P. 2012. Antibacterial activity of selected Cameroonian dietary spices ethno-medically used against strains of *Mycobacterium tuberculosis*. *Journal of Ethnopharmacology*, **142**: 374–382.

Tomás-Barberán, F.A. and Andrés-Lacueva, C. 2012. Polyphenols and health: Current state and progress. *Journal of Agricultural and Food Chemistry*, **60**: 8773–8775.

Torres-Ruiz, R. and Rodriguez-Perales, S. 2015. CRISPR-Cas9: a revolutionary tool for cancer modelling. *International Journal of Molecular Sciences*, **16**: 22151–22168.

Tripathi, I.P. and Mishra, C. 2015. Phytochemical screening of some medicinal plants of Chitrakoot Region. *Indian Journal of Applied Research*, **5(12)**: 56–60.

Tshikalange, T.E., Meyer, J.J.M. and Hussein, A.A. 2005. Antimicrobial activity, toxicity and the isolation of a bioactive compound from plants used to treat sexually transmitted diseases. *Journal of Ethnopharmacology*, **96(3)**: 515–519.

Tzin, V. and Galili, G. 2010. New insights into the Shikimate and Aromatic amino acids biosynthesis pathways in plants. *Molecular Plant*, **3(6)**: 956–972.

Vasudevan, D.M., Sreekumar, S. and Vaidyanathan, K. 2011. Textbook of biochemistry for medical students. 6th edition. Jaypee Brothers Medical Publishers (P) Ltd, New Delhi, India, Pp. 113–116.

Wang, J. H., Luan, F., He, X. D., Wang, Y., & Li, M. X. 2017. Traditional uses and pharmacological properties of *Clerodendrum* phytochemicals. *Journal of traditional and complementary medicine*, **8(1)**: 24–38.

Warner, D.F. 2015. *Mycobacterium tuberculosis* metabolism. *Cold Spring Harbor Perspectives in Medicine*, **5**: a021121.

Webby, C.J., Jiao, W., Hutton, R.D., Blackmore, N.J., Baker, H.M., Baker, E.N., Jameson, G.B. and Parker, E.J. 2010. Synergistic allostery: a sophisticated regulatory network for the control of aromatic amino acid biosynthesis in *Mycobacterium tuberculosis*. *Journal of Biological Chemistry*, **285**: 30567–30576.

Werner, C., Doenst, T. and Scharzer, M. 2016. Chapter 4 - metabolic pathways and cycles. In The scientist's Guide to cardiac metabolism. Academic Press: Doi:10.1016/B978-0-12-802394-5.00004-2.

Williams, V.L., Victor, J.E. and Crouch, N.R. 2013. Red listed medicinal plants of South Africa: status, trends, and assessment challenges. *South African Journal of Botany*, **86**: 23–35.

World Health Organization. 2011. Guidelines for the programmatic management of drug-resistant tuberculosis—2011 update, 6th ed. WHO/HTM/TB/2011 WHO, Geneva.

World Health Organization. 2015. Post 2015 End-TB Strategy. Global Strategy and Targets for Tuberculosis Prevention, Care and Control after 2015. Geneva.

World Health Organization. 2019. Global tuberculosis report. World Health Organization. Geneva.

Yuan, T. and Sampson, N.S. 2018. Hit generation in TB drug discovery: From genome to granuloma. *Chemical Reviews*, **118**: 1887–1916.

Chapter 3

3. Phytochemical analysis of medicinal plant extracts

3.1 Introduction

Medical plants possess phytochemicals that are non-nutritive to the human diet but have pharmacological importance towards human health and managing infectious diseases. The synthesis of these chemicals is for the survival of the plant against environmental challenges, which include but are not limited to, pathogens such as bacteria, fungi, herbivores, parasites and viruses (Mulaudzi *et al*., 2012).

The triumph of phytochemicals towards drug discovery is due to their complex chemical structures and diversity within these families. Majority of phytochemicals have steric density than their synthetic libraries. These differences from synthetics breed new ground for bioactive compounds that may react differently with biological targets and systems (Wolfender, 2009).

Ibekwe and Ameh (2014), comprehensively reviewed medicinal plants and isolated phytochemical compounds used in the treatment of TB from different parts of the world. McGaw *et al*. (2008) reported the potential of South African plants against *Mycobacterium* infections. Studies such as these highlighted the wide use of medicinal plants as alternative or complementary medicine in South Africa for the treatment of TB and confirmed their antimycobacterial potential. Common classes of anti-TB active phytochemicals reviewed belonged to tannins, flavonoids, hydrolyzable tannins, alkaloids, sesquiterpenoids, saponins, glycosylated flavonols, flavanones, phytosterols, proanthocyanidins, lignans, coumarins, anthraquinones (Ibekwe and Ameh, 2014; McGaw *et al*., 2008).

Extraction of phytochemicals is an important step in medicinal plant research because it determines the kind of compounds one will obtain from raw material. The screening and investigation of the phytochemistry of plants is integral towards exploring the mechanism of action of biological activities of interest. As such, various extraction methods have been used by researchers to optimally and exhaustively extract bioactive compounds from plant material. Conventional extraction methods include plant tissue homogenisation, serial exhaustive extraction, soxhlet extraction, maceration, infusion, distillation, decoction, and sonication (Tiwari *et al*., 2011).

The objective of this chapter was to screen, quantify and determine the correlation of phyto-constituents of plant leaves extracts. Phytochemical screening and quantification provide direction towards which extracts contain larger amounts of bioactive compounds. The benefit of this is that there will be an informed decision on the choice of optimal solvents to use in bioassays to determine the pharmacological effects of the medicinal plants.

3.2 Materials and methodology

3.2.1 Plant collection, drying and storage

The selection of the plants in this study was based on their ethnopharmacological use for the treatment of TB infection and management of accompanying symptoms. The investigation of such plants will help to explore their pharmacological properties and to determine their value as a source of nutraceutical antimycobacterial remedies. Table 3.1 shows the selected plants and their summarised traditional uses. The plants were collected from the Lowveld National Botanical Garden, in Mbombela, Mpumalanga, South Africa.

The leaves and branches were separated and dried at an ambient temperature away from sunlight. Once dried, the plant material was ground to fine powder using a commercial blender. The powdered material was stored in airtight glass bottles in closed cabinet compartments.

3.2.2 Extraction and thin layer chromatography

Organic solvents, namely; hexane, dichloromethane, acetone, methanol and water were used to extract leaves from the selected plants. All organic solvents used were of HPLC grade (Sigma Aldrich). These solvents were selected to enable a maximum extraction of different phytochemicals based on their polarity index. Non-polar solvents such as hexane and dichloromethane were expected to extract non-polar compounds and polar solvents, where methanol and water were expected to extract compounds of a higher polarity index (Coklar and Akbulut, 2017). Ten millilitres (10 mL) of organic

Table 3. 1: Medicinal plants used in this study

Plant name (**Family**)	Common names	Part used	Traditional use	Reference	Voucher number
Gardenia volkensii (**Rubiaceae**)	English: *Bushveld gardenia*, Sepedi: *Morala*, Xitsonga: *ntsalala*, isiZulu: *umgongwane*	Fruits and roots	Chest complaints and tuberculosis related infections	Maroyi, 2020	UNIN1220022
Senna petersiana (Bolle) Lock (**Fabaceae**)	English: *Dwarf Cassia*, *Monkey Pod*, *Monkey Senna*, TšhiVenda: *Munembenembe*, Sepedi: *Bohlôko*	Root Leaves	Coughs, colds, syphilis and helminthic infections	Foden and Potter, 2005	SSS511
Carissa bispinosa (L.) Desf. Ex Brenan (**Apocynaceae**)	English: *Forest num-num*, isiZulu: *isibethankunzi*, *isabetha*	Roots	Cough and diarrhoea	Maroyi, 2013	SSS09
Acacia senegal (L.) Willd (**Fabaceae**)	English: White gum tree	Bark, roots, leaves	cold, cough, diarrhoea, gonorrhoea, sore throat	Agrawal, 2018	SSS34
Croton gratissimus var. *gratissimus* Burch. (**Euphorbiaceae**)	English: lavender Croton or lavender fever berry	Leaves	Fever, dysentery, convulsions, anti-microbial (against urinary infections) and to treat malaria-linked fever	Block *et al*., 2002	SSS28
Ficus sur Forssk. (**Moraceae**)	English: Cape fig and broom cluster fig, *mogotshetlo* (Sepedi), *umkhiwane* (Xhosa), *umkhiwane* (Zulu)	Bark, root, bark	pulmonary TB, influenza and skin infections	Olufisayo, 2017	SS89
Clerodendrum glabrum E. Mey.(**Lamiaceae)**	English: glorybower, bagflower and bleeding-heart	Root, bark	oral ulcers, diarrhoea, coughs	Masevhe *et al*., 2015	SSS712
Peltrophorum africanum (Sond.)(**Fabaceae**)	English: Weeping wattle (English) and *Mosetlha* (Sepedi)	Root, bark	Rashes and blisters, venereal diseases, anthelmintic, coughs	Mongalo, 2013	SSS47

solvent was added to 1 g of dried powdered leaves material from each of the plant species in a 50 mL tube. The mixture was shaken at 200 rpm for 30, 20 and 10 minutes. The plant extracts were filtered using Whatman No.1 filter into pre-weighed glass vials after every cycle. The resulting extracts from each extraction time were added together. The glass vials were placed under a stream of air from a bench-top fan to evaporate the solvents while the water extracts were freeze-dried. To prepare for thin layer chromatography (TLC), dried extracts were reconstituted to 10 mg/mL and 10 μL of each extract was loaded onto the TLC plates. The TLC plates were developed in saturated TLC chambers using mobile phases of varying polarities, namely; ethyl acetate/methanol/ water (EMW) (40:5.4:5) (polar/neutral), chloroform/ethyl acetate/formic acid (CEF) (5:4:1) (intermediate polarity/acidic) and benzene/ethanol/ammonia hydroxide (BEA) (90:10:1) (non-polar/basic) (Kotze and Eloff, 2002).

Ultra-violet (UV) light (254 and 365 nm) was used to visualise compounds which have the ability to fluoresce under that electromagnetic spectrum. The TLC plates were sprayed with vanillin spray reagents (0.1 g vanillin, 28 mL methanol, 1 mL sulphuric acid) and heated at 110 °C to optimal colour development of compounds which had not been visualised under UV light.

3.2.3 Phytochemical screening

Tannins, saponins, terpenoids, alkaloids, flavonoids, steroids, anthraquinones, phlobatannins, resins, cardiac glycosides, quinones, anthocyanin and betacynin were among the bioactive phytochemicals screened using standard testing protocols described below.

3.2.3.1 Test for Tannins

A weighed amount of plant material (100 mg) was boiled in 5 mL of distilled water. The mixture was cooled and filtered using laboratory cotton wool. A 1% w/v Ferric chloride ($FeCl_3$) solution, prepared in distilled water was added to the filtrate drop-wise using a medicine dropper. The appearance of blue-black precipitate indicated the presence of tannins (Mujeeb *et al*., 2014).

3.2.3.2 Test for Saponins

The froth test detailed by Mujeeb *et al*. (2014) was used to evaluate the presence of saponins. Plant material (100 mg) was added to 5 mL of distilled water in a test tube, shaken and put to boil. The formation of consistent foam indicated the presence of saponins.

3.2.3.3 Test for Alkaloids

Hundred milligrams of plant material were mixed with 5 mL methanol and boiled briefly. The mixture was cooled and filtered using a filter paper. To this filtrate, Hydrochloric acid (HCl) (1%) followed by Dragendorff reagent were added dropped-wise using a medicine dropper. The appearance of a brown-red to orange coloured precipitate was indicative of the presence of alkaloids (Mujeeb *et al*., 2014).

3.2.3.4 Test for Anthraquinones

Plant material (100 mg) was mixed with 5 mL 10% HCl and boiled for 5 minutes. The mixture was allowed to cool to an ambient temperature and subsequently filtered using a laboratory cotton wool. Chloroform ($CHCl_3$) of equal volume to the recovered filtrate was added followed by a few drops of 10% ammonia (NH_3) solution. The appearance of a rose-pink colour was indicative of the presence of anthraquinones (Mujeeb *et al*., 2014).

3.2.3.5 Test for Flavonoids

Hundred milligrams (100 mg) of plant material was extracted with 5 mL of distilled water, by mixing them in a 50 mL centrifuge tube and shaking for 10 minutes at a 200-rpm speed. The mixture was filtered using a laboratory cotton wool. To this filtrate, 2 mL of ammonia solution (NH_3) was added, followed by a few drops of concentrated sulphuric acid (H_2SO_4) using a glass medicine dropper. The formation a yellow colour in the mixture showed the presence of flavonoids (Mujeeb *et al*., 2014).

3.2.3.6 Test for Terpenoids

The Salkowski procedure was followed, where 100 mg of plant material was extracted with 5 mL of chloroform for 10 minutes in a 50 mL centrifuge tube by shaking at 200-rpm. A cotton wool was used to filter the extract into a glass test tube. To the filtrate, 2 mL of concentrated sulphuric acid (H_2SO_4) was carefully added. The presence of terpenoids was shown by the development of a reddish-brown precipitate (Mujeeb *et al*., 2014).

3.2.3.7 Test for Triterpenoids

Each extract (100 mg) was shaken with chloroform in a test tube; a few drops of acetic anhydride was added to the test tube and the solution was brought to boil in a water bath. Once boiling, the solution was rapidly cooled in iced water. Concentrated H_2SO_4 (2 mL) was added alongside the test tube. Formation of a brown ring at the junction of two layers and turning the upper layer to green showed the presence of steroids while formation of deep red colour indicated the presence of triterpenoids (Joshi *et al*., 2013).

3.2.3.8 Test for Steroids

To detect steroids, the Liebermann-Burchard method detailed by Mujeeb *et al*. (2014) was followed, where, 100 mg of plant material was mixed with 5 mL of chloroform ($CHCl_3$). To this mixture, 5 mL of Acetic anhydride was added. The presence of steroids was signified by the development of blue-green ring in the mixture.

3.2.3.9 Test for Phlobatannins

To detect the presence of phlobatannins, 100 mg of plant material was mixed with 5 mL of distilled water in a glass test tube and put to boil. In the boiling test tube, a few drops of 1% HCl were added using a medicine dropper. A positive result was signified by the appearance of a red coloured precipitate (Mujeeb *et al*., 2014).

3.2.3.10 Test for Resins

Acetone extracts were obtained by mixing 100 mg of plant material with 5 mL of acetone and shaken at 200-rpm for 10 minutes. The extract was filtered using cotton and 1 mL of distilled water was added to the filtrate. The development of turbidity was indicative of the presence of resins (Tripathi and Mishra, 2015).

3.2.3.11 Test for Anthocyanin and Betacynin

Plant material (100 mg) was extracted with 5 mL of acetone in a 50 mL centrifuge tube by shaking for 10 minutes at 200-rpm. The extract was filtered by cotton. One millilitre (1 mL) of the filtrate extract was treated with 1 mL of 1 M sodium hydroxide (NaOH) in a test tube and the mixture was heated. The development of bluish-green colouration indicated the presence of anthocyanins and betacynins presence was indicated by the appearance of a yellow colouration of the mixture (Tripathi and Mishra, 2015).

3.2.3.12 Cardiac glycosides

Aqueous extracts were obtained by mixing 100 mg of plant material with 5 mL of distilled water. The mixture was shaken for 10 minutes at 200-rpm and filtered with cotton. Ferric (III) chloride ($FeCl_3$) (1 mL) followed by 1 mL glacial acetic acid were added to 2 mL of the recovered filtrate. A few drops of concentrated Sulphuric acid (H_2SO_4) was then added to the mixture using a medicine dropper. The presence of cardiac glycosides was shown by the formation of green-blue colouration (Tripathi and Mishra, 2015).

3.2.3.13 Quinones

Hundred milligrams (100 mg) of plant material was extracted with 5 mL of distilled water, shaken for 10 minutes at 200-rpm and filtered with cotton. Each extract was separately treated with 5% potassium hydroxide (KOH) dissolved in ethanol. Red to blue colour formation indicated the presence of quinones (Kumar *et al*., 2013).

3.2.4 Quantification of phyto-constituents

Phenolics, flavonoids, flavonols, tannins, alkaloids and proanthocyanidin contents were determined using UV-Vis spectrometry.

3.2.4.1 Total phenolic content

The Folin-Ciocalteu reagent method, described by Tambe and Bhambar (2014), was adopted. Ten microliters of 10 mg/mL plant extracts were diluted with 490 µL of distilled water, followed by the addition of 0.25 mL of Folin-Ciocaltleu reagent in each test tube. To this solution, 1.25 mL (7%) aqueous sodium carbonate (Na_2CO_3) was added and the mixtures were incubated in the dark at an ambient temperature for 30 minutes. An ultraviolet/visible (UV/VIS) spectrophotometer was used to determine the absorbance of the mixtures at 550 nm. A blank and the standard curve were prepared in a similar manner, except that the plant extracts were replaced by distilled water for the blank and various concentration of gallic acid (1.25, 0.63, 0.31, 0.16, 0.08 mg/mL) were prepared for the standard. The results were expressed as a milligram of tannic acid equivalence/gram of extract (mg GAE/g extract). The experiment was conducted in triplicates and independently repeated three times.

3.2.4.2 Total tannin content

To quantify the tannin content, the Folin-Ciocalteu method, described by Tambe and Bhambar (2014), was used. Briefly, 100 µL of 10 mg/mL extracts were added to a clean test tube containing 7.5 mL of distilled water. The Folin-Ciocalteu reagent (0.5 mL) was added to the mixture and vortexed thoroughly. Ten millilitres (10 mL) of a 35% solution of sodium carbonate (Na_2CO_3) was added to the mixture. The mixture in the tube was transferred to a 10 mL volumetric flask and the volume of the mixture made up to 10 mL with distilled water. The mixture was shaken and kept at an ambient temperature for 30 minutes in the dark. Gallic acid was used as a standard and reference standard solutions (1.0, 0.5, 0.25, 0.125, 0.625 mg/mL) were prepared. The absorbance for the solutions was measured at 725 nm using a UV/VIS spectrophotometer against a blank that was prepared in the same manner as the test solutions without adding any extract. Tannin content was expressed as milligram gallic acid equivalence/gram of extract (mg GAE/g extract). The experiment was conducted in triplicates.

3.2.4.3 Total flavonoid content

Total flavonoid content was determined by the aluminium chloride colorimetric assay described by Tambe and Bhambar (2014). Briefly, 100 µL of 10 mg/mL of plant extracts were added to 4.9 mL of distilled water in a clean test tube followed by an addition of 300 µL of 5% sodium nitrite ($NaNO_2$) dissolved in distilled water. The mixture was allowed to react at an ambient temperature (25 °C) for 5 minutes. Once the reaction period elapsed, 300 µL of 10% aluminium chloride ($AlCl_3$) (dissolved in distilled water) was added to the reaction mixture. The reaction was allowed to proceed for 5 minutes, after which 2 mL of 1 M sodium hydroxide (NaOH) was added. To construct a standard curve, a concentration gradient (500, 250, 125, 62.5, 31.5

µg/mL) of quercetin was prepared and each concentration was reacted in the same manner as the extracts. A UV/VIS spectrophotometer was used to measure absorbance at a wavelength of 510 nm. The blank was prepared in the same manner as samples, but 100 µL of distilled water was added instead. The total flavonoid content of the samples was expressed as milligram quercetin equivalence/ gram of extract (mg QE/g extract). The experiment was conducted in triplicates.

3.2.4.4 Total alkaloid content

A procedure detailed by Mallikarjuna *et al*. (2012) was followed. Working solutions of 1 mg/mL of each plant extract were prepared using dimethyl sulfoxide (DMSO). One millilitre (1 mL) of 2 M HCl was added to 1 mL of DMSO dissolved extracts and the resulting mixture was filtered using filter paper. The filtrate was transferred to a 250 mL separating funnel and to this solution, 5 mL of 0.1% Bromocresol green (dissolved in methanol) was added followed by 5 mL of phosphate buffer (pH 6.6). Chloroform ($CHCl_3$) (1 mL) was added into the separating funnel and the mixture was vigorously shaken, after which the funnel was allowed to stand to allow the mixture to separate into different layers. The lower layer was collected in a 10 mL volumetric flask. The process was repeated with 2, 3 and 4 mL of $CHCl_3$. Atropine was used as a standard and each prepared concentration (1, 0.5, 0.25, 0.125, 0.0625 mg/mL) was performed, as described for the extracts. A UV/VIS spectrophotometer was used to measure absorbance at a wavelength of 470 nm against a reagent blank. The total alkaloid content was expressed as milligram atropine equivalent/ gram of extract (mg AE/g of extract). The experiment was conducted in triplicates.

3.2.4.5 Total flavonol content

The aluminium chloride method detailed by Iqbal *et al*. (2015) was followed to determine total flavonol content. Plant extracts were made to 1 mg/mL and 0.5 mL of these solutions and were added to test tubes followed by the addition of 0.5 mL of 2% aluminium chloride ($AlCl_3$) and 1.5 mL of 5% of sodium acetate. The solution was mixed well using a vortex. The solution was then transferred to a 2 mL Eppendorf tube and centrifuged for 20 minutes to obtain a clear solution. A UV/VIS spectrophotometer was used to measure the absorbance of the clear solution at a wavelength of 440 nm against a blank prepared as described earlier. Quercetin was used as a standard and a standard curve was constructed by subjecting different concentration (250, 125, 62.5, 31.3, 16 µg/mL) to the same methodology. Results were expressed as mg quercetin equivalent per gram of extract (mg QE/g extract). The experiment was conducted in triplicates.

3.2.4.6 Total proanthocyanidin content

Total proanthocyanidin content was quantified by following the procedure described by Sun *et al*. (1998). Concentration of plant extracts prepared were 1 mg/mL. In a test tube, 0.5 mL of 1 mg/mL of plant extracts were prepared. To these extracts, 3 mL of 4% v/v vanillin dissolved in methanol was added, followed by 1.5 mL of 37% HCl. The mixture was vortexed thoroughly and allowed to stand for 15 mins in an ambient temperature. A UV/VIS spectrophotometer was used to measure the absorbance of the solutions at a wavelength of 500 nm against a reagent blank. The blank was prepared by adding the same reagents but omitting the test samples. Gallic acid was used, as standard and concentrations 250, 125, 62.5, 31.3, 16 µg/mL were used to construct a standard curve. Total proanthocyanidin content was expressed as milligram gallic acid equivalence/gram of extract (mg GAE/g extract). The experiment was conducted in triplicates.

3.3 Results
3.3.1 Percentage yield

Various solvents (hexane, dichloromethane, acetone, methanol and water) were used as extractants of the phytochemicals from the leaves material. Methanol and water extracts gave the largest mass of phytochemicals compared to acetone, dichloromethane and hexane (Figure 3.1).

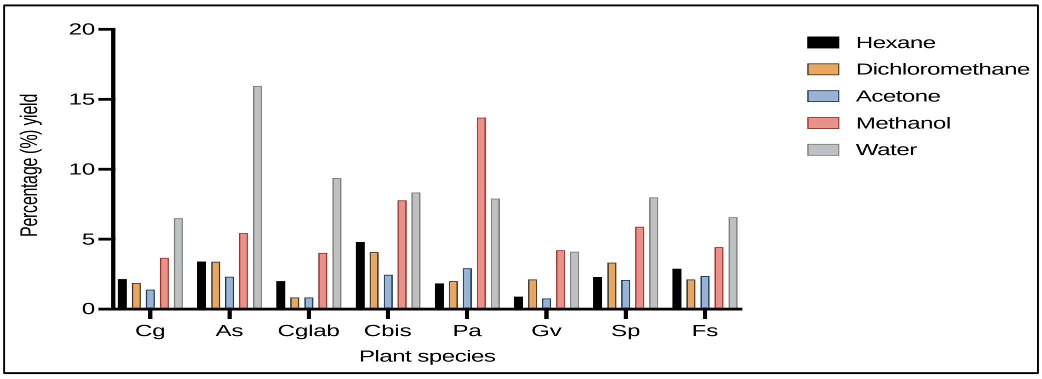

Figure 3. 1: Percentage yield of different solvents from 1 g of dried plant material.

Key: Cg: *Croton gratissimus*, As: *Acacia Senegal*, Cglab: *Clerodendrum glabrum,* Cbis: *Carissa bispinosa*. Pa: *Peltophorum africanum*, Gv: *Gadernia volkensii*, Sp: *Senna petersiana*, Fs: *Ficus sur.*

3.3.2 Thin layer chromatography phytochemical profiles

Thin layer chromatography (TLC) was used to establish the phytochemical profiles of the different plant extracts. Fluorescent compounds on the chromatograms (Figure 3.1-3.4) were observed under ultraviolet (UV) light. Vanillin-sulphuric acid was used to visualise non-fluorescent compounds (Figures 3.5 and 3.6). More varieties of non-polar compounds were observed (BEA chromatograms) from each plant species compared to intermediate (CEF) and polar compounds (EMW).

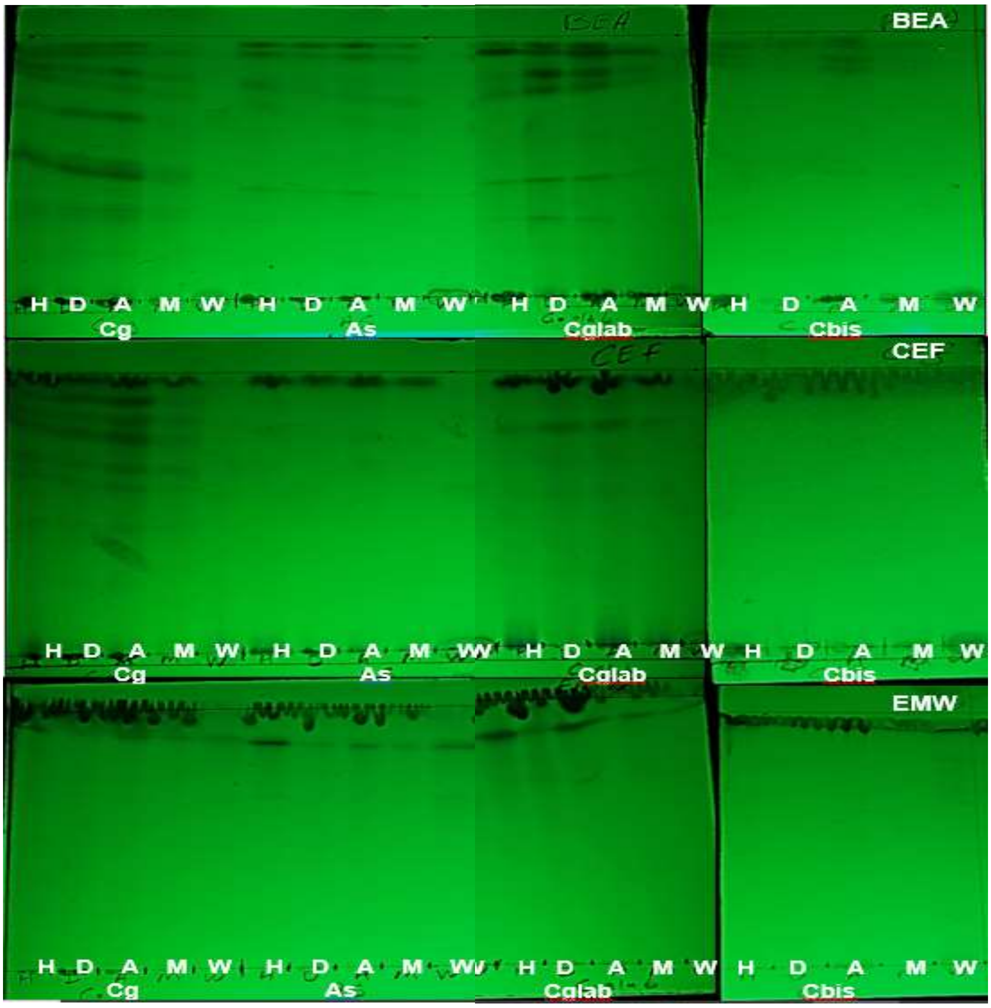

Figure 3. 2: Chromatograms of separated plant extracts developed in various mobiles phases and visualised using ultraviolet light (254 nm).

Key: Cg: *Croton gratissimus*, As: *Acacia Senegal*, Cglab: *Clerodendrum glabrum,* Cbis: *Carissa bispinosa*, H: hexane, D: dichloromethane, A: acetone, M: methanol, W: water.

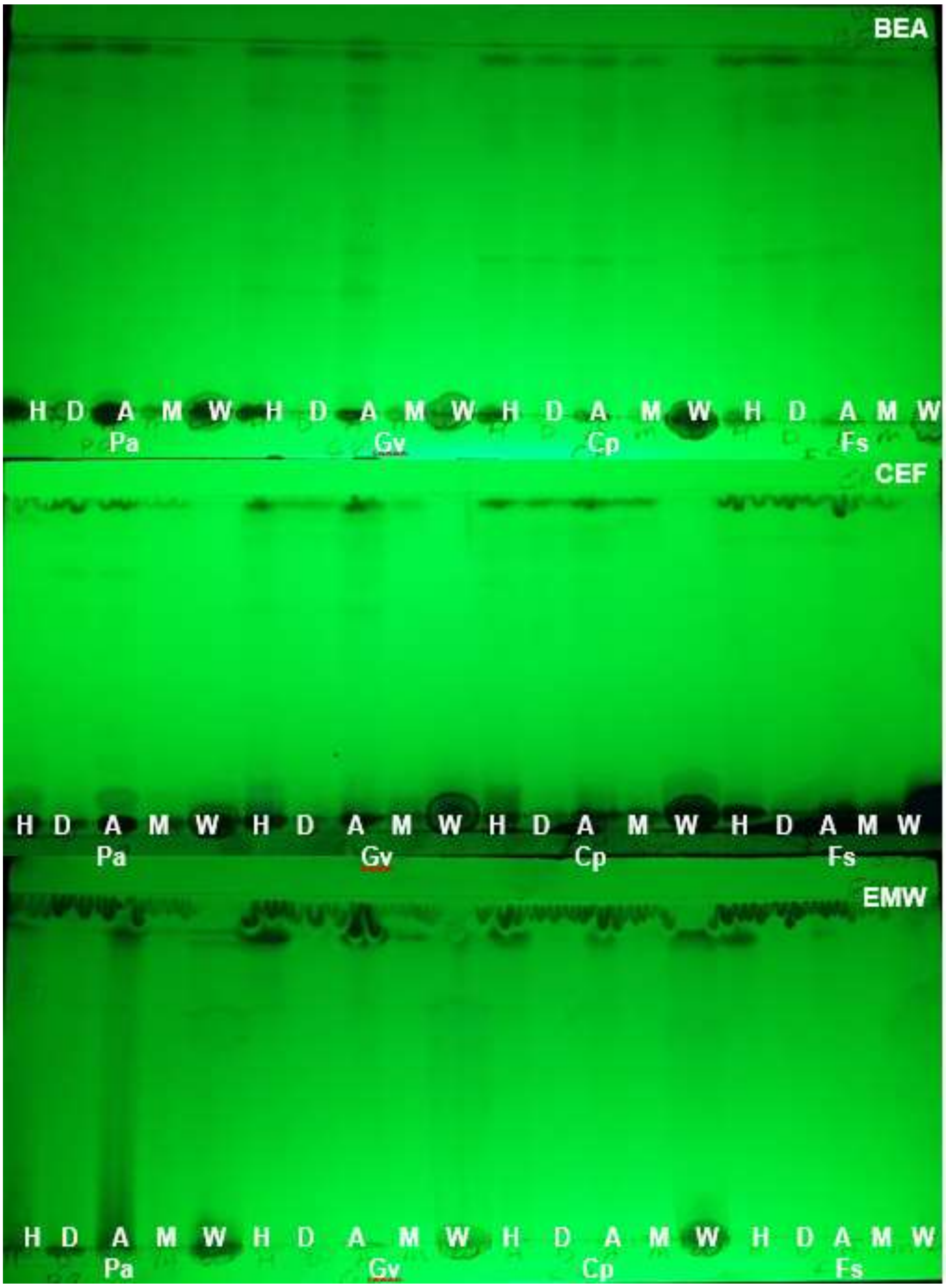

Figure 3. 3: Thin layer chromatograms of leaves extracts viewed under UV Light (254 nm).

Key: Pa: *Peltophorum africanum*, Gv: *Gadernia volkensii*, Cp: *Senna petersiana*, Fs: *Ficus sur,* H: hexane, D: dichloromethane, A: acetone, M: methanol, W: water.

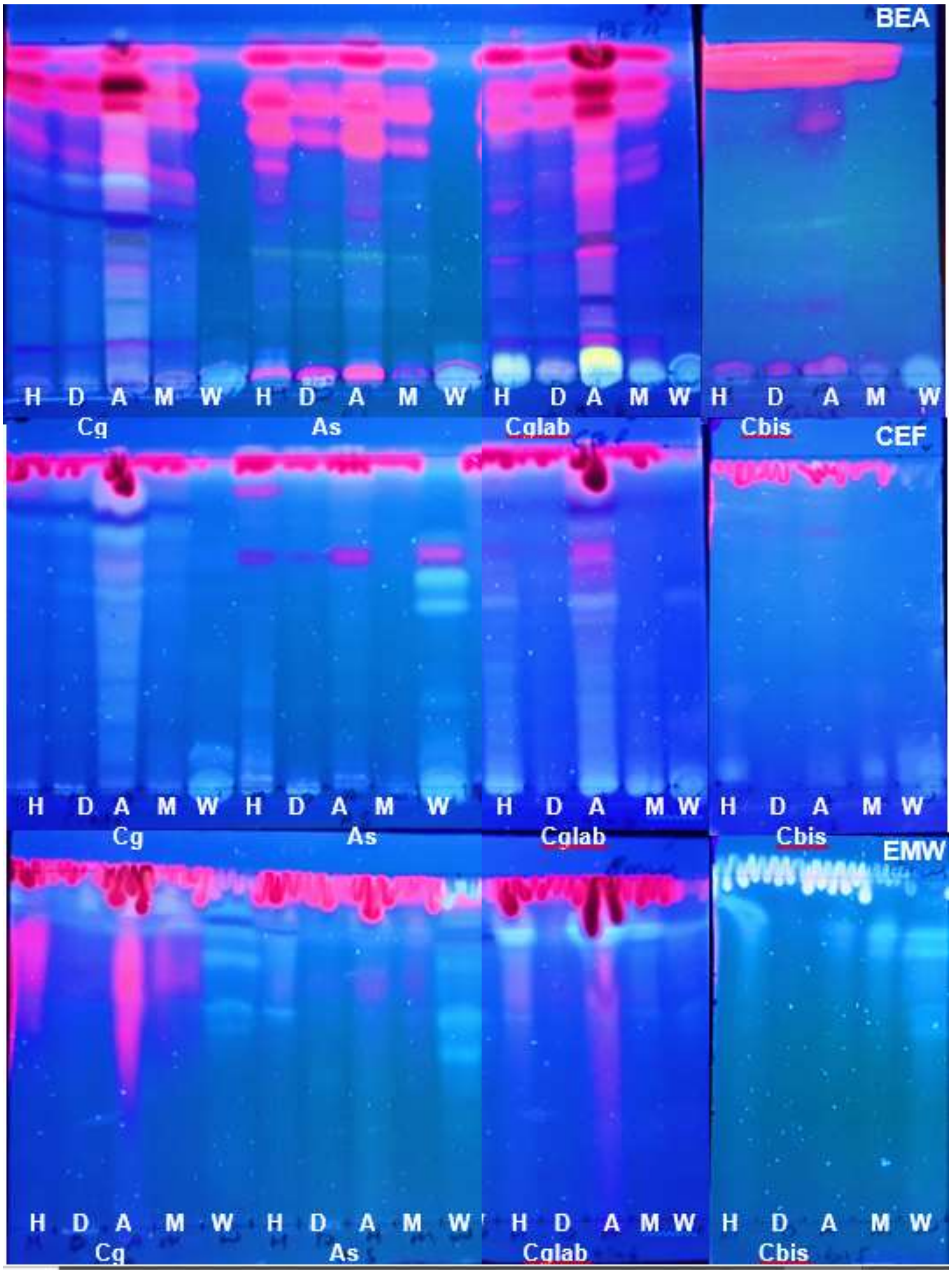

Figure 3. 4: TLC chromatograms of various phytochemicals in the different plant leaves visualised with 365 nm UV light.

Key: Cg: *Croton gratissimus*, As: *Acacia Senegal*, Cglab: *Clerodendrum glabrum*, Cbis: *Carissa bispinosa*, H: hexane, D: dichloromethane, A: acetone, M: methanol, W: water.

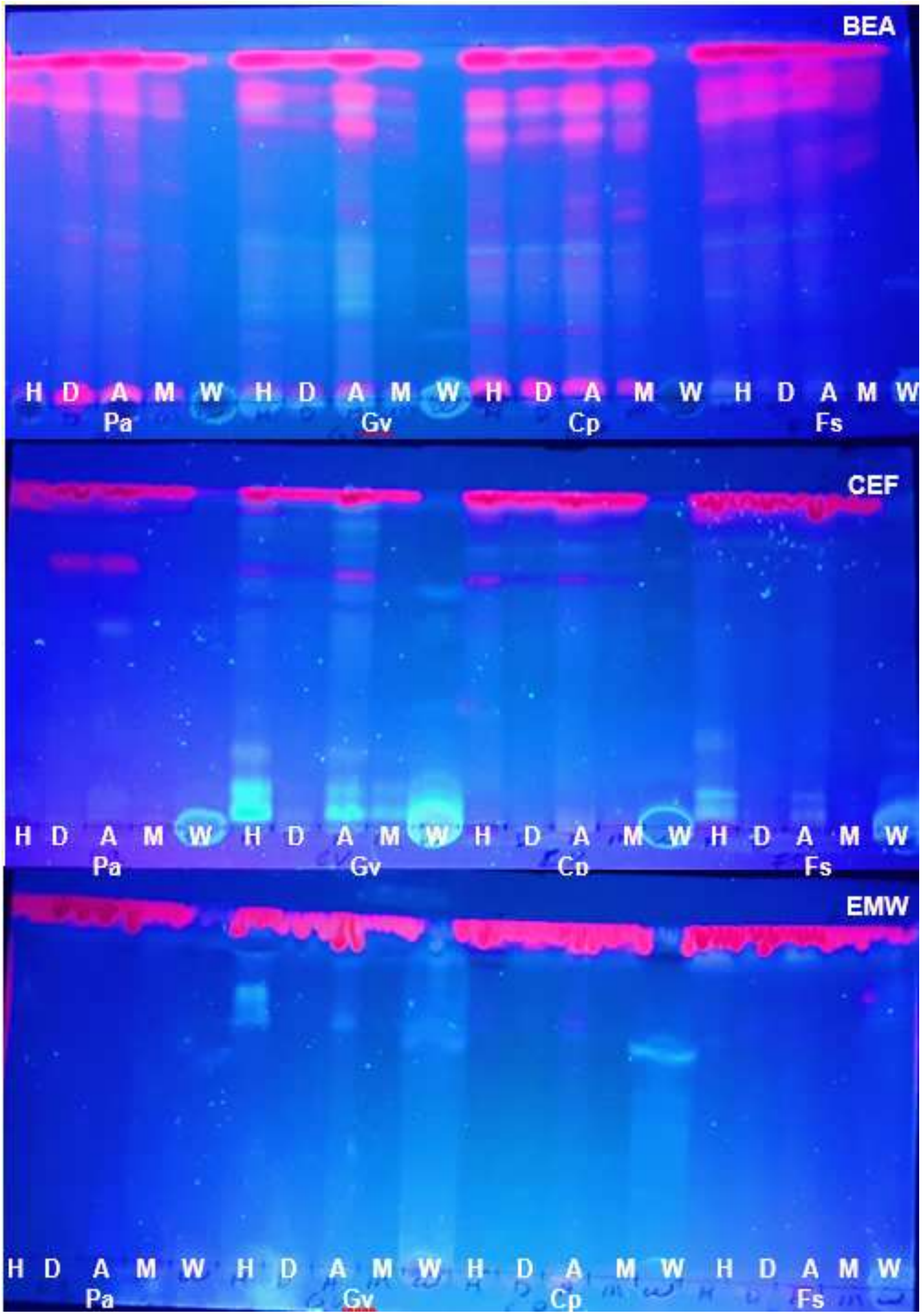

Figure 3. 5: Phytochemicals separated with TLC from crude solvent leaves extracts and visualised under UV (365 nm). Fluorescent compounds are visible under UV light of various wavelengths.

Key: Pa: *Peltophorum africanum*, Gv: *Gadernia volkensii*, Cp: *Senna petersiana*, Fs: *Ficus sur,* H: hexane, D: dichloromethane, A: acetone, M: methanol, W: water.

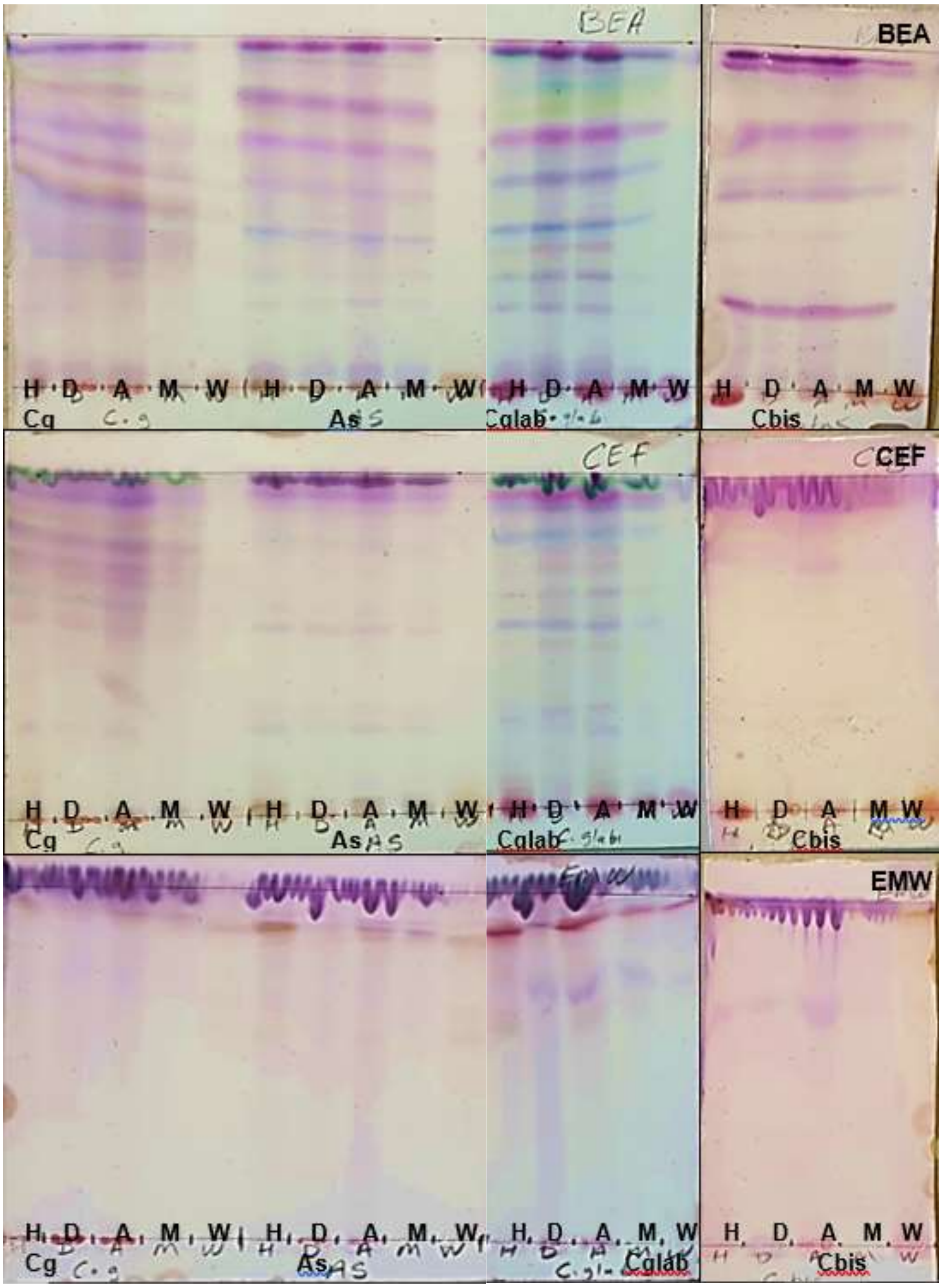

Figure 3. 6: TLC chromatograms of the different plant leaves extracts sprayed with vanillin-sulphuric acid. The chromatograms were heated and treated for optimal colour development.

Key: Cg: *Croton gratissimus*, As: *Acacia Senegal*, Cglab: *Clerodendrum glabrum,* Cbis: *Carissa bispinosa*, H: hexane, D: dichloromethane, A: acetone, M: methanol, W: water.

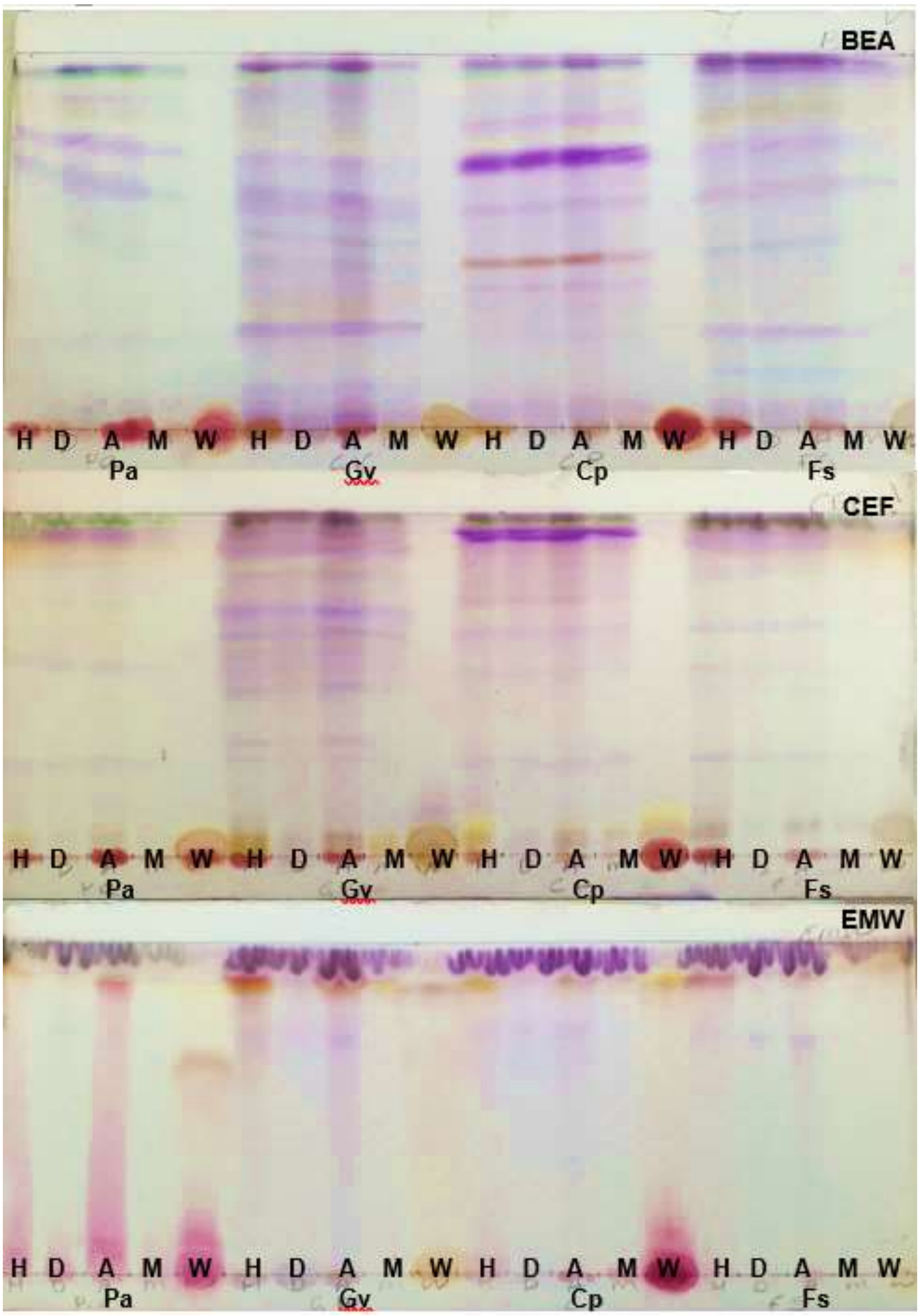

Figure 3. 7: TLC chromatograms developed with various mobile phases and sprayed with vanillin-sulphuric acid spray reagent. Vanillin reacts with different compounds to produce various colours.

Pa: *Peltophorum africanum*, Gv: *Gadernia volkensii*, Cp: *Senna petersiana*, Fs: *Ficus sur,* H: hexane, D: dichloromethane, A: acetone, M: methanol, W: water.

3.3.3 Phytochemical screening

Standard chemical methods based on colour changes for positive identification phytochemical groups. Majority of the screened phytochemicals were detected in all plants, namely, saponins, steroids, terpenoids, triterpenoids, alkaloids, tannins, flavonoids, cardiac glycosides and resins (Table 3.2). The presence of this myriad of phytochemicals are responsible for various biological activities such as antimicrobial, antioxidant and anti-inflammatory activities which are explored further in this current study.

Table 3. 2: Phyto-constituents screened from the different plant leaves.

Phyto-constituents	**Cg**	**As**	**Cglab**	**Cbis**	**Pa**	**Gv**	**Sp**	**Fs**
Saponin	+	+	+	+	+	+	+	+
Steroids	+	+	+	+	+	+	+	+
Terpenoids	+	+	+	+	+	+	+	+
Triterpenoids	+	+	+	+	+	+	+	+
Alkaloids	+	+	+	+	+	+	+	+
Tannins	+	+	+	+	+	+	+	+
Flavonoids	+	+	+	+	+	+	+	+
Phlobatannins	-	-	-	-	+	+	+	+
Antraquinones	-	+	+	-	+	-	+	+
Quinones	-	+	+	+	+	+	+	+
Anthocyanin	+	-	-	+	+	+	+	+
Betacynin	+	+	+	+	-	-	-	-
Resins	+	+	+	+	+	+	+	+
Cardiac glycosides	+	+	+	+	+	+	+	+

Key: (+): Positive, (-): Negative, Cg: *Croton gratissimus*, As: *Acacia Senegal*, Cglab: *Clerodendrum glabrum,* Cbis: *Carissa bispinosa*. Pa: *Peltophorum africanum*, Gv: *Gadernia volkensii*, Sp: *Senna petersiana*, Fs: *Ficus sur*.

3.3.4 Quantification of total phyto-constituent content

The quantified phyto-constituents were present in all the different solvent extracts. The *Senna petersiana* water extract had the most Total phenolic content (1239.94 ± 0.18 mg GAE/g). Total tannin content and proanthnocyanidin content were highest in the water extract of *Peltophorum africanum* (25.51 ± 0.08 mg GAE/g) and acetone extract of *Ficus sur* (679.69 ± 0.93 mg GAE/g), respectively. In general, the flavonol content was (mg QE/g) was higher than the total flavonoid content (Table 3.3).

Table 3. 3: Total phenolic and tannin content determined from various solvent extracts.

Total Phenolic content (mg GAE/g extract)								
	Cg	As	Cglab	CB	Pa	Gv	cp	Fs
H	61.58 ± 0.59	57.87 ± 0.068	94.01 ± 0.18	106.73 ± 0.25	276.38 ± 0.12	172.07 ± 0.14	722.04 ± 0.14	497.96 ± 0.27
DCM	87.31 ± 0.31	49.29 ± 0.12	24.96 ± 0.18	14.70 ± 0.14	238.65 ± 0.12	277.01 ± 0.07	787.90 ± 0.07	698.85 ± 0.41
A	71.82 ± 0.43	23,03 ± 0.18	65.14 ± 0.07	35.80 ± 0.30	417.85 ± 0.07	440.06 ± 0.34	661.22 ± 0.07	412.26 ± 0.12
M	69.01 ± 0.65	17.06 ± 0.35	107.40 ± 0.12	92.27 ± 0.25	533.39 ± 0.12	582.78 ± 0.25	845.81 ± 0.07	582.88 ± 0.25
W	150.33 ± .20	250.02 ± 0.18	35.95 ± 0.14	137.52 ± 0.07	290.65 ± 0.07	1000.43 ± 0.12	1239.94 ± 0.18	914.93 ± 0.65
Total tannin content (mg GAE/g extract)								
H	7.87 ± 0.02	6.86 ± 0.02	9.61 ± 0.01	13.06 ± 0.03	6.33 ± 0.02	1.01 ± 0.01	11.43 ± 0.56	3.57 ± 0.02
DCM	8.89 ± 0.06	4.92 ± 0.02	7.32 ± 0.03	9.91 ± 0.03	1.80 ± 0.04	1.49 ± 0.03	4.31 ± 0.10	4.51 ± 0.04
A	9.34 ± 0.01	2.93 ± 0.04	12.96 ± 0.01	10.39 ± 0.07	23.99 ± 0.09	5.87 ± 0.04	5.62 ± 0.04	5.72 ± 0.61
M	3.43 ± 0.04	1.81 ± 0.04	3.49 ± 0.01	6.39 ± 0.15	7.36 ± 0.04	7.36 ± 0.05	3.81 ± 0.03	5.10 ± 0.03
W	5.05 ± 0.06	3.49 ± 0.02	1.63 ± 0.02	12.79 ± 0.02	25.51 ± 0.08	12.14 ± 0.6	14.14 ± 0.24	7.33 ± 0.1

Key: mg GAE/g extract: milligram gallic acid equivalence/ gram of extract; mg QE/g extract: milligram quercetin equivalence/ gram of extract. Key: Cg: *Croton gratissimus*, As: *Acacia Senegal*, Hp: *H. Pauciflora*, Cglab: *Clerodendrum glabrum,* Cbis: *Carissa bispinosa*, H: hexane, D: dichloromethane, A: acetone, M: methanol, W: water.

Table 3. 4: Total Proanthocyanidin and alkaloid content extracted from plant leaves.

Total proanthrocyanidins content (mg GAE/g extract)								
Extract	Cg	As	Cglab	Cbis	Pa	Gv	Sp	Fs
H	322.04 ± 0.60	579.54 ± 0.32	291.42 ± 0.08	183.06 ± 0.11	47.22 ± 0.32	26.18 ± 0.43	398.49 ± 0.52	393.36 ± 0.52
D	508.21 ± 0.34	356.76 ± 0.08	573.11 ± 0.27	97.17 ± 0.30	74.96 ± 0.52	48.10 ± 0.05	506.33 ± 0.81	571.11 ± 0.73
A	487.11 ± 0.3	505.25 ± 0.29	579.11 ± 0.03	241.59 ± 0.05	152.48 ± 0.52	44.95 ± 0.03	340.66 ± 0.74	679.69 ± 0.93
M	335.53 ± 0.11	441.86 ± 0.23	296.69 ± 0.05	106.74 ± 0.32	168.30 ± 0.16	60.39 ± 0.39	576.91 ± 0.69	493.95 ± 1.38
W	175.20 ± 0.26	297.07 ± 0.32	124.5 ± 0.30	13.22 ± 0.29	174.73 ± 0.03	266.73 ± 0.61	416.66 ± 0.62	169.61 ± 0.34
Total alkaloid content (mg APE/g extract)								
H	0.43 ± 0.45	100.68 ± 1.54	113.72 ± 0.34	13.38 ± 0.28	124.39 ± 0.34	1.54 ± 0.44	10.63 ± 0.01	137.79 ± 0.83
D	0.12 ± 0.92	354.92 ± 1.68	993.48 ± 1.60	10.62 ± 0.17	475.63 ± 0.58	874.30 ± 0.67	0.38 ± 0.78	589.83 ± 0.50
A	0.57 ± 0.71	244.99 ± 0.34	727.02 ± 1.46	11.72 ± 0.11	19.01 ± 0.83	78.26 ± 0.29	0.03 ± 0.63	19.93 ± 1.21
M	0.73 ± 0.06	788.69 ± 0.77	1048.97 ± 0.17	13.26 ± 0.05	252.69 ± 0.6	16.36 ± 1.45	14.91 ± 0.51	25.26 ± 0.29
W	1.58 ± 0.91	14.78 ± 0.73	323.02 ± 0.50	217.48 ± 0.93	38.30 ± 0.44	370.09 ± 0.67	15.76 ± 0.32	13.06 ± 0.44

Key: mg TAE/g extract: milligram tannic acid equivalence/ gram of extract; mg GAE/g extract: milligram gallic acid equivalence/ gram of extract; mg QE/g extract: milligram quercetin equivalence/ gram of extract. Key: Cg: *Croton gratissimus*, As: *Acacia senegal*, Cglab: *Clerodendrum glabrum*, Cbis: *Carissa bispinosa*, H: hexane, D: dichloromethane, A: acetone, M: methanol, W: water.

Table 3. 5: Flavonol and Flavonoid content in plant leaves extracted using various solvents.

Total flavonols content (mg QE/g extract)								
	Cg	As	Cglab	Cbis	Pa	Gv	Sp	Fs
H	65.99 ± 0.17	62.10 ± 0.06	63.76 ± 0.06	64.77 ± 0.04	65.54 ± 0.04	13.71 ± 0.36	2.98 ± 0.16	4.03 ± 0.06
D	60.48 ± 0.04	41.55 ± 0.16	130.43 ± 0.15	57.20 ± 0.07	94.77 ± 0.04	7.69 ± 0.17	3.055 ± 0.87	4.96 ± 0.98
A	100.41 ± 0.14	67.58 ± 0.06	129.85 ± 0.06	77.59 ± 0.11	60.38 ± 0.10	4.62 ± 0.07	10.68 ± 0.67	10.19 ± 1.84
M	27.86 ± 0.06	28.60 ± 0.03	44.01 ± 0.14	16.66 ± 0.06	21.83 ± 0.06	3.06 ± 0.04	17.44 ± 0.03	7.14 ± 0.01
W	0.75 ± 0.07	17.64 ± 0.10	0.04 ± 0.001	5.41 ± 0.04	01.39 ± 0.14	19.66 ± 0.10	10.41 ± 0.03	5.15 ± 0.01
Total flavonoid content (mg QE/g extract)								
H	10.18 ± 0.32	13.42 ± 0.65	15.93 ± 0.47	16.18 ± 0.06	0.66 ± 0.04	1.52 ± 0.27	2.30 ± 0.20	1.60 ± 0.47
D	7.23 ± 0.38	7.18 ± 0.05	19.75 ± 0.41	10.36 ± 0.05	2.36 ± 0.04	5.86 ± 0.87	3.52 ± 0.34	9.93 ± 1.50
A	10.89 ± 0.26	10.86 ± 0.45	27.84 ± 0.29	7.51 ± 0.04	4.56 ± 0.08	4.26 ± 0.85	4.05 ± 0.54	5.11 ± 0.18
M	6.80 ± 0.13	6.69 ± 0.04	7.63 ± 0.04	6.79 ± 0.17	3.31 ± 0.23	6.11 ± 0.61	3.01 ± 0.29	5.77 ± 0.14
W	0.87 ± 0.03	1.19 ± 0.04	0.34 ± 0.04	4.98 ± 0.10	6.40 ± 0.4	9.56 ± 0.01	3.24 ± 0.25	7.13 ± 0.22

Key: mg TAE/g extract: milligram tannic acid equivalence/ gram of extract; mg GAE/g extract: milligram gallic acid equivalence/ gram of extract; mg QE/g extract: milligram quercetin equivalence/ gram of extract Cg: *Croton gratissimus*, As: *Acacia senegal*, Cglab: *Clerodendrum glabrum,* Cbis: *Carissa bispinosa*. Pa: *Peltophorum africanum*, Gv: *Gadernia volkensii*, Sp: *Senna petersiana*, Fs: *Ficus sur*, H: hexane, D: dichloromethane, A: acetone, M: methanol, W: water.

3.3.5 Correlation of quantified phyto-constituents

The relationship between the determined phyto-constituents was evaluated and shown by Pearson's correlation matrix in Table 3.6. The highly significant positive ($R = 0.947$, $p<0.05$) correlation between TPC and TFC observed in the present study was expected because flavonoids can be classified as a group of phenolic compounds.

Table 3. 6: Correlation between the various tested phyto-constituents.

Phytoconstituents	Phenolics	Tannins	Flavonols	Flavonoids	proanthcyanidins	Alkaloids
			C. gratissimus			
Phenolics	1.000					
Tannins	-0.313	1.000				
Flavonols	-0.708	0.836	1.000			
Flavonoids	**0.919***	0.617	**0.918***	1.000		
Proanthcyanidins	-0.621	0.712	0.817	0.714	1.000	
Alkaloids	-0.716	-0.218	0.347	0.588	0.160	1.000
			A. senegal			
Phenolics	1.000					
Tannins	0.026	1.000				
Flavonols	-0.627	0.430	1.000			
Flavonoids	-0.741	0.498	**0.926***	1.000		
proanthcyanidins	-0.655	0.366	0.830	**0.944***	1.000	
Alkaloids	-0.385	-0.536	-0.336	-0.058	0.122	1.000
			C. glabrum			
Phenolics	1.000					
Tannins	0.108	1.000				
Flavonols	-0.207	0.800	1.000			
Flavonoids	-0.030	**0.949***	**0.945***	1.000		
proanthcyanidins	-0.225	0.741	**0.990***	**0.915***	1.000	
Alkaloids	-0.049	-0.063	0.445	0.225	0.550	1.000
			P. africanum			
Phenolics	1.000					
Tannins	0.133	1.000				
Flavonols	-0.425	-0.579	1.000			
Flavonoids	0.189	**0.847***	-0.682	1.000		
proanthcyanidins	-0.060	0.192	0.638	-0.082	1.000	
Alkaloids	-0.205	-0.843	0.537	-0.474	-0.154	1.000
			G. volkensii			
Phenolics	1.000					
Tannins	**0.983***	1.000				
Flavonols	**0.924***	0.859	1.000			
Flavonoids	**0.956***	**0.907***	0.874	1.000		
proanthcyanidins	**0.886***	0.833	**0.966***	0.818	1.000	
Alkaloids	-0.016	-0.164	0.099	0.241	0.112	1.000
S. petersiana						

Phenolics	1.000					
Tannins	0.296	1.000				
Flavonols	-0.269	-0.298	1.000			
Flavonoids	**0.911***	-0.436	0.616	1.000		
proanthcyanidins	0.010	-0.496	-0.680	-0.222	1.000	
Alkaloids	**0.953***	0.430	-0.047	-0.800	-0.295	1.000
			F. sur			
Phenolics	1.000					
Tannins	-0.814	1.000				
Flavonols	-0.769	0.294	1.000			
Flavonoids	-0.392	0.376	-0.009	1.000		
proanthcyanidins	-0.147	-0.438	0.640	0.085	1.000	
Alkaloids	0.432	-0.457	-0.438	0.574	0.279	1.000
			C. bispinosa			
Phenolics	1.000					
Tannins	0.352	1.000				
Flavonols	-0.677	0.193	1.000			
Flavonoids	-0.098	0.374	0.603	1.000		
proanthcyanidins	-0.472	-0.031	0.869	0.453	1.000	
Alkaloids	-0.492	-0.468	0.613	0.569	0.737	1.000

Key: (*): Correlation is significant where $p< 0.05$.

3.4 Discussion

3.4.1 Percentage yield

The percentage yields from 1 g of dry powdered leaf samples are shown in Figure 3.1. It was observed that indeed percentage yields of extraction were dependent on the polarity index of the solvent used, as previously reported by Abdisa *et al*. (2020). In agreement with this, methanol and water extracts gave the largest percentage yield of phytochemicals compared to that of acetone, dichloromethane and hexane (Figure 3.1). Water had the highest polarity index among the solvents and as such, it was expected that it, along with methanol, would generally extract more polar compounds than non-polar. Masoko *et al*. (2008) also reported the same principle.

3.4.2. Thin layer chromatography phytochemical screening

Thin later chromatography (TLC) continues to be used for the phytochemical analysis of medicinal plants (Ochwang'I *et al*., 2016). Fluorescence was used as a chemical property to assess the characteristics of various phytochemicals in the crude plants extracts. Fluorescence under ultraviolet light (254 and 365 nm) was chosen because when a chemical absorbs the UV light, a light of a different colour, usually a longer wavelength is emitted and can be seen with the naked eye.

The TLC chromatograms visualised with UV (366 nm) (Figures 3.4 and 3.5) have bands of red, blue, yellow and green, which corresponds with multiple classes of phytochemicals. The green chlorophyll of leaves fluoresces red (Marshall and Johnsen, 2017). The phytochemical groups in the various extracts demonstrated different Rf values in the different solvent systems (BEA, CEF, EMW). The number of coloured bands on a chromatogram is representative of the number of compounds present in the extracts. Moreover, the chromatogram in which the compounds are observed is representative of their polarities. This difference in Rf values offers a clue to the polarity of the phytochemicals in each of the extracts. It was noted that the BEA chromatogram was able to separate and show more compounds with varied Rf values than the CEF and EMW in both the UV visualised chromatograms and vanillin-sulphuric acid treated chromatograms (Figures 3.2-3.7). The chromatograms suggested that the plant extracts possessed more varieties of non-polar compounds, followed by those of intermediate polarity and polar compounds were present in the least chemical varieties.

Majority of the compounds observed on the vanillin-sulphuric acid treated chromatograms may highlight the presence of steroids because this reagent reacts with most steroidal compounds. Other classes of phytochemicals observed on the chromatograms were the terpenoids/triterpenoids (purple/bluish-purple coloured bands), while flavonoids are yellow/orange coloured and proanthocyanidins were visualised as pink bands (Ahmed *et al*., 2014; Taganna *et al*., 2011) (Figure 3.5 and 3.6). The most ubiquitous polyphenolics are the flavonoids and consist of numerous subclasses, namely; flavan-3-ols, flavanones, flavones, isoflavones, flavonols, anthocyanins and proanthocyanidins (Balentine *et al*., 2015). The presence of these phytochemicals in the plant extracts may have implications and contribution to the biological activities of the plants because they have ethnobotanical applications. Studies have indeed reported on the antimycobacterial potential of terpenoids (Gordien *et al*., 2009) and flavonoids (Soh *et al*., 2017; Chen *et al*., 2015).

3.4.3 Phytochemical screening

It is important to know the various compounds contained in the extracts of the medicinal plants used and cataloguing the phytochemistry of these active constituents is key towards antimycobacterial drug discovery (Kerr, 2013). This information is vital in understanding the mechanisms of the biological activity found in the extracts. Phytochemical screening is a pilot stage in a phytochemical study that aims to offer a summary of the class of compounds contained in the extracts. Phytochemical analyses of the present study revealed the presence of bioactive constituents known to possess important pharmacological activities (Table 3.1). A majority of the screened phytochemicals were detected in all plants, namely, saponins, steroids, terpenoids, triterpenoids, alkaloids, tannins, flavonoids, cardiac glycosides and resins. Various phytochemicals have been associated with antioxidant, antimicrobial, antifungal, antidiabetic, anti-inflammatory, anticancer and antihypertensive properties (Demir and Akpinar, 2020) (Table 3.1). A similar *Senna petersiana* phytochemical profile was reported by Gatsing and Adoga (2007), where alkaloids, flavonoids, cardiacglycosides, anthraquinones, anthocyanins, polyphenols, triterpenes, steroids, saponins, tannins and phlobatannins were detected and reported by Gasting and Adoga, 2007).

3.4.4 Quantification of phytoconstituents

Various important phyto-constituent groups were quantified from the various extracts obtained with different solvents (Tables 3.3-3.5). The water extracts of *S. petersiana* and *G. volkensii* had the most total phenolic content (TPC) of 1239.94 ± 0.18 mg GAE/g and 1000.43 ± 0.12 mg GAE/g, respectively (Table 3.3). The lowest TPC were detected in the DCM extract of *C. bispinosa* (14.70 ± 0.14 mg GAE/g), followed by *A. senegal* methanolic extract (17.06 ± 0.35 mg GAE/g). It was observed that in general, the TPC for the extracts was higher than the total tannin content (TTC) (mg GAE/g) (Table 3.3). However, the TPCs were fairly lower than the total proanthocyanidin content (TPAC) (Tables 3.3 and 3.4). All the plant extracts possessed various concentrations of alkaloids (Table 3.4). The antimycobacterial activity of numerous alkaloids has been thoroughly documented by Mishra *et al*. (2017). The presence of alkaloids in the plant extracts in the current study may reflect potential antimicrobial activity. The alkaloid content was the lowest in both the acetone and DCM extracts of

C. gratissimus and *S. petersiana*. Although flavonols are a subclass of flavonoids (Balentine *et al*., 2015), it was interesting to note that the total flavonol contents (TFOC) were higher than the total flavonoid content (TFC) for the plant extracts. This may indicate that the aluminium chloride protocol used to detect the TFOC may be more sensitive to other types of flavonoid compounds. Nevertheless, a significant positive correlation ($p<0.05$) between flavonoids and flavonols were determined for *C. gratissimus*, *A. senegal* and *C. glabrum* (Table 3.6). Correlation studies indicated a lack of significant correlation between the determined total phyto-constituent contents of the extracts tested for *C. bispinosa* and *F. sur* ($p>0.05$) (Table 3.6).

A previous phytochemical study by Njoya *et al*. (2018) reported TPC of acetone and water leaves extract of *C. gratissimus* to be 222.29 and 121.92 mg GAE/g, respectively. In this study, however, lower TPC was quantified for acetone (71.82 mg GAE/g) and water (150.33 mg GAE/g) extracts of *C. gratissimus*. Similarly, lower TFC was reported for *C. gratissimus* extracts. There is an absence of thorough phytochemical profile of *Carissa bispinosa* leaves. Only the fruits were reported to have bioactive flavonoids (Gwatidzo *et al*., 2018). Through correlation assessment, Saloufou *et al*. (2018) determined that 72% of the phenolic compounds found in the *Ficus sur* may be due to flavonoids. Conversely, lower flavonoid content from *F. sur* leaves was determined. Condensed-flavonoids, terpenoids, flavonoids, and flavonols were reported in *Peltophorum africanum* (Mazimba, 2014). Similar to previous studies by Suwannakud *et al*. (2017) and Juma and Majinda, (2007), tepernoids and phenolics were detected in *G. volkensii* leaves. The crude *G. volkensii* hexane leaf extract was reported to have monoterpenes, diterpenes, terpinenes iridoids genipin and genipin gentiobioside, the pterocarpin medicarpin, coumarins, phenylpropanoids, benzenoids. This study shows that the tannins, flavonoids, flavonols and proanthocyanidins in *G. volkensii* significantly correlated with the total phenolic content (Table 3.6).

The minor differences observed between the phytochemical profiles and previous studies may be due to differences of protocols used for extraction, seasonal variation of phytochemicals, environmental factors; such as temperature, water stress, and light conditions (Upadrasta *et al*., 2011; Wang *et al*., 2009). Results demonstrate that the quantity of phyto-constituents is dependent on the choice of solvent. Indeed, the solvent is important during extraction because the solubility of the phytochemicals is affected by the polarity index of the selected solvent (Tiwari *et al*., 2011).

3. 5 Conclusion

The selected plant species all possessed various important classes of phyto-constituents which have well documentation of pharmacological application. Polar solvents extract a large mass of these compounds. However, thin layer chromatography demonstrated that intermediate and non-polar solvents extracted greater diversity of compounds from respective samples. This indicated that solvents with an intermediate polarity index such as acetone, would be ideal for extracting a variety of the bioactive phytochemicals. Given that some members of phyto-constituent classes identified have been reported to have antimycobacterial activities, their presence in the tested plant extracts may have implications of various biological activities such as the antimycobacterial, antioxidant, anti-inflammatory activity evaluated in this current work.

4.6 References

Abdisa, Z., Kenea, F. and Kishore, C. 2020. Phytochemical screening, antibacterial and antioxidant activity studies on the crude root extract of *Clematis hirsute*. *Cogent Chemistry*, **6(1)**: DOI: 10.1080/23312009.2020.1862389.

Agrawal, T. 2018. Ethnobotany of the *Acacia senegal*. *World Journal of Pharmaceutical Research*, **7(3)**: 384–388.

Ahmed, A.S., McGaw, L.J., Elgorashi, E.E., Naidoo, V. and Eloff, J.N. 2014. Polarity of extracts and fractions of four *Combretum* (*Combretaceae*) species used to treat infections and gastrointestinal disorders in southern African traditional medicine has a major effect on different relevant in vitro activities. *Journal of Ethnopharmacology*, **154(2)**: 339–350

Balentine D.A., Dwyer J.T., Erdman J.W., Jr., Ferruzzi M.G., Gaine P.C., Harnly J.M. and Kwik-Uribe C.L. 2015. Recommendations on reporting requirements for flavonoids in research. *American Journal of Clinical Nutrition*, **101**:1113–1125.

Block, S., Stevigny, C., De Pauw-Gillet, M.C., de Hoffmann, E., Llabres, G., Adjakidje, V. and Quetin-Leclercq, J. 2002. Ent-trachyloban-3beta-ol, a new cytotoxic diterpene from *Croton zambesicus*. *Planta Medica*, **68(7)**: 647–649.

Chen, M., Deng, J., Li, W., Lin, D., Su, C., Wang, M., Li, X., Abuaku, B.K., Tan, H. and Wen S.W. 2015. Impact of tea drinking upon tuberculosis: a neglected issue. *BMC Public Health*, **15**: 515.

Coklar, H. and Akbulut, M. 2017. Anthocyanins and phenolic compounds of *Mahonia aquifolium* berries and their contributions to antioxidant activity. *Journal of Functional Foods*, **35**: 166–174.

Demir, T. and Akpinar, ö. 2020. Biological activities of phytochemicals in plants. *Turkish Journal of Agriculture–Food Science and Technology*, **8(8)**: Doi: 10.24925/turjaf.v8i8.1734-1746.3484.

Foden, W. and Potter, L. 2005. *Senna petersiana* (Bolle) Lock. National assessment: red list of South African plants version 2020.1. http://redlist.sanbi.org/species.php?species=388-12. Accessed on 2021/01/09.

Gatsing, D. and Adoga, G.I. 2007. Antisalmonellal activity and phytochemical screening of the various parts of *Cassia petersiana* Bolle (Caesalpiniaceae). *Research Journal of Microbiology*, **2**: 876–880.

Gordien, A.Y., Gray, A.I., Franzblau, S.G. and Seidel, V. 2009. Antimycobacterial terpenoids from *Juniperus communis* L. (Cuppressaceae). *Journal of Ethnopharmacology*, **126(3)**: 500–505.

Gwatidzo, L.; Dzomba, P. and Mangena, M. 2018. TLC separation and antioxidant activity of flavonoids from *Carissa bispinosa*, *Ficus sycomorus* and *Grewia bicolar* fruits. *Nutrire*, **43**: 1–3.

Ibekwe, N.N. and Ameh, S.J. 2014. Plant natural products research in tuberculosis discovery and development: a situation report with focus on Nigerian biodiversity. *African Journal of Biotechnology*, **13(23)**: 2307–2320.

Iqbal, E., Salim, K.A. and Lim, L.B.L. 2015. Phytochemical screening, total phenolics and antioxidant activities of bark and leaf extracts of *Goniothalamus velutinus* (Airy Shaw) from Brunei Darussalam. *Journal of King Saud University- Science*, **27(3)**: 224–232.

Joshi, A., Bhobe, M., Saatarkar, A. 2013. Phytochemical investigation of the roots of *Grewia microcos* Linn. *Journal of Chemical and Pharmaceutical Research*, **5**: 80–87.

Juma, B.F. and Majinda, R. R.T. 2007. Constituents of *Gardenia volkensii*: their brine shrimp lethality and DPPH radical scavenging properties. *Natural Product Research*, **21(2)**: 121–125.

Kerr, P.G. 2013. Fighting multidrug resistance with herbal extracts, essential oils and their components: chapter 5. In Rai, M.K. and Kon, K.V., *Plants and Tuberculosis: phytochemicals potentially useful in the treatment of Tuberculosis*. Academic Press: pp 45–64.

Kotze, M. and Eloff, J.N. 2002. Extraction of antibacterial compounds from *Combretum microphyllum* (Combretaceae) *South African Journal Botany*, **68**: 62–67.

Kumar, R.S., Venkateshwar, C., Samuel, G. and Rao, S.G. 2013. Phytochemical screening of some compounds from plant leaf extracts of *Holoptelea integrifolia* (Planch.) and *Celestrus emarginata* (Grah.) used by Gondu tribes at Adilabad District, Andhrapradesh, India. *International Journal of Engineering Science Invention*, **2(8)**: 2319–6734.

Mallikarjuna, R.T., Ganga, R.B. and Venkateswara, R.Y. 2012. Antioxidant activity of *Spilanthes acmella* extracts. *International Journal of Phytopharmacology*, **3(2)**: 216–220.

Maroyi, A. 2013. Traditional use of medicinal plants in south-central Zimbabwe: review and perspectives. *Journal of Ethnobiology and Ethnomedicine*, **9(31)**: Doi:10.1186/1746-4269-9-31.

Maroyi, A. 2020. *Gardenia volkensii* K. Schum. (Rubiaceae): review of medicinal uses, phytochemistry and biological activities. *Journal of Pharmacy and Nutrition Sciences*, **10**: 175–181.

Marshall, J. and Johnsen, S. 2017. Fluorescence as a means of colour signal enhancement. *Philosophical Transactions of the Royal Society B: Biological sciences*, **372(1724)**: Doi: 10.1098/rstb.2016.0335.

Masevhe, N.A., McGaw, L.J. and Eloff, J.N. 2015. The traditional use of plants to manage candidiasis and related infections in Venda, South Africa. *Journal of Ethnopharmacology*, **168**: 364–372.

Masoko, P., Mmushi, T.J., Mogashoa, M.M., Mokgotho, M.P., Mampuru, L.J. and Howard, R.L. 2008. *In vitro* evaluation of the antifungal activity of *Sclerocarya birrea* extracts against pathogenic yeasts. *African Journal Biotechnology*, **7(20)**: 3521–3526.

Mazimba, O. 2014. Pharmacology and phytochemistry studies in *Peltophorum africanum*. *Bulletin of Faculty of Pharmacy, Cairo University*, **52(1)**: 145–153.

McGaw, L.J., Lall, N., Meyer, J.J.M. and Eloff. 2008. The potential of South African plants against Mycobacterium infections. *Journal of Ethnopharmacology*, **119**: 482–500.

Mishra, S.K., Tripathi, G., Kishore, N., Singh, R.K., Singh, A. and Tiwari, V.K. 2017. Drug development against tuberculosis: Impact of alkaloids. *European Journal of Medicinal Chemistry*, **137**: 504–544.

Mongalo, N.I. 2013. *Peltophorum africanum* Sond [Mosetlha]: a review of its ethnomedicinal uses, toxicology, phytochemistry and pharmacological activities. *Journal of Medicinal Plants Research*, **7(48)**: 3484–3491.

Mujeeb, F., Bajpai, P. and Pathak, N. 2014. Phytochemical evaluation, antimicrobial activity and determination of bioactive components from leaves of *Aegle marmelos*. *Biomedicine Research International*, **4(10)**: 1–11.

Mulaudzi, R.B., Ndhlala, A.R., Kulkarni, M.G. and van Staden, J. 2012. Pharmacological properties and protein binding capacity of phenolic extracts of some Venda medicinal plants used against cough and fever. *Journal of Ethnopharmacology*, **143**: 185–193.

Njoya, E., Eloff, J. N. and McGaw, L. J. 2018. *Croton gratissimus* leaf extracts inhibit cancer cell growth by inducing caspase 3/7 activation with additional anti-inflammatory and antioxidant activities. *BMC Complementary and Alternative Medicine*, **18(1):** Doi:10.1186/s12906-018-2372-9.

Ochwang'I, D.O., Kimwele, C.N., Oduma, J.A., Gathumbi, P.K., Kiama, S.G. and Efferth, T.I. 2016. Phytochemical screening of medicinal plants of the Kakamega Country, Kenya, commonly used against cancer. *Medicinal and Aromatic Plants*, **5(6)**: Doi: 10.4172/2167-0412.1000277.

Olufisayo, O.O. 2017. Phytochemical, elemental and biological studies of three Ficus species (Moraceae) found in KwaZulu-Natal, South Africa. PhD thesis, school of Chemistry and Physics, College of Agriculture, Engineering and Science, University of KwaZulu-Natal, Westville.

Saloufou, K.I., Boyode, P., Simalou, O., Eloh, K., Idoh, K., Melila, M., Toundou, O., Kpegba, K. and Agbonon, A. 2018. Chemical composition and antioxidant activities of different parts of *Ficus sur*. *Journal of HerbMed Pharmacology*, **7(3)**: 185–192.

Soh A.Z., Pan A., Chee C.B.E., Wang Y.T., Yuan J.M., Koh W.P. 2017. Tea drinking and its association with active tuberculosis incidence among middle-aged and elderly adults: The Singapore Chinese Health Study. *Nutrients.* **9**:544.

Sun, B., Ricardo-da-Silva, J.M. and Spranger, I. 1998. Critical factors of Vanillin Assay for Catechins and Proanthocyanidins. *Journal of Agricultural and Food Chemistry*, **46(10)**: 4267–4274.

Suwannakud, K.S., Chaveerach, A., Sudmoon, R. and Tanee, T. 2017. Chemical constituents of medicinal plants, *Gardenia elata*, *G. gjellerupii*, and *G. volkensii*. *International Journal of Pharmacognosy and Phytochemical Research*, **9(3)**: 293–296.

Taganna, J.C., Quanico, J.P., Perono, R.M.G., Amor, E.C. and Rivera, W.L. 2011. Tannin-rich fraction from *Terminalia catappa* inhibits quorum sensing (qs) in *Pseudomonas aeruginosa*. *Journal of Ethnopharmacology*, **134**: 865–871.

Tambe, V.D. and Bhambar, R.S. 2014. Estimation of total phenol, tannin, alkaloid and flavonoid in *Hibiscus Tiliaceus* Linn. wood extracts. *Journal of Pharmacognosy and Phytochemistry*, **2(4)**: 2321–6182.

Tiwari, P., Kumar, B., Kaur, M., Kaur, G. and Kaur, H., 2011. Phytochemical screening and extraction: a review. *Internationale Pharmaceutica Sciencia*, **1(1)**: 98–106.

Tripathi, I.P. and Mishra, C. 2015. Phytochemical screening of some medicinal plants of Chitrakoot region. *Indian Journal of Applied Research*, **5(12)**: 56–60.

Upadrasta L., Mukhopadhyay M., Banerjee R. 2011. Tannins: chemistry, biological properties and biodegradation. In: Sabu A., Roussos S., Aguilar C.N., editors, *Chemistry and biotechnology of polyphenols*. Cibet Publishers; Thiruvananthapuram, India: pp. 5–32.

Wang, R., Wang, R. and Yang, B. 2009. Extraction of essential oils from five cinnamon leaves and identification of their volatile compound compositions. *Innovative Food Science and Emerging Technologies*, **10(2)**: 289–292.

Wolfender, J-L. 2009. HPLC in natural product analysis: The detection issue. *Planta medica*, **75(719)**: 719–734.

Chapter 4

4 Evaluation of antioxidant and anti-inflammatory activities of plant extracts

4.1 Introduction

Free radicals (oxidants) are chemical species that have either one or more unpaired electrons and seek stability through electron pairing with biomolecules (Box *et al*., 2012). Reactive oxygen species (ROS) represent the furthermost significant group of oxidants and are composed of two main groups, radical oxidant species (hydroxyl $^{\bullet}OH$, superoxide ion $O_2^{\bullet -}$) and non-radical oxidant species (hydrogen peroxide H_2O_2, organic peroxides) (Li *et al*., 2015). Other notable oxidant species include several reactive nitrogen species (RNS) (nitroxide $NO^{\bullet}$) and some sulphur derivatives (alkyl sulfanyl radicals) (Bedlovi˘cová *et al*., 2020). Free radicals are produced by living organisms through numerous biological activities such as aerobic respiration, nutrient metabolism, the progress of aging, peroxisomes and stimulation of macrophages (Klaunig and Kamendulis, 2004). It has been reported that approximately 5 g of ROS are produced daily by the human body (Bedlovicová *et al*., 2020).

The load of free radicals in human increases under pathophysiological conditions such as TB infection, inflammation and metabolism of foreign compounds (Kasote *et al*., 2015). This overload of free radicals causes oxidative stress. During oxidative stress, the functionality, integrity and permeability of cellular membranes can be disrupted and compromised by the action of ROS and RNS due to their ability to oxidise the double bonds of polyunsaturated fatty acids (lipoproteins, membrane structures) (Förstermann, 2010). The effect of oxidative stress transcends to the damage of nucleic acids through deoxyribose ring cleavage, base modification or chain breaks leading to mutations, translation errors or inhibition of protein synthesis (Bedlovicová *et al*., 2020). It is known that inflammation and oxidative stress are interrelated processes (Chatterjee, 2016).

Inflammation has been associated with pain, increase in temperature (heat), swelling and loss of function in the affected area, membrane alteration and an increase of vascular permeability and protein denaturation, among others (Dharsana and Mathew, 2014; Kandikattu *et al*., 2013). During an inflammatory response, ROS and RNS are produced in high concentrations by macrophages due to their physiological activities, which include presenting antigens and producing chemical mediators, such as cytokines (Marrassini *et al*., 2018).

Protein denaturation occurs due to the disruption of the electrostatic, hydrogen, hydrophobic and disulphide bonds in the protein structure (Bailey-Shaw *et al*., 2017). It has been reported that inhibition of denaturation of bovine serum albumin at physiological pH (6.2-6.5) was a measure of anti-inflammatory activity of various NSAIDs such as salicylic acid, diclofenac sodium, flufenamic acid and indomethacin (Hasan, 2017). Therefore, chemical agents that can inhibit protein conformational changes and may possess therapeutic value as anti-inflammatory agents and may assist mediate microbial infection (Bailey-Shaw *et al*., 2017; Anyasor, *et al*., 2015). Results from Marrassini *et al*. (2018) suggested that anti-inflammatory activity may also be induced by antioxidant activity.

Antioxidants prevent or delay the damage of cells caused by oxidants (ROS, RNS, free radicals, other unstable molecules) through the stabilisation or deactivation of free radicals, often before they attack targets in biological cells (Jing *et al*., 2011). There is no universal antioxidant, as different antioxidants react with different reactive species by various mechanisms, at various locations and protect specific molecular targets (Jing *et al*., 2011). Antioxidants can be thought of as the opposition of oxidants and may be of natural or synthetic origins (Jing *et al*., 2011). Synthetic antioxidants such as butylated hydroxyl anisole (BHA), propyl gallate (PG), butylated hydroxyl toluene (BHT), which have been used to prevent oxidation, have been found to cause internal and external bleeding in rats and guinea pigs at a high dose (Borneo *et al*., 2009; Lee *et al*., 2003).

The antioxidant potential of plant extracts can be determined using various methods. Moreover, it is recommended that at least two different procedures be used to quantify the antioxidant activity (Milan *et al*., 2010). There are a number of available methods, which are grouped into two main groups: the hydrogen-atom transfer (HAT) (involves the transfer of hydrogen atom) and single electron transfer (SET), which involves reduction reactions through electron transfer from an antioxidant (Prior *et al*., 2005). The most commonly used SET methods by researchers include 2,2-di-phenyl-1-picrylhydrazyl (DPPH radical scavenging capacity assay), ferric reducing (FRAP) assay, Trolox equivalent antioxidant capacity assay, copper reduction (CUPRAC) assay and reducing power assay (RPA). Popular HAT methods commonly used to evaluate antioxidant activity are the crocin bleaching assay, the total peroxyl radical-trapping antioxidant parameter (TRAP) assay, total oxyradical scavenging capacity assay, and the oxygen radical absorbance capacity assay (Chaves *et al*., 2020; Prior *et al*., 2005).

4.2 Materials and Methods

4.2.1 Qualitative free radical scavenging assay

Thin layer chromatography (TLC) sprayed with DPPH was used to screen for free radical scavenging activity. The chromatograms were prepared and developed identically to phytochemical fingerprinting (Section 3.2.3.1). DPPH solution (0.2% w/v) was prepared by dissolving 0.2 g of the DPPH (Sigma) in 100 mL of methanol. This solution was sprayed onto the air-dried chromatograms. The presence of antioxidant activity was indicated by the development of yellow bands against a purple background (Deby and Margotteaux, 1970). The DPPH free radical scavenging assay measures the decolouration of purple/violet DPPH solution to a yellow colour in the presence of an antioxidant agent. The degree of colour change is proportional to the concentration and potency of the antioxidants, i.e., a great reduction in the absorbance of the reaction mixture indicates significant free radical scavenging activity (Krishnaiah *et al*., 2011).

4.2.2. Free radical scavenging activity assay

Free radical scavenging activity of the plant extracts was quantified using 2,2-Diphenyl-1-picrylhydrazyl (DPPH) method reported by Chigayo *et al*. (2016) with modifications. Briefly, different concentrations of the extracts (250-15.63 µg/mL) were prepared to a volume of 1 mL of the solution. L-ascorbic acid was used as a standard by preparing the same concentration range as the extracts. To this 1 mL solution, 2 mL of 0.2 mmol/L DPPH solution (dissolved in methanol) was added and vortexed thoroughly. All the prepared mixtures were left to stand in the dark for 30 minutes. The control solution was prepared by adding 2 mL of 0.2 mmol/L DPPH to 1mL of distilled water. After the elapsed time, the solutions were analysed with a UV/VIS spectrophotometer. The experiment was conducted in triplicates and independently repeated three times. The absorbance of the solutions was read at 517 nm and the percentage antioxidant potential was calculated using the formula:

$$\%Inhibition = \frac{Ac-As}{Ac} \text{ x } 100$$

Where Ac is absorbance of the control solution, As is the absorbance of the extracts.

4.2.3 Ferric reducing power

The ferric reducing power of the plant extracts was determined using the methods of Ahmed *et al*. (2012) and Vijayalakshmi and Ruckmani (2016). The ferric reducing power of plant extracts may serve as an indicator of antioxidant activity of bioactive phytochemicals. This reducing power of the extracts is attributed to their ability to donate electrons to ferric ion (Fe^{3+}) to a ferrous (Fe^{2+}). Five different concentrations of the samples (625-39 µg/mL) were prepared by serially diluting a stock solution of 1 250 µg/mL. The different concentrations (2.5 mL) were mixed with 2.5 mL of sodium phosphate buffer (0.2 M, pH 6.6) and 2.5 mL of (1% w/v in distilled water) potassium ferricyanide (Rochelle) in test tubes, respectively. The mixtures were vortexed after the addition of solutions. The mixtures were incubated at 50 ºC for 20 minutes. Two millilitres of trichloroacetic acid (Sigma) (10% w/v in distilled water) were added to the test tubes after incubation. The mixtures were centrifuged at 3000 rpm for 10 minutes and 5 mL of the resulting supernatant was transferred to a clean test tube. To this solution, 5 mL of distilled water and 1 mL ferric chloride (0, 1% w/v in distilled water) were added consecutively with thorough vortexing after each addition. A UV/VIS spectrophotometer was used to read the absorbance of solutions at 700 nm wavelength. The blank for this procedure was prepared in the same manner, however, the extracts were replaced by an equal amount of distilled water. L-Ascorbic acid (Sigma) (625-39 µg/mL) was used as a positive control and was prepared similar to the extracts. The experiment was conducted in triplicates and independently repeated three times.

4.2.4 Bovine serum albumin (BSA) denaturation inhibition assay

The anti-inflammatory activities of the methanol crude plant extracts were determined using a BSA assay reported by Bailey-Shaw *et al*. (2017) and Anyasor *et al*. (2019). Bovine serum albumin (BSA) solution (0.5%, w/v) was prepared in 0.05 M Tris

Buffered Saline. Tris Buffered Saline was prepared by preparing 0.05 M Tris and 0.15 M sodium chloride (NaCl), pH 7.6 at room temperature. The pH was adjusted to 6.4 with hydrochloric acid (HCl). Stock solutions of each plant extract were reconstituted in their appropriate solvent at a concentration of 10 mg/mL. Various concentrations of test solutions (2, 1, 0.5, 2.5 mg/mL) of extracts were taken respectively in a volume of 50 µL and mixed with 950µL (0.5% w/v BSA). Product (negative) control solution (1000 µL) consisted of 950µL of 0.05 M Tris Buffered Saline and 50 µL of each extract solution in order to consider the colouration of the extracts. BSA solution (0.5%) 950µL with 50 µL of Tris buffered saline was used as the test solution control. The test solution control represented 100% protein denaturation. The results were compared with diclofenac sodium. The solutions were then heated in a heat block at 72 °C for 5 minutes, and cooled for 20 minutes under laboratory conditions. The turbidity of the solutions (level of protein precipitation) was measured at 660 nm in a UV/Vis Spectrophotometer. Tris buffered saline (0.05 M) was used as a blank. The experiments were conducted in a duplicate and the mean absorbance values were recorded. The percentage inhibition of precipitation (protein denaturation) was determined on a percentage basis.

%Inhibition of Protein Denaturation = $\frac{Absorbance\ of\ control - Absorbance\ of\ test\ sample*}{Ansorbance\ of\ control} \times 100$

*Absorbance of test sample = absorbance of test solution – absorbance of negative control.

4.2.5 Egg albumin denaturation inhibition assay

The reaction mixture (5 mL) consisted of 0.2 mL of egg albumin (from a fresh hen's egg), 2.8 mL of 0.05 M Tris buffered saline (PBS, pH 6.4) and 2 mL of varying concentrations (2, 1, 0.5, 0.25 mg/mL) of the plant extracts and standard drug (diclofenac sodium) (1, 0.5, 0.25 mg/mL). Product (negative) control solution (5 mL) consisted of 3 mL of 0.05 M Tris Buffered Saline and 2 mL of each extract solution in order to consider the colour of the extracts when using the UV/Vis spectrophotometer. The egg albumin solution (0.2 mL and 4.8 mL Tris buffered saline) was used as the test solution (positive) control. The positive control represented 100% protein denaturation. The mixtures were incubated at 37 ± 2°C in a biochemical oxygen demand (BOD) incubator for 15 minutes and then heated at 70°C for 5 minutes. After heating, the solutions were allowed to cool to room temperature for 30 minutes. After cooling, their absorbance was measured at 660 nm by using the Tris buffered saline as a blank (Uttra and Alamgeer, 2017; Rahman *et al*., 2015). The percentage inhibition of protein denaturation was calculated by using the following formula:

$$\% \text{ Anti-Denaturation activity} = \frac{Absorbance\ of\ control - Absorbance\ of\ test\ sample*}{Ansorbance\ of\ control} \times 100$$

*Absorbance of test sample = absorbance of test solution – absorbance of negative control.

4.2.6 Statistical Analysis

Where appropriate, results were expressed as means ± standard deviation (SD) of triplicate determinations. Statistical analysis was performed by Graphpad prism v8.9 by a two-way analysis of variance (ANOVA) followed by Tukey multiple or Duncan's comparison post hoc test as required. Significant difference was considered when $p<0.05$ and conversely, non-significance was indicated by $p>0.05$ values.

4.3 Results

4.3.1 Free radical (DPPH) scavenging potential screening

DPPH was used as a free radical to detect the scavenging activity of the plant extracts to stabilise reactive chemical species with the result of potentially reducing the effects of oxidative stress.

4.3.1.1 Qualitative free radical (DPPH) scavenging activity

Thin layer chromatography coupled with DPPH was used to screen and localise antioxidant compounds in the plant extracts. Yellow zones on the chromatograms against a purple background indicated antioxidant compounds (Figure 4.1 and 4.2). All the plant extracts, except *Croton gratissimus*, had one or more bioactive compounds. All bioactive compounds migrated in the polar chromatogram (EMW), indicating that the antioxidant compounds were polar in nature.

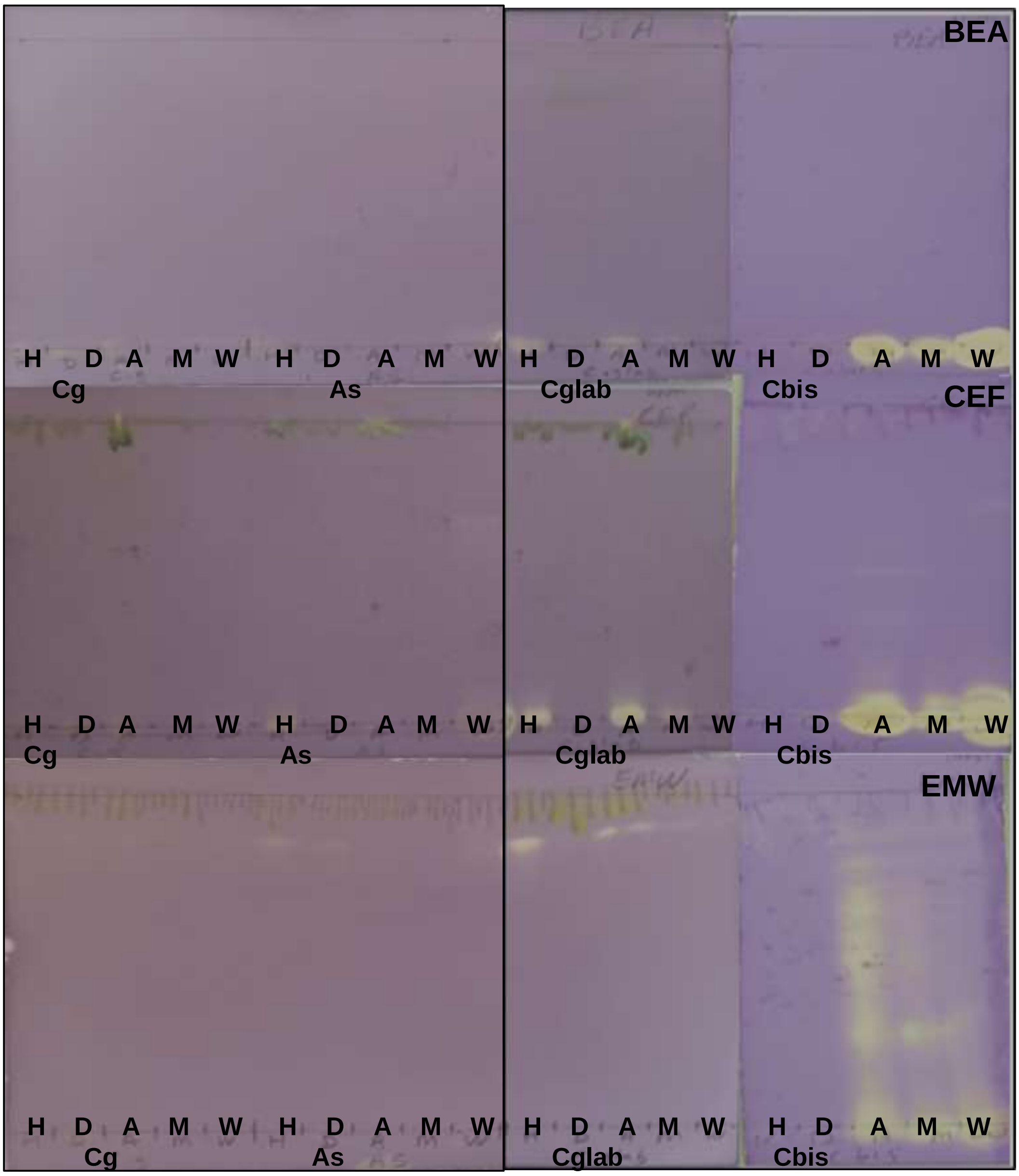

Figure 4. 1: Antioxidant screening of plant extracts using DPPH as a free radical. Chromatograms were developed in the mobile systems (BEA, CEF and EMW) that varied in polarity.

Key: H: hexane; D: dichloromethane; A: acetone; M: methanol; W: water; C.g: *Croton gratissimus*; AS: *Acacia Senegal*; C.glab: *Clerodendrum glabrum*; Cbis: *Carissa bispinosa*; BEA: benzene/ethanol/ammonium hydroxide; CEF: chloroform/ethyl acetate/formic acid; EMW: ethyl acetate/methanol/water.

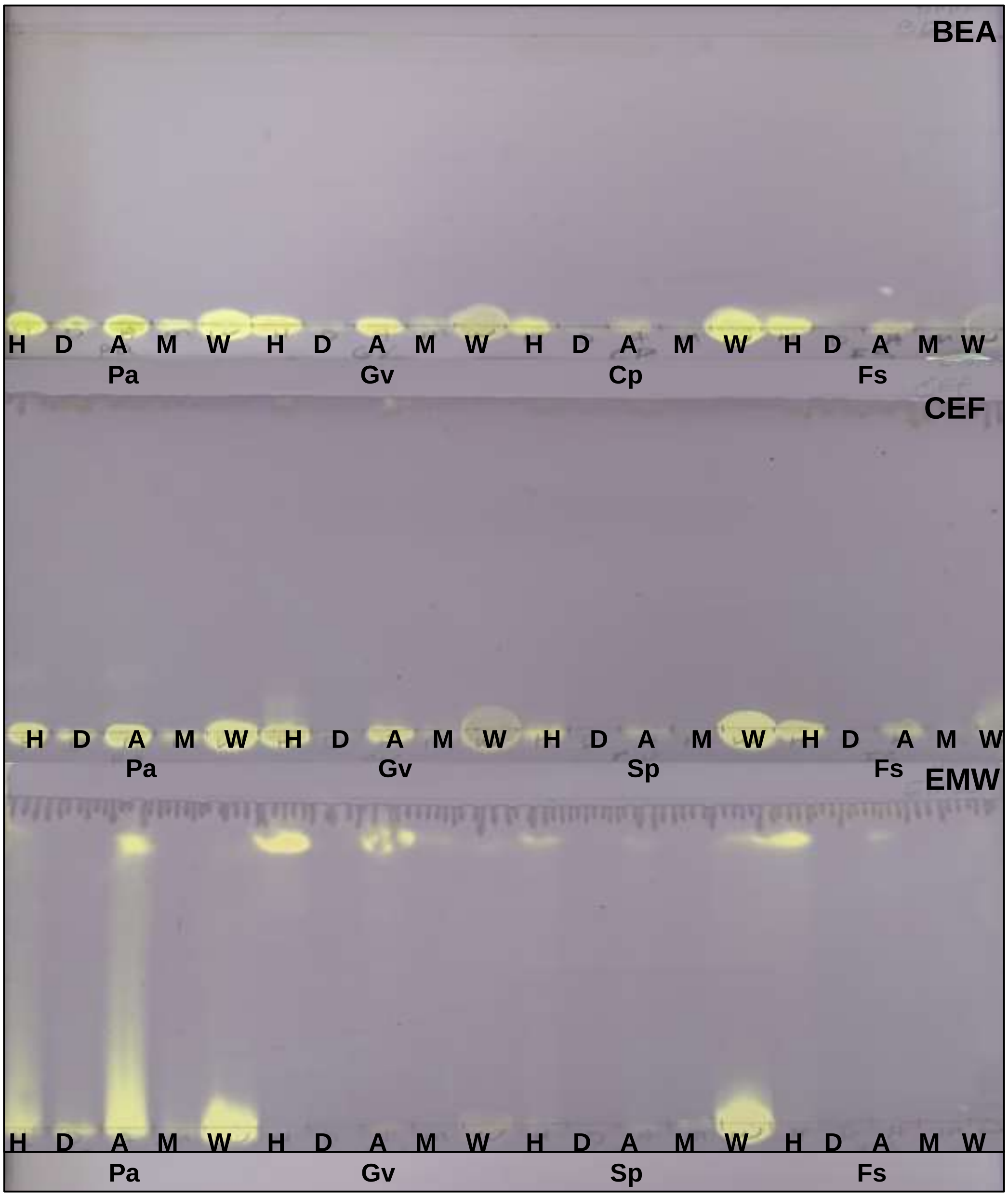

Figure 4. 2: Antioxidant screening of bioactive compounds from plant extracts using thin layer chromatography and DPPH free radical.

Key: H: hexane; D: dichloromethane; A: acetone; M: methanol; W: water; Pa: *Peltophorum africanum*; Gv: *Gardenia volkensii*, Sp: *Senna petersiana*; Fs: *Ficus sur*; BEA: benzene/ethanol/ammonium hydroxide; CEF: chloroform/ethyl acetate/formic acid; EMW: ethyl acetate/methanol/water.

4.3.1.2 Quantitative free radical (DPPH) scavenging activity

Quantification of free radical scavenging activity showed that intermediate and polar solvents had the best ability to extract antioxidant compounds. *P. africanum* methanol extract had the best activity (EC_{50}: 56.63 ± 0.77 μg/mL) and the lowest activity was observed from *C. gratissimus* (1994.9 ± 0.71 μg/mL) (Table 4.1). The percentage of DPPH inhibition was observed in all the plant extracts in a concentration dependent manner up to the highest tested concentration.

Table 4. 1: Free radical (DPPH) scavenging activity of extracts represented as Ec50 (µg/mL) determinations.

Plant extract	**Hexane**	**Dichloromethane**	**Acetone**	**Methanol**	**Water**
C. gratissimus	850.18 ± 0.70^{dd}	197.77 ± 0.03^{g}	545.14 ± 0.53^{t}	688.70 ± 0.12^{bb}	1994,9 ± 0.71^{ii}
A. senegal	353.80 ± 0.07^{m}	864.30 ± 0.42^{ee}	646.42 ± 0.35^{z}	932.40 ± 0.32^{gg}	272.56 ± 0.21^{i}
C. bispinosa	160.65 ± 0.21^{d}	514.57 ± 0.28^{q}	312.83 ± 0.16^{j}	452.06 ± 0.42^{p}	205.78 ± 0.46^{h}
C. glabrum	170.88 ± 0.19^{f}	353.53 ± 0.21^{m}	137.58 ± 0.54^{c}	326.55 ± 0.34^{l}	536.46 ± 0.23^{s}
P. africanum	440.77 ± 0.08^{o}	322,76 ± 0.62^{k}	100.07 ± 0.16^{b}	56.63 ± 0.77^{a}	167.40 ± 0.37^{e}
G. volkensii	559.95 ± 0.37^{u}	568.32 ± 0.99^{v}	442.8 ± 0.46^{o}	376.66 ± 0.81^{n}	543.85 ± 0.78^{t}
S. petersiana	718.85 ± 0.59^{cc}	889.76 ± 0.77^{ff}	636.56 ± 0.77^{y}	670.12 ± 0.5^{aa}	271.77 ± 0.76^{i}
F. sur	579.53 ± 1.03^{w}	1438.4 ± 0.06^{hh}	588.9 ± 0.34^{x}	525.68 ± 0.20^{r}	311.28 ± 0.39^{j}
Ascorbic acid					

Key: EC_{50} concentration that leads to 50% reduction in DPPH activity (the lower the value the higher the activity). Same alphabets denote non-significance where $p>0.05$ and different alphabets denote significant difference where $p<0.05$.

4.3.2 Ferric reducing power of the plant extracts

For ferric reducing power, the initial yellow colour of the test solution changes to various shades of green and blue depending on the reducing power (conversion of Fe^{3+} to Fe^{2+}) of each extract. Table 4.1 shows the EC_{50} of the extracts. The non-polar solvents (hexane and dichloromethane) did not extract ferric reducing compounds from *F. sur*. The best activity was observed from *C. gratissimus* water extract (13.22 ± 0.57 µg/mL) followed by *C. glabrum* acetone extract (68.62 ± 0.23 µg/mL).

Table 4. 2: Ferric reducing power (EC_{50} µg/mL) of different plant extracts.

Plant extract	Hexane	Dichloromethane	Acetone	Methanol	Water
C. gratissimus	61.13 ± 0.09^{b}	193 ± 0.07^{h}	307.13 ± 0.66^{m}	83.08 ± 1.12^{c}	13.22 ± 0.57^{a}
A. senegal	193.05 ± 0.1^{h}	188.64 ± 0.21^{h}	158.33 ± 0.19^{f}	726.83 ± 0.12^{s}	493.28 ± 1.72^{q}
C. glabrum	229.71 ± 0.61^{k}	1106 ± 2.86^{t}	68.62 ± 0.23^{b}	207.95 ± 0.25^{i}	1455.17 ± 3.41^{w}
C. bispinosa	237.8 ± 0.1^{k}	411.03 ± 0.15^{o}	308.82 ± 0.13^{m}	3688.67 ± 3.31^{y}	139.92 ± 0.11^{e}
P. africanum	255.63 ± 0.07^{l}	149.76 ± 0.06^{f}	124.49 ± 0.12^{d}	206.32 ± 0.34^{i}	133.99 ± 0.31^{e}
G. volkensii	219.3 ± 0.22^{j}	213.59 ± 0.35$^{i, j}$	442.0 ± 3.55^{p}	374.83 ± 1.51^{n}	1135 ± 0.82^{u}
S. petersiana	1223.58 ± 1.03^{v}	1231.25 ± 0.35^{v}	1127.08 ± 1.03^{u}	1558.33 ± 0.27^{x}	178.23 ± 0.107^{g}
F. sur	-	-	6942.86 ± 2.33^{aa}	4915.33 ± 3.09^{z}	683.93 ±1.15^{r}
Ascorbic acid	-	-	-	-	12.14 ± 1.23^{a}

Key: (-): Not determined; Same alphabet denote non-significant difference where $p>0.05$ and different alphabets denote significant difference where $p<0.05$.

4.3.3 Anti-inflammatory activity of the plant extracts

Anti-inflammatory activity of the extracts was determined using bovine serum albumin and egg albumin denaturation assays.

4.3.3.1 Bovine serum albumin (BSA) denaturation inhibition

In this study, the plant extracts and the used standard, diclofenac sodium, demonstrated the concentration dependent inhibition of BSA denaturation (Figures 4.3-4.5). It was generally observed that the hexane extracts (non-polar compounds) from the various plant species exhibited higher BSA denaturation inhibition, followed by methanol (Figure 4.4) and water extracts (Figure 4.3), respectively. Only *C. glabrum* and *G. volkensii* hexane extracts demonstrated BSA denaturation inhibition comparable to diclofenac sodium (Figure 4.5).

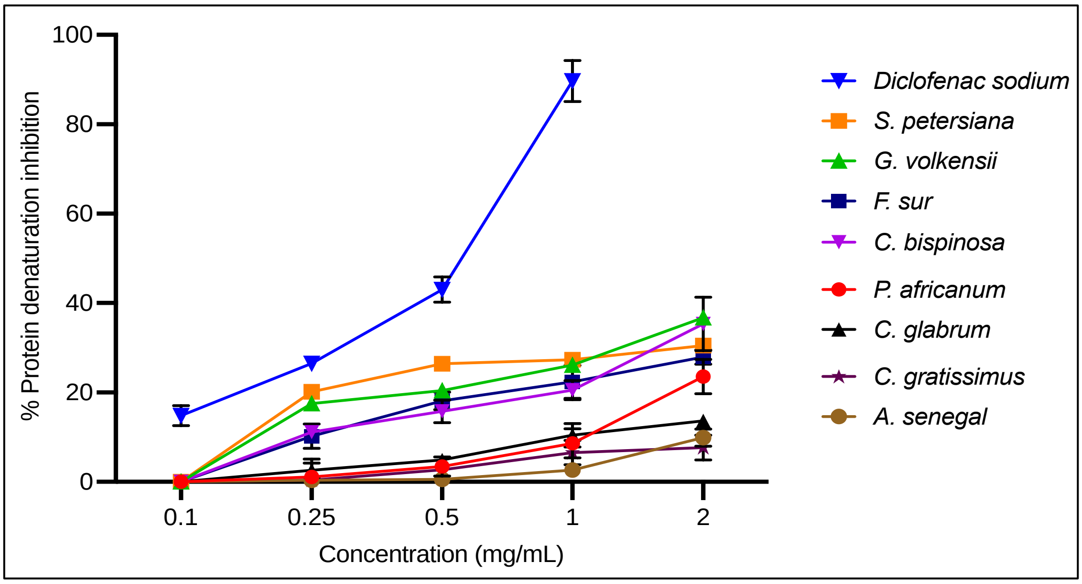

Figure 4. 3: Inhibition of bovine serum albumin denaturation by water extracts of various plant leaves.

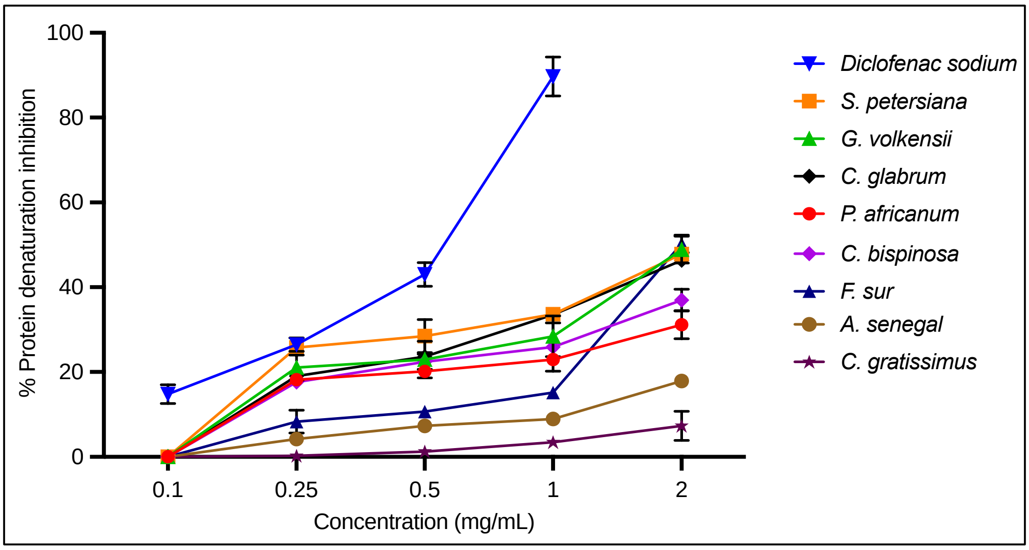

Figure 4. 4: Anti-inflammation by inhibition of bovine serum albumin denaturation using different methanol leaves extracts.

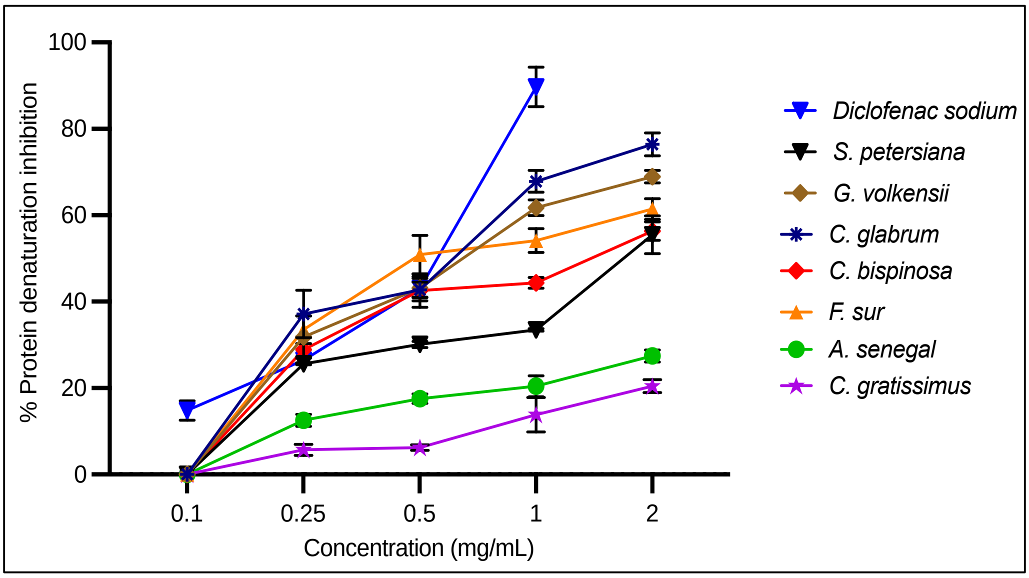

Figure 4. 5: Inhibition of bovine serum albumin denaturation by hexane plant extracts.

4.3.3.2 Egg albumin denaturation inhibition

Inhibition of egg albumin denaturation from a fresh hen's egg was used to determine the anti-inflammatory activity of the extracts. Figures 4.6 and 4.7 represent the anti-inflammatory activity of the plant extracts (2 mg/mL) compared to the standard drug (1 mg/mL). *S. petersiana* water extract showed better inhibition (62.13%) among the extracts (Figure 4.6). *A. senegal* methanol inhibition (50.57%) was the highest among methanol extracts (Figure 4.7). Diclofenac sodium demonstrated higher inhibition than both the water and methanol extracts.

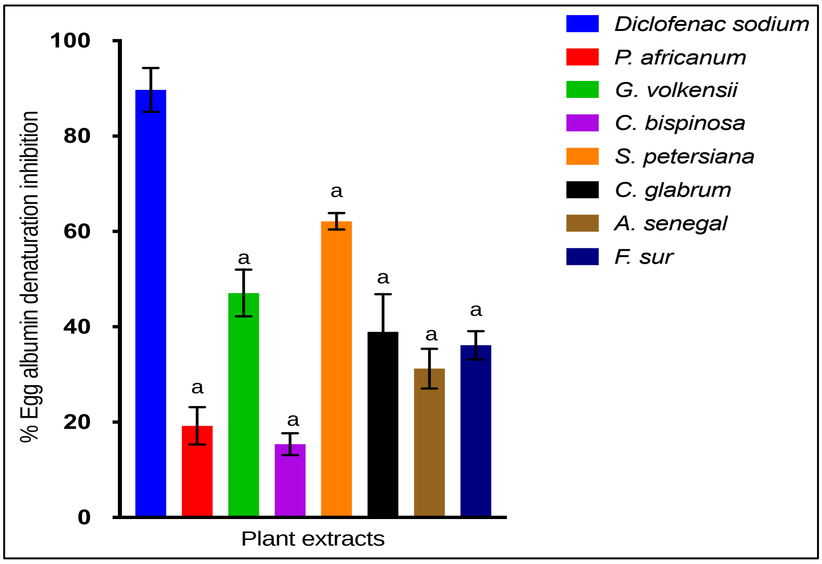

Figure 4. 6: Inhibition of egg albumin denaturation by water plant extracts was compared to the used standard (diclofenac sodium).

Key: a: Significant difference compared to diclofenac sodium.where p<0.0001.

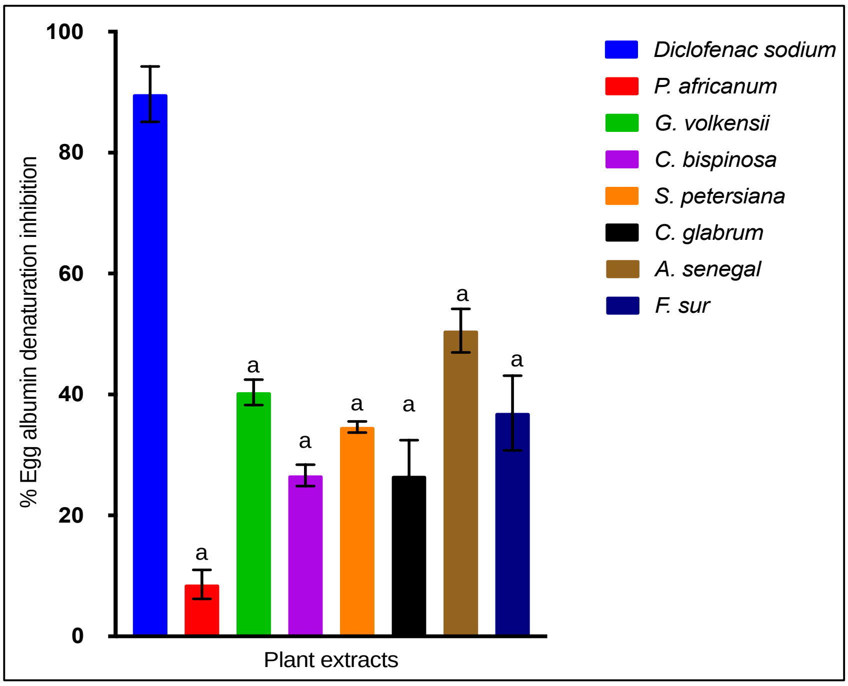

Figure 4.7: Anti-inflammatory activities of methanol plant extracts by egg albumin denaturation inhibition. Activity was compared diclofenac sodium.

Key: a: Significant difference compared to diclofenac sodium, where p<0.0001.

4.3.4 Correlation between phyto-constituent content and bioactivity of the plant extracts

The correlation between the determined bioactivity and the different groups of phyto-constituents quantified from the extracts was evaluated. Polyphenols (tannins, flavonoids and proanthocyanidins) were responsible for antioxidant activity and BSA denaturation inhibition for some plant species such as *C. gratissimus*, *C. bispinosa*, *A. senegal*, and *G. volkensii* due to significant correlation ($p<0.05$). Free radical scavenging activity significantly correlated with ferric reducing power for *S. petersiana* where, $p<0.05$ (Table 4.3).

Table 4. 3: Pearson's correlation coefficient (r) and p (two-tailed) for total phyto-constituent content versus EC50 values of antioxidant and anti-inflammatory activity of various plant extracts.

Plant species	**EC_{50} (µg/mL)**	**Phenolics**		**Tannins**		**Flavonols**		**Flavonoids**		**proanthocyanidins**		**Alkaloids**		**DPPH (EC_{50})**		**FRP (EC_{50})**	
		r	*p*	*r*	*p*	*R*	*p*	*r*	*p*	*r*	*p*	*r*	*p*	*r*	*p*	*r*	*p*
Cg	DPPH	0.812	0.095	-0.515	0.374	-0.722	0.167	-0.772	0.125	-0.925	**0.024***	-0.331	0.585	1	-	-0.687	0.19
	FRP	-0.438	0.460	0.716	0.174	0.846	0.073	0.645	0.239	-0.887	**0.044***	0.223	0.718	-0.687	0.199	1	-
	BSA	0.392	0.513	-0.968	**0.006*****	-0,861	0.065	-0,641	0.235	-0,857	0.063	0,151	0.807	0.675	0.211	-0.825	0.08
As	DPPH	-0.715	**0.04.**	-0.464	0.430	-0.018	0.976	0.069	0.911	-0.042	0.946	0.552	0.333	1	-	0.221	0.72
	FRP	0.206	0.739	-0.661	0.223	-0.775	0.123	-0.588	0.296	-0.365	0.551	0.812	0.094	0.220	0.721	1	-
	BSA	0.627	0.257	-0.143	0.817	-0.679	0.206	-0.512	0.377	-0.246	0.689	0.389	0.517	-0.467	0.426	0.736	0.15
C. glab	DPPH	0.597	0.286	0.646	0.238	0.116	0.851	0.426	0.474	0.074	0.905	0.285	0.519	1	-	-0.793	0.10

	FRP	-0.815	0.092	-0,629	0.255	-0,345	0.568	-0.539	0.348	-0,324	0.593	0.122	0.871	-0.793	0.109	1	-
	BSA	-0.228	0.711	-0.809	0.096	-0.877	0.053	-0.883	**0.044**	-0.836	0.077	-0.066	0.577	-0.290	0.635	0.644	0.24
Pa	DPPH	-0.799	0.104	-0.523	0.365	0.116	0.551	-0.715	0.178	0.011	0.986	0.285	0.642	1		-0.793	
	FRP	0.060	0.923	-0.616	0.267	-0.345	0.689	-0.783	0.116	-0.395	0.509	0.122	0.844	0.512	0.377	1	
	BSA	0.598	0.286	0.140	0.821	-0.877	0.905	0.445	0.452	-0.779	0.120	-0.066	0.916	-0.627	0.257	0.061	0.92
Gv	DPPH	-0.178	0.773	-0.320	0.598	0.183	0.767	-0.121	0.845	0.245	0,690	0.579	0.305	1		0.504	
	FRP	0.749	0.144	0.645	0.239	-0.941	**0.016***	0.719	0.174	-0.936	**0.018***	0.272	0.657	0.504	0.386	1	-
	BSA	0.816	0.091	0.791	0.111	0.821	0.088	0.732	0.159	0.676	0.215	-0.255	0.678	-0.171	0.782	0.658	0.22
Sp	DPPH	0.303	0.619	-0.720	0.169	0.253	0.680	-0.024	0.968	0.312	0.608	0.201	0.745	1	-	0.837	
	FRP	0.316	0.603	-0.798	0.105	0.182	0.768	-0.123	0.842	0.444	0.453	0.171	0.782	0.837	0.076	1	
	BSA	-0.227	0.717	0.775	0.122	-0.519	0.370	-0.104	0.867	-0.117	0.850	-0.183	0.767	-0.917	**0.028***	-0.904	**0.03**
Fs	DPPH	0.294	0.630	-0.482	0.411	-0.193	0.751	0.590	0.294	0.516	0.372	0.962	**0.008****	1	-	-0.285	0.64
	FRP	-0.164	0.792	0.044	0.943	0.159	0.797	0.005	0.993	-0.023	0.969	-0.372	0.536	-0.285	0.641	1	
	BSA	-0.220	0.722	0.676	0.209	-0.306	0.611	0,021	0.972	-0.897	**0.038***	-0.515	0.373	-0.672	0.214	0.337	0.57
Cbis	DPPH	-0.672	0.214	-0.821	0.087	-0.031	0.960	-0.277	0.652	-0.106	0.864	0.336	0.579	1		0.525	
	FRP	0.101	0.870	-0.881	**0.043***	-0.451	0.445	-0.287	0.638	-0.113	0.855	0.387	0.519	0.525	0.362	1	
	BSA	0.885	**0.044***	-0.096	0.877	-0.887	**0.044***	-0.332	0.584	-0.619	0.265	-0.394	0.510	-0.260	0.671	0.504	0.38

Key: C.g: *Croton gratissimus*; AS: *Acacia senegal*; C.glab: *Clerodendrum glabrum*; Cbis: *Carissa bispinosa*, Pa: *Peltophorum africanum*; Gv: *Gardenia volkensii*, Sp: *Senna petersiana*; Fs: *Ficus sur*; FRP: ferric reducing power assay; BSA: Bovine serum albumin inhibition assay; DPPH: Free radical (DPPH) assay. Non-significance is where $p>0.05$ and significant is where $p<0.05$.

4.4 Discussion

Supplementation of external antioxidants or boosting endogenous antioxidant defences of the body are known to be a promising method to improve oxidative stress linked to the pathophysiology of diseases (Kasote *et al*., 2015).

Recent studies aimed at determining the usefulness of medicinal plants as the host's immune system boosters against *M. tuberculosis* have emerged and demonstrate that those substances that can restore the balance between inflammatory and anti-inflammatory processes contribute to the overall antimycobacterial action. Even plants inactive or weakly active *in vitro* against bacilli can provoke bacteria clearance by mainly acting synergistically when combined with established anti-TB drugs. The introduction of phytochemicals as immunomodulatory agents administered as adjuvants in TB chemotherapy could thus contribute to the efficacy of antimycobacterial activity *in vivo* (Sieniawska *et al*., 2020).

4.4.1 Qualitative antioxidant screening

The DPPH free radical scavenging activity coupled with thin layer chromatography (TLC) was used to screen for antioxidant compounds in the plant extracts. Antioxidant compounds from the various plant extracts were appropriately eluted and separated by the polar mobile phase (EMW), suggesting that the observed antioxidant compounds are polar in nature (Figure 4.1).

Polyphenolic compounds are polar compounds that have chiefly been reported to be fundamental in the antioxidant activity of plant species because of their ability to readily donate hydrogen and/or electrons (Chaves *et al*., 2020; Nićiforović *et al*., 2010). González-Burgos and Gómez-Serranillos (2012) reported the antioxidant activity of terpenes. This could explain the presence of antioxidant compounds in the non-polar BEA chromatograms, as seen in *Peltophorum africanum*, *Clerodendrum glabrum*, *Gardenia volkensii*, *Ficus sur* and *Acacia Senegal* extracts. The acetone extract of *Carissa bispinosa* demonstrated multiple active antioxidant compounds on the EMW chromatogram (Figure 4.1).

4.4.2 Quantitative antioxidant activity

Two spectrometry-based methods were used to quantify the observed antioxidant activity of bioactive extracts, namely, the free radical scavenging and ferric reducing power assay.

4.4.2.1 Free radical (DPPH) scavenging activity

Ascorbic acid was chosen as the reference antioxidant for this test. Free radical scavenging activity was represented as the concentration of the extract required to scavenge/reduce 50% of DPPH in solution (EC_{50}) (Table 4.1) and percentage DPPH inhibition at the highest tested concentration (250 µg/mL) (Figure 4.2).

The methanol and acetone extracts of *Peltophorum africanum* significantly ($p<0.05$) demonstrated the best free radical scavenging activity of all the extracts with EC_{50} values of 56.63 ± 0.77 and 100.07 ± 0.16 µg/mL, respectively (Table 4.1). At 250 µg/mL, percentage free radical scavenging activity of *P. africanum* acetone extract was the best among the extracts and had non-significant difference ($p>0.05$) with ascorbic acid (Figure 4.2). In a different study, Adebayo *et al*. (2015) reported that 70% acetone leaf extract of *P. africanum* had the best free radical (DPPH and ABTS) scavenging activity, with 4.67 ± 0.31 and 7.71 ± 0.36 µg/mL IC_{50} concentrations respectively, out of 25 plant species evaluated.

Acetone extract of *C. glabrum* (137.58 ± 0.54 µg/mL) and hexane extract of *C. bispinosa* (160.65 ± 0.21 µg/mL) respectively followed *P. africanum* activity. These results are consistent with those reported by Adamu *et al*. (2014). The lowest free radical scavenging activity was observed from the water extract of *C. gratissimus* (1994.9 ± 0.71 µg/mL) and *Ficus sur*'s dichloromethane extract (1438.4 ± 0.06 µg/mL). Similarly, Njoya *et al*. (2018) also reported weak free radical (DPPH) scavenging activity from the *C. gratissimus* water extract and the higher antioxidant activity from its ethanol extract with an EC_{50} of 32.18 ± 2.11 µg/mL). In a study conducted to determine the DPPH scavenging activity of *C. bispinosa* fruits, Gwatidzo *et al*. (2018) reported that at 200 µg/mL, the flavonoids from the fruit achieved above 80% DPPH inhibitory activity. In this study, the best activity of *C. bispinosa* was recorded to be 69.62% at 250 µg/mL (Figure 4.1), demonstrating that its fruits have a greater antioxidant activity than the leaves.

4.4.2.2 Ferric reducing power

Ferric reducing power was expressed as EC_{50} values in Table 4.1. Interestingly, the *C. gratissimus* water extract demonstrated the greatest ferric reducing power (13.22 ± 0.57 µg/mL), followed by the *C. glabrum* acetone extract (68.62 ± 0.23 µg/mL) and the *C. gratissimus* methanol extract (83.08 ± 1.12 µg/mL). The *C. gratissimus* activity was consistent with the findings reported by Ndhlala *et al*. (2013), where the highest FRP was observed from polar solvent extracts (70% methanol, butanol). Except for *C. gratissimus* and *C. bispinosa*, moderate to good free radical scavenging activity was observed in the polar extracts, particularly water and methanol.

Garry *et al*. (2013) recommended that based on high correlation between DPPH and FRAP methods, the use of both methods or more than one method in parallel to quantify antioxidant activity is redundant. Taking these prior findings by Garry *et al*. (2013), one might be led to prematurely conclude that any of the methods used in this study could be used to quantify and rank the antioxidant activity of the different plant species without significant differences between them. The results of this study show that this assertion may not be correct/universal. Similar findings to this study were reported by Chaves *et al*. (2020) and González-Burgos and Gómez-Serranillos (2012), where it was generally observed that selecting plant species with high antioxidant activity requires knowing the method to be applied. Thus, antioxidant compounds can respond in a different manner to different radical or oxidant compounds.

4.4.3 Anti-inflammatory assay

There are indeed commercially available non-steroidal anti-inflammatory drugs (NSAIDs) that are efficacious against inflammation. However, the adverse effects such as gastric ulcers, gastric pain, cardiovascular, hepatic and renal dysfunctions that are brought about by the NSAIDs prompt alternatives to be explored (Heendeniya *et al*., 2018).

Anti-protein denaturation effects of the extracts in heat treated bovine serum albumin were used as an assay to evaluate anti-inflammatory activity (Al-Shidhani *et al*., 2015, Williams *et al*., 2008). The rationale behind implementing this assay is that the denaturation of albumin protein leads to the formation of antigens which initiate type III hypersensitive reaction leading to inflammation (Agrawal and Paridhavi, 2007). Furthermore, albumin protein denaturation is widely used, validated, sensitive, quick and a reliable *in vitro* technique to investigate anti-inflammatory activity of natural products (Chandra *et al*., 2012).

Figures 4.3-4.5 represent the bovine serum albumin (BSA) denaturation inhibition of the extracts. As expected, the reference NSAID drug used, diclofenac sodium, demonstrated a concentration-dependent *in vitro* anti-inflammatory activity. The plant extracts also demonstrated a concentration-dependent inhibition. Diclofenac sodium showed a better anti-inflammatory activity than the plant extracts.

The hexane extracts (Figure 4.5), which consist of predominantly non-polar phytochemicals, had a higher BSA denaturation inhibitory activity compared to their polar counterparts, (methanol and water extracts) (Figures 4.3 and 4.4). At 0.25 and 0.5 mg/mL concentrations, hexane extracts from *F. sur*, *C. bispinosa*, *C. glabrum*, *G. volkensii* demonstrated comparable anti-inflammatory activity to diclofenac sodium (Figure 4.5). Previously, Madikizela *et al*. (2014) reported 73.9% cyclooxygenase-2 (COX-2) inhibition by *F. sur* dichloromethane bark extract.

Only polar solvents (methanol and water) extracts demonstrated egg albumin denaturation inhibition (Figures 4.6 and 4.7). The exact mechanism through which the extract mediated its anti-denaturation effect in the heat induced protein denaturation test is unknown at present. But, it may be due to the interaction of phytochemicals with aliphatic region around the lysine residue on the albumin protein (Williams *et al*., 2008). One dimensional and two-dimensional protein nuclear magnetic resonance (1D and 2D ‘H NHR) studies have shown that agents which have albumin anti-denaturation action bind and/or interact at these two sites (Williams *et al*., 2008).

On the other hand, a weak to moderate BSA and egg albumin denaturation inhibition was recorded for *P. africanum*. Adebayo *et al*. (2015) reported that the *P. africanum* 70% acetone extract demonstrated a higher inhibitory activity of lipoxygenase activity (IC_{50} = 12.42 μg/mL) compared with quercetin controls (IC_{50} = 8.75 μg/mL). This highlights that the phytochemicals from *P. africanum* deploy different mechanisms of action to reduce inflammation. This observation may extend to other plant extracts because in this study, weak activity was observed for *C. gratissimus* extracts. Njoya *et al*. (2018) reported better anti-inflammatory activity from the ethanol extract of *C. gratissimus* compared to quercetin (p<0.05) through lipoxygenase activity inhibition.

4.4.4 Correlation matrices between phyto-constituents and bioactivity

Table 4. shows the correlation between quantified phyto-constituents present in the extracts, antioxidant and anti-inflammatory activities through the assessment of EC_{50} values from free radical (DPPH) scavenging assay, ferric reducing power and BSA protein denaturation assay. The coefficient of Pearson's correlation was significantly negative, if $-0.61 \leq r \geq -0.97$, and significantly positive, if $0.61 \leq r \geq 0.97$ (Thaipong *et al*., 2006). From Table 4.4, negative Pearson's correlation coefficients represent instances where, when one variable increases, the value of the other variable decreases (inverse proportion). Given that lower EC_{50} values demonstrate higher activity (antioxidant and anti-inflammatory), negative Pearson's correlation coefficients indicated that as the phyto-constituent content increase, EC_{50} values decrease (Trieu *et al*., 2021).

For *Acacia senegal*, no significant correlation between DPPH and FRP was observed. However, the total phenolic content significantly correlated with DPPH scavenging activity ($r=-0.715$, $p=0.04$) indicating that the polyphenolic compounds were largely responsible for the free radical scavenging activity of this plant. This was consistent with the findings reported by Mirghani *et al*. (2018). Proanthocyanidin content was responsible for FRP for *G. volkensii* ($r=-0.936$, $p=0.018$), DPPH scavenging activity ($r=-0.925$, $p=0.024$) of *C. gratissimus* while they consequently reduced the FRP for *C. gratissimus* ($r=0.887$, $p=0.044$). This observation further demonstrated the different mechanisms the phytochemicals use. Flavonoids were responsible for the BSA denaturation inhibition of *C. glabrum* ($r=-0.883$, $p=0.044$). Anti-inflammatory properties have been linked to the presence of bioactive antioxidants such as polyphenols (Trieu *et al*., 2021). Both DPPH scavenging activity ($r=-0.917$, $p=0.028$) and FRP were responsible for the BSA activity of *S. petersiana* ($r=-0.904$, $p=0.035$). Indeed, antioxidant activity has also previously been associated with anti-inflammatory activity (Marrassini *et al*., 2018).

4.5 Conclusion

The plant extracts demonstrated moderate to good antioxidant and anti-inflammatory activity. Since a variety of bioactive phyto-constituents were found in the crude extracts, it becomes difficult to attribute both antioxidant and anti-inflammatory properties to one specific compound without further studies. However, correlation studies narrowed the bioactivity determined to specific groups of the phyto-constituents, which include but not limited to, proanthocyanidins, flavonoids, tannins and alkaloids. The administration of medicinal plants as adjunct therapy in TB treatment may be beneficial in preventing and diminishing hepatotoxicity caused by anti-TB drugs. Furthermore, the anti-inflammatory activities of the plant extracts may have the potential to reduce the inflammation induced by *M. tuberculosis* during infection.

4.6 References

Adamu, M., Naidoo, V. and Eloff, J.N. 2014. The antibacterial activity, antioxidant activity and selectivity index of leaf extracts of thirteen South African tree species used in ethnoveterinary medicine to treat helminth infections. *BMC Veterinary Research*, **10(52)**: Doi:10.1186/1746-6148-10-52.

Adebayo, S.A., Dzoyem, J.P., Shai, L.J. *et al*. 2015. The anti-inflammatory and antioxidant activity of 25 plant species used traditionally to treat pain in southern African. *BMC Complementary Medicine and Therapies*, **15 (159)**: Doi: 10.1186/s12906-015-0669-5.

Agrawal, S.S. and Paridhavi, M. 2007. Herbal drug technology. Edn 2, University press Pvt. Ltd. Hyderabad.

Ahmed, A.S., Esameldin, E., Elgorashi, E.E., Moodley, N., McGaw, L.J., Naidoo, V. and Eloff, J.N. 2012. The antimicrobial, antioxidative, anti-inflammatory activity and cytotoxicity of different fractions of four South African *Bauhinia* species used traditionally to treat diarrhoea. *Journal of Ethnopharmacology*, **143**: 826–839.

Al-Shidhani, A., Al-Rawahi, N. and Al-Rawahi, A. 2015. Nonsteroidal Anti-inflammatory Drugs (NSAIDs) use in primary health care centers in A'Seeb, Muscat: a clinical audit. *Oman Medical Journal*, **30(5)**: 366–371.

Anyasor, G.N., Funmilayo, O., Odutola, O., Olugbenga, A. and Oboutor, E.M. 2015. Evaluation of Costus afer Ker Gawl. *in vitro* anti-inflammatory activity and its chemical constituents identified using gas chromatography-mass spectrometry analysis. *Journal of Coastal Life Medicine*, **3(2)**: 132–138.

Bailey-Shaw, Y., Williams, L.A.D., Green, C.R., Rodney, S. and Smith, A.M. 2017. *In vitro* evaluation of the anti-inflammatory potential of selected Jamaican plant extracts using the bovine serum albumin protein denaturation assay. *International Journal of Pharmaceutical Sciences Review and Research*, **47(1)**: 145–153.

Bedloviˇcová, Z., Strapáˇc, I., Baláž, M. and Salayová, A. 2020. A brief overview on antioxidant activity determination of silver nanoparticles. *Molecules*, **25**: Doi:10.3390/molecules25143191.

Borneo, R., Leon, A.E., Aguirre, A., Ribotta, P. and Cantero, J.J. 2009. Antioxidant capacity of medicinal plants from the Province of Cordoba (Argentina) and their *in vitro* testing in a model food system. *Food Chemistry*, **112**: 664–670.

Box, H.C., Patrzyc, H.B., Budzinski, E.E., Dawidzik, J.B. and Freund, H.G, *et al*. 2012. Profiling oxidative DNA damage: effects of antioxidants. *Cancer Science*, 103: 2002–2006.

Chandra, S., Chatterjee, P., Dey, P. and Bhattacharya, S. 2012. Evaluation *of in vitro* anti-inflammatory activity of coffee against the denaturation of protein. *Asian Pacific Journal of Tropical Biomedicine*, **2(1)**: S178–S180.

Chatterjee, S. 2016. Chapter two—oxidative stress, inflammation, and disease Oxidative stress and biomaterials. New York: Academic Press, Elsevier. p. 35–58.

Chaves, N., Santiago, A. and Alías, J.C. 2020. Quantification of the antioxidant activity of plant extracts: analysis of sensitivity and hierarchization based on the method used. *Antioxidants*, **9(1)**: Doi: 10.3390/antiox9010076.

Chigayo, K., Mojapelo, P.E.L. and Moleele, S.M. 2016. Phytochemical and antioxidant properties of different solvent extracts of *Kirkia wilmsii* tubers. *Asian Pacific Journal of Tropical Biomedicine*, **6(12)**: 1037–1043.

Deby, C. and Margotteaux, G. 1970. Relationship between essential fatty acids and tissues antioxidant levels in mice. *CR Science Society of Biological Fil*, **165**: 2675–2681.

Dharsana, J.N. and Mathew, S.M. 2014. Preliminary screening of anti-inflammatory and antioxidant activity of *Morinda umbellata*. *International Journal of Pharmacy and Life Sciences*, **5(8)**: 3774–3779.

Förstermann, U. 2010. Nitric oxide and oxidative stress in vascular disease. *European Journal of Applied Physiology*, **459**: 923–939.

Garry, C., Kang, N.T., Christophe W. and Jeffrey, F. 2013. High correlation of 2,2-diphenyl-1-picrylhydrazyl (DPPH) radical scavenging, ferric reducing activity potential and total phenolics content indicates redundancy in use of all three assays to screen for antioxidant activity of extracts of plants from the Malaysian rainforest. *Antioxidants*, **2**: 1–10.

González-Burgos, E. and Gómez-Serranillos, M.P. 2012. Terpene compounds in nature: a review of their potential antioxidant activity. *Current Medicinal Chemistry*, **19**: 5319–5341.

Gwatidzo, L., Dzomba, P. and Mangena, M. 2018. TLC separation and antioxidant activity of flavonoids from *Carissa bispinosa*, *Ficus sycomorus*, and *Grewia bicolar* fruits. *Nutrire*, **43(3)**: Doi: 10.1186/s41110-018-0062-5.

Hasan, A.U.H. 2017. Evaluation of in vitro and in vivo therapeutic efficacy of Ribes alpestre Decne in Rheumatoid arthritis. *Brazilian Journal of Pharmaceutical Sciences*, Doi: 10.1590/s2175-97902019000217832.

Heendeniya, S.N., Ratnasooriya, W.D. and Pathirana, R.N. 2018. *In vitro* investigation of anti-inflammatory activity and evaluation of phytochemical profile of *Syzygium caryophyllatum*. *Journal of Pharmacognosy and Phytochemistry*, **7(1)**: 1759–1763.

Jing, M., Ah, K., Kyung, I., Sun, H., Kim, S., Yun, J., Choi, J. and Won, J. 2011. Silver nanoparticles induce oxidative cell damage in human liver cells through inhibition of reduced glutathione and induction of mitochondria-involved apoptosis. *Toxicology Letters*, **201**: 92–100.

Kandikattu, K., Bharath, R.K.P., Venu, P.R., Sunil, K.K. and Ranjith-Singh, BR. 2013. Evaluation of anti-inflammatory activity of *Canthium parviflorum* by *in vitro* method. *Indian Journal of Research in Pharmacy and Biotechnology*, **1(5)**: 729–730.

Kasote, D. M., Katyare, S. S., Hegde, M. V. and Bae, H. 2015. Significance of antioxidant potential of plants and its relevance to therapeutic applications. *International Journal of Biological Sciences*, **11(8)**: 982–991.

Klaunig, J.E. and Kamendulis, L.M. 2004. The role of oxidative stress in carcinogenesis. *Annual Review of Pharmacology and Toxicology*, **44**: 239–267.

Krishnaiah, D., Sarbatly, R. and Nithyanandam, R.R. 2011. A review of the antioxidant potential of medicinal plant species. *Food and Bioproducts Processing*, **89**: 217–233.

Lee, S.E., Hwang, H.J., Ha, J.S., Jeong, H. and Kim, J.H. 2003. Screening of medicinal plant extracts for antioxidant activity. *Life Sciences*, **73**: 167–179.

Li, Z., Jiang, H., Xu, C. and Gu, L. 2015. Food hydrocolloids a review: using nanoparticles to enhance absorption and bioavailability of phenolic phytochemicals. *Food Hydrocolloids*, **43**: 153–164.

Madikizela, B., Ndhlala, A. R., Finnie, J. F., and Van Staden, J. 2014. Antimycobacterial, anti-inflammatory and genotoxicity evaluation of plants used for the treatment of tuberculosis and related symptoms in South Africa. *Journal of Ethnopharmacology*, **153(2)**: 386–391.

Marrassini, C., Peralta, I. and Anesini, 2018. Comparative study of the polyphenol content-related anti-inflammatory and antioxidant activities of two *Urera aurantiaca* specimens from different geographical areas. *Chinese Medicine*, **13(22)**: Doi.org/10.1186/s13020-018-0181-1.

Milan, C., Hana, C., Petko, D., Maria, K., Anton S. and Antonín L. 2010. Different methods for control and comparison of the antioxidant properties of vegetables. *Food Control*, **21**: 518–523.

Mirghani, M.E.S., Elnour, A.A.M., Kabbashi, N.A., Alam, M.D.Z., Musa, K.H. and Abdullah, A. 2018. Determination of antioxidant activity of gum arabic: An exudation from two different locations. *Science Asia*, **44**: 179–186.

Ndhlala, A.R., Aderogba, M.A., Ncube, B. and Van Staden, J. 2013. Anti-oxidative and cholinesterase inhibitory effects of leaf extracts and their isolated compounds from two closely related croton species. *Molecules*, **18**: 1916–1932.

Nićiforović, N., Mihailović, V., Mašković, P., Solujić, S., Stojković, A. and Muratspahić, D.P. 2010. Antioxidant activity of selected plant species; potential new sources of natural antioxidants. *Food and Chemical Toxicology*, **48**: 3125–3130.

Njoya, E.M., Eloff, J.N. and McGaw. 2018. *Croton gratissimus* leaf extracts inhibit cancer cell growth by inducing caspase 3/7 activation with additional anti-inflammatory and antioxidant activities. *BMC Complementary and Alternative Medicine*, **18**: 305.

Prior, R.L., Wu, X. and Schaich, K. 2005. Standardized methods for the determination of antioxidant capacity and phenolics in foods and dietary supplements. *Journal of Agricultural and Food Chemistry*, **53**: 4290–4302.

Rahman, H., Eswaraiah, M.C. and Dutta, A.M. 2015. *In vitro* anti-inflammatory and anti-arthritic activity of *Oryza sativa* Var. Joha Rice (an aromatic indigenous rice of Assam). *American-Eurasian Journal of Agricultural and Environmental Sciences*, **15(1)**: 115–121.

Sieniawska, E., Maciejewska-Turska, M., Świątek, L. and Xiao, J. 2020. Plant-based food products for antimycobacterial therapy. *eFood*, **1(3)**: 199–216.

Thaipong, K., Boonprakob, U., Crosby, K., Zevallos, L.C. and Byrne, D.H. 2006. Comparison of ABTS, DPPH, FRAP, and ORAC assays for estimating antioxidant activity from guava fruit extracts. *Journal of Food Composition and Analysis*, **19(6-7)**: 669–675.

Trieu, L.H., Trang, L.V., Minh, N.T. and Dao, P.T.A. 2021. Effect of different polarity solvents on the anti-inflammatory activity of *Symplocos cochinchinensis* leaves and correlation with total polyphenol content. *Vietnam Journal of Chemistry*, **59(1)**: 106–114.

Uttra, A.M. and Alamgeer. 2017. Assessment of anti-arthritic potential of *Ephedra gerardiana* by *in vitro* and *in vivo* methods. *Bangladesh Journal of Pharmacology*, **12**: 403–409.

Vijayalakshmi, M. and Ruckmani, K. 2016. Ferric reducing anti-oxidant power assay in plant extract. *Bangladesh Journal of Pharmacology*, **11**: 570–572.

Williams, L.A.D., O'Connar, A., Latore, L., Dennis, O., Ringer, S., Whittaker, J.A. and Kraus W. 2008. The *in vitro* anti-denaturation effects induced by natural products and non-steroidal compounds in heat treated (immunogenic) bovine serum albumin is proposed as a screening assay for the detection of anti-inflammatory compounds, without the use of animals. *The West Indian Medical Journal*, **57(4)**: 327–351.

Chapter 5

5. Antimycobacterial activity of plant extracts

5.1 Introduction

Conventional TB drug combinational chemotherapy yields cure rates of about 85% for new pulmonary TB cases, after about 6 months of strict adherence to the treatment (WHO, 2015). Combinational therapy was necessitated by the difficulty in treating *M. tuberculosis* cells because of the cellular structure and metabolism, which also plays in the microorganisms pathogenicity (Kerantzas and Jacobs, 2017). The selected drugs, rifampicin, isoniazid, and ethambutol exert different mechanisms of action towards *M. tuberculosis* growth inhibition to increase the chances for complete sterilisation in the lung parenchyma and remnant lesions. The current TB combinational therapy may be improved by further incorporating natural products from bioactive medicinal plants (Kerantzas and Jacobs, 2017). Numerous other studies have demonstrated the antimycobacterial potential of various plant species (Singh *et al*., 2021a; Ravindran *et al*., 2020).

The *M. tuberculosis* H37Rv is the commonly used *M. tuberculosis* strain in laboratories. This is mainly because the drug susceptibility of this strain is typically representative of clinical isolates from patients. However, in the initial steps of anti-TB drug discovery, it becomes a challenge and daunting task to test each plant extract against this strain (Gupta *et al*., 2017). The challenge of working with the H37Rv strain is its high infectious nature, which requires level 3 biosafety infrastructure. In addition, the slow doubling time makes studies on *M. tuberculosis* tedious and time consuming (Nema, 2012). As a result, screening a large number of plant extracts becomes problematic in laboratories lacking the level 3 biosafety infrastructure. To solve this problem, most laboratories have opted to utilise fast growing non-pathogenic surrogate model microorganisms, which can be handled under lower biosafety levels. Although the approach of surrogate model microorganisms has limitations, it does allow for vigorous screening of large amounts of plant extracts under an economical platform and a non-hazardous environment (Gupta *et al*., 2017).

Commonly used surrogates include *M. avium*, which causes disease upon contact with an immunosuppressed host. In this study, *M. smegmatis* was used as a model to screen for antimycobacterial activity in the selected plant extracts. The choice of *M.*

smegmatis was compounded by the presence of conserved housekeeping genes similar to *M. tuberculosis*. Morever, *M. smegmatis* shares more than 200 homologs with *M. tuberculosis*. Thus, pathways that are conserved in both species could be studied in *M. smegmatis* to gain insights into specific aspects of physiological adaptation in a shorter time period than is currently possible with *M. tuberculosis*.

5.2 Methods and Materials

5.2.1 Microorganism strains used in this study

The slow growing *M. tuberculosis* H37Rv and fast growing *M. smegmatis* mc^2 155 were obtained from the Centre of Excellence for Biomedical Tuberculosis Research, Division of Molecular Biology and Human Genetics, Department of Biomedical Sciences, Stellenbosch University, South Africa. All work performed using *M. tuberculosis* was conducted in a Biosafety level 3 (BSL3) laboratory. Work conducted with *M. smegmatis* was conducted in a biosafety level 2 (BSL2) laboratory.

5.2.1.1 Maintenance of *Mycobacterium tuberculosis* H37Rv

M. tuberculosis was grown and maintained in Middlebrooks 7H9 (Fluka) broth containing glycerol (Sigma), tween-80 and supplemented with Oleic Albumin Dextrose Catalase (OADC) growth supplement (Sigma) and Tween-80. Ten millilitres of the prepared Middlebrook 7H9 media was transferred to a sterile squared medium bottle, to which, 100 µL of a thawed strain stock was inoculated. The starter culture was incubated at 37 °C for 2 weeks.

5.2.1.2 Maintenance of *Mycobacterium smegmatis* mc^2 155

One hundred microlitres (100 µL) of a thawed freezer stock was inoculated into 10 mL of Middlebrooks 7H9 (Fluka) broth containing glycerol (Sigma) and Middlebrooks Oleic Albumin Dextrose Catalase (OADC) growth supplement (Sigma) and Tween-80 and incubated at 37 °C for 48 hrs.

5.2.1.3 Ziehl-Neelsen staining

A standard protocol of the Ziehl-Neelsen (ZN) staining was used to check the purity of the *M. tuberculosis* before progression to bioassays. 2 drops (~100 µL) of culture in broth was added onto a glass microscope slide and spread to cover approximately 1 x 2 cm area. The smeared samples were allowed to air-dry in the level 3 biosafety

safety cabinet for 30 mins and heat-fixed at 70 °C for 2 hrs. For ZN staining, the slides were flooded with carbol fuchsin and heated to steaming for 5 mins. During the 5 mins, the carbol fuchsin was neither allowed to dry-off nor boil; thus, additional stain was added onto the slide when necessary. The stain was washed off with distilled water and the slides were flooded with 3% v/v acid-alcohol then allowed to stand for 3 mins to sufficiently decolourise the smear, i.e., pale pink. The acid-alcohol was washed off with distilled water. Malachite green was used to flood the slides and the stain allowed to stand for 2 mins, were after, the stain was washed off with distilled water. A bright field microscope, Ziehl-Neelsen smears are examined with the 100X oil objective.

5.2.2 Direct bioautography using *Mycobacterium smegmatis*

Direct bioautography was performed according to Singh *et al*. (2021a) with modifications. The various extracts were reconstituted with acetone to a concentration of 10 mg/mL and 20 µL of this concentration was loaded onto the TLC plates. The TLC plates were prepared and developed in chambers saturated with mobile phases of varying polarity indices as described in Chapter 3, Section 3.2.3.1. The developed chromatograms were dried at room temperature for 5 days ensure that all the solvents have evaporated. *M. smegmatis* culture was grown for 24 hrs in a shaking incubator (200 rpm) at 37 °C in Middlebrook 7H9 broth media (supplemented with OADC and glycerol). The culture was sprayed onto the dried chromatograms until damp/wet. The moistened chromatograms were incubated in humidified chambers for 24 hrs at 37 °C. After incubation, the developed chromatograms were sprayed with the 0.22 filter sterilised 2.0 mg/mL ρ-iodonitrotetrazolium violet (INT) (Sigma, South Africa) dissolved in distilled water. The plates were further incubated for 24 hrs. The presence of clear bands on the chromatograms against a purple background indicated *M. smegmatis* growth inhibition.

5.2.3 Broth microdilution assay

Minimum inhibitory concentrations (MIC) of the extracts were determined against *M. smegmatis* (mc^2 155) and *M. tuberculosis* (H37Rv) using the broth microdilution assay. The broth microdilution assay used was the resazurin microtitre assay and was performed as described by Singh *et al*. (2021a) and Ravindran *et al*. (2020). *M. tuberculosis* and *M. smegmatis* inoculums were grown in Middlebrook 7H9 broth base containing Middlebrook 7H9 broth containing glycerol and Middlebrook oleic albumin dextrose catalase (OADC) growth supplement. *M. smegmatis* starter culture was prepared in 10 mL media, incubated in a shaker, with 200 rpm shaking at 37 °C until OD600 between 0.4-0.6 was reached. Thereafter, the culture was sub cultured in 50 mL OADC-glycerol supplemented Middlebrooks 7H9 media at OD600 of 0.005 and incubated in a shaker, with 200 rpm shaking at 37 °C until an OD600 between 0.2-0.3 was reached (approximately 12 hours). The culture was 100x diluted before adding to plates.

One hundred microlitres (100 µL) of Middlebrook 7H9 broth base containing glycerol (Fluka 49769) and OADC growth supplement and was added into the 96-well microtitre plates. Each plant extract (20 mg/mL) was filter sterilised using a 0.22 µm nylon syringe filter. The extracts (100 µL) were serially diluted two folds with the broth base added in the plate. This was followed by the separate inoculation of 100 µL of the prepared mycobacterial cultures into each well to complete a two-fold broth microdilution. Negative control cells contained only culture medium without the extracts while positive controls contained a standard drug, rifampicin. The plates inoculated with *M. smegmatis* were incubated at 37 °C for 48 hrs, thereafter, 20 µL of 0.22 µm syringe filtered 0.02% Resazurin dissolved in distilled water was added. The plates were incubated for 4 hrs for optimal colour development. Bacterial growth in the wells was indicated by a change in colour from blue to pink. The plates inoculated with M. tuberculosis were incubated for 5 days after adding to the extracts. To determine the MIC values of the active plant extracts against *M. tuberculosis*, freshly prepared and filter sterilised 0.02%. Resazurin dissolved in distilled water was added to each well and plates re-incubated at 37 °C for 24 hrs. Similar to *M. smegmatis* plates, the MIC was determined by the change of colour from blue to pink, where pink colour (formazan) indicated cell viability and blue showed inhibition of cell growth.

5.2.3 Combinational effects

The combinational effects of the extracts was carried out using extracts that were active against *M. smegmatis*. The method described by van Vuuren and Vijoen (2011) was used to determine the fractional inhibitory concentration (FIC). The broth microdilution assay described in Section 6.2.2 was used to determine the combinational effects on the antimicrobial activity of various mixtures. The fractional inhibitory concentration (FIC) of each plant extract was calculated to determine types of chemical interactions that occur when they are mixed, i.e., synergistic, additive, indifferent and antagonistic. The FIC value for each extract in a combination was calculated by dividing the MIC value of the combination by the MIC value of each plant decoction placed in the combination (Equation 5.1). The fraction inhibitory index ($\sum FIC$) was then calculated by adding the two FIC values of the plant extracts in a combination (Equation 6.2).

$$FIC = \frac{MIC\ (combination\ a,b)}{MIC\ (a)} \qquad (5.1)$$

$$FIC\ index = \sum FIC = FICA + FICB \qquad (5.2)$$

Where MIC is the minimum concentration of the extract that was able to inhibit microbial growth. FIC_A is the FIC for the first extract in the combination and FIC_B is of the second extract.

Table 5. 1: The definitions on the interpretation of the combinational effects of plant extracts at a 1:1 ratio.

FIC index value	Outcome of combination
$\sum FIC \leq 0.5$	Synergistic
$\sum FIC > 0.5 - 1.00$	Additive
$\sum FIC > 1.00 - \leq 4.00$.	Indifferent
$\sum FIC > 4.00$	Antagonistic

5.3 Results

Different plant extracts were qualitatively and quantitatively evaluated for possible antimycobacterial activities against *M. smegmatis* (mc^2 155) and *M. tuberculosis* (H37Rv).

5.3.1 Ziehl-Neelsen staining

Ziehl-Neelsen staining was used check the purity of *M. smegmatis* (Figure 5.1A) and *M. tuberculosis* (Figure 5.1B) before use for bioassays.

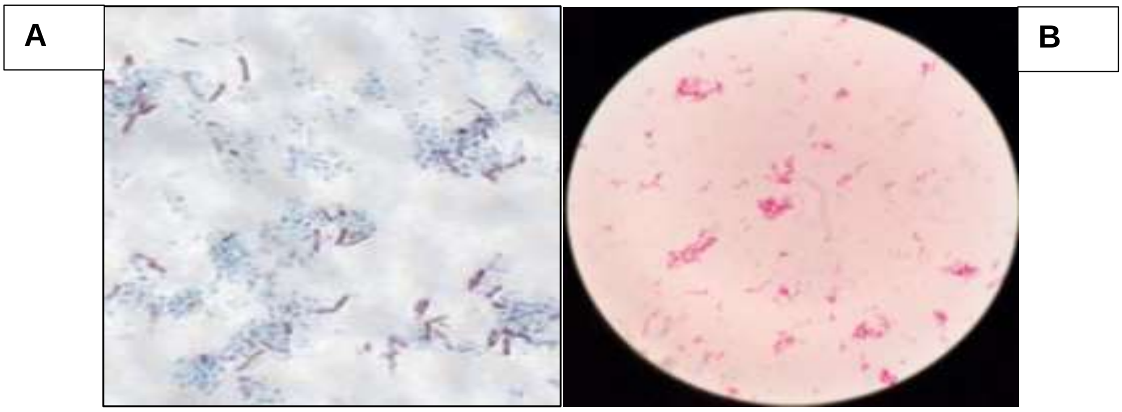

Figure 5. 1: Ziehl-Neelsen staining showing pink rod shaped cells of pure mycobacterial cultures of visualised under a 100x oil objective. A: *M. smegmatis* (mc^2 155) and B: *M. tuberculosis* (H37Rv).

5.3.2 Bioautography

The non-polar bioautograms (BEA) in the leaves extracts showed multiple bioactive compounds (Figures 5.2 and 5.3) with varying retention factors (Table 5.1). *Gardenia volkensii* acetone extract had the most bioactive compounds (7). *Senna petersiana* and *Ficus sur* each had a total of 8 bioactive compounds (Table 5.2).

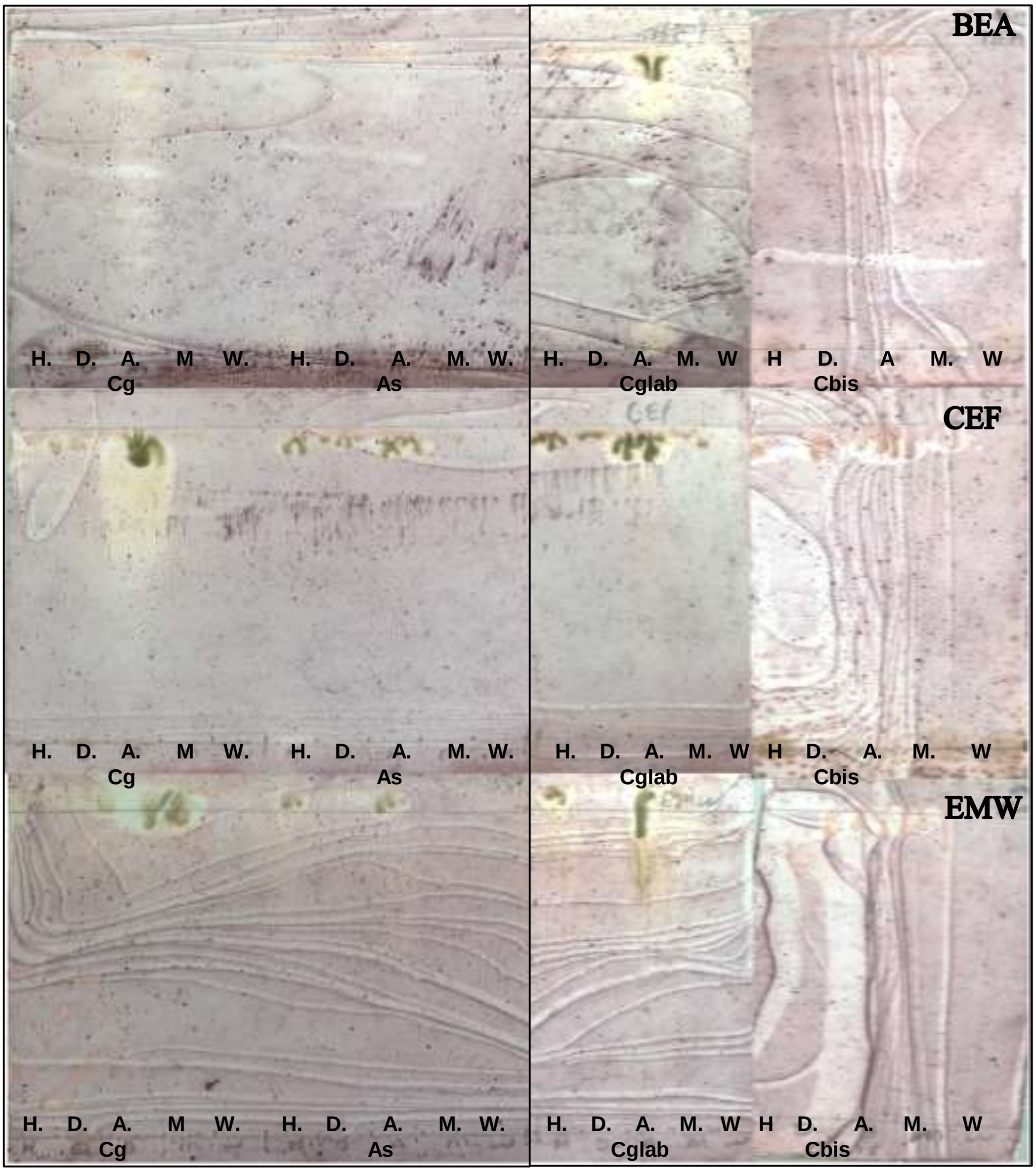

Figure 5. 2: *Mycobacterium smegmatis* bioautogram showing bioactive compounds leaves are clear bands against the purple background.

Key: Cg: *Croton gratissimus*, As: *Acacia Senegal*, Cglab: *Clerodendrum glabrum*, Cbis: *Carissa bispinosa*, H: hexane, D: dichloromethane, A: acetone, M: methanol, W: water.

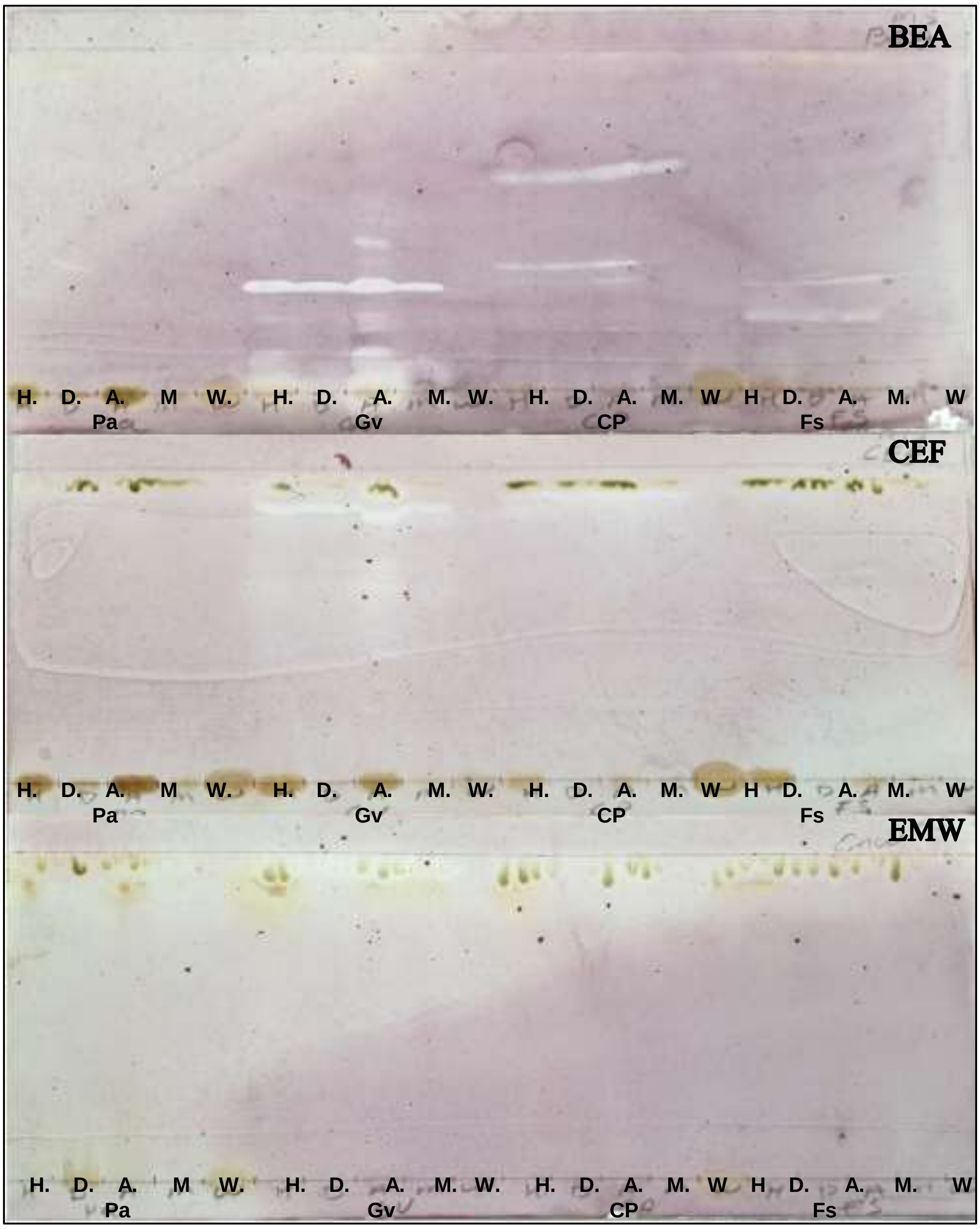

Figure 5. 3: Bioautogram of leaves against *Mycobacterium smegmatis*.

Key: Pa: *Peltophorum africanum*, Gv: *Gadernia volkensii*, Cp: *Senna petersiana*, Fs: *Ficus sur,* H: hexane, D: dichloromethane, A: acetone, M: methanol, W: water.

Table 5. 2: Rf values of TLC separated anti-*Mycobacterium smegmatis* compounds.

			M. smegmatis		
Plant species	Solvent system	Extracts	Rf values	Active bands	Total
C. grattissimus	BEA	A	0.48	1	1
C. glabrum	BEA	A	0.56	1	1
P. africanum	BEA	D	0.49	1	1
C. bispinosa	BEA	H	0.41	1	4
		D	0.41	1	
		A	0.41	1	
		M	0.41	1	
G. volkensii	BEA	H	0.11, 0.23, 0.31	3	16
		D	0.31	1	
		A	0.11, 0.19,0.21, 0.23, 0.31, 0.38, 0.44	7	
		M	0.31	1	
	CEF	H	0.86	1	
		D	0.86	1	
		A	0.86	1	
		M	0.86	1	
Senna petersiana	BEA	H	0.38, 0.65	2	8
		D	0.38, 0.65	2	
		A	0.33, 0.38, 0.65	3	
		M	0.65	1	
Acacia senegal	BEA	H	0.65	1	3
		D	0.65	1	
		A	0.65	1	
Ficus sur	BEA	H	0.21, 0.27	2	8
		D	0.21, 0.27	2	
		A	0.21, 0.27, 0.3	3	
		M	0.27	1	

Key: Rf: retention factor, BEA: benzene/ethanol/ammonium hydroxide, CEF: chloroform/ethyl acetate/formic acid, EMW: ethyl acetate/methanol/ water, H: hexane, D: dichloromethane, A: acetone, M: methanol.

5.3.3 Broth microdilution assay

High Dimethyl sulfoxide (DMSO) concentrations have been reported to be toxic to bacterial cells. To determine the non-toxic concentrations of DMSO, various concentrations were tested against *M. smegmatis*. DMSO concentrations of 1.56 and 3.15% showed non-significant effects on mycobacterial growth (Figure 5.4). Antimycobacterial activity of the extracts was tested against *M. smegmatis* and *M.*

tuberculosis using as a growth indicator, where, pink colour (formazan) shows the presence of viable cells and the blue colour/unchanged wells demonstrate the inhibition of cell growth (Figure 5 and 6, respectively). The acetone extract of *Clerodendrum glabrum* was the most active with MIC values of 0.98 and 0.63 mg/mL against *M. smegmatis* and *M. tuberculosis*, respectively (Table 5.3). *Carissa bispinosa*, *Acacia senegal*, *Ficus sur* and *Senna petersiana* did not demonstrate inhibitory effects on *M. tuberculosis*, but should moderate activity against *M. smegmatis*.

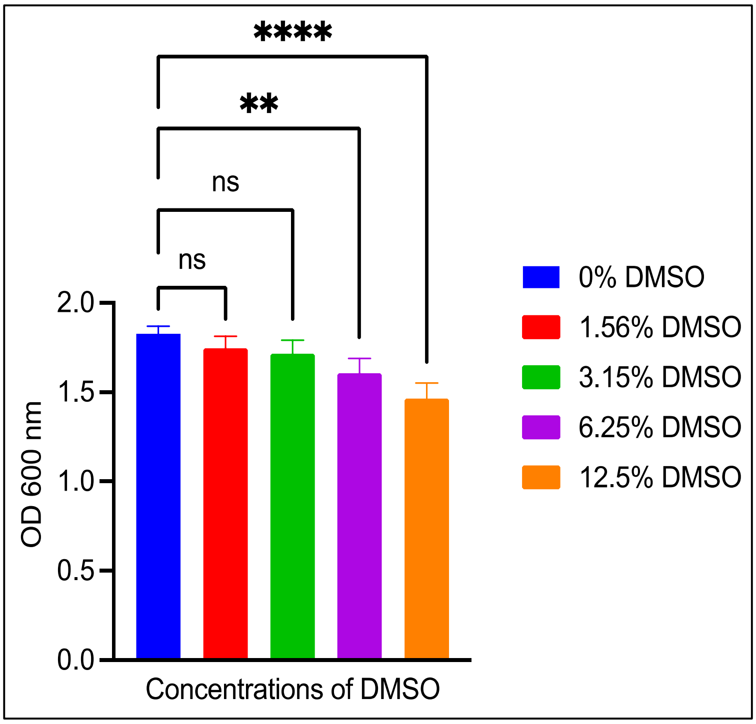

Figure 5. 4: The influence of different concentrations of Dimethyl sulfoxide (DMSO) on *M. smegmatis* mc^2 155. *M. smegmatis* was grown in 7H9-OADC broth and exposed to the different concentrations of DMSO in 96-well microplates.

Key: (****): $p < 0.0001$, (**): $p<0.01$, ns: non-significant difference ($p>0.05$). Values are the mean ± SD for N = 4.

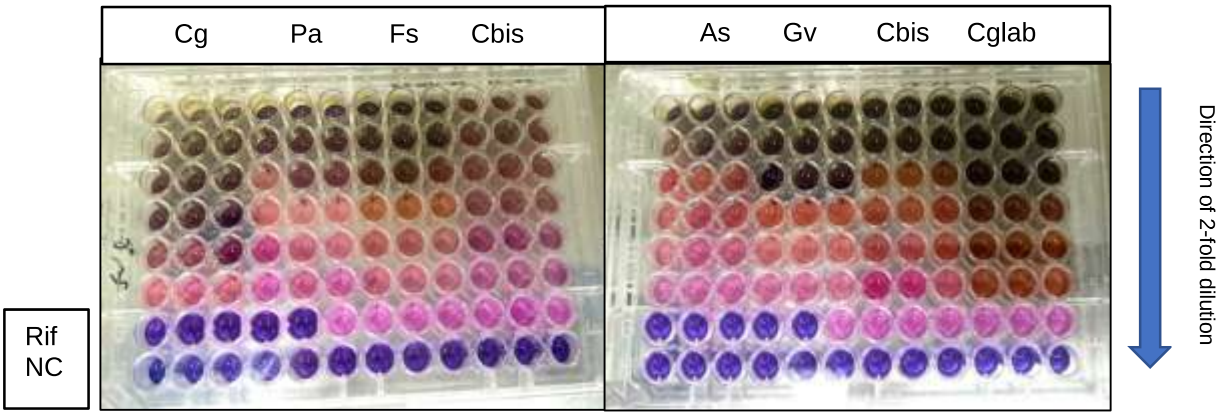

Figure 5. 5: Broth microdilution assay used to determine antimycobacterial activity of plant extracts against *Mycobacterium smegmatis*. Rifampicin was used as a standard.

Key: Cg: *Croton gratissimus*, As: *Acacia Senegal*, Cglab: *Clerodendrum glabrum*, C.bis: *Carissa bispinosa*, *Peltophorum africanum*, Gv: *Gadernia volkensii*, Cp: *Senna petersiana*, Fs: *Ficus sur*

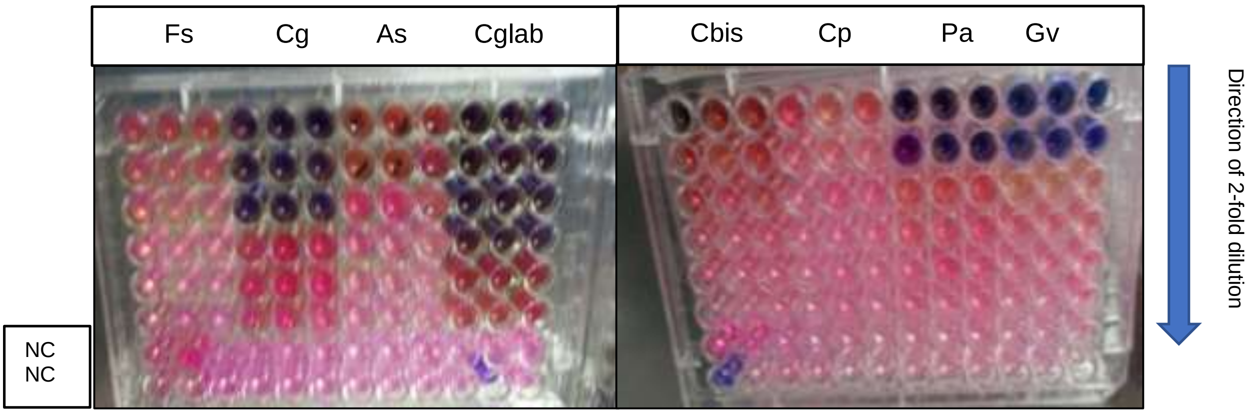

Figure 5. 6: Antimycobacterial activity against *Mycobacterial tuberculosis* H37Rv. Bacterial growth in the wells was indicated by a change in colour, whereas clear wells indicated inhibition by the extracts.

Key: Cg: *Croton gratissimus*, As: *Acacia Senegal*, Cglab: *Clerodendrum glabrum*, C.bis: *Carissa bispinosa*, *Peltophorum africanum*, Gv: *Gadernia volkensii*, Cp: *Senna petersiana*, Fs: *Ficus sur*

Table 5. 3: Antimycobacterial activities of extracts against *Mycobacterium smegmatis* and *Mycobacterium tuberculosis*.

		Hexane			Dichloromethane			Acetone			Methanol			Water		
Plant	Plant part	MIC	MBC	TA	MIC	MBC	TA	MIC	MBC	TA	MIC	MBC	TA	MIC	MBC	TA
M. smegmatis																
Cg	Leaf	>2.5	-	-	>2.5	-	-	**1.25**	-	11.16	>2.5	-	-	>2.5	-	-
	Branch	>2.5	-	-	**1.25**	-	16.12	**1.25**	-	7.16	>2.5	-	-	>2.5	-	-
As	Leaf	>2.5	-	-	>2.5	-	-	**2.5**	-	9.3	>2.5	-	-	>2.5	-	-
	Branch	>2.5	-	-	>2.5	-	-	>2.5	-	-	>2.5	-	-	>2.5	-	-
Cglab	Leaf	>2.5	-	-	>2.5	-	-	**0.98**	-	12.04	>2.5	-	-	>2.5	-	-
	Branch	>2.5	-	-	>2.5	-	-	>2.5	-	-	>2.5	-	-	**2.5**		18.77
Cbis	Leaf	**2.5**	-	19.20	**2.5**	-	16.34	**1.25**	-	19.68	>2.5	-	-	>2.5	-	-
	Branch	>2.5	-	-	>2.5	-	-	>2.5	-	-	>2.5	-	-	>2.5	-	-
Pa	Leaf	**1.25**	-	6.57	**2.5**	-	3.40	**1.25**	-	8.80	1.25		12.80	>2.5	-	-
	Branch	>2.5	-	-	>2.5	-	-	>2.5	-	-	>2.5	-	-	>2.5	-	-
Gv	Leaf	**1.25**	-	5.92	**2.5**	-	3.80	**1.25**	-	7.70	2.5	-	6.00	>2.5	-	-
	Branch	>2.5	-	-	>2.5	-	-	**1.25**	-	5.90	>2.5	-	-	>2.5	-	-
Sp	Leaf	**2.5**	-	4.00	>2.5	-	-	**2.5**	-	4.20	1.25	-	6.45	**0.63**		19.05
	Branch	>2.5	-	-	>2.5	-	-	>2.5	-	-	>2.5	-	-	>2.5	-	-
Fs	Leaf	**1.25**	-	6.40	>2.5	-	-	**1.25**	-	7.36	>2.5	-	-	>2.5	-	-
	Branch	>2.5	-	-	>2.5	-	-	>2.5	-	-	>2.5	-	-	>2.5	-	-
M. tuberculosis																
Cg	Leaf	-	-	-	-	-	-	1.25	>5	11.16	-	-	-	-	-	-
Gv	Leaf	-	-	-	-	-	-	2.5	>5	3.60	-	-	-	-	-	-
Pa	Leaf	-	-	-	-	-	-	2.5	>5	4.40	-	-	-	-	-	-
Cglab	Leaf	-	-	-	-	-	-	**0.63**	>5	26.60	-	-	-	-	-	-

Key: (-): Not determined, Cg: *Croton gratissimus*, As: *Acacia Senegal*, Cglab: *Clerodendrum glabrum*, Cbis: *Carissa bispinosa*, Pa: *Peltophorum africanum*, Gv: *Gardenia volkensii*, Sp: *Senna petersiana*, Fs: *Ficus sur*, MIC: Minimum inhibitory concentration (mg/mL), MBC: Minimum bactericidal concentration (mg/mL), TA: total activity (mL).

5.3.5 Combinational effects of plant extracts

Combinational effects between the different crude extracts resulted in indifferent and antagonistic interactions. *C. glabrum*, *P. africanum*, *F. sur* and *C. bispinosa* had additive effects with rifampicin (Table 5.4).

Table 5. 4: Combinational effects of extracts on anti-*M. smegmatis* activity.

Combination	MIC mg/mL	FIC(A)	FIC(B)	FIC index (ΣFIC)	Outcome
Pa+Cg	1.25	1	1	2	Indifferent
Pa+Cglab	1.25	1	1.28	2.28	Indifferent
Pa+Gv	1.25	1	1	2	Indifferent
Pa+Fs	1.25	1	1	2	Indifferent
Pa+Cb	1.25	1	1	2	Indifferent
Pa+As	1.25	1	0.5	1.5	Indifferent
Pa+Cp	1.25	1	0.5	1.5	Indifferent
Cg+Cglab	2.5	2	2.55	4.55	Antagonistic
Cg+Gv	5	4	4	8	Antagonistic
Cg+Fs	5	4	4	8	Antagonistic
Cg+Cb	5	4	4	8	Antagonistic
Cg+As	5	4	2	6	Antagonistic
Cg+Cp	5	4	2	6	Antagonistic
Cglab+Gv	5	5.1	4	9.1	Antagonistic
Cglab+Fs	5	5.1	4	9.1	Antagonistic
Cglab+Cb	>5	>5	>4	>9	Antagonistic
Cglab+As	>5	>5	>2	>7	Antagonistic
Cglab+Cp	5	5.1	2	7.1	Antagonistic
Gv+Fs	5	4	4	8	Antagonistic
Gv+Cb	5	4	4	8	Antagonistic
Gv+As	5	4	2	6	Antagonistic
Gv+Cp	5	4	2	6	Antagonistic
Fs+Cb	>5	>4	>4	>8	Antagonistic
Fs+As	>5	>4	>2	>6	Antagonistic
Fs+Cp	>5	>4	>2	>6	Antagonistic
Cb+As	>5	>4	>2	>6	Antagonistic
Cb+Cp	>5	>4	>2	>6	Antagonistic
Extract combination with Rifampicin					
Pa+Rif	0.00156	0.0012	1	1.00	Additive
Cg+Rif	0.00313	0.0025	2	2.00	Indifferent
Cglab+Rif	0.00156	0.0016	1	1.00	Additive
Gv+Rif	0.00313	0.0025	2	2.00	Indifferent
Fs+Rif	0.00156	0.0012	1	1.00	Additive
Cbis+Rif	0.00156	0.0012	1	1.00	Additive
As+Rif	0.00313	0.0013	2	2.00	Indifferent
Cp+Rif	0.00313	0.0013	2	2.00	Indifferent
Rif only	0.00156	-	-	-	-

Key: Cg: *Croton gratissimus*, As: *Acacia Senegal*, C.glab: *Clerodendrum glabrum*, C.bis: *Carissa bispinosa*, *Peltopphorum africanum*, Gv: *Gadernia volkensii*, Cp: *Senna petersiana*, Fs: *Ficus sur*, A: FIC of extract 1, B: FIC of extract 2.

5.4 Discussion

In South Africa, many plants and derivatives have been recorded to be used by local communities for the treatment of various respiratory infections, including TB. It is important to report and elucidate the activities of such plants because they could lead to the discovery of new novel antimycobacterial agents. This prompted the selection and investigation of the antimycobacterial potential of these medicinal plants.

5.4.1 Bioautography

Bioautography is a specialised form of planar chromatography where the separated compounds are not made visible by treating with a spray reagent, but are sprayed with a live microorganism, incubated and then sprayed with a tetrazolium salt that indicates whether the microorganism grew or not. This makes it possible to detect and determine how many different antimicrobial compounds were separated and also to calculate the Rf value to determine their location for further studies (Runyoro *et al*., 2006).

All the selected plants possessed bioactive antimycobacterial compounds in one or more of the different solvent extracts (Figures 5.2 and 5.3). With the BEA and CEF solvent systems used, a total of 42 bioactive bands across the various solvent leaves extracts of the 8 selected plants were detected. No active bands were detected on the polar EMW bioautograms from all the tested extracts, reflecting that singular polar compounds were inactive against *M. smegmatis* (Figures 5.2 and 5.3). The BEA system was remarkably responsible for the appropriate separation of 90.48% of bioactive compounds across all the tested extracts followed by CEF bioautograms (9.52%) (Table 5.1). This indicated that most of the antimycobacterial compounds were non-polar. In agreement, it has previously been reported that non-polar extracts or compounds from plant extracts frequently exhibited higher antibacterial activity and polar compounds commonly show weaker antibacterial activity (Masoko and Makgapeetja, 2015; Adamu *et al*., 2014). *Gardenia volkensii* had the most detectable active compounds against *M. smegmatis* (16), followed by *S. petersiana* (8) and *F. sur* (8). It was noted that there were occurrences where the same Rf value of active compounds was determined within the same plant species was the same across the various solvent extracts. This may mean that the same antibacterial compound showed the ability to become extracts by the different solvents. Direct bioautography showed the antimycobacterial potential of the separated compounds from the crude extracts of various plant extracts.

5.4.2 Broth microdilution assay

The broth micro-dilution assay was used to determine the minimum inhibitory concentration (MIC) of the extracts against M. smegmatis. The MIC represents the lowest concentration of the crude extracts (mg/mL) that is able to inhibit mycobacterial growth. This method served to quantify the antimycobacterial activity observed on the bioautograms. The non-fluorescent blue resazurin dye (low OD readings) used is converted through reduction by viable cells to red fluorescent resorufin dye (high OD readings) (Figures; 5.5 and 5.6).

It has been shown that organic solvents used in the extraction of plant material may also be toxic to microorganisms (Eloff, 1998). During antimicrobial activity investigation, it is important that the extractant does not interfere with the experiments by contributing to the activity/death of the test microbe. In this study, the plant extracts were redissolved in Dimethyl sulfoxide (DMSO); therefore, the effects of different DMSO concentrations were investigated. DMSO concentrations greater than 3.15% in solution were found to be toxic to *M. smegmatis* DMSO concentrations whereas $\leq$ 3.15% were found to be non-toxic to *M. smegmatis* cells (Figure 5.4). Based on these results, a final concentration of 2% DMSO was selected for the broth micro-dilution assays. Other researchers have reported similar findings, where, 2.5% DMSO was found not to have a significant effect on *M. smegmatis* viability (Nyambuya *et al*., 2017). Rifampicin was used as a standard and the antibiotic-containing control wells showed appropriate antimycobacterial activity with MIC value of 1.56 μg/mL against *M. smegmatis* (Figure 5.7).

Gardenia volkensii and *Peltophorum africanum* extracts had the same activity for the hexane (1.25 mg/mL MIC), dichloromethane (2.5 mg/mL MIC) and acetone extracts (1.25 mg/mL MIC) against *M. smegmatis*. Similarly, the acetone extracts from both plant extracts had the same MIC of 2.5 mg/mL against *M. tuberculosis*. Early antimicrobial studies by Mutta (1995) revealed the potential antimycobacterial activity of *G. volkensii* methanol root extract against *Mycobacterium phlei*. In addition, the stem bark of *G. volkensii* was reported to be used for treatment of chest complaints and TB related infections (Mongalo and Makhafola, 2018). Theo *et al*. (2009) isolated betulinic acid, a triterpenoid from the methanol crude extract of *P. africanum*. Betulinic acid had been reported to have MIC of 32 μM against *M. tuberculosis* H37Rv (Cantrell *et al*., 2001). Accordingly, the phytochemical analysis of *P. africanum* in the current study also revealed the presence of triterpenoids (Chapter 3) in the leaves. It is likely that the antimycobacterial activity of *P. africanum* in part, could be due to the presence of these compounds.

The aqueous and methanol leaf extracts of *F. sur* have previously been reported to not to have any detectable antimycobacterial activity against *M. smegmatis*, *M. tuberculosis* H37Rv, clinical isolate of MDR-TB and XDR-TB at a concentration of 1 mg/mL (Singh *et al*., 2021a). These observations are in agreement with the current findings since both the aqueous and methanol leaves and stem extracts did not have antimycobacterial activity at 2.5 mg/mL. It was interesting that the hexane and acetone extracts of *F. sur* inhibited *M. smegmatis* at 1.25 mg/mL. This could be contributed by specific bioactive compounds in the crude extracts as seen on the bioautogram in Figure 5.5.

The aqueous leaves extract of *S. petersiana* had a notable low MIC of 0.63 mg/mL compared to the rest of the plant extracts tested. This result indicates that the antimycobacterial activity may be due to the synergistic interaction of polar compounds present in the aqueous extracts. This is because no single antimycobacterial compound was detected by bioautography. A flavonoid called Luteolin, has been isolated from *S. petersiana* (Tshikalange *et al*., 2005), and has been shown that when added to conventional therapy (particularly administered adjunct to isoniazid), the development of *M. tuberculosis* drug resistance may be avoided and disease therapy can be improved (Singh *et al*., 2021b). Flavonoids and their subclasses have also been detected in *S. petersiana* in this study (Chapter 3), having a high possibility that luteolin is present in various concentrations.

The decoction of *A. senegal* root is commonly used by Bapedi local communities to treat respiratory ailments such as asthma, TB, sore throat, chronic cough, sinusitis (Semenya and Maroyi, 2018). Contrary to the weak antimycobacterial determined for *A. senegal* branch extracts (>2.5 mg/mL MIC), Mariita *et al.* (2010) indicated that 1 mg/mL of *A. senegal* bark methanol extract was able to completely inhibition, *M.*

tuberculosis, *M. smegmatis* and *M. fortuitum* (Mariita *et al.*, 2010). *Clerodendrum glabrum* acetone leaves extract showed the highest antimycobacterial activity among all other extracts, demonstrating MIC values of 0.98 mg/mL and 0.63 mg/mL against *M. smegmatis* and *M. tuberculosis*, respectively. It appeared that *C. glabrum* extract was more active against *M. tuberculosis* H37Rv than *M. smegmatis* mc^{155}. These results are corroborated by Dzoyem *et al*. (2015), where it was shown that the *C. glabrum* acetone extract had higher antimycobacterial activity against *M. tuberculosis* (0.156 mg/mL MIC) and *M. smegmatis* (0.312 mg/mL MIC) (Dzoyem *et al*., 2015). However, contrary to Dzoyem *et al*. (2015), this study reports weaker broad-spectrum antimycobacterial activity of *C. glabrum*.

Kuete, (2010) recommended that antimicrobial activity of crude plant extracts should be considered significant when MIC values are less than 100 μg/mL, moderate when MIC values are between 100 and 625 µg/mL and low when MIC are greater than 625 µg/mL. Other researchers have considered a lesser stringent criteria, where MIC values less than 8000 μg/mL were recommended as noteworthy antimicrobial activity (Fabry *et al*., 1998). Applying this less stricter criteria, the activity recorded from the tested crude extracts could be considered important.

The MIC values reported in this current study reflect the activity of crude/impurified extracts, thus, the bioactive compounds showed on the bioautograms may be in lower concentrations to interfere with mycobacterial cell growth in liquid media (Nguta *et al*., 2016). Although moderate antimycobacterial activity was observed, it is expected that a fractionation of these crude extracts with lesser polar solvents (or solvent combinations) will improve the MIC observed. In addition, further investigations should focus on isolating and elucidating the structures of these bioactive phytochemicals responsible for the observed antimycobacterial activities.

One of the important parameters in assessing the microbial activity of plant extracts is total activity (TA). Calculated by dividing the mass in mg extracted from 1 g of plant material with the MIC in mg/mL a value, TA is the volume of a solvent that can added to the extract obtained from 1 g of plant material that will still inhibit the MIC of the pathogen (Adamu *et al*., 2014; Eloff, 2000). TA is valuable because it takes into consideration, not only the antimicrobial activity, but also relates it to the quantity of compounds extracted from plant material. Between the hexane, DCM and acetone extracts of *P. africanum*, *G. volkensii*, *S. petersiana* and *F. sur*, low TA was determined (3.4-7.70 mL/g plant extract) against *M. smegmatis*. *P. africanum* and *G. volkensii* acetone extracts also had low TA values of 4.40 and 3.60 mL/g, respectively against *M. tuberculosis*. These results highlight the possibility that the solvents used may have extracted the bioactive compounds in low concentrations from 1 g of plant material. The highest TA determined was from *C. glabrum* acetone extract against 26.60 mL/g against *M. tuberculosis*. This indicated that the MIC of the acetone extract of *C. glabrum* can be diluted to 26.60 mL and still demonstrate antimycobacterial activity

5.4.3 Combinational effects of plant extracts

Combinational effects between the different crude extracts yielded antagonistic and indifferent interactions (Table 5.3). Similar results were obtained from adding the extracts with rifampicin at a 1:1 ratio. These results showed that the crude extracts lose antimycobacterial activity when mixed together or have no significant change on the activity of a single extract. This may suggest that the antimycobacterial activity of bioactive phytochemicals may be interrupted by other chemicals. All the extracts did not demonstrate a detectable anti-mycobactericidal activity (MBC) against both *M. smegmatis* and *M. tuberculosis*. This showed that the extracts do not kill the tubercle cells (or stop all metabolic activity); rather, they inhibit or elongate the lag phase of the test organisms.

5.5 Conclusion

The current data provides evidence that the screened leaves are a potential source of molecules against TB and in part, the findings of this study validate the ethnopharmacological use of the leaves by local communities. These results demonstrated that the activity of a plant species is dependent on the solvent used for extraction. Results from bioautography highlight the need for a further fractionation of the crude extracts to evaluate the individual activity of the bioactive antimycobacterial compounds. This prompts intensified studies focusing on isolation and elucidation of anti-tb bioactive constituents from the medicinal plant.

5.6 References

Adamu, M., Naidoo, V. and Eloff, J.N. 2014. The antibacterial activity, antioxidant activity and selectivity index of leaf extracts of thirteen South African tree species used in ethnoveterinary medicine to treat helminth infections. *BMC Veterinary Research*, **10**: 52.

Cantrell, C., Franzblau, S. and Fischer, N. 2001. Antimycobacterial plant terpenoids. *Planta Medica*, **67(8)**: 685–694.

Dzoyem, J.P., Aro, A.O., McGaw, L.J. and Eloff, J.N. 2015. Antimycobacterial activity against different pathogens and selectivity index of fourteen medicinal plants used in southern Africa to treat tuberculosis and respiratory ailments. *South African Journal of Botany*, **102**: 70–74.

Eloff, J.N. 1998. Which extractant should be used for the screening of antimicrobials components from plants? *Journal of Ethnopharmacology*, **60(1)**:1–8.

Eloff, J.N. 2000. On expressing the antibacterial activity of plant extracts - a small first step in applying scientific knowledge to rural primary health care. *South African Journal Science*, **96**: 116–118.

Fabry, W., Okemo, P.O. and Ansorg, R. 1998. Antibacterial activity of East African medicinal plants. *Journal of Ethnopharmacology*, **60**: 79–84.

Gupta, V.K., Kumar, M.M., Bisht, D. and Kaushik, A. 2017. Plants in our combating strategies against *Mycobacterium tuberculosis*: progress made and obstacles met. *Pharmaceutical Biology*, **55(1)**: 1536–1544.

Kerantzas, C.A. and Jacobs, W.R. 2017. *Origins of combination therapy for tuberculosis: lessons for future* antimicrobial development and application*. mBio*, **8(2)**: Doi:10.1128/mbio.01586-16.

Kuete, V. 2010. Potential of Cameroonian plants and derived products against microbial infections: a review. *Planta Medica*, **76**: 1479–1491.

Mariita, R.M., Ogol, C.K.P.O., Oguge, N.O. and Okemo, P.O. 2010. Antitubercular and phytochemical investigation of methanol extracts of medicinal plants used by the Samburu community in Kenya. *Tropical Journal of Pharmaceutical Research*, **9(4)**: 379–385.

Masoko, P. and Makgapeetja, D.M. 2015. Anti-bacterial, antifungal and antioxidant activity of *Olea africana* against pathogenic yeast and nosocomial pathogens. *BMC Complementary and Alternative Medicine*, **15**: 409.

Mongalo, N. I. and Makhafola, T. J. 2018. Ethnobotanical knowledge of the lay people of Blouberg area (Pedi tribe), Limpopo Province, South Africa. *Journal of Ethnobiology and Ethnomedicine*, **14(1)**: Doi: 10.1186/s13002-018-0245-4.

Mutta, D.N. 1995. Antibiotic screening of plants used to treat infectious diseases in Kenya. MSc Dissertation. Vancouver: University of British Columbia.

Nema, V. 2012. Tuberculosis diagnostics: Challenges and opportunities. *Lung India*, **29**: 259–66.

Nguta, J. M., Appiah-Opong, R., Nyarko, A. K., Yeboah-Manu, D., Addo, P. G., Otchere, I. and Kissi-Twum, A. 2016. Antimycobacterial and cytotoxic activity of selected medicinal plant extracts. *Journal of Ethnopharmacology*, **182**: 10–15.

Nyambuya, T., Mautsa, R. and Mukanganyama, S. 2017. Alkaloid extracts from *Combretum zeyheri* inhibit the growth of *Mycobacterium smegmatis*. *BMC Complementary and Alternative Medicine*, **17(1)**: Doi: 10.1186/s12906-017-1636-0.

Ravindran, R., Chakrapani, G., Mitra, K. and Doble, M. 2020. Inhibitory activity of traditional plants against Mycobacterium smegmatis and their action on Filamenting temperature sensitive mutant Z (FtsZ)-A cell division protein. *Public Library of Science One*, **15(5)**: Doi: 10.1371/journal.pone.0232482.

Runyoro, D.K.B., Matee, M.I.N., Ngassapa, O.D., Joseph, C.C. and Mbwambo, Z.H. 2006. Screening of Tanzanian medicinal plants for anti-candida activity. *BMC Complementary and Alternative Medicine*, **6(11)**: 6882–6886.

Semenya, S.S. and Maroyi, A. 2018. Ethnomedicinal uses of Fabaceae species for respiratory infections and related symptoms in the Limpopo Province, South Africa. *Journal of Pharmacy and Nutrition Sciences*, **8**: 219–229.

Singh, A., Venugopala, K.N., Pillay, M, Shode, F, Coovadia, Y. and Odhav, B. 2021a. Antimycobacterial activity of aqueous and methanol extracts of nine plants against *Mycobacterium* bacteria. *Tropical Journal of Pharmaceutical Research*, **20(4)**: 849–858.

Singh, D.K., Tousif, S., Bhaskar, A., Devi, A., Negi, K., Moitra, B., Ranganathan, A., Dwivedi, V.P. and Das, G. 2021b. Luteolin as a potential host-directed immunotherapy adjunct to isoniazid treatment of tuberculosis. *Public Library of Science Pathogens*, **17(8)**: Doi: 10.1371/journal.ppat.1009805.

Theo, A., Masebe, T., Suzuki, Y., Kikuchi, H., Wada, S., Obi, C. L., Hattori, T. 2009. *Peltophorum africanum*, a traditional South African medicinal plant, contains an anti-HIV-1 constituent, Betulinic acid. *Tohoku Journal of Experimental Medicine*, **217(2)**: 93–99.

Tshikalange, T.E., Meyer, J.J.M. and Hussein, A.A. 2005. Antimicrobial activity, toxicity and the isolation of a bioactive compound from plants used to treat sexually transmitted diseases. *Journal of Ethnopharmacology*, **96(3)**: 515–519.

Van Vuuren, S. and Viljoen, A. 2011. Plant-based antimicrobial studies–methods and approaches to study the interaction between natural products. *Planta Medica*, **77(11)**: 1168–1182.

World Health Organization. 2015. Global tuberculosis report 2015, Geneva, Switzerland, p 1–126.

CHAPTER 6

6. Utilization of CRISPR interference to study the shikimate pathway as a drug target

6.1 Introduction

Typically, antimycobacterial drugs under development target well-characterised functions in macromolecular biosynthesis such as cell wall, protein, and nucleic acids (Lott, 2020; Wellington *et al*., 2018). The current anti-TB chemotherapy consists of isoniazid and ethambutol, both of which inhibit cell wall biosynthesis; rifampicin, which inhibits mRNA production; and pyrazinamide, which is thought to inhibit coenzyme A biosynthesis (Wellington *et al*., 2018; Tam, 2008). The duration, toxicity, and complexity of the required drug regimens are some of the prominent challenges facing current TB treatment drugs (Lott, 2020). The main challenging task facing researchers involved in TB drug discovery has to be the lack of knowledge about targets required for mycobacterial growth and survival of the tubercle bacilli *in vivo* (Blumenthal *et al*., 2010).

Aromatic amino acid (AAA) biosynthesis is vital for *M. tuberculosis* survival and pathogenesis *in vivo*. Upon *M. tuberculosis* infection, the host's immune system recruits various immune cells such as $CD4^+$ T-cells and macrophages. More immune processes are activated and some of them involve attempts to starve tubercle bacilli of essential amino acids, with tryptophan starvation being one of the highly studies mechanisms (Zhang *et al*., 2013). However, *M. tuberculosis* is competent to synthesise tryptophan *de novo* (through the shikimate pathway). The ability of infecting bacilli to survival for long allows it to disrupt and escape acidification by the macrophages. This renders the host's defence mechanisms inefficient (Zhang *et al*., 2013). Moreover, metabolic pathways for AAA biosynthesis play an important role in the viability of *M. tuberculosis* bacilli by serving as sources of carbon and nitrogen (Yelamanchi and Surolia, 2021). Some of the essential AAs for *M. tuberculosis* metabolism include histidine, isoleucine, leucine, methionine, phenylalanine, threonine, tryptophan, and valine (Abrahams *et al*., 2017).

The requirement of AAAs for *M. tuberculosis* survival makes their biosynthetic pathways very attractive for drug targeting. It has been suggested that the clinical use of inhibitors of essential AA biosynthesis can have an advantage of having fewer negative effects on normal gut flora because the gut is abundant in AA (Grandoni *et al*., 1998). Therefore, when targeting the biosynthetic pathways of essential AAs, one should consider pathways or key enzyme homologs that are absent in the hosts (humans) but essential for pathogen survival and viability (Yelamanchi and Surolia, 2021).

In this work, the researcher studied the inhibition of the *Mycobacterium* pentose phosphate and shikimate pathway enzymes. The shikimate pathway, used by microorganisms to synthesis AAA, is an attractive target for antimycobacterial agents, as it is essential for bacterial growth, but absent in humans (Nirmal *et al*., 2015). In *M. tuberculosis*, the shikimate pathway is linked to carbohydrate metabolism through glycolysis and pentose phosphate pathway (PPP). The former pathway provides phosphoenolpyruvate (PEP) to the shikimate pathway, and the latter provides the erythrose 4-phosphate (E4P) by receiving help from the transketolase enzymes encoded by *tkt* gene (Pereira *et al*., 2007). The DAHP synthase, encoded by the *aroG*, gene is responsible for the first reaction of seven shikimate pathway steps. It catalyses the aldol condensation reaction between PEP and E4P to produce 3-deoxy-D-arabino-heptulosonate 7-phosphate (DAHP) and inorganic phosphate (Tzin *et al*., 2012). Enzyme inhibition assays against DAHPS synthase of *M. tuberculosis* confirmed their inhibitory potential, suggesting that their structure or biosynthesis could be exploited for future drug development (Nirmal *et al.*, 2015). The PPP is essential for the *in vitro* survival and viability of *M. tuberculosis* and evidence of this essentiality lies in the conservation of its housekeeping genes in other *Mycobacterium* species such as *M. leprai* (Fullam *et al*., 2011). In addition, the proportion of available E4P was found to influence the proportion of DAHP produced, which effectively compromised AA biosynthesis (Patnaik and Liao, 1994). As such, this demonstrated the importance of the transketolase enzyme in suppling E4P to the DAHP synthase of the shikimate pathway. The essentiality of the transketolase enzyme was demonstrated by Kolly *et al.* (2014a) using the RNA silencing and protein degradation (RSPD) system, which showed that depleting *tkt* gene arrested *M. tuberculosis* growth.

Anti-TB drug discovery is hampered by only focusing on essential drug targets whose vulnerability to chemical inhibition has not been determined (Blumenthal *et al*., 2010). Gene knockdown methods have long been used in molecular biology to study gene essentiality and vulnerability in a given genome of a species (Rock *et al*., 2017). Unlike gene knockout methods which permanently modify genomic DNA sequences, gene knockout methods temporarily alter the expression of the targeted gene(s) (Singh *et al*., 2016; Choudhary *et al*., 2015). Therefore, new genetic tools, that can combine the study of gene essentiality and vulnerability for new therapeutic targets without causing permanent gene deletions, is highly required. Clustered regularly interspaced short palindromic repeats (CRISPR)-Cas9 is a simple two-component system that allows researchers to precisely edit any sequence in the genome of an organism. Of the various CRISPR systems available, the least complex and commonly used is the type II CRISPR from *Streptococcus pyogenes* (Choudhary *et al*., 2015). Many adaptations were made to the classical CRISPR system to achieve many different goals and on such adaptation is the use of catalytically inactive dCas9 protein in CRISPR interference (CRISPRi) system. CRISPRi technique involves the expression of a small guide RNA (sgRNA) that targets and binds the target gene sequence in a genome. The binding of the sgRNA to the target sequence is achieved through a complementary nucleotide base pairing of 12-20 nucleotides where the sequence is homologous to the target gene (Singh *et al*., 2016; Choudhary *et al*., 2015). Following sgRNA binding, a catalytically inactive endonuclease enzyme, dCas9 is expressed and recruited to the binding site of the sgRNA-DNA complex (Singh *et al*., 2016). The presence of the dCas9 at the sgRNA-DNA complex leads to the interference of transcription initiation or elongation based on the choice of the target gene (Qi *et al*., 2013). The DNA sequence is not altered, so, when the cell naturally clears the dCas9 enzyme, the targeted gene is free to be expressed again (Choudhary *et al*., 2015). Important for the CRISPRi system, are short sequences of about 2-6 nucleotides called protospacer adjacent motifs (PAM) which are located downstream the target sequence. Their role in CRISPRi is to increase precision and binding as they are recognised by the dCas9 and this endonuclease binds upstream of the PAM sequences where it blocks transcription by RNA polymerase (Singh *et al*., 2016; Choudhary *et al*., 2015). Therefore, PAM sequences increase specificity of the sgRNA for target sequence recognition (Singh *et al*., 2016; Choudhary *et al*., 2015). Hence, the selection a PAM for the target gene is critical for the functioning of the CRISPRi system (Rock *et al*., 2017).

In this chapter, optimised CRISPR-dCas-mediated transcription interference system (Rock *et al*., 2017) was utilised to transcriptionally knockdown two shikimate pathway genes *tkt* and *aroG* in order to generate screening models suitable for application for isolation of novel shikimate targeting (inhibiting) hits from compound mixture such as plant extracts. The hypothesis was based on previous observations that hypomorphs of enzymes mediating essential pathways are hypersensitive to inhibitors targeting any of the enzymes within the pathway. For that reason, the hypomorphs of shikimate pathway were ideal for the isolation inhibitors of shikimate enzymes.

With this approach, a sustained knockdown of the *tkt* and aroG genes showed their essentiality and vulnerability in *M. smegmatis* hypomorphs. Furthermore, the use of CRISPRi/dCas9 system targeted with *tkt* gene knockdown was showed to be able to potentiate plant extracts with moderate antimycobacterial activity to possess improved activity.

6.2 Materials and methods

An *Escherichia coli-Mycobacterium smegmatis* shuttle plasmid, PLJR962, was used for the CRISPRi/dCas9 gene knockdown experiments. The integrating CRISPRi plasmid expressed both sgRNA with the targeting region and the dCas9 handle which was under the control of the anhydro-tetracycline (ATC) inducible promoters. To generate the CRISPRi/dCas9 system, short oligonucleotides of ~ 21 bases were synthesised and ligated into the Esp3I digested pLJR962 vector backbone (Rock *et al*., 2017). PAM sequences located ahead of the *tkt* (encode transketolase enzyme) and *aroG* (3-Deoxy-D-arabinoheptulosonate 7-phosphate (DAHP) synthase genes were used to guide the design of the target specific oligonucleotides. These designed oligos represent the single guide RNAs (sgRNA) handle on the CRISPRi recombinant plasmid. To create hypomorphs (targeted gene knockdown mutants of *M. smegmatis*), the reconstructed PLJR962, (*tkt* and aroG- CRISPRi/dCas9 plasmids) were transformed into *Escherichia coli* and consequently electroporated into wild type *M. smegmatis*, the details of which are outlined below.

6.2.1 Bacterial growth conditions and maintenance

E. coli and *M. smegmatis* strains used in this study are derivatives of XYL blue and mc^2155, respectively, and their cultures were kept at -80 °C in 66% (v/v) glycerol for storage.

E. coli was cultured in Luria-Bertani (LB) broth (supplemented with 25 µg/mL of Kanamycin when working with transformants), while *M. smegmatis* was cultured in Middlebrook 7H9 supplemented with 0.02% (v/v) glycerol, 10% (v/v) Middlebrook Oleic Acid Dextrose Catalase (OADC), 0.02% (v/v) of 25% Tween80 and 25 μg/ml kanamycin (Kan) in 50 ml Erlenmeyer flasks at 37 °C and incubated in a shaking incubator (IncoShake incubator, Labotec). *E. coli* culture was also grown on LB agar supplemented with 25 µg/mL where required, and Middlebrook 7H10 agar supplemented with 0.05% (v/v) glycerol and 10% (v/v) OADC (± 25 µg/ml Kan).

6.2.2 Isolation of the plasmid PLJR962 (CRSPRi backbone)

Escherichia coli XL1 blue cell containing the PLJR962 plasmid (CRSPRi backbone**)** were purchased from Addgene and stored at the Culture Bank library of Stellenbosch University (Contact: S007015, MTA Order: 582237) (Figure 6.1). The frozen *E. coli* cells were thawed, and a starter culture was prepared by inoculating 10 µL of the cells into 10 mL of fresh Luria-Bertani (LB) broth and incubating overnight at 37 °C with shaking at 200 rpm. The culture (200 µL) was innoculated into 20 mL of LB broth to achieve a 1:100 dilution, followed by incubation until OD600nm of 0.8 was reached. The cells were harvested by centrifugation after overnight incubated at 37^{o}C with 200 rpm shaking. The plasmid was isolated by using the plasmid Miniprep kit following the manufacturer’s protocol. Plasmid concentration was determined using nanodrop spectrophotometer.

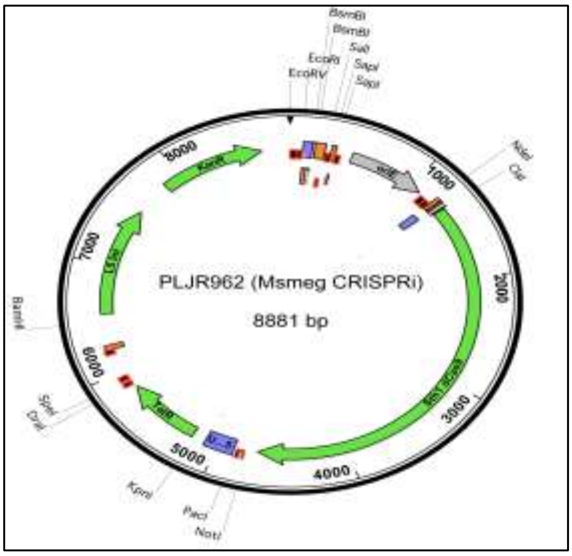

Figure 6. 1: Plasmid PLJR962 designed for the CRISPRi knockdown experiments and used in this study (Rock *et al*., 2017). Anhydrotetracycline inducible TetR expressing Sth1 and dCas9, a single-copy L5 integrating backbone, KanR.

6.2.3 Plasmid digestion with Esp3I restriction enzyme

The PLJR962 plasmid, as shown in Figure 6.1, has Esp3l restriction sites (5' CGTCTC 3') where the sgRNA sequences (inserts) for genes of interest (*tkt* and *aroG*) could be designed to be ligated. Accordingly, PLJR962 plasmid was digested with Esp3I restriction enzyme (Thermo Scientific™). The plasmid digestion was carried out in a 1.5 mL Eppendorf tube and the reagents were added, as described in Table 6.1, in that order. The reaction mixture was mixed by gentle pipetting and centrifuged at 5000 rpm for 60 secs. The tube was incubated in a heat block at 37 °C for 6 hrs. Following incubation, the Esp3I enzyme was deactivated by incubating the reaction at 65 °C for 20 mins in the heat block.

Table 6. 1: Plasmid digestion using Esp3I restriction enzyme.

Reagent	Concentration	Volume (µL)
Nuclease free water	-	16
Tango buffer	10x	2
PLJR962 plasmid	1 µg/µL	1
Dithiothreitol (DTT)	20 mM	1
Esp3I		2

6.2.4 Agarose gel electrophoresis

Digested plasmid was purified from the partially or undigested fragments in the mixture using agarose gel electrophoresis. The agarose gel was prepared by adding 1 g of agarose into 100 mL of 1X Tris base, acetic acid and EDTA (TAE) buffer to make 1% solution. The agarose was completely dissolved by heating and once dissolved, the solution was cooled down by gentle swirling and 10 µL of SYBR green was added and mixed by swirling. The solution was added onto a gel tray before the gel could set while carefully avoiding bubbles and placing the comb immediately after pouring. Once the gel had solidifed, the comb was removed and 1X TAE buffer was poured in the electrophoresis tank until the gel was slightly submerged. A 1 kb plus ladder was used and prepared for loading by adding 18 µL of nuclease free water, 1 µL of the ladder and 2 µL of loading dye. The undigested plasmid was used as the positive control. Two microlitres (2µL) of loading dye was added to all the digested samples to track electrophoresis run progression. Samples were loaded into the wells and electrophoresis was run for approximately 3 hrs at 95 V. Gels were visualised using ultraviolet light (UV) to locate the position of the CRISPRi backbones as green fluorescing bands. The bands were cut out of the gel using sterile surgical blades and transferred to 2 mL Eppendorf tubes. The plasmid was recovered from the agarose gel using a gel recovery kit following the manufacturer's protocol. Concentration of the purified plasmid was determined using NanoDrop ND-1000 spectrophotometer (Thermo Scientific). The samples were stored at -20 °C until further use.

6.2.5 Design and annealing of oligonucleotides

To construct the *tkt* and *aroG* CRISPRi system in *M. smegnatis*, a 20-bp oligonucleotide sequences (sgRNA) were selected by first identifying the PAMs (Table 6.2) in the promoter region, 5'untranslated region (UTR) and coding sequence of these genes. The strengths of gene knockdown, expressed as fold repressions, could be guided by PAM sequence as previously determined, and were used in this study to choose a PAM with the strongest rest fold repression (see table 6.2 (Rock *et al*., 2017). Given previous studies showing that targeting of the nontemplate strand of a gene's promoter or coding region as most efficient for CRISPRi-mediated gene silencing (Rock *et al*., 2017), sgRNAs that target the non-template strand of *tkt* and *aroG* sequences, located between the transcription start site and the coding region, were generated. The exact location was dependent on the location of species-specific

PAMs for each gene. The selected target-specific complementary oligonucleotides, *forward* and *reverse* were synthesised. The oligos were designed to have sticky ends, which easily form complementary bonds with the sticky ends on the CRSPRi backbone created by Esp3I restriction enzyme.

The synthesised oligonucleotides were annealed prior to ligation into the CRISPRi backbone. The annealing buffer contained 50 mM Tris, 50 mM NaCl and 1 mM EDTA and the solution pH was adjusted to 7.5. Into a PCR tube, 42 µL of the annealing buffer was added, followed by the addition of 4 µL of the forward oligonucleotides and 4 µL of the reverse oligonucleotides, respectively. The oligonucleotides concentration was 100 µM in nuclease free water. The oligonucleotides were annealed using a PCR program in the thermocycler. The annealing conditions were set at a denaturation phase of 95 ^{o}C for 2 min followed by an annealing step incorporating a decline in temperature from 95 ^{o}C to 25 ^{o}C at a 0.1 ^{o}C per second interval (T100TM Thermal cycler, BioRad). After the program ran, the annealed oligonucleotides were stored at -20 °C until further use.

6.2.6 Ligation of oligonucleotides and CRISPRi backbone

DNA ligase was used to ligate the annealed *tkt* and *aroG* oligonucleotides from PCR and CRISPRi backbone obtained from the digestion of the PLJ962 plasmid (Section 6.2.3). The ligation reaction was prepared by first adding 1 µL of the annealed oligonucleotides to a 0.5 mL tube, followed by addition of 0.5 µL of ± 50 ng/µL CRISPRi backbone (Esp3I digested plasmid). A volume of 1 µL of T4 DNA ligase buffer (amount?) was added to the reaction followed by 0.5 µL of T4 DNA ligase enzyme (NEB; 2 000 000 unites/mL). The reaction was topped up with 7 µL of nuclease free water to make 10 µL of ligation reaction. The reaction was incubated at room temperature and allowed to progress overnight. Thermal deactivation of the T4 DNA ligase was achieved by incubating the tubes at 65 °C in a heat block for 10 mins. The samples were stored at 4 °C until required for transformation. These resulting recombinant PLJR962 plasmids as shown in Figure 6.1 contained sites for cloning the target specific complementary sequences of the *tkt* and *aroG* genes followed by dCas9-binding hairpin sequence (dCas9 handle) and a transcriptional terminator (Rock *et al*., 2017).

Table 6. 2: Oligonucleotide sequences designed for different protospacer adjacent motif (PAM) of the *tkt* and *aroG* genes.

Gene	Direction	Oligo sequence	PAM	Fold repression
Transketolase genes				
tkt gene PAM 1	Forward	5'-GGGAGCCGCATGTAATCCGAGAACTG-3'	CTTCC	145.2
	Reverse	5'-AAACCAGTTCTCGGATTACATGCGGC-3'		
tkt gene PAM 2	Forward	5'-GGGAGTCAGGCTCGAATGCCCGCAGG-3'	ATCCT	64.7
	Reverse	5'-AAACCCTGCGGGCATTCGAGCCTGAC-3'		
DAHP synthase gene				
aroG gene PAM 1	Forward	5'-GGGAATCGCGGAGCATCTCCGCGAC-3'	GTTCT	120.5
	Reverse	5'-AAACGTCGCGGAGATGCTCCGCGAT-3'		
aroG gene PAM 2	Forward	5'-GGGAGTCTCGGCCGGGTTGGACAGGC-3'	ATGCT	84.6
	Reverse	5'-AAACGCCTGTCCAACCCGGCCGAGAC-3'		

6.2.7 Cloning of recombinant *tkt* and aroG-PLJR962 plasmids in *E. coli*

6.2.7.1 Generation of competent *Escherichia coli* XL1 blue cells

Escherichia coli cells were made competent to enable an increased permeability for the uptake of the plasmid. Competency was achieved using the Rubidium chloride protocol. Briefly, a starter culture was prepared by inoculationg 10 µL of thawed *E. coli* freezer stock into 10 mL of fresh Luria-Bertani (LB) broth and incubating overnight at 37 °C with shaking at 200 rpm. The resulting culture was sub-cultured into 20 mL of LB broth at a 1:100 dilution and incubated until OD600nm of 0.5 was reached. The culture was transferred to a 50 mL tube and incubated on ice for 15 mins. Cells were harvested by centrifugation at 4 °C for 10 mins at 4500 rpm. The supernatant was discarded, and the cells were resuspended to a volume of 30 mL using the Tbf I buffer and then incubated on ice for 15 mins. The cells were centrifuged at 4500 rpm for 10 mins at 4 °C, the supernatant was discarded, and the pellet was resuspended with 6 mL of Tbf II buffer on ice. Aliquots were made into cryotubes, and cells were stored at -80 °C until further use. Table 6.3 shows the composition of reagents used for the preparation of the Tbf I and II buffers.

Table 6. 3: Composition of Tbf buffer I and II.

Tbf I buffer		
Chemical	Concentration	Composition in 500 mL
Rubidium chloride (RbCl)	100 mM	7.25 g
Manganese(II) chloride tetrahydrate ($MnCl_2 \cdot 4H_2O$)	50 mM	5 g
Potassium acetate (CH_3COOK)	30 nM	14.7 g
Calcium chloride dihydrate ($CaCl_2 \cdot 2H_2O$)	10 mM	0.75 g
Glycerol	15%	75 mL
Distilled water (H_2O)	-	425 mL
Tbf II buffer		Composition in 400 mL
0.2 M MOPS	10 mM	20 mL
Rubidium chloride (RbCl)	10 mM	0.48 g
Calcium chloride dihydrate (CaCl2·2H_2O)	75 mM	4.4 g
Glycerol	15%	60 mL
Distilled water (H_2O)	-	320 mL

Key: MOPS: 4-Morpholinepropanesulfonic acid, 3-(N-Morpholino) propane sulfonic acid.

6.2.7.2 Transformation of competent *Escherichia coli*

The heat-shock protocol was used for the transformation of competent *E. coli* cells. Briefly, -80 °C stocks of competent *E. coli* cells were thawed on ice and 50 µL of the cells were transferred to a sterile 2 mL Eppendorf tube containing 5 µL of the recombinant PLJR962 plasmid with the inserted *tkt* and *aroG* oligos. This mixture was immediately incubated on ice for 30 mins. The undigested PLJR962 plasmid was used as a positive control, as such, it was also transformed into *E. coli*. After 30 mins, the cells were heat-shocked in a heat block at 42 °C for 90 secs. The tubes were immediately incubated on ice for 5 mins. Luria-Bertani (LB) broth pre-warmed to 37 °C was used to rescue the transformed cells by adding 950 µL of this media to the transformation mixture and incubated for 2 hrs at 37 °C with shaking at 200 rpm. The cells were harvested by centrifugation at 5000 rpm for 5 mins and the 900 µL of the supernatant was removed to leave 100 µL with the pellet. The pellet was mixed with the remainder of the supernatant and spread-plated onto LB agar plates containing kanamycin at a final concentration of 0.02 mg/mL and incubated at 37 °C for 24 hrs or until visible colonies appear.

6.2.8 DNA sequencing

Random single colonies of the transformants that grew on the LB-kanamycin plates were picked from the agar plates and inoculated into LB broth containing kanamycin (0.02 mg/mL). The culture was incubated at 37 °C for 24 hrs, and thereafter, sub-cultured to OD600nm of 0.1. The subculture was allowed to grow to OD600nm of 0.8, where aliquots were made for freezer stocks (-80 °C storage). The remaining culture was used to isolate the transformed plasmid. Plasmid isolation was achieved using Qiagen miniprep kit by following the protocol described by the manufacturer. The isolated plasmid samples were sent for sequencing to validate the successful insertion of the *tkt* and *aroG* sgRNAs into the CRISPRi backbone (plasmid PLJR962).

The presence of all sgRNA inserts in respective constructs was validated by sequencing, conducted by the Central Analytical Facility (CAF) at the University of Stellenbosch using Sanger sequencing methods. Sequencing results were read using the FinchTv 1.4.0 free software (https://digitalworldbiology.com/finchTv). The received sequencing reads were compared to the predicted sgRNA sequence to verify successful cloning.

6.2.9 Cloning of recombinant CRISPRi constructs in *M. smegmatis*

6.2.9.1 Preparation of competent wild type *M. smegmatis* (mc^2 155)

From a thawed freezer stock, a 100 µL of *M. smegmatis* culture was inoculated in 10 mL fresh Middlebrooks 7H9 (Fluka) broth containing glycerol (Sigma) and Middlebrooks Oleic Albumin Dextrose Catalase (OADC) growth supplement (Sigma) and Tween-80 and incubated at 37 °C for 48 hrs with shaking at 200 rpm. The culture was sub cultured to OD600nm of 0.05 and incubated at 37 °C shaking at 200 rpm until OD600nm reached 0.8. The cells were harvested by a centrifugation of 45 mL of the culture at 3901 rcf for 10 mins at a temperature of 4 °C in two separate 50 mL centrifuge tubes. The supernatant was discarded, and the pellet was resuspended in a 20 mL of filter-sterilised 10% glycerol while keeping the cells on ice. The cells were centrifuged at 3901 rcf for 10 mins at a temperature of 4 °C. The supernatant was discarded, and the pellet was resuspended in 15 mL of 10% filter-sterilised glycerol while keeping the cells on ice. The resuspension was centrifuged again using the same parameters described in the protocol. The supernatants were discarded, and the pellets resuspended with 10 mL of 10% filter-sterilised glycerol. The resuspensions from the two 50 mL tubes were mixed together to make a 20 mL total resuspension and subsequently centrifuged at 3901 rcf for 10 mins at a temperature of 4 °C. The pellet was resuspended in a 2 mL 10% glycerol, and 400 µL were aliquoted into 1.5 mL cryotubes and stored at -80 °C until use for electroporation.

6.2.9.2 Transformation of competent *Mycobacterium smegmatis* cells

An electroporation method was used to transform competent *M. smegmatis* cells with sequence verified CRISPRi plasmids. Freezer stocks of competent *M. smegmatis* cells (400 µL) were thawed on ice. 2µL of 5 ng/µL of the recombinant CRISPRi plasmid was added to 400 µL competent cells. The cells were maintained on ice during the entire electroporation procedure. PLJR962 plasmid without an insert was used as a positive control. Electroporation was carried out with a Biorad gene pulser II in a 0.2 cm electroporation cuvette with the following parameters set for gene pulser, current: 2500V, capacitance; 25 µF and resistance of 1000 Ω. After electroporation, the cells were immediately rescued using Middlebrooks 7H9 (Fluka) broth containing glycerol (Sigma) and Middlebrooks Oleic Albumin Dextrose Catalase (OADC) growth supplement (Sigma) and Tween-80, and incubated at 37 °C for 4 hrs with shaking at 200 rpm. The tubes were centrifuged at 16100 rcf for 60 secs. The supernatant was discarded leaving 100 µL was left behind, which was used to resuspend the pellet. The electroporated culture (100 µL) was inoculated on Middlebrooks 7H10 agar media containing glycerol (Sigma), OADC growth supplement (Sigma) and 0.02 mg/mL kanamycin as the selectable marker. Competent *M. smegmatis* cells (100µL) were used as negative control and were also inoculated in the 7H10-kanamycin selective media. The plates were incubated at 37 °C for 3 days for appropriate colony formation.

Randomised selection was used to pick colonies that were able to grow on the kanamycin supplemented 7H9 plates. The picked colonies were inoculated in 10 mL of Middlebrooks 7H9 (Fluka) broth containing glycerol (Sigma), OADC growth supplement (Sigma), Tween-80 and 0.02 mg/mL kanamycin. ThIs starter culture was sub-cultured to OD600nm of 0.05 and incubated at 37 °C shaking at 200 rpm until OD600nm reached 0.8. Glycerol freezer stocks were prepared and stored in 1.5 mL cryotubes and stored at -80 °C until further use.

6.2.10 Phenotypic characterisation

6.2.10.1 Testing *tkt* and *aroG* CRISPRi constructs functionality in *M. smegmatis*

The spot assay was used to test the essentiality of the selected gene on *M. smegmatis* growth and consequently confirming the functionality of the designed CRISPRi system in *M. smegmatis*. The CRISPRi strains were cultured in Middlebrooks 7H9 (Fluka) broth containing glycerol (Sigma), OADC growth supplement (Sigma), Tween-80 and 0.02 mg/mL kanamycin for 24 hrs. For the spot assay, petri-dish plates with Middlebrooks 7H10 agar plates containing glycerol (Sigma), OADC growth supplement (Sigma), 0.02 mg/mL kanamycin (KAN) were split into those supplemented with or without 0.5 µg/mL anhydrotetracycline (ATC). A grid was drawn on the outer surface lid of the petri dish as a guide to the inoculation of culture dilutions. Culture dilutions (10^0, 10^{-1}, 10^{-2}, 10^{-3}) (20 µL) of the overnight culture at log phase were inoculated onto the petri dishes. Plates only supplemented with KAN were used as controls. The plates were incubated for 48 hrs at 37 °C.

6.2.10.2 Determination of MIC in liquid media using broth micro-dilution assay

Minimum inhibitory concentrations (MICs) of ATC and shikimate inhibitors; naringin and 2-amino-benzothiazole were determined against the generated *M. smegmatis tkt* CRISPRi mutants using the broth microdilution assay. Inoculum of the mutant strains were grown in Middlebrook 7H9 broth base containing glycerol and Middlebrook oleic albumin dextrose catalase (OADC) growth supplement. A Starter culture was prepared in 10 mL media, incubated in a shaker, with 200 rpm shaking at 37 °C until OD600nm between 0.4-0.6 was reached. Thereafter, the culture was sub-cultured in 50 mL OADC-glycerol-Middlebrooks 7H9 media at OD600nm of 0.005 and incubated in a shaker, with 200 rpm shaking at 37 °C until an OD600nm between 0.2-0.3 was reached (approximately 12 hours). The culture was 100x diluted before adding to plates.

One hundred microlitres (100 µL) of Middlebrook 7H9 broth base containing glycerol (Fluka 49769) and OADC growth supplement and was added into the 96-well microtitre plates. Working concentrations of Rifampicin (400 µg/mL), anhydrotetracycline (400 µg/mL), naringin (10 mg/mL) and 2-amino-benzothiazole (10 mg/mL) were filter sterilised using a 0.22 µm nylon syringe filter. The drugs were serially diluted into two folds with the Middlebrook's 7H9 broth base added in the plate. This was followed by the separate inoculation of 100 µL of the prepared *M. smegmatis tkt* mutant cultures into each well. Negative control cells contained only a culture medium without the extracts while the positive controls contained was rifampicin. The plates inoculated with *M. smegmatis* were incubated at 37 °C for 48 hrs, thereafter, 20 µL of 0.22 µm syringe filtered 0.02% Resazurin dissolved in distilled water was added. The plates were incubated for 4 hrs for optimal colour development. Bacterial growth in the wells was indicated by a change in colour from blue to pink, where blue showed the inhibition of cell growth and pink showed cell viability.

6.2.10.3 Phenotypic assessment of CRISPRI strain exposed to varying concentrations of ATC and aminoB

Cultures od CRISPRi strains targeting *tkt* PAM 1 (stronger PAM) and PAM 2 (weaker PAM) allowed to grow overnight at 37 ºC to reach exponential phase OD600nm of approximately 0.5 (Incoshake incubator, LaboTech). The cultures were then inoculated to a final OD600nm of 0.1 in 25 mL of OADC-glycerol Middlebrook's 7H9 broth media containing 25 µg/ml Kan and different concentrations of ATC (2, 1, 0.5, 0.25, 0.1, 0.05 µg/mL), 2-amino-benzothiazole (200, 100, 20, 2, 1, 0.5, 0.1 µg/mL) and Naringin (200, 20, 2, 1, 0.5, 0.1 µg/mL) in relevant flasks. Cultures inoculated in media without ATC, 2-amino-benzothiazole and Naringin were used as controls. Cultures were incubated at 37 ºC with shaking at 200 rpm for 24 hrs, were at the 24th hr, the OD600 of the cultures was recorded using Novaspec Plus visible spectrophotometer (Amersham Biosciences).

6.2.10.4 Growth curves of CRISPRi strains to evaluate gene knockdown by CRISPRi system

To monitor the growth effect upon CRISPRi activation, CRISPRi mutant strains were inoculated from log phase cultures into Middlebrooks 7H9 (Fluka) broth containing glycerol (Sigma), OADC growth supplement (Sigma), Tween-80 and 0.02 mg/mL kanamycin. Cultures were incubated at 37◦C with shaking at 200 rpm. When the OD600nm reached 0.5-0.6, the cultures were split into equal volumes to an initial OD600nm of 0.1 and then incubated with or without ATC. The ATC was added to the media to a final concentration of 500 ng/mL to moderately induce the expression of dcas9 and the sgRNA targeting the *tkt* and *aroG* sequences, respectively. The cultures were incubated at 37◦C with shaking at 200 rpm and sampled in 3, 6, 9, 18, 24 hr intervals, where OD600nm was determined using a UV/VIS spectrophotometer. *M. smegmatis* strain containing an empty insert (PLJR962 without target genes) was used as a positive control. Results were expressed as means of duplicate ± standard deviation (SD) of two biological replicates.

6.2.10.5 Effect of medicinal plants in the CRISPRi *M. smegmatis* mutants

Growth curves of *tkt* CRISPRi strains were performed to evaluate the effect of the plant extracts on their growth. Briefly, a final OD600nm of 0.1 of log phase *tkt* mutants were prepared in 20 mL Middlebrooks 7H9 (Fluka) broth containing glycerol (Sigma), OADC growth supplement (Sigma), Tween-80 and 0.02 mg/mL kanamycin and/or 0.5 µg/mL ATC. The plant extracts (1 mg/mL) were added to relevant flasks containing KAN and/or ATC. Cultures inoculated in media with only KAN were used as a control. The cultures were incubated at 37◦C with shaking at 200 rpm and sampled in 3, 6, 9, 18, 24 hr intervals, where OD600 was determined using a UV/VIS spectrophotometer. Results were expressed as means of duplicate ± standard deviation (SD) of two biological replicates.

6.2.10.6 Combinational effects of 2-amino-benzothiazole and plant extracts

To evaluate possible interactions between the shikimate inhibitor 2-amino-benzothiazole and the plant extracts, growth curves of treated *tkt* CRISPRi strains were performed. *M. smegmatis tkt* mutants in a log phase were cultured to a final OD600 0.1 in Middlebrook's Middlebrooks 7H9 (Fluka) broth containing glycerol (Sigma), OADC growth supplement (Sigma), Tween-80, 0.02 mg/mL kanamycin supplemented with 20 µg/mL of 2-amino-benzothiazole and 1 mg/mL of each respective plant extract. Cultures inoculated in media with only KAN were used as a control. The cultures were incubated at 37◦C with shaking at 200 rpm and sampled in 3, 6, 9, 18, 24 hr intervals, where OD600nm was determined using a UV/VIS spectrophotometer.

6.2.11 Rescue experiments

The rescue experiments were conducted to evaluate whether the gene depleted knockdown strains of the *aroG* and *tkt M. smegmatis* CRISPRi strains could regain growth metabolism when exogenously provided with some essential shikimate intermediates. The possibility that host-derived metabolites might rescue antibiotic-mediated nutrient auxotrophy is a key concern in targeting metabolic pathways for new TB drug development. Briefly, *tkt* and *aroG* CRISPRi strains were cultured to maintain an OD600nm of 0.1 in 20 mL Middlebrooks 7H9 (Fluka) broth containing glycerol (Sigma), OADC growth supplement (Sigma), Tween-80 and 0.02 mg/mL kanamycin and 0.5 µg/mL ATC, respectively. The cultures were incubated at 37◦C with shaking at 200 rpm and samples collected after 24 hrs, where OD600nm was determined using a UV/VIS spectrophotometer. These cultures represented the first passage of ATC and non-ATC treated *tkt* and *aroG M. smegmatis* mutants. For the rescue experiment using plant extracts, the first passage of the cultures included those treated with 1 mg/mL of each extract and incubated similarly under the same conditions.

This first passage (after 24 hr treatment with ATC and extracts) consists of *M. smegmatis* mutants that had been moderately depleted of their *tkt* and *aroG* gene expressions and gene products, thus growth inhibition. To evaluate the possibility of rescue, 20 mL of Middlebrook's 7H9 media supplemented with 20 mM of L-tyrosine, L-tryptophan (20 mM), L-phenylalanine (20 mM) and 0.05 mg/mL shikimic acid were prepared. The ability of each intermediate to mitigate *tkt* or *aroG* gene depletion would result in improved growth relative to the un-supplemented ATC-exposed culture. The culture from the first passage was inoculated from ATC and AAA supplemented media and incubated for a further 24 hrs. This represented the second passage. OD600 was determined using a UV/VIS spectrophotometer. Cultures inoculated in Middlebrook's media with only KAN were designated as the controls for this experiment.

6.2.12 Quantitative real time polymerase chain reaction

6.2.12.1 RNA extraction protocol

M. smegmatis culture grown in Middlebrooks 7H9 (Fluka) broth containing glycerol (Sigma), OADC growth supplement (Sigma), Tween-80 and 0.02 mg/mL kanamycin and 0.5 µg/mL ATC were appropriate. The culture at OD600nm 0.5 was pelleted by centrifuging at 5000 rpm for 10 mins at 25 ^{o}C. The supernatant was decanted, and the pellet was resuspended in 1 mL RNApro Solution/TRIzol. The suspension was transferred to a Lysing Matrix tube and through ribolysation, the cells were disrupted (speed = 4 m/s^{-1}, 40 sec, 3 times and cooling on ice for 1 min between each session.

Cellular debris was cleared from the solution by centrifugation at 12 00 x g for 15 mins at 4 C. The supernatant was transferred to a clear 1.5 mL microcentrifuge tube and incubated at room temperature for 5 mins. This process allowed for the dissociation of nucleoprotein complexes. To this solution, 300 μL of chloroform was added and the solution vortexed for 20 mins followed by periodic inversion of the tubes at room temperature for 5 mins. The solution was centrifuged for 10 mins at 12 000 x g at 4 C and the upper aqueous phase (250 μL) was transferred to a new clean 1.5 mL Eppendorf tubes taking care not to disrupt the interphase containing the DNA and protein. Absolute ethanol (500 μL) was added to the aqueous phase in the Eppendorf tube and the solution was gently inverted several times (~5 times) and carefully loaded directly onto the membrane of a NucleoSpin RNA II column. For RNA isolation and washing, the tube was incubated at room temperature for 2 mins followed by centrifugation for 30 sec at 11 000 x g and the resulting supernatant was transferred to new 2 mL collection tubes. To this supernatant, 350 μL of membrane desalting buffer was added and the solution incubated at room temperature for 2 mins. The solution was centrifuged at 11 000 x g for 30 sec. Dnase solution (96 μL) was added to the column membrane and incubated at room temperature for 30 mins. A RAW2 buffer (200 μL) was added and the solution incubated for 2 mins at room temperature. The solution centrifuged at 11 000 x g for 30 sec and a column was placed in a new 2 mL tube followed by the addition 600 μL of RAW3 buffer and 2 min incubation at room temperature. The solution was centrifuged for 2 mins at 11 000 x g and to now elute the RNA, the column was placed in a nuclease free 1.5 mL Eppendorff tube. Rnase-free water (30 μL) was used to elute the RNA and the tubes were centrifuged for 1 min at 11 000 x g. The concentration of the RNA was determined using a nanodrop spectrophotometer. The RNA samples were stored at -80 C until further use.

6.2.12.2 qRT PCR

Purification through denaturing agarose gel electrophoresis and determination of RNA sample intensities was conducted by the Central Analytical Facility (CAF) at the Stellenbosch University. TapeStation Analysis Software 4.1 and RNA ScreenTape® were used for RNA analysis. Quantitative polymerase chain reaction (qPCR) was used to evaluate the level of *tkt* gene inhibition, through comparing the quantity of mRNA expression from ATC treated and untreated *tkt* CRISPRi strain. The RNA samples were sent to Inqaba (Pty) Ltd for qPCR and the designed primers are shown in Table 6.4.

Table 6. 4: A list of primers for qRT-PCR in this study.

Primer	Primer sequence	Length of primer	Amplicon size
tkt PAM 1			
Forward	5’-CTCGCGTACACGCTGTT-3’	17	
Reverse	5’-CCGAGGTAGAGCTGGATGTA-3’	20	128
RT primer			
Reverse	5’-GAAGAGCGTGCTGGAGC-3’		

6.2.13 Bioinformatics analysis tools

Gene identifier: The Mycobrowser (http://mycobrowser.epfl.ch) database was used to identify the gene of interest, *tkt* (MSMEG_3103) and *aroG* (MSMEG_4244), and homologs found in other mycobacterial species such as *M. smegmatis*.

6.3 Results

6.3.1 Plasmid digestion and agarose gel electrophoresis

Agarose gel electrophoresis was used to check the progression of digestion by Esp3I restriction enzyme, which has two restriction sites on PLJR962 plasmid. Therefore, Esp3I produced two linearised DNA fragments, one larger than the other (Figure 6.2). The undigested PLJR962 plasmid (P) was used as control and demonstrated various conformations; supercoiled, linear, and open circular (Figure 6.2).

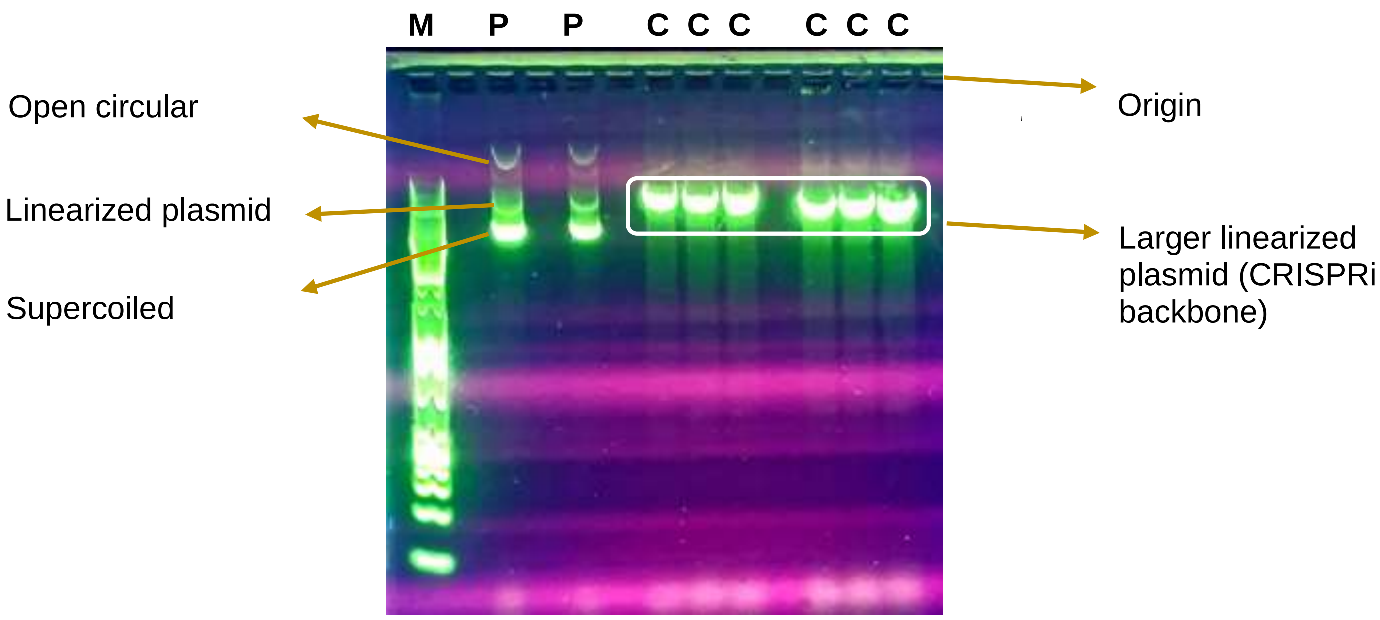

Figure 6. 2: Agarose gel electrophoresis of PLJR962 plasmid DNA (P) digested with Esp3I type II endonuclease enzyme to introduce double-stranded cuts, which produced linearised plasmid fragments (C). Agarose gel was visualised by the fluorescence of SYBR™ Green gel stain under ultraviolet light.

Key: M: Molecular marker, P: Undigested PLJR962 plasmid, C: Linearised plasmid to be used as the CRISPRi backbone in recombination with target-specific oligonucleotides.

6.3.2 Transformation of *E. coli* with recombinant *tkt* and *aroG* plasmids

The *tkt* and *aroG* recombinant plasmids were transformed into competent *Escherichia coli* cells by heat shock. Selection of successful transformants was achieved by plating cells on kanamycin supplemented LB agar plates where kanamycin was used as a selectable marker (Figure 6.3). As expected, only cells that were able to assimilate functional recombinant PLJR962 plasmid grew in kanamycin-supplemented plates.

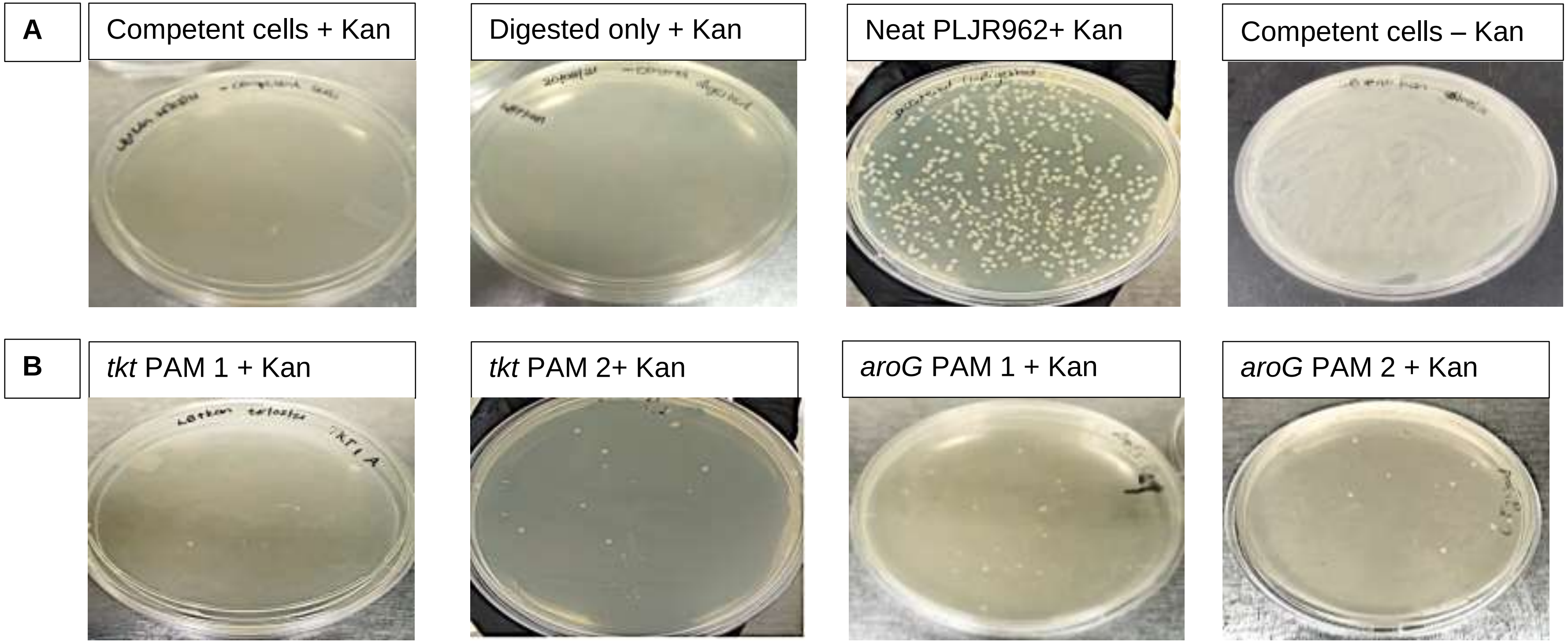

Figure 6.3: Transformed *Escherichia coli* cells cultured on LB agar supplemented with kanamycin. Kanamycin was used as a selectable marker for selection of positive transformants.

Key: A: Experiment controls, B: *tkt* and *aroG E. coli* transformants

6.3.3 Transformation of *M. smegmatis* with recombinant *tkt* and *aroG* plasmid

Sequence validated *tkt* and *aroG* recombinant plasmids were electroporated into competent *M. smegmatis* cells. Kanamycin supplemented 7H10 Middlebrooks agar plates were used to select successful transformants. Figure 6.4 shows that colonies of the *M. smegmatis* mutants. Growth on Kanamycin plated indicated that they possessed functional CRISPRI plasmid with tet^R gene.

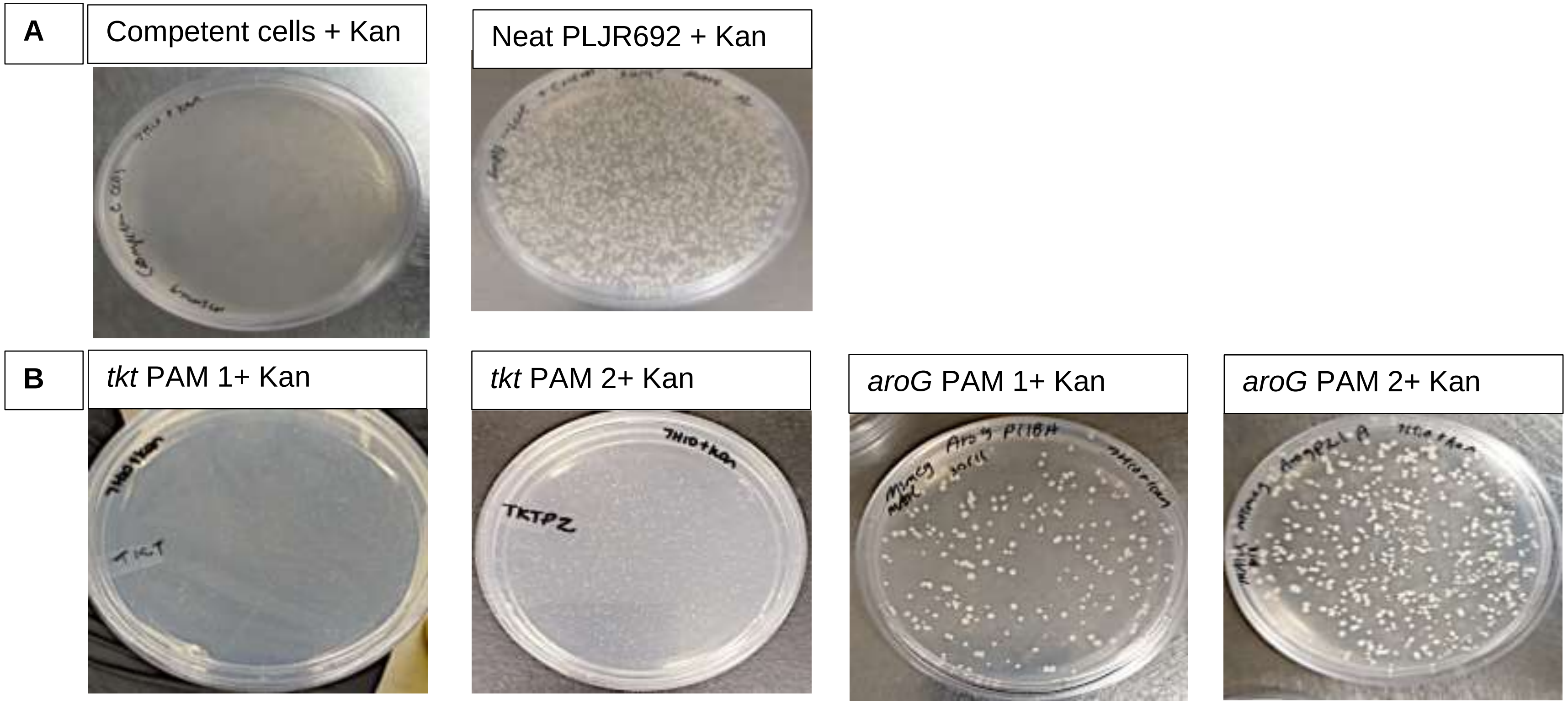

Figure 6. 4: Transformed *M. smegmatis* ells cultured on Middlebrook's 7H10 agar supplemented with kanamycin. Kanamycin was used as a selectable marker for selection of positive transformants.

Key: A: Experiment controls, B: *tkt* and *aroG E. coli* transformants

6.3.4 Evaluation of CRISPRi functionality in *M. smegmatis tkt* and *aroG* hypomorphs

To assess the functionality of the designed CRISPRi system and validate the gene essentiality of the *tkt* and *aroG* genes, a spot assay was conducted. The activation of the CRISPRi system by ATC demonstrated that the depletion of the *tkt* gene in the *M. smegmatis* hypormphs had a greater inhibition of growth compared to *aroG* depletion (Figure 6.5). These results demonstrated the ability of CRISPRi to achieve substantial inhibition of gene expression in *M. smegmatis* sufficient to cause a clear growth phenotype.

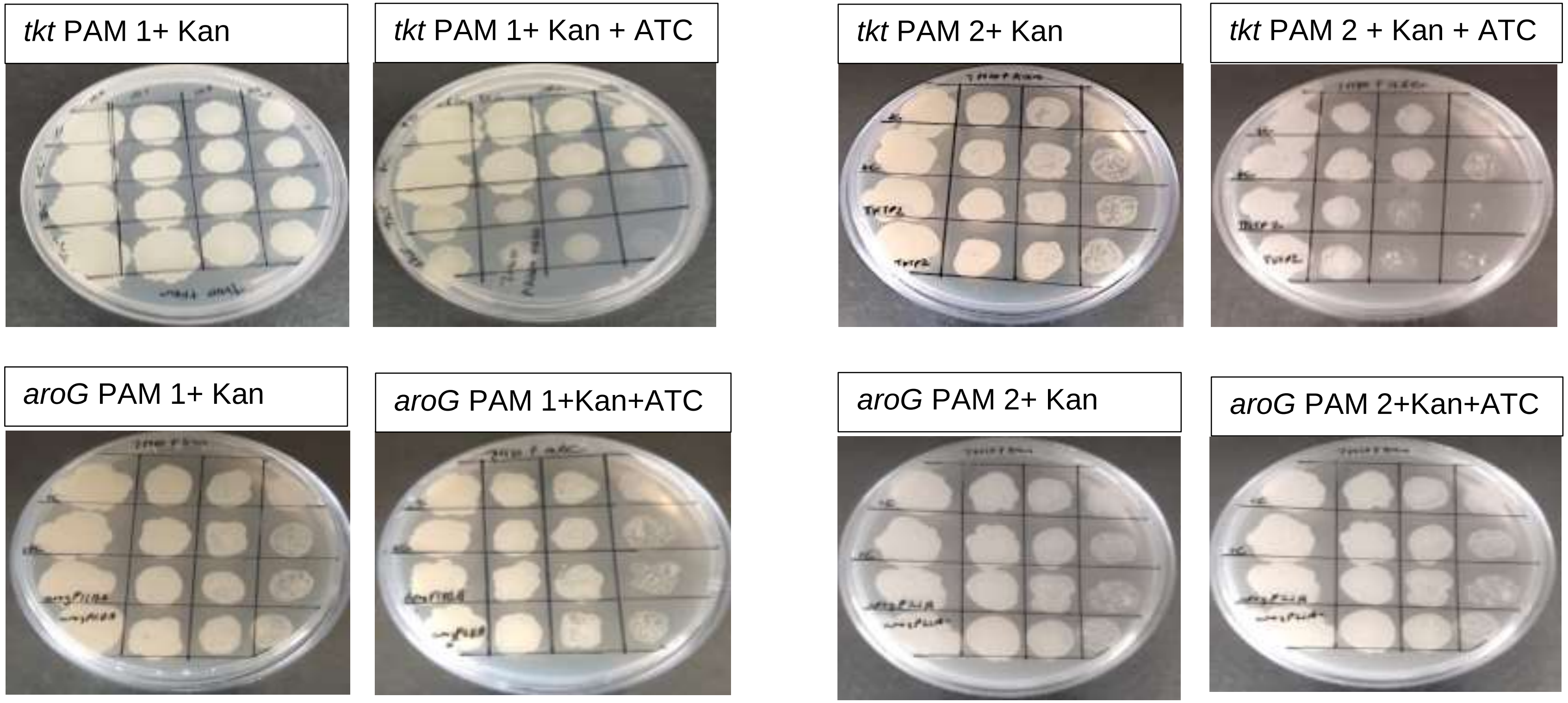

Figure 6. 5*:* Spot assay used to assess the functionality of CRISPRi system in *Mycobacterium smegmatis tkt and aroG hypomorpths*

Key: A: Experiment controls, B: *tkt* and *aroG E. coli* transformants

6.3.5 Growth curves

To study the effect of depletion of *tkt* and *aroG*, the various *M. smegmatis* CRISPRi strains were grown with and without ATC. No difference was observed for any of the mutants during the first 9 hrs of ATC treatment compared with the neat controls, suggesting that the mRNA, the corresponding proteins and/or metabolites were still present and functional in the cells, and needed to be depleted before a phenotype could be observed. A decrease in bacterial growth from 18 hrs in the presence of ATC was detected (Figure 6.6). This indicated that the *tkt* and *aroG* CRISPRi\dCas9 gene silencing became significantly active from about 18 hrs.

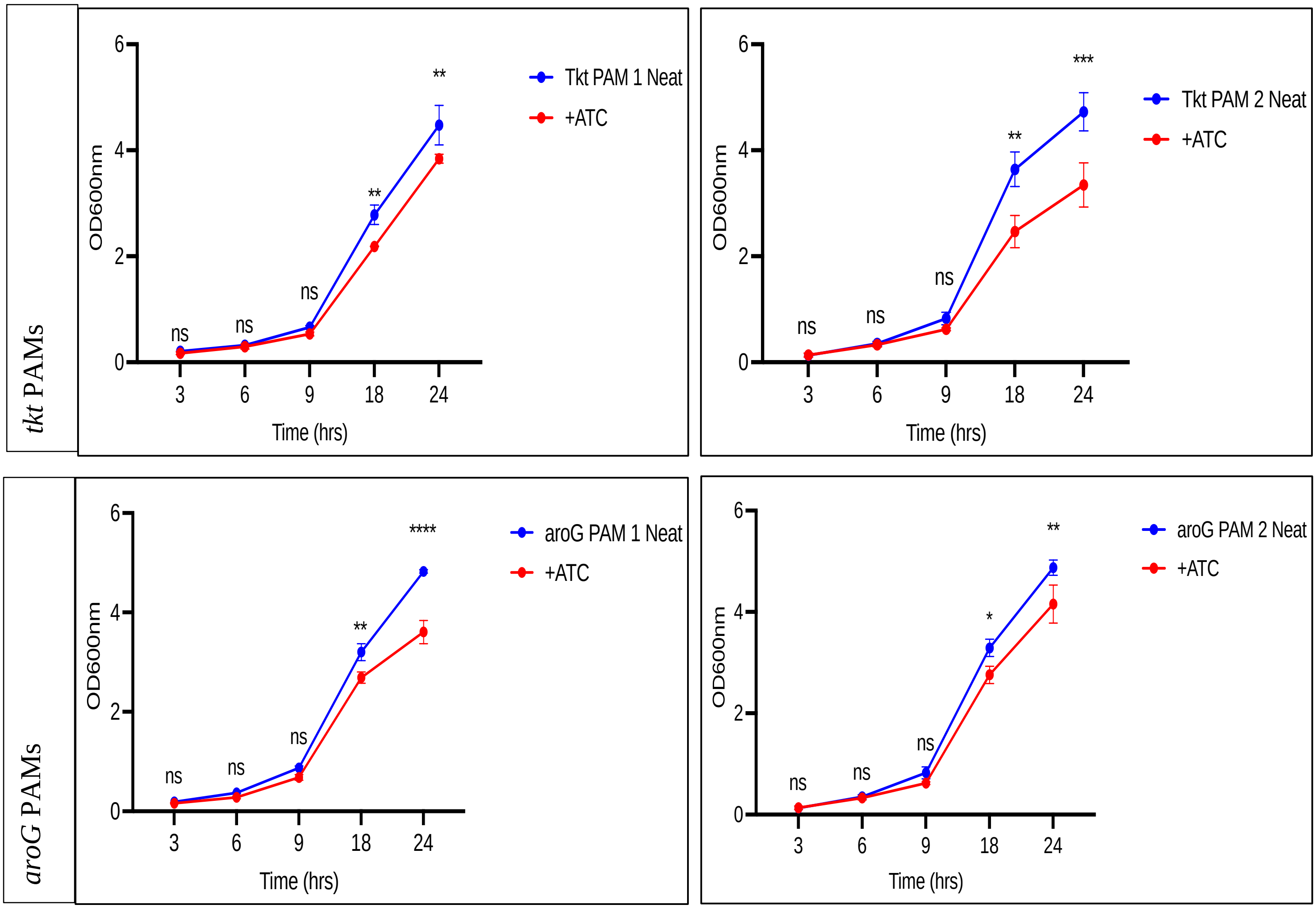

Figure 6.6: Growth curves of *M. smegmatis tkt* and *aroG* hypomorphs. Induction of target specific gene knockdown of *tkt* and *aroG* genes by anhydrotetracycline (ATC) activated CRSPRi/dCas9 system results in growth inhibition of *M. smegmatis* hypomorphs.

6.3.6 RNA isolation and qRT-PCR

The denaturation agarose gel showed that the RNA samples had two bands of different intensities (Figure 6.7), which represented the 16S and 23S. As expected, the larger 23S unit had a larger band and higher intensity than the smaller 15S unit as seen on the agarose gel in Figure 6.8. The same band patterns were observed in the control; however, it was observed that the control bands were slightly more fluorescent than the mutant isolated RNA, suggesting the control had more RNA than the *tkt* CRISPRi strain. This was confirmed by comparing the relative fluorescence intensities, in Figure 6.8, where the RNA isolated from *tkt* PAM1 and PAM 2 mutants have a slightly lower fluorescent intensity than the untreated control. Based on the normal fold change in gene expression evaluation using qRT-PCR, it was clear that indeed, the designed CRISPRi/dCas system depleted the expression of the *tkt* gene (Figure 6.9).

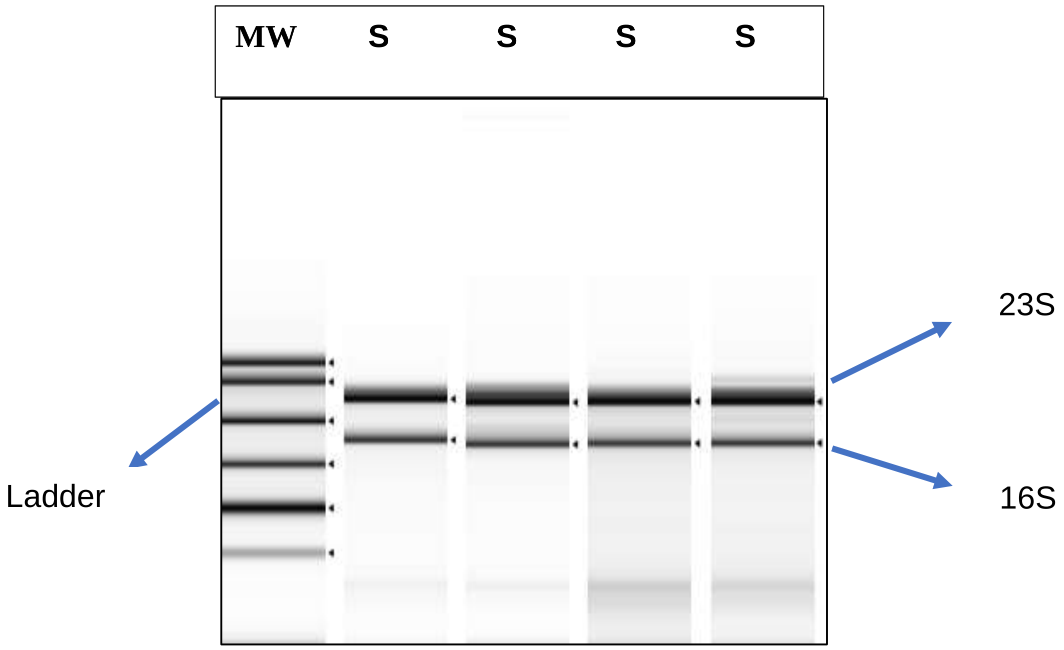

Figure 6. 7: Agarose gel electrophoresis of isolated RNA from *M. smegmatis* wild type untreated control and ATC treated *M. smegmatis* tkt PAM 1 and PAM 2 CRISPRi strains.

Key: MW: Molecular marker, S: RNA samples isolated from ATC treated M. smegmatis tkt PAM 2 hypomorphs

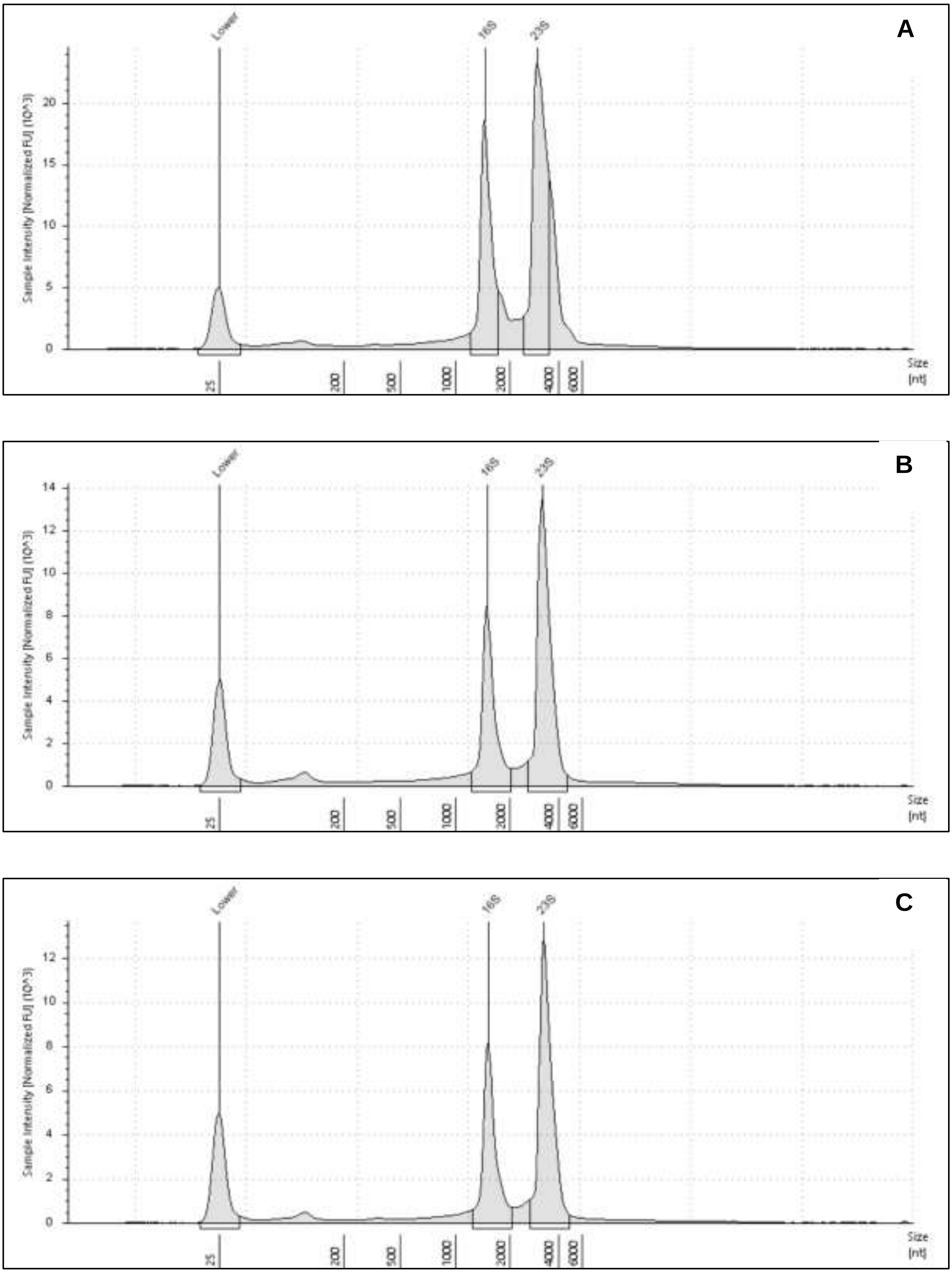

Figure 6. 8: Relative fluorescence intensities of RNA samples isolated from M. smegmatis untreated control (A), *M. smegmatis tkt* PAM 1 mutant and *M. smegmatis tkt* PAM 2 CRISPRi strains.

Table 6. 5: Concentrations of eluted RNA samples from various strains.

Sample	Concentration (ng/μL)
M. smegmatis WT control	212
M. smegmatis tkt PAM 1	109
M. smegmatis tkt PAM 2	102

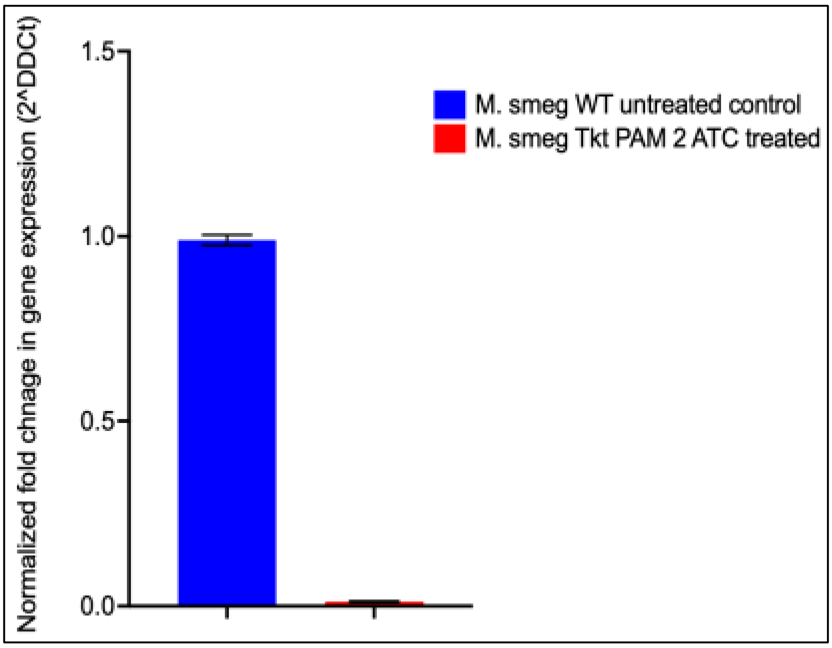

Figure 6. 9: Analysis of transcript levels of tkt gene was determined in ATC induced (red bar) and uninduced (blue bar) *M. smegmatis tkt* PAM 2 cultures by qRT-PCR at 24 hours post CRISPRi induction. Transcript levels were normalised to the ATC uninduced strain control.

6.3.7 Determination of MIC of different antimycobacterial drugs

Consistent with the growth curves and spot assay, *M. smegmatis tkt* PAM 2 CRISPRi strain was more sensitive to ATC compared to the PAM 1 variant where MIC values of 0.488 and 0.976 µg/mL were determined, respectively (Table 6.6). Of the shikimate inhibitors, 2-amino-benzothiazole had lower MIC values, making it a more efficient antimycobacterial agent than naringin. No synergistic effects were detected between gene depleted hypormorphs and selected antimycobacterial drugs (Table 6.5).

Table 6. 6: MIC of anhydrotetracycline, 2-amino-benzothiazole and Naringin.

Chemical species	*M. smegmatis tkt* PAM 1	*M. smegmatis tkt* PAM 2
MIC (µg/mL)		
Rifampicin	1.56	1.56
Anhydrotetracycline (ATC)	0.976	0.488
Naringin	1250	1250
2-amino-benzothiazole	320	320
Combinational effects with 500 ng/mL ATC		
Naringin	1250	1250
2-amino-benzothiazole	320	320
Rifampicin	1.56	1.56

6.3.8 Treating hypomorphs with different ATC concentrations

M. smegmatis CRISPRi strains were treated with a range of ATC concentrations and a strong correlation between the high concentrations of ATC and culture growth inhibition was observed (Figure 6.10). The results confirmed that the inhibitory effect of *tkt* gene knockdown was ATC concentration dependent. Moreover, 2 µg/mL ATC led to significant growth inhibition.

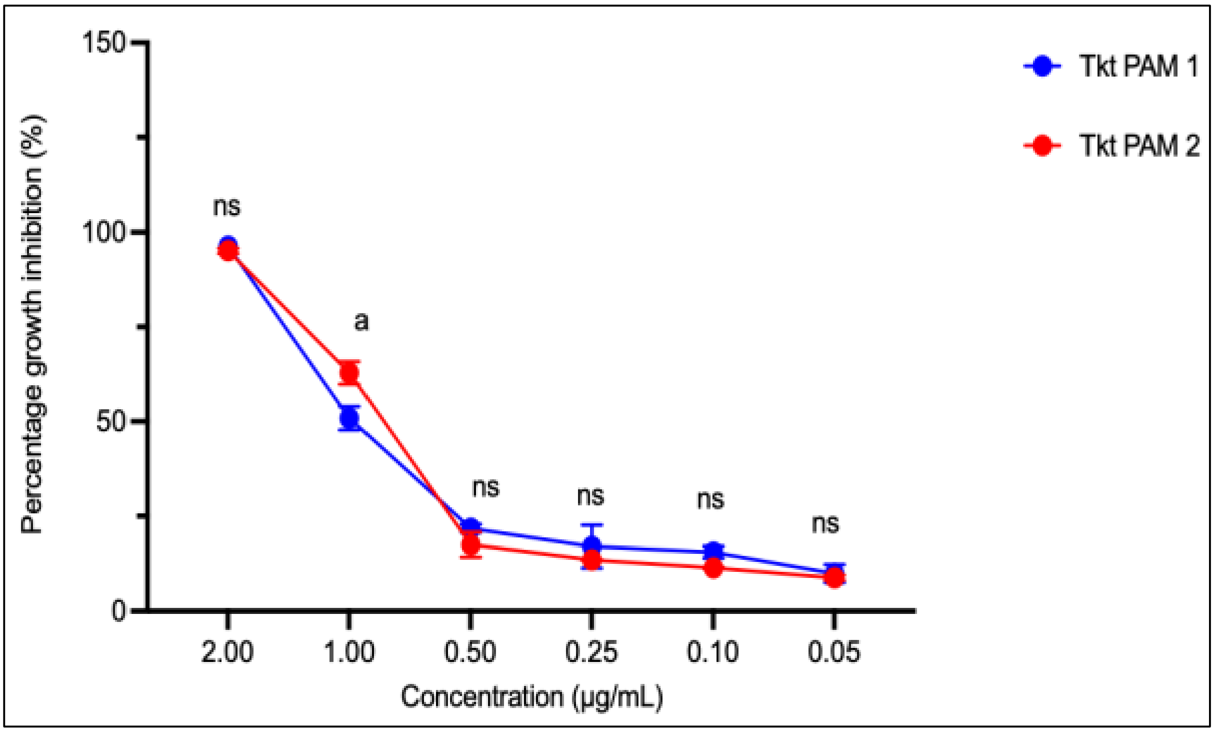

Figure 6. 10: Anhydrotetracycline (ATC) titration of *M. smegmatis tkt* PAM1 (A) and PAM 2 (B) CRISPRi strains with OD600 nm determined after 24 hrs of treatment. Two-way ANOVA was used followed by Šidák Multiple comparisons test.

Key: a= p< 0.05, b= p<0.01, c= p<0.001, d= p<0.0001, ns: non-significant difference.

6.3.9 Treating hypomorphs with different concentrations of shikimate inhibitors

M. smegmatis tkt CRISPRi mutants were treated with different concentrations of shikimate inhibitors. A clear dose-response was observed between the concentration of the shikimate pathway inhibitors and culture growth. Consistent with the broth micro-dilution assay, 2-amino-benzothiazole was more efficacious at inhibiting *M. smegmatis* hypomorphs than naringin (Figure 6.11).

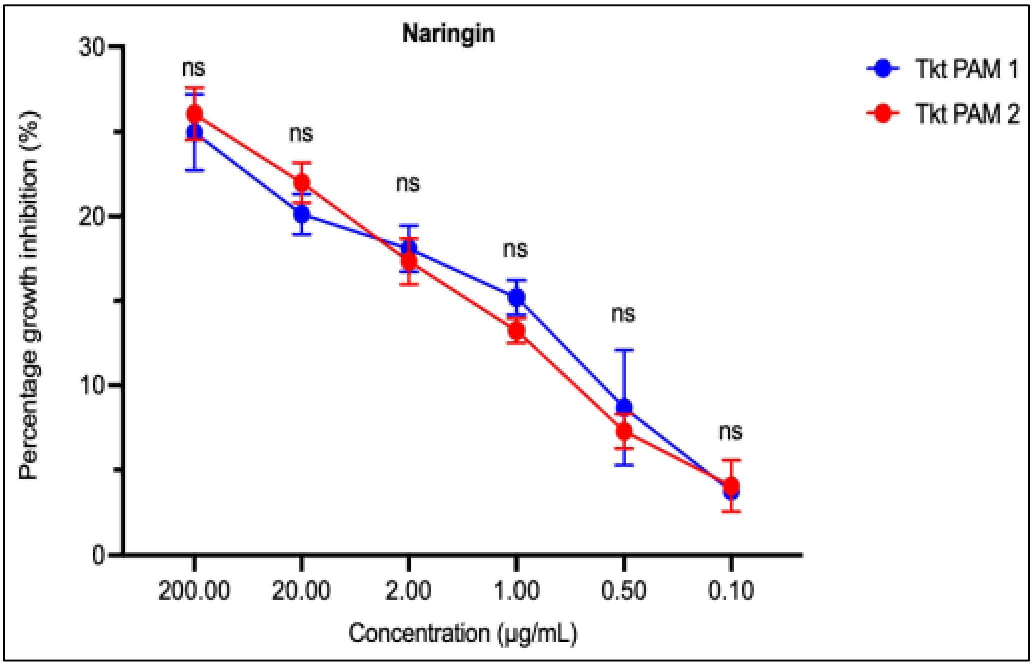

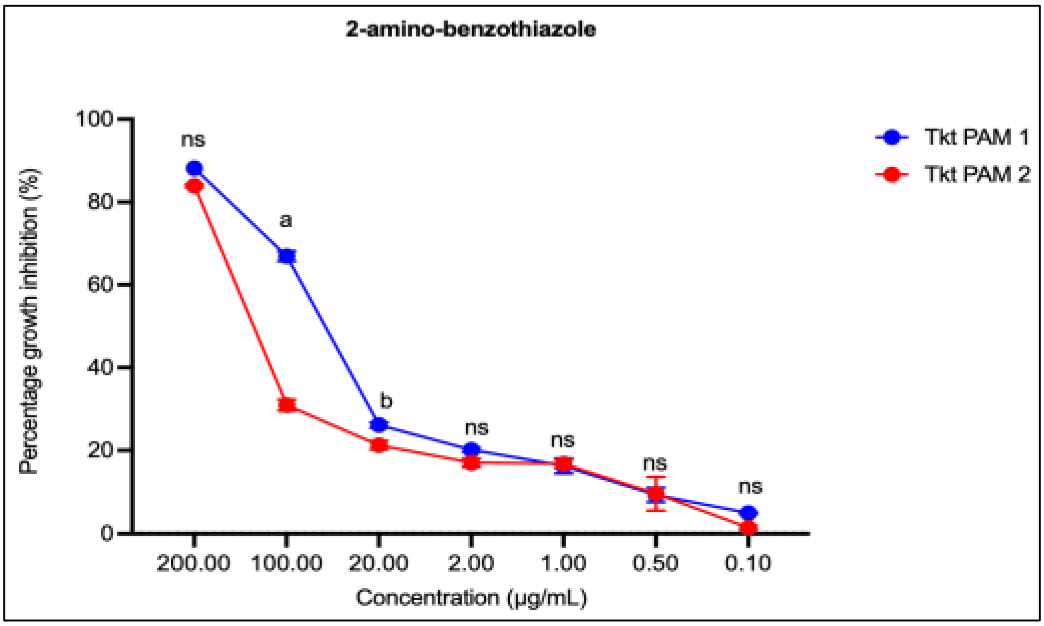

Figure 6. 11: Titration of *M. smegmatis tkt* PAM1 and PAM 2 hypomorphs with shikimate inhibitors, naringin and 2-amino-benzothiazole sampled after 24 hrs. Two-way ANOVA was used followed by Šidák Multiple comparisons test.

Key: a= $p < 0.05$, b= $p<0.01$, c= $p<0.001$, d= $p<0.0001$, ns: non-significant difference.

6.3.10 Evaluation of the effect of plant extracts on *M. smegmatis tkt* gene knockdown strains

Accordingly, anhydrotetracycline (ATC) was used to induce *tkt* gene knockdown. Extracts from *Acacia senegal*, *Peltophorum africanum*, *Carissa bispinosa*, *Senna petersiana* and *Ficus sur* did not inhibit *M. smegmatis* CRISPRi strains after 24 hr (Figure 6.12). However, when *tkt* gene knockdown was initiated by activation of the CRSPRi system, these plant extracts demonstrated increased inhibitory activity to *tkt* CRISPRi hypomorphs. The antimycobacterial activity of the extracts from *Clerodendrum glabrum*, *Croton gratissimus*, *Carissa bispinosa*, *Senna petersisana* and *Ficus sur* significantly improved in *tkt* gene knockdown mutants, both PAM1 and PAM 2 cultures (Figure 6.12). The synergy of the extracts and ATC was evaluated by determining the fold change that results from their combination (Figure 6.13). *C. glabrum* and *P. africanum* have the highest fold changes of -1.892 and -2.299, respectively.

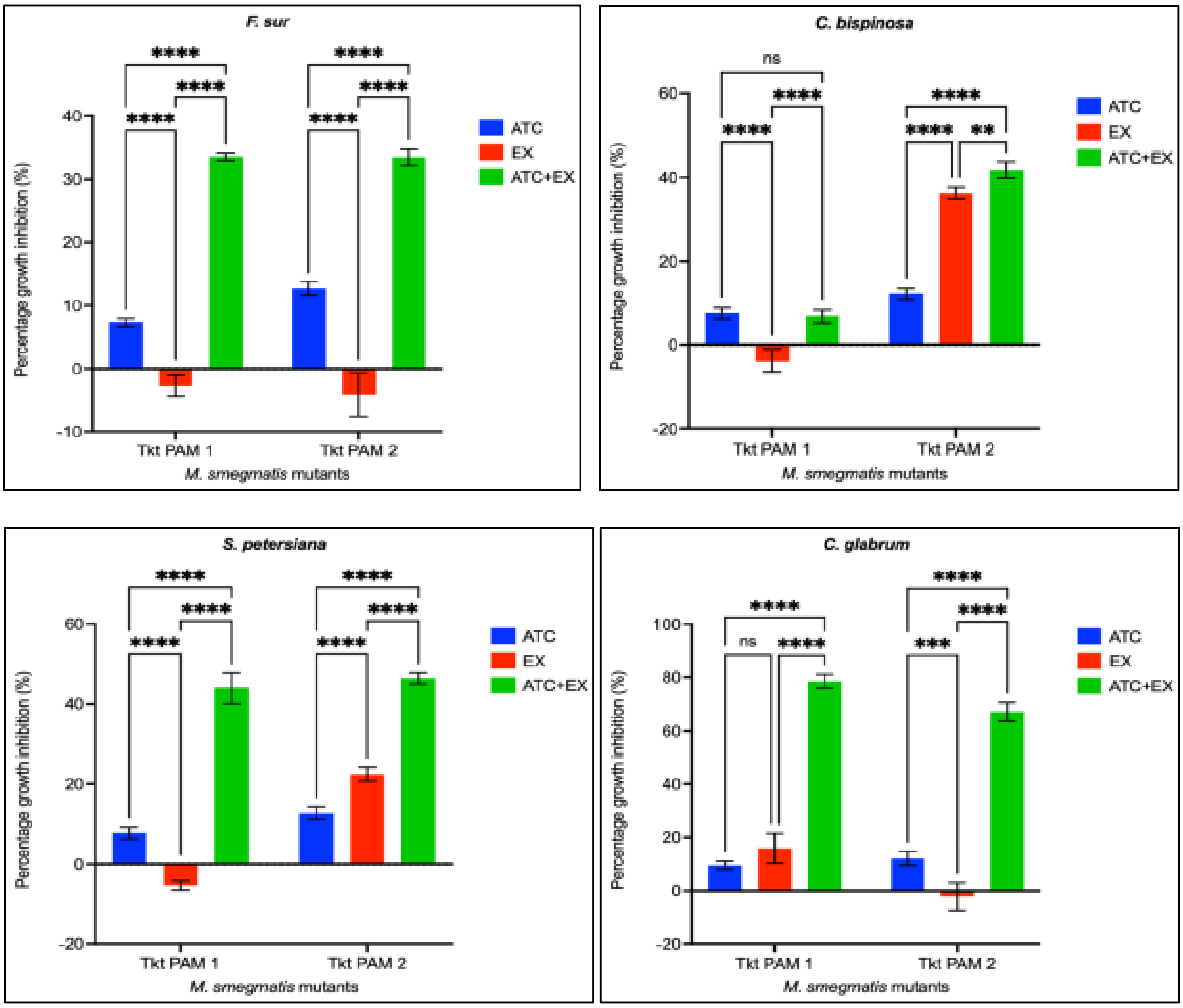

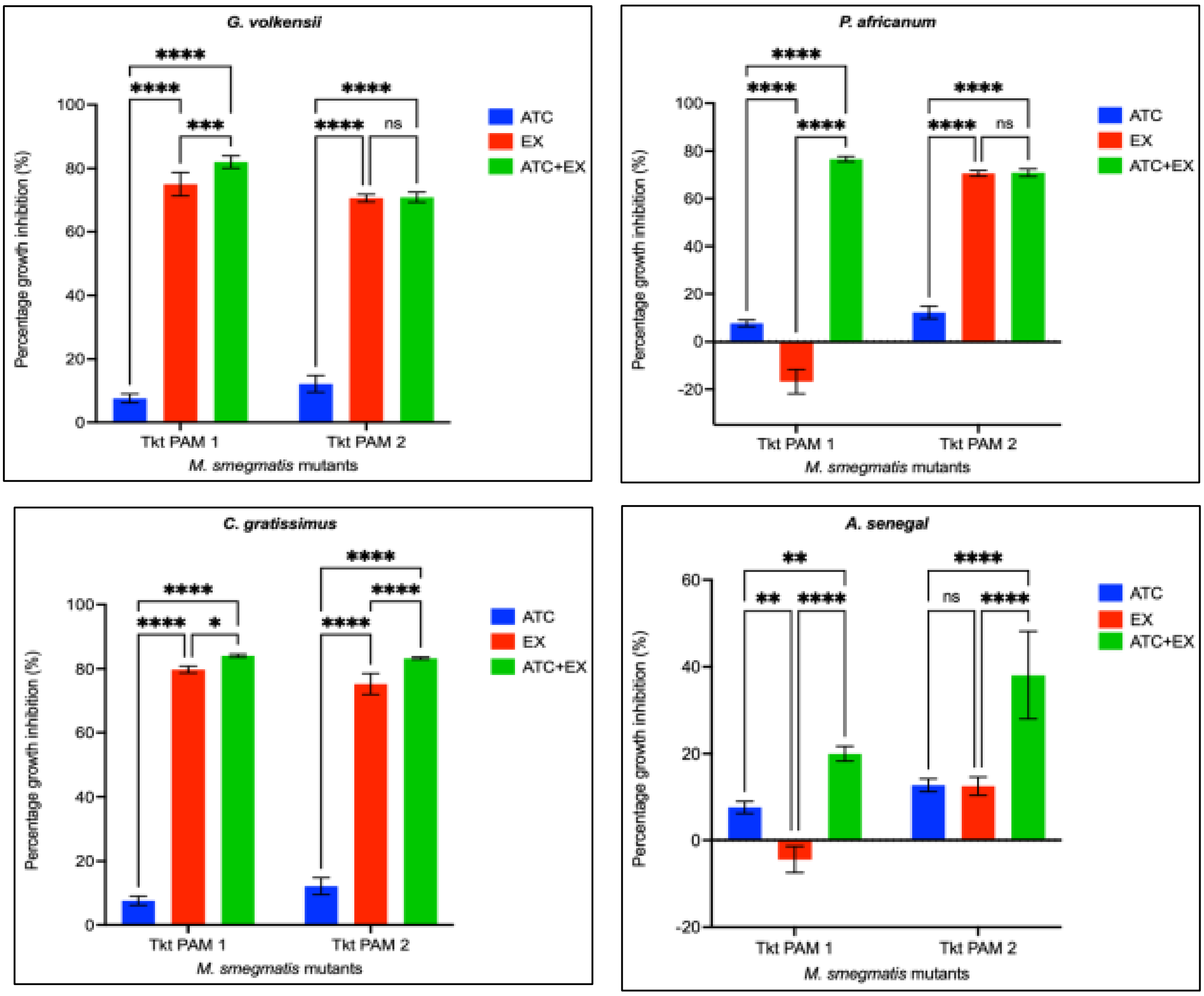

Figure 6. 12: Evaluation of the effect of extracts on the growth of *tkt* depleted *M. smegmatis tkt* PAM 1 and PAM 2 after 24 hrs of treatment. A Two-way ANOVA was used to determine statistical significance coupled with Tukey multiple comparisons.

Key:(****): p<0.0001, (***): p<0.001, (**): p<0.01, (*): p<0.05, ATC: anhydrotetracycline, EX: extract.

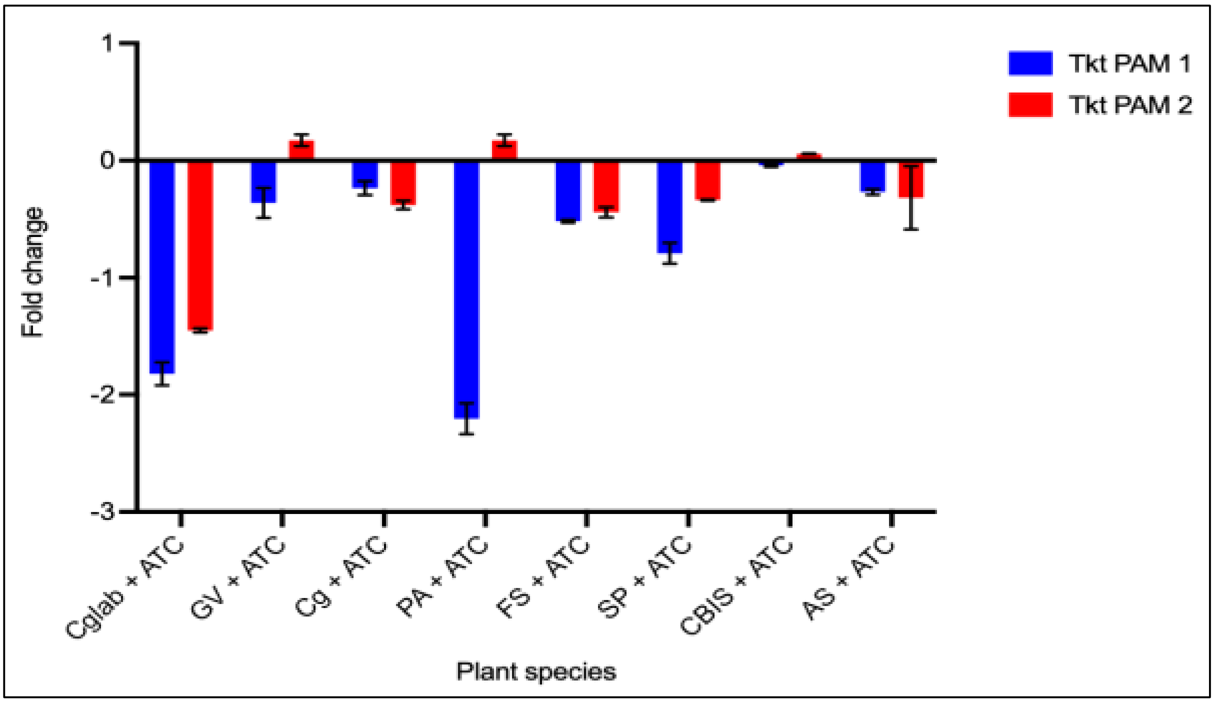

Figure 6. 13: Synergistic effects of anhydrotetracycline (ATC) (0.5 µg/mL) and the plant extracts (1 mg/mL) was evaluated by quantifying the inhibition of *M. smegmatis tkt* mutants relative to untreated controls. This was the fold change.

6.3.11 Combinational effects of extracts and shikimate inhibitor on the growth of the CRISPRi hypomorphs

Initially, 2 µg/mL of 2-amino-benzothiazole was tested with the plant extracts and no interactions were observed (results not shown). However, with an increased concentration of 20 µg/mL, 2-amino-benzothiazole and *Croton gratissimus* extract demonstrated synergistic interaction at 24 hrs (Figure 6.14). Similarly, synergistic interaction of 2-amino-benzothiazole and *Gardenia volkensii* was only observed for *M. smegmatis tkt* PAM 1 and not *tkt* PAM 2 mutants. Accordingly, the synergy between *C. gratissimus* and aminoB resulted in a fold change of -0.356 and -0.61 on *tkt* PAM 1 and 2, respectively (Figure 6.15). There was a general lack of synergy between 2-amino-benzothiazole and the rest of the tested extracts from the different plant species.

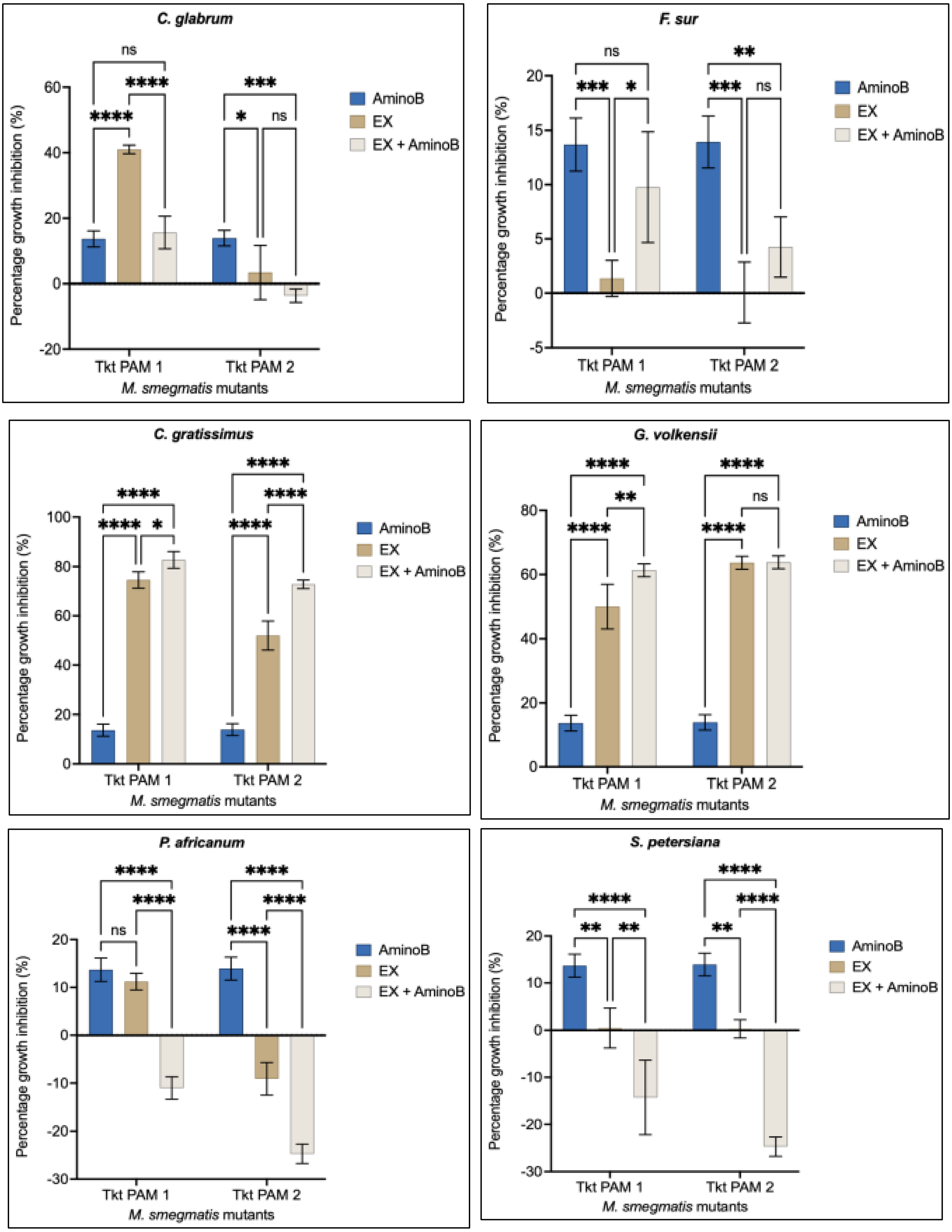
C. glabrum
F. sur
C. gratissimus
G. volkensii
P. africanum
S. petersiana
Percentage growth inhibition (%)
Tkt PAM 1
Tkt PAM 2
M. smegmatis mutants
AminoB
EX
EX + AminoB
ns
*
**
***
****

.

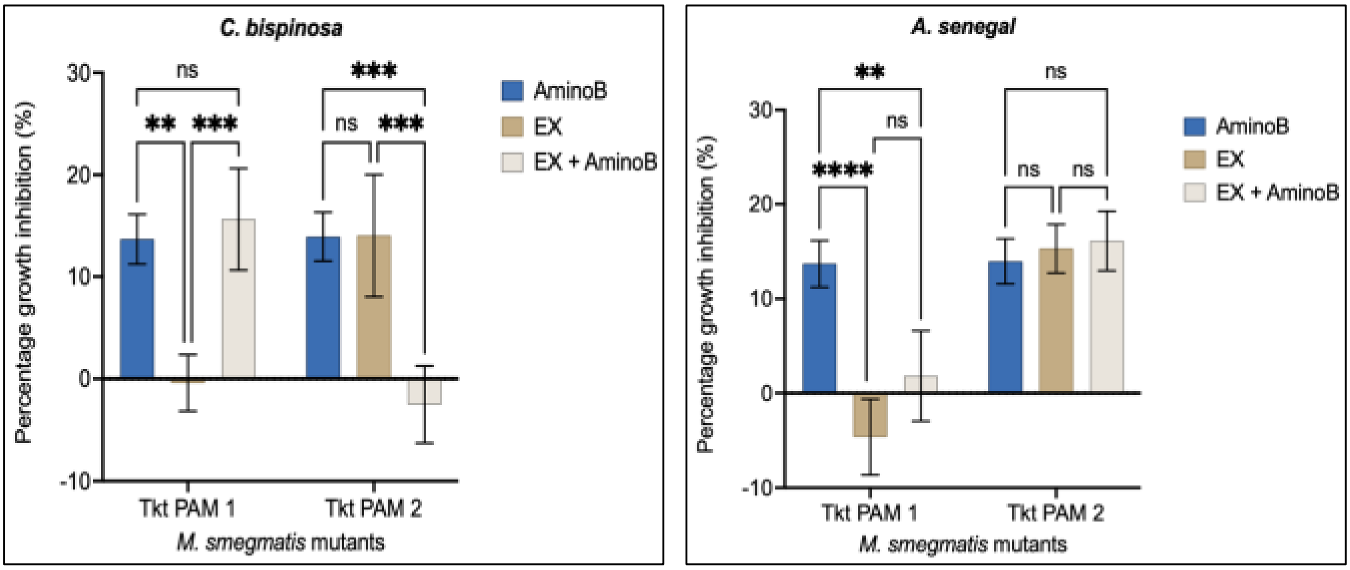

Figure 6. 14: Combinational effects of 2-amino-benzothiazole (20 μg/mL) and various plant extracts (1 mg/mL) on cell growth of *M. smegmatis tkt* hypomorphs, PAM 1 and PAM 2, after 24 hr ATC treatment.

Key: (****): p<0.0001, (***): p<0.001, (**): p<0.01, (*): p<0.05, EX: extract, AminoB: 2-amino-benzothiazole

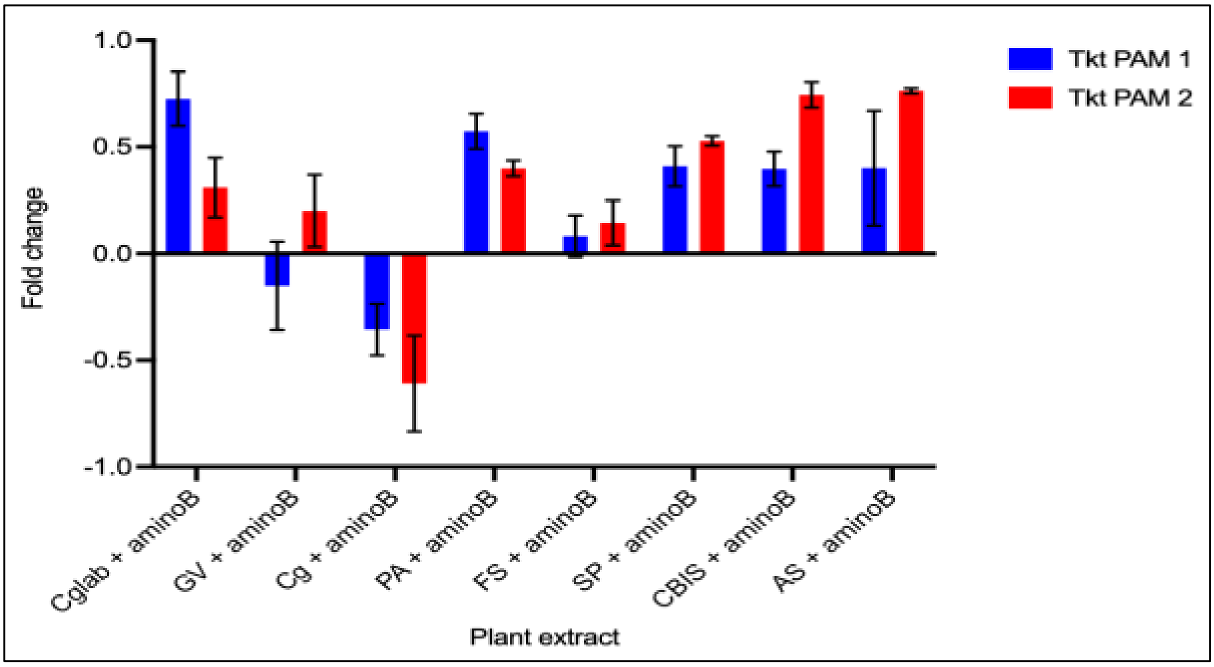

Figure 6.15: Fold change of *M. smegmatis tkt* mutants because of combinational effects of the plant extracts and 2-amino-benzothiazole relative to untreated control.

6.3.12 Rescue experiment for *M. smegmatis tkt* hypomorphs

The possibility that host-derived metabolites might rescue antibiotic-mediated nutrient auxotrophy is a key concern in targeting metabolic pathways for drug development. For this reason, the potential for uptake and assimilation of exogenous amino acids and intermediates by *tkt* and *aroG* depleted *M. smegmatis* hypomorphs was evaluated by a rescue experiment (Figure 6.16). Rescue was demonstrated by higher OD600nm of hypomorphs cultured with AAAs. In all mutants, shikimic acid (0.05 mg/mL) was able to rescue growth, while l-tryptophan failed to rescue growth. L-tryrosine largely rescued the growth of all the mutants, except for *aroG* PAM 2. In contrast, L-l-phenylalanine was able to rescue the growth of only *aroG* PAM 1 strain.

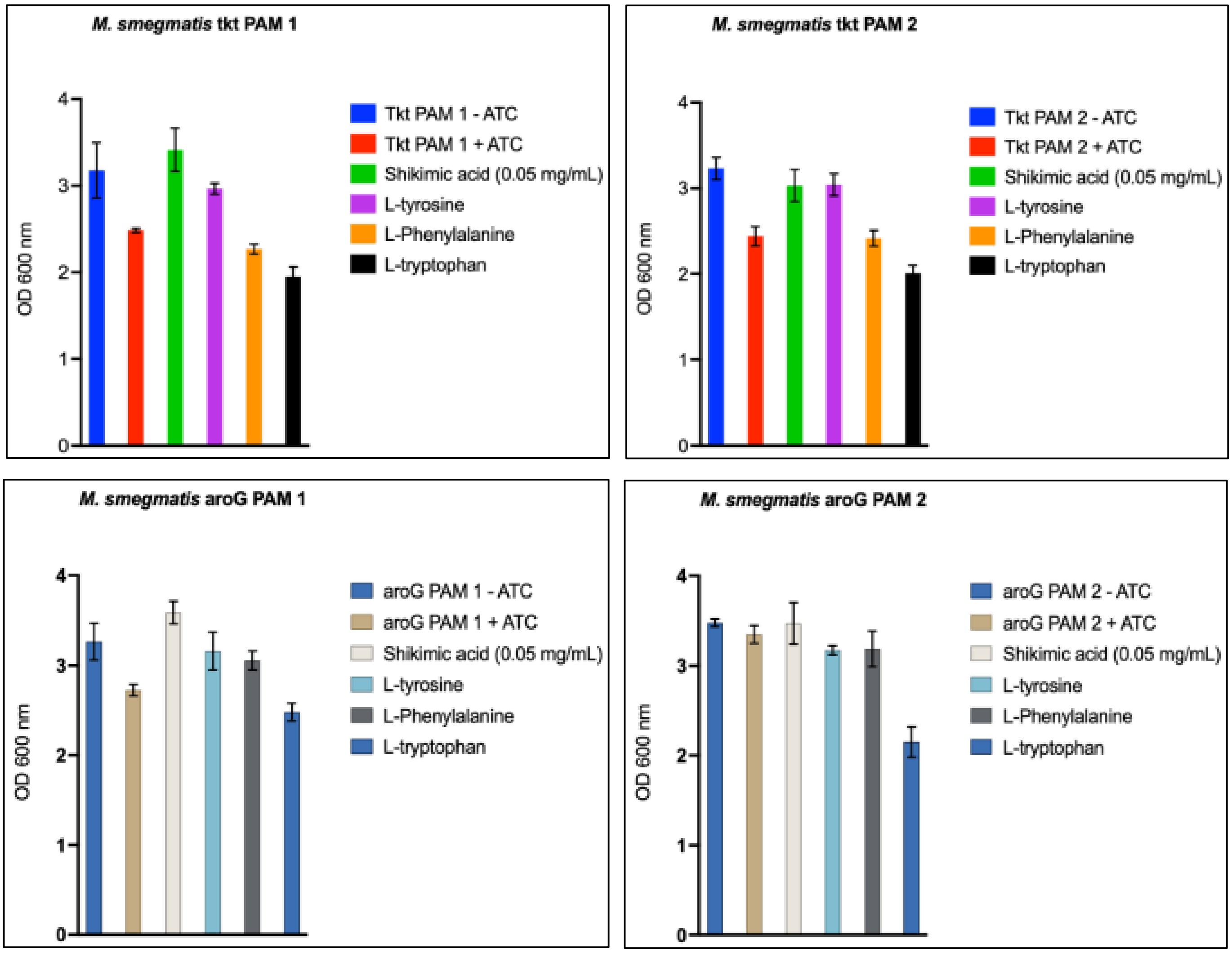

Figure 6. 16: The growth rescue of *tkt* and *aroG M. smegmatis* hypomorphs by various aromatic amino acids produced through the shikimate pathway.

Key: ATC: anhydrotetracycline

6.3.13 Rescue of by shikimate metabolites of *tkt* hypomorphs inhibited by plant extracts

Of the plant species investigated, only *Gardenia volkensii* and *Croton gratissimus* demonstrated persistent growth inhibition of the *tkt M. smegmatis* hypomorphs. L-tyrosine was the only AAA that was able to rescue the *tkt* PAM 1 strain (Figure 6.17). All the other tested shikimate intermediates, L-phenylalanine, shikimic acid and L-tryptophan failed to rescue the growth of *tkt* hypomorphs that had been inhibited by the plant extracts.

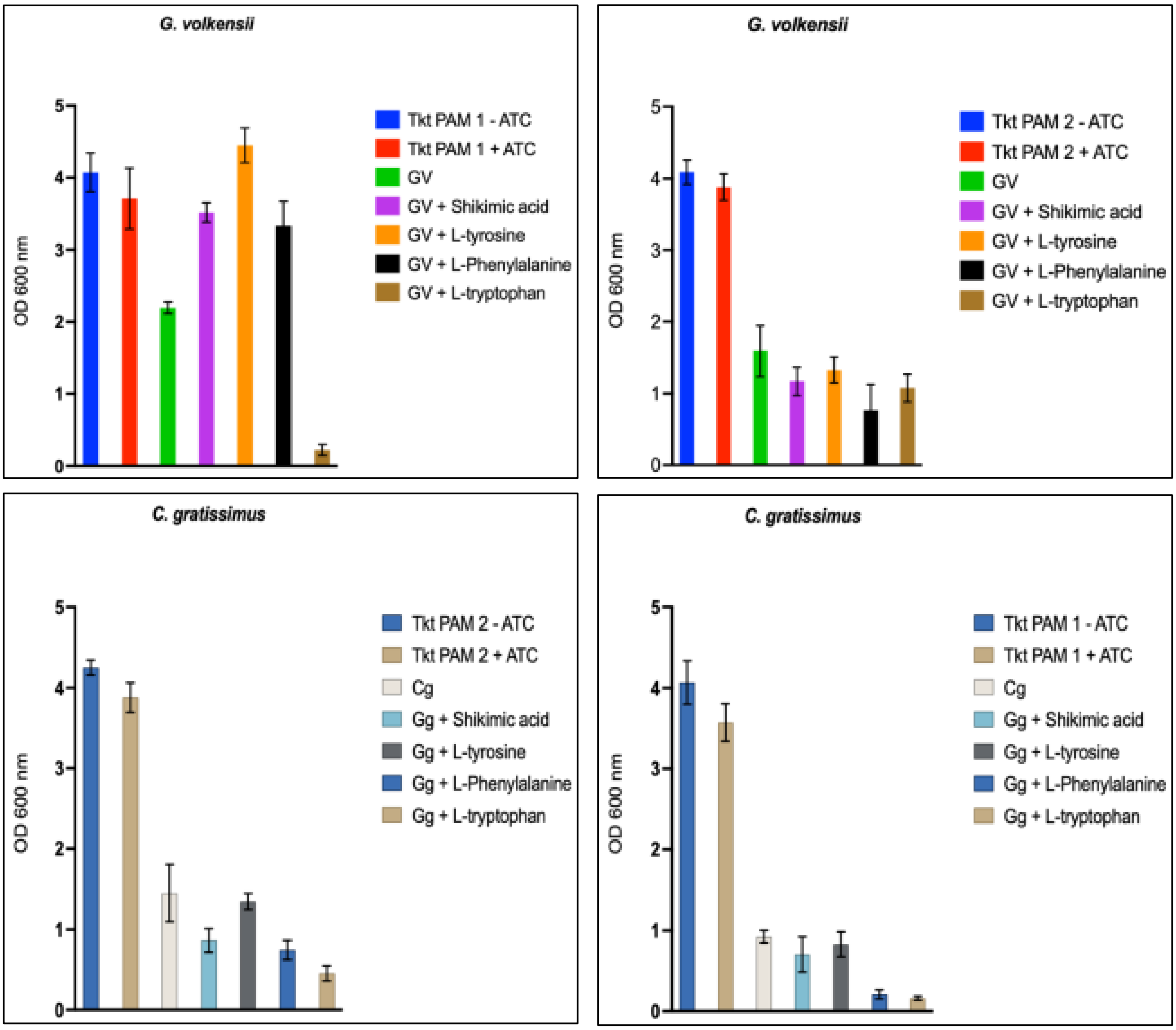

Figure 6. 17: Rescue experiment of *tkt* PAM 1 and PAM 2 *M. smegmatis* CRISPRi strains treated with *Gardenia volkensii* and *Croton gratissimus* acetone extracts for the second passage.

Key: ATC: anhydrotetracycline

6.4 Discussion

6.4.1 Endonuclease plasmid digestion, agarose gel electrophoresis and transformation

The isolated PLJR962 plasmid appeared in three different conformations: open circular, linear and supercoiled (Figure 6.2). The applied current during electrophoresis migrated the loaded samples by size, because the supercoiled conformation of the plasmid was the smallest and most compact, it travelled faster than the linear and the open circular. The open circular conformation is the largest of the three conformations and as such, it traveled the least. Similar observations were detailed by other researchers for the pUC series of plasmids (Higgins and Vologodskii, 2015; De Mattos *et al*., 2004). The presence of the linearised conformation of PLJR962 in lane P may have been caused by the contamination of nucleases. Digestion of PLJR962 plasmid by Esp3I linearised the plasmid and as expected, only single bands were observed. Moreover, these restricted bands migrated a similar distance to the linear conformation of PLJR962 on the control lane. SYBR green was used to visualise the DNA samples via UV light where high concentrations DNA in a band give a more intense fluorescence of that band (Green *et al*., 2019). For the control PLJR962, the band with the highest intensity was the supercoiled conformation compared to the open circular and linear (Figure 6.2). *In vivo*, plasmid DNA is a tightly supercoiled circle to enable it to fit inside the cell. In the laboratory, following a careful plasmid prep, most of the DNA will remain supercoiled (Higgins and Vologodskii, 2015; De Mattos *et al*., 2004). The separation of these conformations demonstrated the importance of electrophoresis as a purification technique.

The agarose gel recovered plasmid fragments, alternatively known as the CRISPRi backbone, were ligated with PAM designed oligonucleotides for both *tkt* and *aroG* genes using DNA ligase. Kanamycin was used as a selectable marker for successful transformants, i.e., transformants *E. coli* and *M. smegmatis* with a functional CRISPRi plasmid, and as expected, were able to express the KAN^R and therefore, were able to grow on the plates supplemented with the antibiotic (Figures 6.3 and 6.4). As expected, competent cells (without CRISPRi plasmid) were unable to grow in the presence of KAN.

6.4.2 Spot assay

To assess the essentiality of the selected genes on Mycobacteria, the use of conditional knockdown strains enables the validation of the vulnerability of the targets (Kolly *et al*., 2014b). The essentiality of a target for microbial growth and/or survival is a critical feature of an attractive drug target and the validation of a selected target as essential to the growth of the test microorganism is critical in antimicrobial drugs discovery.

Figure 6.5 shows the spot assay used to qualitatively determine the functionality of the integrated CRSPRi/dCas9 system (Figure 6.5). In the control plates, where ATC was not added to the media, it is worthy to highlight the indifference in the growth of the *M. smegmatis* mutants and the control with an empty insert. This indifference in growth indicated that the integration of the CRISPRi plasmid into competent *M. smegmatis* cells did not impose any notable adverse effects on their *in vitro* growth.

Culturing the *M. smegmatis* hypomorphs on ATC supplemented plates enabled the activation of the CRISPRi/dCas9 system. The gene silencing method utilised for the construction of the cKD mutants is based on the transcriptional repression by both the TetR and Pip regulators (Kolly *et al*., 2014b). An addition of ATC induces expression of Pip that, in turn, represses the P_{ptr} promoter, which is driving the expression of the gene of interest (Kolly *et al*., 2014b). These results demonstrated that in the gradual intracellular depletion of a fully functional copy of the *tkt* and/or *aroG* gene, the *M. smegmatis* hypomorphs undergo gradual growth impairment, thus confirming the essentiality of these two genes *in vitro*.

6.4.3 Growth curves

It was observed that within the first 9 hours of incubation, the growth of all the hypomorphs in ATC were non-significantly affected compared to the control with an empty insert (Figure 6.6). The results demonstrated that the *M. smegmatis tkt* and *aroG* hypomorphs required a minimum of 18 hours of incubation (shaking at 200 rpm) for the growth inhibition to become evident. This observation was consistent with other CRISPRi-mediated essential gene knockdowns in *M. smegmatis* mutants (de Wet *et al*., 2018). The kinetics of gene knockdown have been reported to be driven primarily by the rate at which dCas9 is expressed and its subsequent accumulation (Guzzo *et* *al*., 2020). Therefore, the growth curves in Figure 6.6 suggested that the expression of the dCas9 in the *M. smegmatis* hypomorphs was minimal during the lag phase and accordingly, higher during exponential phase (incubation time> 18 hrs).

At 18 and 24 hrs, it appeared that compared to the untreated control, the growth of *M. smegmatis tkt* PAM 2 hypomorph was the most significantly impaired. Consistent with the spot assay, where *M. smegmatis tkt* PAM 2 hypomorph was more sensitive to ATC induced gene knockdown. These combined results indicated that although, both the *aroG* and the *tkt* genes are essential for *M. smegmatis* growth and survival, the *tkt* gene was more essential for growth and therefore, might be a better target than the *aroG* gene because the interference of the expression of the *tkt* gene led to a more notable growth inhibition (Figure 6.6). In the context of AAA biosynthesis, the non-oxidative pentose phosphate pathway supplies erythrose-4-phosphate (E4P) to the shikimate pathway through reactions catalysed by the transketolase enzyme. The E4P is used in the first reaction of the shikimate pathway by the DAHP synthase. These results demonstrated that the knockdown of the *tkt* gene might have caused metabolic deficiency downstream shikimate pathway reduced the normal AAA biosynthesis for the hypomorph, as observed in Figures 6.6.

Apart from its central role in the shikimate pathway, the transketolase enzymes Rv1449c (*tkt*) have been shown to be important to the decaprenyl-phospho-D-arabinofuranose (DPA) biosynthetic pathway because they catalyse the first reaction where D-ribose 5-phosphate (R5P) is produced by the transketolase from the non-oxidative pentose phosphate pathway intermediates (Fullam *et al*., 2011). The DPA is the only precursor of arabinofuranose used in the production of arabinogalactan (AG) and lipoarabinomannan (LAM), which are also major components of the mycobacterial cell wall (Kolly *et al*., 2014b). Furthermore, Kolly *et al* (2014b) showed that the DPA is essential for *M. tuberculosis* growth. The role of the *tkt* gene product in both these essential pathways, shikimate and DPA pathways might explain the greater growth repression from the *M. smegmatis tkt* PAM 1 hypomorph than both the *aroG* hypomorphs.

6.4.4 RNA isolation and qPCR

Given that it was once activated by ATC, the designed CRISPRi/dCas9 system interfered with the rate of transcription of both *tkt* and *aroG* genes (Section 6.3.5), qRT-PCR was conducted to further evaluate the consequence at an RNA transcriptional level. RNA was isolated from the untreated *M. smegmatis* wild type control and *M. smegmatis tkt* hypomorphs, PAM 1 and PAM 2 after ATC for 24 hrs.

The electrophoresis of the RNA samples yielded two distinct bands of 16S and 23S subunits (Figure 6.7). The RNA samples isolated from both *M. smegmatis tkt* hypomorphs had slightly lesser brightness than the control RNA from ATC untreated control. Qualitatively, the results indicated that the mutants had lesser amounts of RNA than the untreated control. This was further validated by the evaluation of the normalised intensities (Figure 6.8), where the control *M. smegmatis* RNA had the highest detected fluorescence compared to the ATC treated *M. smegmatis* mutants. The higher the intensity, the larger the amount of RNA because the amount of fluorescence given off by SyBr green reflects the amount of RNA it is bound to. RNA analysis of the isolated RNA samples indeed indicated that with the introduction of ATC, the expression of the target specific sgRNA from the CRISPRi/dCas system inserted in the *M. smegmatis* interferes with or blocks the expression of the *tkt* gene.

Quantitative measurement of transcript levels of target genes (*tkt* PAM 2 depleted strains) by qRT-PCR were performed and these were compared to that in the uninduced strains controls of *M. smegmatis* (Figure 6.9). The qPCR results further confirmed the significant reduction of the amount of RNA, demonstrating the interreference of the expression of the target gene when ATC activated the CRISPRi/dCas system.

6.4.5 Minimum inhibitory concentrations of ATC and shikimate inhibitors

Both *M. smegmatis tkt* hypomorphs, PAM 1 and PAM 2, were most susceptible to ATC with MIC values of 0.976 and 0.488 µg/mL, respectively (Figure 6.10 and Table 6.5). In a study by McNeil and Cook (2019), ATC concentrations as low as 1 ng/mL were shown to affect *M. tuberculosis hypomorphs* containing the mmpL3-targeting sgRNA. Moreover, MIC values of 19.3 ± 0.6 ng/mL were determined against the *M. tuberculosis* mutants. This showed that, compared to mmpL3, a higher level of *tkt* depletion was required to inhibit mycobacterial growth. It was further found that a moderate *tkt* knockdown (by low concentrations of ATC) had no synergistic effects with the shikimate inhibitors and rifampicin (Table 6.5). This indicated that a moderate depletion of the *tkt* gene neither potentiated the activity of the used drugs, nor did it sensitise the mutants. This demonstrated that higher levels of ATC-induced gene depletion were required for synergistic interactions.

Compound 2-amino-benzothiazole and other benzothiazole derivatives were shown to inhibit mycobacterial growth by inhibiting the shikimate kinase (encoded by aroK) (Mehra *et al*., 2016; Simithy *et al*., 2014). Being the fifth enzyme in the shikimate pathway, the shikimate kinase is downstream to the transketolase enzymes (*tkt* gene) (Ducati *et al*., 2007). Therefore, the activity of MtSK is dependent on the efficacy of the *tkt* gene to provide the erythrose-4-phosphate into the shikimate pathway. This explained the lower MIC values of ATC compared to 2-amino-benzothiazole and naringin. These results were important because they showed and validated that the knockdown of an essential upstream gene may lead to an increased growth inhibition. However, the role played by *tkt* in other essential pathways might have also contributed to the lower ATC MICs. The MIC of rifampicin (1.56 µg/mL) remained unchanged when tested against both the *M. smegmatis tkt* hypomorphs. This indicated that the presence of the CRISPRi plasmid in the *M. smegmatis* cells did not interfere with the mechanism of action of rifampicin.

ATC had lowest MIC values than rifampicin, 2-amino-benzothiazole and naringin against both *M. smegmatis* CRISPRi hypomophs. These results suggested that high concentrations of ATC over saturated the activation/overexpression of the CRISPRi/dCas9 cascade which led to a corresponding increase in *tkt* gene knockdown. The consequence of this high level of gene knockdown is increased cell death. To validate this speculation, the two *M. smegmatis* hypomorphs (at exponential phase) were cultured with different ATC concentrations over a 24 hr period.

6.4.6 Treating hypomorphs with different concentrations of ATC and shikimate inhibitors

The treatment of the *M. smegmatis tkt* hypomorphs with the different ATC concentrations indeed showed that CRISPRi efficacy is ATC concentration dependent. Lower concentrations led to a minimal growth inhibition and higher concentrations (1 and 2 µg/mL) significantly reduced the growth of both the *M. smegmatis tkt* hypomorphs (Figure 6.11). McNeil and Cook (2019) and Singh *et al*. (2016) also reported observing a dose-response between ATC concentrations and mutant cultures. Accordingly, it has been reported that a high expression of dCas9 from *S. pyrogenes* has cidal effects on *M. smegmatis* (Rock *et al*., 2017). On the other hand, a poor expression of the dCas9 in a CRISPRi system may lead to low knockdown efficiencies (Rock *et al*., 2017). A vector for the expression of dCas9 at levels that do not interfere with bacterial growth but are sufficient to achieve consistent, physiologically relevant inhibition of gene expression 500 ng/mL was therefore chosen for this study.

Similarly, the growth inhibition of the *M. smegmatis tkt* hypomorphs in liquid medium was dependent on the concentration of the shikimate inhibitors (Figure 6.12). Notably, 0.1 µg/mL, 2-amino-benzothiazole had a significant growth reduction of the *M. smegmatis tkt* PAM 1, but had a non-significant inhibition for *M. smegmatis tkt* PAM 2 hypomorph. These results suggested that the fold repressions of the selected PAMs (Rock *et al*., 2017) affected the activity of the 2-amino-benzothiazole, with the inhibitor showing a stronger inhibition effect when more *tkt* was intracellularly depleted.

6.4.7 Evaluation of the effect of plant extracts on *M. smegmatis tkt* gene knockdown strains

Earlier results showed that a significant growth inhibition of the *M. smegmatis* mutants due to *tkt* gene knockdown was evident from 18 hrs of incubation (Figure 6.6). Therefore, a sampling of extract-treated hypomorphs was conducted at 18 and 24 hrs. Based on the pre-determined MIC values of the various plant extracts against both *M. smegmatis tkt* hypomorphs, 1 mg/mL of the extracts was selected for growth. This was to enable a moderate growth inhibition of the hypomorphs to allow an efficient evaluation of the effects of the extracts on *tkt* gene knockdown strains. In general, the results indicated that an antimycobacterial activity of the extracts against *M. smegmatis* increased when the *tkt* gene was knocked down using a PAM sequence with a higher fold repression (PAM 1) than with a lower fold repression (PAM 2) (Figure 6.13). Except for the *C. bispinosa* extract, all tested plant extracts had a higher antimycobacterial activity after 24 hrs against *M. smegmatis tkt* PAM 1 mutants (Figure

6.13). The synergistic interaction of the extracts and ATC was further quantified by defining the fold change in the growth inhibition they exerted on the *M. smegmatis tkt* hypomorphs (Figure 6.14). *P. africanum* and *G. volkensii* extracts did not have synergy towards *M. smegmatis tkt* PAM 2 mutants compared to their effects on *tkt* PAM 1 *M. smegmatis* mutants (Figure 6.14). Interestingly, *P. africanum* and *C. glabrum* had the most efficacious synergy with ATC against *tkt* PAM 1 of *M. smegmatis* mutants. It appeared that significant depletion (higher fold repression) of the *tkt* gene is required to observe an improved antimycobacterial activity of the plant extracts. The increased antimycobacterial activity of the plant extracts demonstrated that CRISPRi/dCas9 mediated the essential gene knockdown can be taken as an effective tool to potentiate/improve inhibitory activity of compounds with moderate antimycobacterial activity.

6.4.8 Combinational effects of extracts and shikimate inhibitors on the growth of *M. smegmatis tkt* hypomorphs

Given that 2-amino-benzothiazole inhibits Mycobacterial shikimate kinase (Simithy *et al*., 2014), it was observed that the combination of 20 µg/mL of this shikimate pathway inhibitor with *C. gratissimus* acetone extract resulted in synergistic effects against both *M. smegmatis tkt* mutants after 24 hrs of incubation (Figure 6.15 and 6.16). The acetone extract of *G. volkensii* had a synergistic interaction with 2-amino-benzothiazole against *tkt* PAM 1 *M. smegmatis* mutant, but not for PAM 2 of the *tkt* mutant. This might indicate that the plant extract had various modes of mechanism of action. No synergistic effects were observed on the *A. senegal*, *C. glabrum*, *G. volkensii*, *F. sur* extracts with 2-amino-benzothiazole. These results demonstrated that the mycobacterial *tkt* CRISPRi/dCas9 system produces a robust and proportional impairment of *tkt* expression that when treated with the combination of the shikimate pathway inhibitor, 2-amino-benzothiazole and acetone extracts of *C. gratissimus* and *G. volkensii* antimycobacterial activity increased and that bioactive components in the plant targeted shikimate pathway.

6.4.9 Rescue experiment of *tkt* knocked down *M. smegmatis* mutants

Because of the essentiality of the shikimate pathway, an intracellular depletion of *tkt* and *aroG* genes (Figure 6.6), led to cell death, possibly due to the starvation of the essential aromatic amino acids (AAA) such as L- tryptophan, L-tyrosine, and L-phenylalanine. In general, *M. tuberculosis* has been reported to use AAA as a source of nitrogen, among others (Agapova *et al*., 2019). One of the main challenges with targeting the shikimate pathway is that the same AAA (amino acids) (L- tryptophan, L-tyrosine, and L-phenylalanine) that are essential for *M. tuberculosis* viability, are also essential to animals and humans. Due to a lack of enzymatic machinery for *de novo* synthesis of these AAA, animals and human obtain them from their diet (Han *et al*., 2019).

In the conducted rescue experiments, it was noted that, though having varying OD600nm values, the *tkt M. smegmatis* hypomorphs shared a similar rescue pattern, where both phenotypes were rescued most significantly by shikimic acid (0.05 mg/mL), followed by L-tyrosine (25 mM) (Figure 6.17). The *M. smegmatis aroG* strains did not share a similar rescue pattern, where the *aroG* PAM 1 strain was rescued by the shikimic acid, L-tyrosine (25 nM) and L-phenylalanine (25 nM), but the *aroG* PAM 2 strain was not rescued by L-phenylalanine. The results of this study indicated that while the *tkt* and *aroG* gene expression are essential for the *in vitro* survival of Mycobacteria, under unfavorable conditions, the species can indeed assimilate exogenous AAA and compensate for the loss of *tkt* and *aroG* gene functions. These findings further indicated that the exogenous AAA were able to permeate through the mycobacterium cell wall, which is well known to be most impermeable to chemical species. Previous investigations by Agapova *et al*. (2019) also demonstrated higher and improved growth and biomass yields when *M. tuberculosis* was cultured in media containing various essential amino acids.

6.4.10 Determination of mechanism of action of the plant extracts using rescue experiment

As previously established, acetone extracts of *G. volkensii* and *C. gratissimus* were the only samples able to synergistically interact with the shikimate pathway inhibitor, 2-amino-benzothiazole. With the rescue experiments, only the *M. smegmatis tkt* hypomorphs treated with the *G. volkensii* and *C. gratissimus* extracts struggled to recover when incubated with AAA. It was also notable that though L-tyrosine was able to rescue *tkt* PAM 1 of the *M. smegmatis* strain treated with *G. volkensii*, *tkt* PAM 2 was not able to recover from the inhibition of the plant extract (Figure 6.18). Compared with the rescue experiments of the *M. smegmatis tkt* strains (Figure 6.18), the inability of the treated extracts' struggle to recover growth in the presence of either one of the AAA demonstrated that the mechanism of *C. gratissimus* extract was to inhibit some element of the shikimate pathway.

The results of this study are important because they provide more data in understanding the essentiality and role of the tryptophan biosynthesis in mycobacterium metabolism and pathogenesis. In addition, these results demonstrate the sensitivity of *M. smegmatis* auxotrophs to tryptophan depletion because the culture struggled to gain full metabolic activity in the rescue experiment. This finding builds on previous work by Smith *et al*. (2001) and Zhang *et al*. (2013), where, through auxotrophic knockout experiments, it was demonstrated that indeed tryptophan is essential for host (mice) colonisation by *M. tuberculosis*. It follows that the inhibition of enzymes involved in tryptophan biosynthesis, as demonstrated in this current study, may impede its production and subsequent supply to the microbe. This may have implications in enhancing/improving the starvation-phagocytosis mechanism of the host (Nunes *et al*., 2020; Zhang *et al*., 2013). Similar sensitivity to tryptophan depletion by other intracellular microbial species; *Chlamydophila psittaci*, *Chlamydia trachomatis*, *Streptococcus agalactiae* and *Leishmania donovani* have been reported (Lott, 2020). Much still needs to be studied and understood about the bioavailability of host tryptophan to clinical *M. tuberculosis* at the various phases of disease progression, and whether the bacterium can bypass inhibition of tryptophan biosynthesis by using environmental sources of the essential amino acids.

6.5 Conclusion

This study supports the hypothesis that, at least in the case of the shikimate pathway, amino acid metabolism is essential for Mycobacterial viability and survival. The combination of the shikimate inhibitors and *C. gratissimus* showed that the shikimate pathway is a druggable target and this necessitates more research to investigate the various forms in which it may be inhibited. Future work in this area should focus on: (1) screening and developing drugs that inhibit tryptophan biosynthesis pathway enzymes, and (2) exploring the role that dysregulation and tryptophan depletion might play in persister populations during TB infection.

6.6 References

Abrahams, K.A., Cox, J.A.G., Fütterer, K., Rullas, J., Ortega-Muro, F., Loman, N.J., Moynihan, P.J., Pérez-Herrán, E., Jiménez, E., Esquivias, J., Barros, D., Ballell, L., Alemparte, C. and Besra, G.S. 2017. Inhibiting mycobacterial tryptophan synthase by targeting the inter-subunit interface. *Scientific Reports*, **7(1)**: 9430.

Agapova, A., Serafini, A., Petridis, M., Hunt, D.M., Garza-Garcia, A., Sohaskey, C.D., and de Carvalho, L.P.S. 2019. Flexible nitrogen utilisation by the metabolic generalist pathogen *Mycobacterium tuberculosis*. eLife, **8**: e41129.

Agapova, A., Serafini, A., Petridis, M., Hunt, D.M., Garza-Garcia, A., Sohaskey, C.D. and de Carvalho, L.P.S. 2019. Flexible nitrogen utilisation by the metabolic generalist pathogen *Mycobacterium tuberculosis*. *eLife*, **8**: e41129.

Blumenthal, A., Trujillo, C., Ehrt, S. and Schnappinger, D. 2010. Simultaneous analysis of multiple *Mycobacterium tuberculosis* knockdown mutants in vitro and in vivo. *Public Library of Science one*, **5(12)**: Doi.org/10.1371/journal.pone.0015667.

Choudhary, E., Thakur, P., Pareek, M. and Agarwal, N. 2015. Gene silencing by CRISPR interference in *Mycobacteria*. *Nature communications,* **6**: Doi: 10.1038/ncomms7267.

De Mattos, J.C.P., Dantas, F.J.S., Caldeira-de-Araujo, A. and Moraes, M.O. 2004. Agarose Gel Electrophoresis System in the classroom. *The International Union of Biochemistry and Molecular Biology*, **32(4)**: 254–257.

De Wet, T.J., Gobe, I., Mhlanga, M.M. and Warner, D.F. 2018. CRISPRI-Seq for the identification and characterisation of essential mycobacterial genes and transcriptional units. *Cold Spring Harbor Laboratory*: Doi: 10.1101/358275.

Fullam, E., Pojer, F., Bergfors, T., Jones, T.A. and Cole, S.T. 2011. Structure and function of the transketolase from *Mycobacterium tuberculosis* and comparison with the human enzyme. Open Biol, **2**: Doi: 10.1098/rsob.110026.

Grandoni, J. A., Marta, P. T. and Schloss, J. V. 1998. Inhibitors of branched-chain amino acid biosynthesis as potential antituberculosis agents. J. Antimicrob. Chemother. **42**: 475–482.

Green, M. R. and Sambrook, J. 2019. Agarose Gel Electrophoresis. *Cold Spring Harbor Protocols*, **2019(1)**: Doi:10.1101/pdb.prot100404.

Guzzo, M., Castro, L.K., Reisch, C.R., Guo, M.S. and Laub, M.T. 2020. A CRISPR Interference System for efficient and rapid gene knockdown in *Caulobacter crescentus*. mBio, **11(1)**: Doi: 10.1128/mBio.02415-19.

Han, Q., Phillips, R. S. and Li, J. 2019. Editorial: aromatic amino acid metabolism. *Frontiers in Molecular Biosciences*, **6**: doi:10.3389/fmolb.2019.00022.

Higgins, N. P. and Vologodskii, A. V. 2015. Topological behavior of plasmid DNA. *Microbiology Spectrum*, **3(2)**: Doi: 10.1128/microbiolspec.PLAS-0036-2014.

Kolly, G. S., Boldrin, F., Sala, C., Dhar, N., Hartkoorn, R. C., Ventura, M., … Cole, S. T. 2014b. Assessing the essentiality of the decaprenyl-phospho-d-arabinofuranose pathway in *Mycobacterium tuberculosis* using conditional mutants. *Molecular Microbiology*, **92(1)**: 194–211.

Kolly, G.S., Sala, C., Vocat, A. and Cole, S.T. 2014. Assessing essentiality of transketolase in *Mycobacterium tuberculosis* using an inducible protein degradation system, *FEMS Microbiology Letters*, **358(1)**: 30–35.

Lott, J.S. 2020. The tryptophan biosynthetic pathway is essential for *Mycobacterium tuberculosis* to cause disease. *Biochemical Society Transactions*, **48(5)**: 2029–2037.

McNeil, M.B. and Cook, G.M. 2019. Utilization of CRISPR interference to validate MmpL3 as a drug target in *Mycobacterium tuberculosis*. *Antimicrobial Agents and Chemotherapy*, **63**: Doi: 10.1128/AAC.00629-19.

Mehra, R., Rajput, V. S., Gupta, M., Chib, R., Kumar, A., Wazir, P., Nargotra, A. 2016. Benzothiazole derivative as a novel *Mycobacterium tuberculosis* shikimate kinase inhibitor: Identification and elucidation of its allosteric mode of inhibition. *Journal of Chemical Information and Modeling*, **56(5)**: 930–940.

Nirmal, C.R., Rao, R. and Hopper, W. 2015. Inhibition of 3-deoxy-D-arabino-heptulosonate 7-phosphate synthase from *Mycobacterium tuberculosis*: *In silico* screening and *in vitro* validation. *European Journal of Medicinal Chemistry*, **105**: 182–193.

Nunes, J.E.S., Duque, M.A., de Freitas, T.F., Galina, L., Timmers, L.F.S.M., Bizarro, C.V., Machado, P., Basso, L.A. and Ducati, R.G. 2020. *Mycobacterium tuberculosis* shikimate pathway enzymes as targets for the rational design of anti-tuberculosis drugs. *Molecules*, **25**: Doi.10.3390/molecules25061259.

Patnaik, R. and Liao, J. C. 1994. Engineering of *Escherichia coli* central metabolism for aromatic metabolite production with near theoretical yield. *Applied and Environmental Microbiology*, **60**: 3903–3908.

Pereira, J.H., Vasconcelos, I.B., Oliveira, J.S., Caceres, R.A., de Azevedo Jr, W.F., Basso, L.A. and Santos, D.S. 2007. Shikimate Kinase: a potential target for development of novel antitubercular agents. *Current Drug Targets*, **8**: 459–468.

Qi, L.S., Larson, M.H., Gilbert, L.A., Doudna, J.A., Weissman, J. S., Arkin, A.P. and Lim, W.A. 2013. Repurposing CRISPR as an RNA-guided platform for sequence-specific control of gene expression. *Cell*, **152**: 1173–1183**.**

Rock, J.M., Hopkins, F.F., Chavez, A., Diallo, M., Chase, M.R., Gerrick, E.R., Pritchard, J.R., Church, G.M., Rubin, E. J., Sassetti, C.M., Schnappinger, D. and Fortune, S.M. 2017. Programmable transcriptional repression in Mycobacteria using an orthogonal CRISPR interference platform. *Nature Microbiology*, **2**: 16274.

Simithy, J., Reeve, N., Hobrath, J.V., Reynolds, R.C. and Calderón, A.I. 2014. Identification of shikimate kinase inhibitors among anti-*Mycobacterium tuberculosis* compounds by LC-MS. *Tuberculosis*, **94(2)**: 152–158.

Singh, A.K., Carette, X., Potluri, L.-P., Sharp, J. D., Xu, R., Prisic, S. and Husson, R.N. 2016. Investigating essential gene function in *Mycobacterium tuberculosis* using an efficient CRISPR interference system. *Nucleic Acids Research*, **44(18):** e143–e143. doi:10.1093/nar/gkw625.

Smith, D.A., Parish, T., Stoker, N.G. and Bancroft, G.J. 2001. Characterization of auxotrophic mutants of *Mycobacterium tuberculosis* and their potential as vaccine candidates. *Infect. Immun*. **69**: 1142–1150.

Tam, C-M. 2008. Development of new antituberculosis drugs: Its relevance worldwide and in the Asia–Pacific region. *Respirology*,**13**: 125–131.

Tzin, V.; Galili, G.; Aharoni, A. 2012. Shikimate pathway and aromatic amino acid biosynthesis. eLS. John Wiley & Sons 2012.

Wellington, S. and Hung, D.T. 2018. The expanding diversity of *Mycobacterium tuberculosis* drug targets. *ACS Infect. Dis.*, **4**: 696–714.

Wolucka, B.A. 2008. Biosynthesis of D-arabinose in mycobacteria–a novel bacterial pathway with implications for antimycobacterial therapy. *FEBS J.*, **275**: 2691–2711.

Yelamanchi, S.D. and Surolia, A. 2021. Targeting amino acid metabolism of *Mycobacterium tuberculosis* for developing inhibitors to curtail its survival. *IUBMB Life*, **73(4)**: 643–658.

Zhang, Y.J., Reddy, M.C., Ioerger, T.R., Rothchild, A.C.; Dartois, V.; Schuster, B.M., Trauner, A., Wallis, D.;Galaviz, S. and Huttenhower, C *et al.* 2013. Tryptophan biosynthesis protects mycobacteria from CD4 T-cell-mediated killing. *Cell*, **155**: 1296–1308.

Chapter 7

7. Toxicological evaluation of the plant extracts

7.1 Introduction

Chemotherapeutic drugs exert toxicity to normal cells, which in turn causes unpleasant side effects to the patients. Administration of antibiotics in TB treatment is related to serious adverse effects such as gastrointestinal disorders, nephrotoxicity, skin rashes, fever, peripheral neuritis and hepatotoxicity (Yang *et al*., 2017). Anti-TB drug-related hepatotoxicity affects 5–28% of treated patients and negatively affects clinical outcome, leading to therapeutic doses reduction and treatment failure (Babalik *et al*., 2012).

The evaluation of kidney damage or dysfunction due to nephrotoxic effects of toxic compounds is complicated by the presence of different cell types exhibiting distinct morphologies and functions and, consequently, diverse responses to toxic compounds. Vero cells (African Green Monkey Kidney cell line) is a widely used model in toxicology and pharmacology research (Menezes *et al*., 2013). Vero cells, are homologous with human body cells and easy to be cultured (Liao *et al*., 2009), as such, the use of this cell line has been representative of human normal cells (Moghe *et al*., 2011). The sensitivity of the Vero cells to toxicity allows them to be ideal *in vitro* models to be used to evaluate cytotoxicity (Njeru and Muema, 2021; Afagnigni *et al*., 2020).

Monocytes are a type white blood cells and belong to the innate immune system. Monocytes can differentiate into macrophages with primary roles such as identifying invasive substances such as bacteria, viruses, fungi, etc. Human macrophage cell lines in their primary form are difficult to obtain and/or isolate in adequate amounts and are usually replaced by the cancer-derived THP-1 cell lines. Differentiation of the THP-1 cell line by stimuli triggers the spherical monocytic cells to acquire functional and morphological resemblance to macrophages (Balon and Wiatrak, 2021). The need to differentiate THP-1 cells to constitute a macrophage model is widely recognised in the scientific community (Balon and Wiatrak, 2021; Hu *et al*., 2016; Chanput *et al*., 2014).

Earlier studies reported the high similarity of the THP-1 cell line to primary monocytes and macrophages, particularly in the cellular function characteristics, differentiation markers and morphological phenotype (Ueki *et al*., 2002; Sakamoto *et al*., 2001). As such, this cell line has been extensively used in immune response studies and investigating monocyte structure and function in both health and disease (Hu *et al*., 2016). Stimuli such as phorbol-12-myristate-13-acetate (PMA), 1α, 25-dihydroxyvitamin D3 (vD3) or macrophage, colony-stimulating factor (M-CSF) play a critical role in the *in vitro* differentiation of monocytic THP-1 cell line into macrophage-like phenotype (Chanput *et al*., 2014). Various studies have reported that among the differentiation agents to obtain mature THP-1 monocyte-derived macrophage, PMA is the most optimal and efficient. Complete differentiation of the cell line may be achieved by treatment with 100 ng/mL PMA for at least 48 hours (Bastiaan-Net *et al*., 2013; Chanput, 2012; Chanput *et al*., 2013).

The 3-(4,5-dimethylthiazol-2yl)-2,5-diphenyl tetrazolium bromide (MTT) calorimetric assay is a widely used method to assess cytotoxic effects of drugs on selected cell lines by determining cell viability after prescribed treatment period. Living/viable cells convert the yellow water-soluble substrate 3-(4,5dimethylthiazol-2-y1)-2,5-diphenyl tetrazolium bromide (MTT) into a dark purple formazan product that is insoluble in water. The conversion of MTT is achieved by dehydrogenases enzymes associated with the endoplasmic reticulum and mitochondria (Senthilraja and Kathiresan, 2015).

The produced purple formazan precipitates within the cytosol from which, it can be dissolved following cell lysis. DMSO is a commonly used agent to dissolve the formazan product. Cells being dead following a toxic damage, cannot transform MTT to formazan. Therefore, the formation of the formazan products is directly proportional to the number of viable cells after drug treatment.

TB is easily contagious as it can be spread through the air commonly infects a subject's lung parenchyma through the inhalation of tubercle infected aerosols (Tekwu *et al*., 2012). Consequently, the alveolar macrophages are the first target and engagement of the host's immune system and Mycobacterium TB (Hiraiwa and Van Eeden 2013). The plant extracts were tested on THP-1 cells, which are monocytic cell line that can be differentiated *in vitro* to macrophages for toxicity (Pick *et al*., 2004).

The data may further give an insight on the potential interaction of the extracts and the respiratory system.

7.2 Materials and methods

7.2.1 Cell culture and maintenance

The THP-1 cell line was cultured in Royal Park Medical Institute-1640 (RPMI-1640) (Invitrogen) medium, supplemented with 10% fetal bovine serum (FBS) (Sigma-Aldrich) and incubated in a 5% CO_2/95% air fully humidified atmosphere at 37°C. Vero cells (African green monkey kidney cells, ATCC CCL-81), obtained from Stellenbosch University were grown in Dulbecco's modified Eagle's medium with low glucose, (DMEM-LG) (Invitrogen) supplemented with 10% fetal bovine serum.

7.2.1.1 THP-1 cell line

Start cultures were prepared by thawing stock cultures and inoculating 5 mL of RPMI supplemented media adding a volume of fresh medium every 48 h until they reached $1x10^5$ cells/mL in 20 mL RPMI supplemented media. Throughout the study procedures, THP-1 cells were maintained in a logarithmic growth phase where the cells were split every 2-3 days and were not allowed to exceed $1x10^6$ cells/mL. Cell counts and viability using the trypan blue dye exclusion method. Briefly, 20 μL of culture was mixed with 80 μL of trypan blue solution and the cells were counted on a hemacytometer. Passages were prepared by first harvesting the cells by centrifugation of 10 mL of the culture at 5000 rpm for 5 mins. The pellet was resuspended in 5 mL of media, and 1 mL of this resuspension was added to 19 mL RPMI supplemented media. The morphology of the cells was observed using the ZOE™ Fluorescent Cell Imager (Bio-RAD). Scale bars were added to the pictures.

7.2.1.2 Vero cell line

Start cultures were prepared by thawing stock cultures and inoculating 5 mL of RPMI supplemented media adding a volume of fresh medium every 48 h until they reached $1x10^5$ cells/mL in 20 mL RPMI supplemented media. Cells were maintained at 37 °C under a humidified 5% CO_2 atmosphere. The cultured Vero cells were harvested by trypsinization and pooled in a 50 mL vial. Cell counts and viability using the trypan blue dye exclusion method. Briefly, 20 μL of culture was mixed with 80 μL of trypan blue solution and the cells were counted on a hemacytometer. The cells were maintained for 5 passages for bioassay (Chan *et al*., 2015). The morphology of the cells was observed using the ZOE™ Fluorescent Cell Imager (Bio-RAD). Scale bars were added to the pictures.

7.2.2 MTT assay to evaluate cell viability

The cell viability assay measures the amount of the blue-colored formazan produced intracellularly following cleavage of the 3-(4,5-dimethylthiazol-2-yl)-2,5-diphenyltetrazolium bromide (MTT) reagent by mitochondrial dehydrogenases of the viable cells. The absorbance of the produced intracellular formazan which is proportional to the number of viable cells present was determined at 570 nm.

THP-1 cells were differentiated into macrophages by exposure to phorbol 12-myristate 13-acetate (PMA). Both the PMA concentration and the duration of treatment affect maturation. Differentiation of THP-1 cell line with PMA treatment has been previously reported to be optimal when incubated for 2-5 days (Starr *et al*., 2018). Growing THP-1 culture was diluted to a 2×10^5 cell/mL in a 50 mL vial. In this study, the THP-1 cells were pre-treated with 25 μL of 100 μg/mL PMA to yield a final concentration of 50 ng/μL in the 50 mL vial and the cells were seeded at 2×10^5 cell/mL (per well) in flat bottom 96 well plates for 72 hrs in 5% CO_2 at 37°C to induce maturation of the monocytes into macrophage-like adherent cells. THP-1 cells per well were seeded in 96 well plates to a final volume of 100 µL. It is vital to arrest the differentiation of the cell line after 48 hr treatment with PMA to increase macrophage markers (Chanput *et al*., 2014). After treatment with PMA, the spent media was removed, and the cells were washed with pre-warmed 1X PBS and fresh media was added followed by 24 hr incubation (Safar *et al*., 2019 THP1 reference*).

Extract concentrations were prepared separately, briefly, each extract was pre-solubilized in DMSO at 37 °C to give a stock solution of 200 mg/mL. The extracts were diluted with complete RPMI 40 media for THP-1 cell line and complete DMEM media for the Vero moneky cells. The dilutions were made to give working concentrations of 1000, 500 and 100 µg/mL, ensuring that the final concentration of DMSO in the tested dilutions was not higher than 1%.

A confluent Vero cell monolayer with the cell density of 4×10^4 cells/well (100 µL) was seeded in 96-well plates and incubated at 37 °C in a 5 % CO_2 incubator for 24 hrs. For the Vero cell line, the culture medium was replaced by new complete DMEM medium containing plant extracts with the concentrations 100, 500 and 1000 µg/mL. For the differentiated THP-1 macrophages, the culture medium was replaced by new complete RPMI medium containing plant extracts with the concentrations 100, 500 and 1000 µg/mL. The plates were incubated for another 24 hrs at 37 °C in a 5 % CO2 incubator and the cell viability was evaluated using the MTT colorimetric assay. A 20 µL of MTT solution (5 mg/mL in phosphate buffered saline (PBS) was pipetted into each well followed by a 4-hr incubation period at 37 °C in the 5 % CO_2 incubator until purple precipitates were clearly visible under a microscope. The MTT solution was filter sterilised before adding to the 96 well plates. Flowing, the medium together with MTT were aspirated off the wells and 100 µL of DMSO was added to the wells to dissolve the MTT formazan. The absorbance was determined at 570 nm using a microplate reader. Absorbance of wells filled with media alone was used as a blank and untreated control wells were seeded with cells that incubated without any extracts. Results were obtained from three independent experiments and duplicate assays were performed for each experiment (Chan *et al*., 2015).

The 50% cytotoxic concentration (CC_{50}) (µg/mL) was defined as the extract/compound concentration required for the reduction of cell viability by half. The CC_{50} value and the standard error mean (SEM) were calculated using a non-linear regression curve contained in the Graphpad PRISM® 9.0 statistical software. The percentage cell viability (CV) was calculated manually using the equation (7.1). To determine the selectivity index (SI) of the solvent extract fractions, we divided their CC_{50} with their antitubercular MIC (all in µg/mL) as previously done by others (Njeru and Muema, 2021; Afagnigni *et al*., 2020; Mongalo *et al*., 2017).

Percentage (%) cell viability: $\frac{\text{Average absorbance plant extract wells}}{\text{Average absorbance of control wells}} \times 100$ (7.1)

Statistical analysis

Data were expressed as the mean percentage of cell viability. Significance levels among were analysed using analysis of variance (ANOVA), with Software Graphpad

PRISM® 9.0. For multiple comparisons among groups, control group and intra-group, we used the Dunnett test, with significance set at $p < 0.05$.

7.3 Results

7.3.1 Morphological evaluation

The morphology of the cell lines were observed with fluorescent Cell Imager (Bio-RAD). The THP-1 monocytic cell line was in media in suspension and the cells appeared spherical and regular in shape and grew singularly (Figure 7.1A). After stimulation with PMA for 2 days, it was seen that the cells adhered to the surface of the culture plates and had adopted a macrophage-like morphology, where they appeared flat and amoeboid shaped (Figure 7.1B).

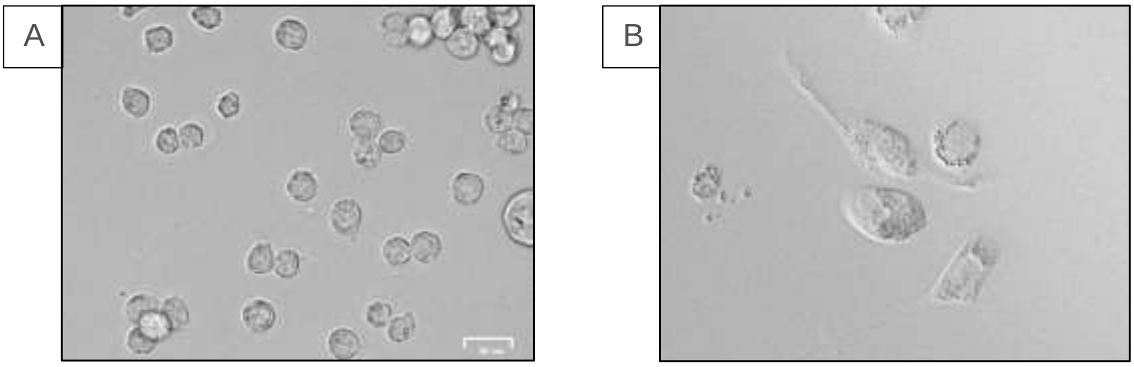

Figure 7.1: THP-1 cell line grown in RPMI. A: Undifferentiated THP-1 cell line (monocytes), B: PMA treated THP-1 cell line in the process of differentiating into macrophage-line cells.

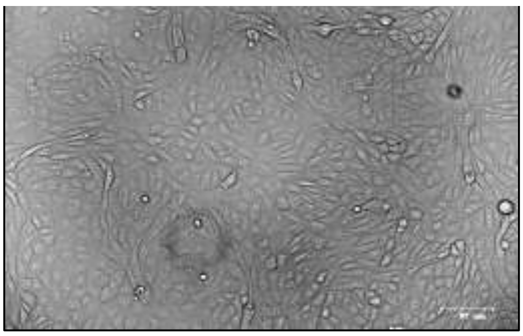

Figure 7. 2: Vero cell line cultured in DMEM media supplemented with 10% fetal bovine serum.

7.3.2 Toxicological studies on plant extracts using MTT assay

Acacia senegal, *Gadernia volkensii*, *Ficus sur*, *Senna petersiana* and *Clerodendrum glabrum* significantly reduced the number of viable Vero cells (p<0.01) at all tested concentrations compared to untreated control cells (Figure 7.). At concentrations 100 and 500 μg/mL, *Croton gratissimus* and *Peltophorum africanum* extracts had a non-significant effect on both the Vero cell line and THP-1 macrophages (Figure). In addition, the results suggested that *P. africanum* increased the number of viable THP-1 macrophages at 100 μg/mL concentration. Similarly, *Carissa bispinosa* increased the number of viable Vero cells at 100 μg/mL. However, *C. bispinosa* was toxic to THP-1 macrophages at the tested concentrations. No effect was obtained with DMSO at the effective extract concentrations.

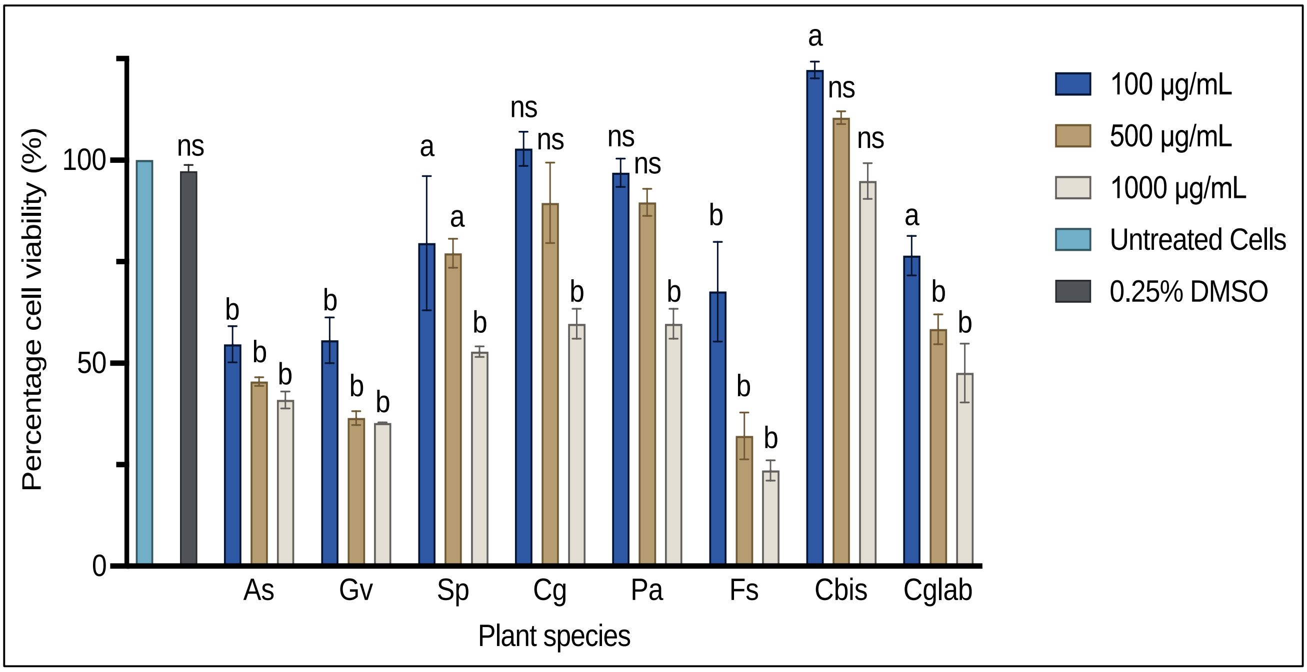

Figure 7. 3: Vero cell line exposed to varying concentrations of plant extracts. Cell viability is expressed as percentage of untreated cells that were seeded.

Key: Two way ANOVA, a: Significant difference where p<0.01, b: Significant difference where p<0.0001, ns: non significance whereby p>0.05.

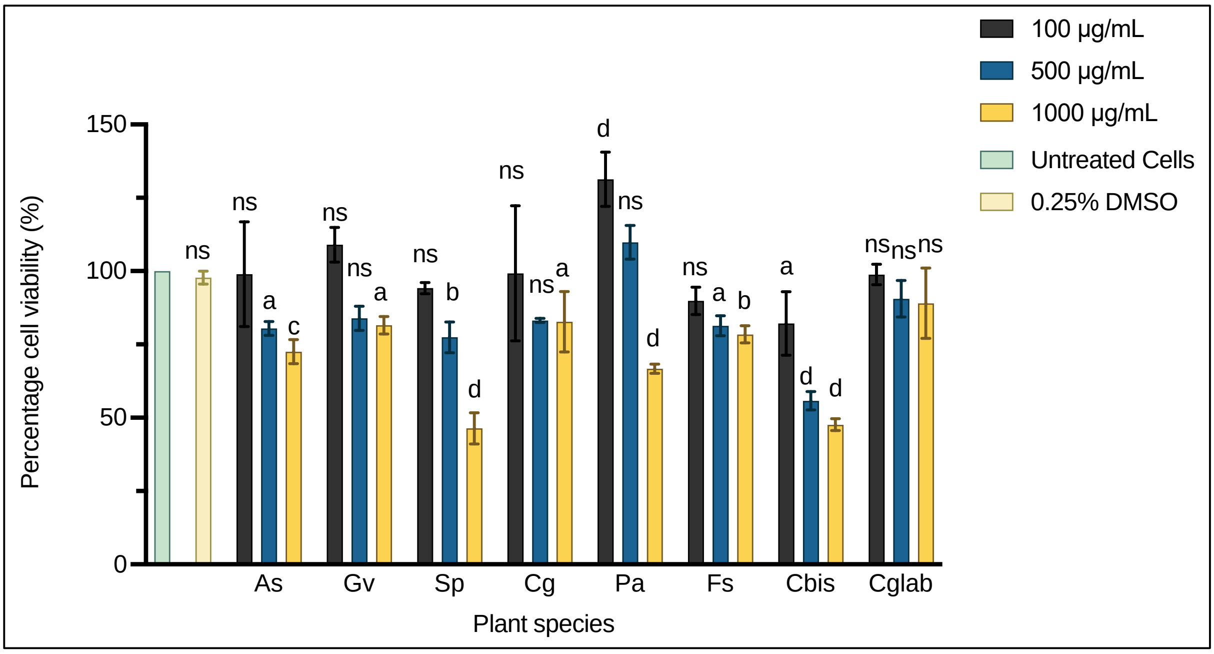

Figure 7. 4: THP-1 macrophages exposed to various concentrations of plant extracts.

Table 7. 1: Half maximal inhibitory concentration and selective indices of plant extracts.

Plant extract	Vero cell line				THP-1 macrophages			
	IC_{50} (µg/mL)	r^2	SI Smeg	SI Tb	IC_{50} (µg/mL)	r^2	SI Smeg	SI Tb
A. senegal	31.34	0.992	0.012	ND	372.70	0.941	0.149	ND
G. volkensii	68.30	0.993	0.054	0.027	188.00	0.920	0.15	0.075
S. petersiana	122.00	0.837	0.048	ND	134.90	0.910	0.054	ND
C. gratissimus	184.10	0.959	0.187	0.147	156.20	0.956	0.158	0.124
P. africanum	515.60	0.973	0.412	0.206	699.20	0.960	0.559	0.280
F. sur	121.70	0.973	0.097	ND	329.80	0.894	0.264	ND
C. bispinosa	704.10	0.947	0.563	ND	114.50	0.902	0.092	ND
C. glabrum	184.14	0.958	0.188	0.29	181.60	0.914	0.185	0.288

Key: SI Smeg: Selectivity index calculated with *M. smegmatis* MIC, SI Tb: Selectivity index calculated for *M. tuberculosis*, IC_{50}: Half maximal inhibitory concentration, r2: coefficient of determination.

7.4 Discussion

Plants and plant-based products remain an important source of novel leads in therapeutic drug discovery and have long been used by people as a form of complementary and alternative medicine. Although the contribution of plants to health is immense, it has been shown and highlighted by various studies that plant-derived medicines and extracts are not always safe and possess potential for patient poisoning (Makhafola *et al*., 2014; Bussmann *et al*., 2011). It is therefore necessary to assert the safety of bioactive medicinal plant extracts. Vero cells were selected as a model to evaluate the safety of the plant extracts on normal cell line.

7.4.1 Morphological evaluation

In this study phorbol-12-myristate-13- acetate (PMA) differentiated THP-1 monocyte cell line were used to evaluate the potential toxicity of the plant extracts on the immune system and the respiratory system because their macrophage-like phenotype mimics human peripheral blood mononuclear cell (PBMC) monocyte-derived macrophages (Chanput *et al*., 2014). The morphology of the monocytic THP-1 cell line was altered to flat and amoeboid shaped cells, which adhered to the culture plates. The cells appeared to have displayed well defined golgi apparatuses, rough endoplasmic reticula, and large numbers of ribosomes in the cytoplasm (Figure 7.1). Similar observations of the THP-1 macrophage-like phenotypes were reported by (Chanput *et al*., 2013).

7.4.2 Broth micro-dilution assay

MTT assay was central to study the toxicity by determining the cell viability of the different cell lines after exposure to the plant extracts. This assay measures cytotoxicity by measuring the conversion of yellow water-soluble substrate 3-(4,5-dimethylthiazol-2-y1)-2,5-diphenyl tetrazolium bromide (MTT) into a dark blue formazan product. This formation production is proportionate to the viable cell number and inversely proportional to the degree of cytotoxicity.

Cell viability is the cell's ability to maintain its life. Percentage of inhibition indicates the amount of inhibition of cells by a test drug. Untreated cells were used as a control to compare the effect of the plant extracts on the selected cell lines. The final concertation of DMSO was maintained at 0.25%. Cell culture sensitivity to DMSO has been well documented (Berger *et al*., 2017). The potential effect of DMSO was evaluated by incubating the cell cultures with final concentration of 0.25% DMSO as a negative control. No significant effect of DMSO on the cell cultures was observed between both the Vero cells and THP-1 macrophages (Figures). This gives confidence that the effect of the extracts on the cell viability of the selected cells would be due to the phytochemicals in the extracts only with no contribution by DMSO, the solvent of choice.

The results of this study showed that *Acacia senegal*, *Gadernia volkensii* and *Ficus sur* had all significantly reduced viable Vero cells were $p<0.0001$. The methanolic extract of *F. sur* fruit was found to be toxic using the higher grade of heart rate reduction method and caution was recommended on the use of *F. sur* (Sinan et al., 2022). Ethanol extracts of *F. sur* have also been indicated to have toxicity towards Vero cell line where IC_{50} was 0.75 μg/mL (Madikizela, 2014). In addition, *F. sur* ethanol extract was reported to have toxic, deleterious and fatal effects at doses beyond 1000mg/kg body weight on adult mice after 24-hr treatment (Akomas *et al*., 2014). The aqueous extract of *A. senegal* showed 57.59 %± 0.09 cell inhibition at 125 μg/mL with IC_{50} 23.5 μg/mL normal cell cultures Raw 264.7 (Hilmi and Abushama, 2014). However, at lower concentrations (250 and 25 μg/mL), 70% ethanol *A. senegal* extract was reported be increase of viable human keratinocyte cells (Magnini *et al*., 2021). The dichloromethane extract of *G. volkensii* have been reported to be toxic in a comet assay whilst the DCM extract and methanol extracts of the twigs/bark were toxic both in the micronuclei and comet assays (Taylor *et al*., 2003). The fruit extract (methanol and chloroform) of *G. volkensii* moderate lethality against brine shrimps (Artemia salina) (Juma and Majinda, 2007). The data provide evidence that these extracts could potentially contain selective cytotoxic agents.

At 100 μg/mL and 500 μg/mL, *Croton gratissimus* and *Peltophorum africunum* extracts were non-toxic towards both the viable Vero cells and THP-1 macrophages. Studies by Bizimenyera *et al*. (2007) corroborate the non-cytotoxicity of the acetone leaf extract of *P. africanum* on Vero monkey cell line and the brine shrimp larval mortality assay (Bizimenyera et al., 2007). It has been proven that the co-administration of plant-derived chemical species with anti-TB drugs reduced the damaged caused by these chemotherapeutic drugs (isoniazid) on vital organs such as the liver in mice (Tousif *et al*., 2017). Interestingly, at 100 μg/mL, *P. africanum* significantly increased the number of THP-1 macrophages. Strong evidence has revealed that some plant extracts can indeed improve and stimulate the function of macrophages (Albrahim *et al*., 2020; Chueh *et al*., 2015).

Likewise, *C. bispinosa* extract demonstrated significant proliferative activity towards the Vero cells at 100 μg/mL compared to untreated control. The *C. bispinosa* fruit is popular around locals in KwaZulu Natal, South Africa and commonly sold in the summer months of the year (Patel, 2013). The widespread use of the fruit and the lack of acute toxicology effects may demonstrate that it is not being consumed at toxic concentrations. Although, no sufficient toxicological studies exist for *C. bispinosa*, other members of the genus Carissa, such as aqueous *Carissa edulis* have been reported to be non-toxic on female Wistar rats after 28-day sub-chronic toxicity (Osseni *et al*., 2016).

Macrophages are vital during *M. tuberculosis* infection and have been proven to further serve as reservoirs of the tubercle cells. Patients with weak immune systems have been reported to be more prone to latent TB infection or reactivation of the active disease (Hasan *et al*., 2018). This array of plants and their components hold immunomodulating properties. Medicinal plants have been reported to be adjuvants to traditional remedy for promoting the immune response (Varma *et al*., 2016, Zhang *et al*., 2018). *Clerodendrum glabrum* extract was the most non-toxic to THP-1 macrophages with a non-significant decrease of viable cells at all tested concentrations. Except *C. bispinosa*, all plant extracts were not toxic to the THP-1 macrophages at 100 μg/mL. *C. bispinosa* was most toxic to the THP-1 macrophages than all other plant extracts tested because at 500 μg/mL, only 55.77% of THP-1 macrophages were viable after the 24-hr treatment.

7.4.3 Half maximal inhibitory concentration and selective indices of plant extracts

Higher IC_{50} values indicate that it would require a large quantity of the plant extract to cause a toxic response, while small IC_{50} values imply high toxicity and could be harmful to human health. The IC_{50} µg/mL of the extracts on Vero cell line and THP-1 macrophages ranged between 31.34-515 μg/mL and 114,50-699.2 μg/mL respectively. In genal, the Vero cell lines was more sensitive to the plant extracts than THP-1 macrophages. *A. senegal* (31.34 μg/mL IC_{50}) and *G. volkensii* (68.30 μg/mL IC_{50}) were the most toxic to the Vero cell line as previously established in this work. Similar results were reported were Sibandze, (2009) found that the fruit and leaf acetone extracts of *G. volkensii* exhibited cytotoxic activities with IC_{50} values of 21.3 µg/mL and 89.5 µg/mL, respectively against human kidney epithelial (Graham) cells (Sibandze, 2009).

Clerodendrum glabrum acetone leaves extracts were previously reported to be non-toxic to Vero cell line (357.11 μg/mL LC50) (Dzoyem *et al*., 2015). The IC_{50} of the *C. glabrum* acetone leaves in this study against Vero cells (184.11 μg/mL) was lower than previously reported.

As expected, *P. africanum* extract demonstrated non-toxic IC_{50} values towards both cell lines, where, 515 μg/mL and 699 μg/mL were determined as IC_{50} values for Vero cells and THP-1 macrophages, respectively. Low toxicity of *P. africanum* was also reported by Adebayo *et al*. (2015) were an IC_{50} of 103 μg/mL of 70% acetone extract against Vero cell lines was determined at a concentration of 5 mg/mL, each yielding LC_{50} >1000 µg/ml (Bizimenyera *et al*., 2007). Commonly, recent toxicological studies have set the threshold of cytotoxic concentrations of extracts, such that IC_{50} concentrations below 20 µg/mL are to be regarded as toxic, and above 20 µg/mL to be non-toxic as previously reported (Njeru and Muema, 2021; Afagnigni *et al*., 2020, Elisha *et al*., 2017). The toxicological results in this study highlight the importance of assessing the percentage cell viability concurrently with IC_{50} values. This is because the IC_{50} values fails to provide data about the interaction of the cell line with the extracts at different concentrations. However, determining the cell viability provides that extra data on the effect of the extracts at all selected concentrations.

Another important aspect of the toxicological evaluation of the plant extract was the determination of selectivity index. The selectivity index values indicate the plant extract’s relative safety. In this work, selectivity index values of the extracts were calculated by dividing the cytotoxicity IC_{50} (in μg/mL) by MIC (μg/mL). The MIC values that were chosen where those determined against *M. smegmatis* and *M. tuberculosis*

(Chapter 5). The selectivity indices were calculated this way to evaluate the selectivity of the extracts between the mammalian and mycobacterial cells. Plant extracts may present good inhibitory activities against test microorganisms, however, should the extracts be highly toxic to normal human cells, that indicates the lack of safety of the extracts to be used for the treatment of the infectious microorganism. All the extracts had relatively low SI values between both Vero cell line and THP-1 macrophages and were all less than 1 (Table 7.1). Plant extracts with SI values >1 imply that the extracts are more toxic mycobacterial cells then mammalian cells. In contrast, when the SI values are less than one (<1), this indicates the extracts are more toxic to mammalian cells than the mycobacterial pathogens (Elisha *et al*., 2017). The results indicate that at the high extract concentrations required to inhibit mycobacterial growth (MIC), the extracts would have caused deleterious and toxic effects to the host normal cells and possibly, the immune system (monocytes and macrophages).

7.5 Conclusion

The toxicological results of this study show that in crude form, the acetone plant extracts were generally non-toxic to THP-1 macrophages and Vero cell line at low concentrations. The proliferative activity of *P. africanum* and *C. bispinosa* extracts on THP-1 macrophages and Vero cell line respectively warrant further investigations as potential immune booster agents. The low SI values indicate that the extracts in their crude form may not be safe to treat *M. tuberculosis* infections. It may be worthwhile to confirm the reported toxic effects on in vivo. models should the extract are intended to be used in this therapeutic context of TB treatment. The toxicity of the extracts may be circumvented by the use of chromatography techniques to separate bioactive compounds of interest from those that are toxic (Masoko *et al*., 2010; Eloff *et al*., 2005). Through fractionation and further purification using chromatography techniques, the active antimycobacterial compounds can be separated from the toxic compounds.

7.6 References

Adebayo, S.A., Dzoyem, J.P., Shai, L.J. and Eloff, J.N. 2015. The anti-inflammatory and antioxidant activity of 25 plant species used traditionally to treat pain in southern African. *BMC Complementary and Alternative Medicine*, **15(1)**: Doi:10.1186/s12906-015-0669-5.

Afagnigni, A.D., Nyegue, M.A., Djova, S.V. and Etoa, F-X. 2020. LC-MS analysis, 15-lipoxygenase inhibition, cytotoxicity, and genotoxicity of *Dissotis multiflora* (Sm) triana (melastomataceae) and *Paullinia pinnata* Linn (Sapindaceae). *Journal of Tropical Medicine*, **2020**: Doi: 10.1155/2020/5169847.

Akomas, S.C., Ijioma, S.M. and Emelike, C.U. 2014. *In vivo* and *In vitro* spasmolytic Effect of *Ficus sur* Forssk Ethanol Leaf Extract on the Gastrointestinal. *Tract British Biotechnology Journal***, 4(11)**: 1182–1190.

Albrahim, T., Alnasser, M.M., Al-Anazi, M.R., ALKahtani M.D., Alkahtani, S., Al-Qahtani, A.A. 2020. *In vitro* studies on the immunomodulatory effects of *Pulicaria crispa* extract on human THP-1 monocytes. *Oxidative Medicine and Cellular Longevity*, **2020**: Doi: 10.1155/2020/7574606.

Babalık, A., Arda, H., Bakırcı, N., Ağca, S., Oruç, K., Kızıltaş, S., Cetintas, G. and Calisir, H.C. 2012. Management of and risk factors related to hepatotoxicity during tuberculosis treatment, *Tüberk Toraks*, **60(2)**: 136–144.

Balon, K. and Wiatrak, B. 2021. PC12 and THP-1 Cell Lines as Neuronal and Microglia Model in Neurobiological Research. *Applied Sciences*, **11**: Doi: 10.3390/app11093729.

Bastiaan-Net, S., Chanput, W., Hertz, A., Zwittink, R.D., Mess, J.J. and Wichers, H.J. 2013. Biochemical and functional characterization of recombinant fungal immunomodulatory proteins (rFIPs). *International Immunopharmacology*, **15(1)**: 167–175.

Berger, E., Breznan, D., Stals, S., Jasinghe, V.J., Gonçalves, D., Girard, D., Faucher, S., Vincent, R., Thierry, A.R. and Lavigne, C. 2017. Cytotoxicity assessment, inflammatory properties, and cellular uptake of Neutraplex lipid-based nanoparticles in THP-1 monocyte-derived macrophages. *Nanobiomedicine*, **4**: Doi: 10.1177/1849543517746259.

Bizimenyera, E.S., Aderogba, M.A., Eloff, J.N. and Swan, G.E. 2007. Potential of neurodegenerative antioxidant-based therapeutics from *Peltophorum africanum* Sond

(Fabaceae). *African Journal of Traditional, Complementary and Alternative Medicines*, **4(1)**: 99–106.

Bussmann, R. W., Malca, G., Glenn, A., Sharon, D., Nilsen, B., Parris, B. and Townesmith, A. 2011. Toxicity of medicinal plants used in traditional medicine in Northern Peru. *Journal of Ethnopharmacology*, **137(1)**, 121–140.

Chan, S.M., Khoo, K.S. and Sit, N.W. 2015. Interactions between plant extracts and cell viability indicators during cytotoxicity testing: implications for ethnopharmacological studies. *Tropical Journal of Pharmaceutical Research*, **14 (11)**: 1991–1998.

Chanput, W.R., Kleinjans, L., Mes. J.J., Savelkoul, H.F.J. and Wichers, H.J. 2012. β-Glucans are involved in immune-modulation of THP-1 macrophages. *Molecular Nutrition and Food Research*, **56(5)**: 822–833.

Chanput, W.R., Mes, J. J. and Wichers, H. J. 2014. *THP-1 cell line: An in vitro cell model for immune modulation approach. International Immunopharmacology*, **23(1)**: 37–45.

Chanput, W.R., Mes, J.J., Savelkoul, H.F.J. and Wichers, H.J. 2013. Characterization of polarized THP-1 macrophages and polarizing ability of LPS and food compounds. *Food and Function*, **4(2)**: 266-276.

Chueh, F.S., Lin, J.J., Weng, S.W., Huang, Y.P and Chung, J.G. 2015. Crude extract of *Polygonum cuspidatum* stimulates immune responses in normal mice by increasing the percentage of Mac-3-positive cells and enhancing macrophage phagocytic activity and natural killer cell cytotoxicity. *Molecular Medicine Reports*, **11(1)**: 127–132.

Elisha, I. L., Jambalang, A. R., Botha, F. S., Buys, E. M., McGaw, L. J. and Eloff, J. N. 2017. Potency and selectivity indices of acetone leaf extracts of nine selected South African trees against six opportunistic Enterobacteriaceae isolates from commercial chicken eggs. *BMC complementary and alternative medicine*, **17(1)**: 90. Doi: 10.1186/s12906-017-1597-3.

Eloff, J. N., Famakin, J. O. and Katerere, D. R. P. 2005. *Combretum woodii* (Combretaceae) leaf extracts have high activity against Gram-negative and Gram-positive bacteria. *African Journal of Biotechnology*, **4(10)**: 1161–1166.

Hasan, T., Au, E., Chen, S., Tng, A. and Wong, G. 2018. Screening and prevention for latent tuberculosis in immunosuppressed patients at risk for tuberculosis: a systematic review of clinical practice guidelines. *BMJ Open*, **2018(8)**: Doi: 10.1136/ bmjopen-2018-022445.

Hilmi, Y. and Abushama, M. 2014. *In-vitro* cytotoxicity of selected Sudanese medicinal plants with potential antitumor activity. *Qatar Foundation Annual Research Conference Proceedings, Qatar Foundation Annual Research Conference Proceedings*, **2014(1)**: Doi: 10.5339/qfarc.2014.HBPP0213.

Hiraiwa, K. and van Eeden, S. F. 2013. Contribution of lung macrophages to the inflammatory responses induced by exposure to air pollutants. *Mediators of Inflammation*, **2013**: Doi: 10.1155/2013/619523.

Hu, Z.D., Wei, T.T., Tang, Q.Q., Ma, N., Wang, L., Qin, B. D., Yin, J. R., Zhou, L. Zhong, R. Q. 2016. Gene expression profile of THP-1 cells treated with heat-killed *Candida albicans*. *Annals of Translational Medicine*, **4(170)**: DOI: 10.21037/atm.2016.05.03.

Juma, B. F., and Majinda, R. R. T. 2007. Constituents of *Gardenia volkensii*: their brine shrimp lethality and DPPH radical scavenging properties. *Natural Product Research*, **21(2)**: 121–125.

Liao, T., Wang, L. and Shi, Y. 2009. Cytotoxic characteristics and sensitivities of Vero Cells exposed to organic chemicals pollutant and the feasibilities in bio-toxicity test of drinking water concerning*. International Conference on Bioinformatics and Biomedical Engineering:* Doi: 10.1109/icbbe.2009.5162570.

Madikizela, B. 2014. Pharmacological evaluation of South African medicinal plants used for treating tuberculosis and related symptoms. PhD thesis, University of KwaZulu-Natal, Pietermaritzburg, South Africa.

Magnini, R.D., Nitiéma, M., Ouédraogo, G.G. et al. 2021. Toxicity and bacterial anti-motility activities of the hydroethanolic extract of *Acacia senegal* (L.) Willd (Fabaceae) leaves. *BMC Complementary Medicine and Therapies*, **21(178)**: Doi: 10.1186/s12906-021-03348-5.

Makhafola, T.J., McGaw, L.J. and Eloff, J.N. 2014. *In vitro* cytotoxicity and genotoxicity of five Ochna species (Ochnaceae) with excellent antibacterial activity. *South African Journal of Botany*, **91**: 9–13.

Masoko, P., Picard, J., Howard, R. L., Mampuru, L. J. and J. N. Eloff. 2010. *In vivo* antifungal effect of Combretum and Terminalia species extracts on cutaneous wound healing in immunosuppressed rats. *Pharmaceutical Biology*, **48(6)**: 621–632.

Menezes, C., Valério, E. and Dias, E. 2013. The Kidney Vero-E6 Cell Line: a suitable model to study the toxicity of microcystins, new insights into toxicity and drug testing, sivakumar gowder. *IntechOpen*: DOI: 10.5772/54463.

Moghe, A.S., Gangal, S.G. and Shilkar. 2011. In vitro cytotoxicity of *Bryonia laciniosa* (Linn.) Naud. On human cancer cell lines. *Indian Journal of Natural Products and Resources*, **2(3)**: 322–329.

Mongalo, N.I., McGaw, L.J., Finnie, J.F. and Staden, J.V. 2017. Pharmacological properties of extracts from six South African medicinal plants used to treat sexually transmitted infections (STIs) and related infections. *South African Journal of Botany*, 112: 290–295.

Njeru, S.N. and Muema, J.M. 2021. *In vitro* cytotoxicity of *Aspilia pluriseta* Schweinf. extract fractions. BMC Research Notes, **14(57)**: Doi: 10.1186/s13104-021-05472-4.

Osseni, R., Akoha, S., Adjagba, M., Azonbakin, S., Lagnika, L., Awede, B., Bigot, A., Diouf, A., Darboux, R. and Laleye, A. 2016. *In vivo* toxicological assessment of the aqueous extracts of the leaves of *Carissa edulis* (Apocynaceae) in Wistar rats. *European Journal of Medicinal Plants*, **15(1)**: 1–10.

Patel, S. 2012. Food, pharmaceutical and industrial potential of Carissa genus: an overview. Food, pharmaceutical and industrial potential of Carissa genus: an overview. *Reviews in Environmental Science*, **11(4)**: Doi: 10.1007/s11157-012-9306-7.

Pick, N., Cameron, S., Arad, D. and Av-Gay, Y. 2004. Screening of compounds toxicity against human monocytic cell line-THP-1 by Flow Cytometry. *Biological Procedures Online*, **6**: 220–225.

Safar, R., Doumandji, Z., Saidou, T., Ferrari, L., Nahle, S., Rihn, B.H. and Joubert, O. 2019. Cytotoxicity and global transcriptional responses induced by zinc oxide nanoparticles NM 110 in PMA-differentiated THP-1 cells. *Toxicology Letters*, **308**: 65–73.

Sakamoto, H., Aikawa, M., Hill, C.C., Weiss, D., Tayler, W.R., Libby, P. and Lee, R.t. 2001. Biomechanical strain induces class A scavenger receptor expression in human monocyte/macrophages and THP-1 cells: a potential mechanism of increased atherosclerosis in hypertension. *Circulation*, **104(1)**: 109–114.

Senthilraja, P. and Kathiresan, K. 2015. *In vitro* cytotoxicity MTT assay in Vero, HepG2 and MCF -7 cell lines study of Marine Yeast. *Journal of Applied Pharmaceutical Science*, **5(3)**: 80–84.

Sibandze, G.F. 2009. Pharmacological properties of Swazi medicinal plants. MSc Dissertation. University of the Witwatersrand, Johannesburg.

Sinan, K.I., Mahomoodally, M.F., Sadeer, N.B., Jeko, J., CZiaky, Z., Chiavaroli, A., Recinella, L., Leone, S., Simone, S.C., Brunetti, L., Orlando, G., Menghini, L., Ferrrante, C. and Zengin, G. 2022. Chemical characterization and biopharmaceutical properties of three fruits from Côte d'Ivoire. *International Journal Dealing with all Aspects of Plant Biology*, Doi: 10.1080/11263504.2021.2024909.

Starr, T., Bauler, T.J., Malik-Kale, P. and SteeleMortimer, O. 2018. The phorbol 12-myristate-13acetate differentiation protocol is critical to the interaction of THP-1 macrophages with *Salmonella Typhimurium*. *Public Library of Science* ONE, **13(3)**: e0193601.

Taylor, J. L. S., Elgorashi, E. E., Maes, A., Van Gorp, U., De Kimpe, N., van Staden, J. and Verschaeve, L. 2003. Investigating the safety of plants used in South African traditional medicine: testing for genotoxicity in the micronucleus and alkaline comet assays. *Environmental and Molecular Mutagenesis*, **42(3)**, 144–154.

Tekwu, E.M., Askun, T., Kuete, V., Nkengfack, A.E., Nyasse, B., Etoa, F.X. and Beng, V.P. 2012. Antibacterial activity of selected Cameroonian dietary 179 spices ethno-medically used against strains of *Mycobacterium tuberculosis*. *Journal of Ethnopharmacology*, **142**: 374–382.

Tousif, S., Singh, D.K., Mukherjee, S., Ahmad, S., Arya, R., Nanda, R. *et al*. 2017. Nanoparticle-formulated curcumin prevents post-therapeutic disease reactivation and reinfection with *Mycobacterium tuberculosis* following isoniazid therapy. *Frontiers in Immunology*, **8**: Doi: 10.3389/fimmu.2017.00739.

Ueki, K, Tabeta,K., Toshie, H. Yamazaki, K. 2002. Self-heat shock protein 60 induces tumour necrosis factor-α in monocyte-derived macrophage: possible role in chronic inflammatory periodontal disease. *Clinical and Experimental Immunology,* **127(1)**: 72–77.

Varma, R.S., Guruprasad, K.P., Satyamoorthy, K., Kumar, L.M.S., Babu, U.V. and Patki, P. 2016. IM-133N modulates cytokine secretion by RAW264.7 and THP-1 cells, *Journal of Immunotoxicology*, **13(2)**: 217–225.

Yang, T.W., Park, H.O., Jang, H.N., Yang, J.H., Kim, S.H., Moon, S.H. 2017. Side effects associated with the treatment of multidrug-resistant tuberculosis at a tuberculosis referral hospital in South Korea: a retrospective study. *Medicine*, **96**: e7482.

Zhang, G., Gao, X., Zeng, H., Li, Y. and Guo. X. 2018. Virosecurinine induces apoptosis in human leukemia THP-1 cells and other underlying molecular mechanisms. *Oncology Letters*, **15(1)**: 849–854.

CHAPTER 8

8. General discussions and conclusions

8.1 General discussions

Natural products have been used since ancient times for the treatment of many diseases. Before the 20th century, 80% of all medicines used to treat human and animal illness were obtained from the leaves, barks and roots of medicinal plants. It is noteworthy to mention that about 70% of the drugs used today are models of natural products (Newman and Cragg, 2016). Between 1981 and 2010, approximately 700 natural products or natural product derived new chemical entities were approved (Ogbourne, 2014).

Despite remarkable achievements in the development of antimicrobial natural products, a major bottleneck in the drug discovery process had remained target identification (Farha and Brown, 2015). One of the main conundrums of antimicrobial drug discovery is that not all viable targets can be relevant towards the pathogenesis of a microorganism. In turn, this exerts an emphasis on target validation for a particular organism (Yuan and Sampson, 2018). *M. tuberculosis* metabolism has been a focus of intense research towards TB drug discovery (Beste and McFadden, 2010). Genetic tools used in molecular biology to disrupt enzymatic activities and regulatory functions have provided critical insights into the pathways (either anabolic or catabolic) that are essential for the survival and pathogenesis of *M. tuberculosis* (Beste and McFadden, 2010). The three preferable main pillars of an ideal drug target is essentiality, vulnerability and druggability (Nunes *et al*., 2020). Understanding these characteristics is important in targeting *M. tuberculosis* and developing new screening models for anti-TB drug discovery. TB infections remain one of the leading causes of death (WHO, 2020).

In this study, the biosynthesis of aromatic amino acids in Mycobacteria was evaluated as a potential target for the development/discovery of novel chemical species. The essentiality, vulnerability and draggability of the *tkt* and *aroG* genes in *M. tuberculosis* were studied using clustered regularly interspaced short palindromic repeat (CRISPR)/ CRISPR-associated proteins (Cas) is a gene editing approach. The *tkt* gene encode for transketolase enzyme involved in the pentose phosphate pathway and *aroG* gene encodes for the biosynthesis of 3-Deoxy-D-Arabino-Heptulosonate-7-Phosphate Synthase (DAHPS) in the shikimate pathway. The transcriptional interference (gene knockdown) by the CRISPRi/dCas9 system was stimulated by anhydrotetracycline (ATC), where the ability of the designed single guide ribonucleic acids (sgRNAs) were able to recognise non-canonical protospacer adjacent motifs (PAMs). The attachment of the dCas9 handle after binding of the sgRNA to the target sequence then leads to gradient of *tkt* and *aroG* gene knockdowns (Rock *et al*., 2017). *M. smegmatis* was used as a surrogate to study the AAA metabolism.

The growth inhibition of *M. smegmatis tkt* and *aroG* hypomorphs due to the knockdown of the *tkt* and *aroG* genes through the activation of the CRISPRi system confirmed their essentiality for the survival of the organism (Figures). In addition, the results showed that the *tkt* gene in *M. smegmatis* is more vulnerable to drug interaction than the *aroG* gene (Figure), thus suggesting that the *tkt* gene is better target than *aroG* gene. To assess the druggability of the *tkt* gene as a drug as a potential drug target, *M. smegmatis tkt* PAM 1 and PAM 2 mutants were then used as screening models to assess the antimycobacterial activity of selected plant extracts. Remarkably, acetone extracts from plants such as *Senna petersiana*, *Acacia senegal*, *Carissa bispinosa*, *Peltophorum africanum* and *Croton gratissimus* that had moderate to low antimycobacterial activity against wild-type *M. smegmatis* (mc^2 155) demonstrated improved inhibitory activity against the *tkt* PAM1 *M. smegmatis* hypomorph. These results were important because they demonstrated that the depletion of the *tkt* gene potentiate the activity of the extracts and this effects may extend to other kind of antimicrobial agents. Given that not all essential genes or their products are similarly vulnerable to the mechanism of action of a drug (Yuan and Sampson, 2018), the results of this study were encouraging because they showed that indeed, the *tkt* gene in the *M. smegmatis* hypomorph was accessible to chemical inhibition because the rescue experiments showed that *C. gratissimus* and *G. volkensii* indeed targeted the AAA biosynthesis for antimycobacterial inhibition. The results of this study further build on previously work by Rock *et al*., 2017; Singh *et al*., 2016; Choudhary *et al*., 2015; Kolly *et al*., 2014) were various *M. smegmatis* CRISPRi mutants were generated as models for the study gene essentiality in Mycobacterium metabolism and pathogenesis and discovery of chemical agents that may interact with various pathways to induce cell death.

The limitation of this study is that the metabolism of *M. tuberculosis* may also be influenced by the host-pathogen interaction possesses the ability to switch between various carbon sources (Warner, 2015). The exact type of nutrients that *M. tuberculosis* can access from its host and the mechanism involved in their assimilation is still ongoing research (Mashabela *et al*., 2019). Nevertheless, several mechanisms of nutrient acquisition by *M. tuberculosis* have been described by several studies (Maueröder *et al*., 2016; Danilchanka *et al*., 2015).

An added advantage of the plant extracts is their antioxidant and anti-inflammatory activities which may benefit the host immune system during treatment of infection by reducing free radicals and pro-inflammatory agents that perpetuate the infection. Although, extracts from plant such as *Acacia senegal*, *Gadernia volkensii*, *Ficus sur*, *Senna petersiana* and *Clerodendrum glabrum* were found to be toxic to the Vero cell line, these results are not an absolute toxicological evaluation. This is because one of the main drawbacks of the use of *ex vivo* models of the cell lines to evaluate toxicity is that their cultivation and culturing is under controlled conditions as opposed to their natural environment within a host (Chanput *et al*., 2014). Eukaryotic cells *in vivo* function in so-called "*cross talks*" with other cells or tissues in the form of a network (Chanput *et al*., 2014).

The combination of results from the phytochemical analysis and bioautography indicated that non-polar compounds such as terpenoids present in the bioactive crude extracts were likey responsible for the observed antimycobacterial activity than phenolic compounds (Chapter 3 and Chapter 5). These results were not surprising because it has been previously reported that due to the high lipid content of the mycobacterial cell envelope, mycobacterium spp. was highly susceptible to non-polar compounds and impermeable to polar compounds (Mazlun *et al*., 2019).

8.2 Conclusions

This study confirmed validated the essentiality of the biosynthesis of aromatic amino acids towards the survival of Mycobacterial species. The use of CRISPRi technique was invaluable in the validating of the *tkt* and *aroG* genes of the shikimate pathway as potential drug targets and demonstrating that the *tkt* gene is vulnerable to chemical interaction by exogenous chemical species. This is because *tkt* gene knockdown seemed to increase the antimycobacterial activity of some plant extracts. Therefore, targeting the shikimate pathway using seems to be a promising approach to screening antimycobacterial agents. The information is pivotal in future studies aimed studying the Mycobacterium metabolism and screening for target-specific antimycobacterial drugs.

8.3 Recommendations

It may be worthwhile to confirm the reported toxicological studies by employing *in vivo* models where activity warrants the exploration. Although mimicking the natural environment proves challenging, it has been suggested that co-culture systems (culturing THP-1 cells with normal somatic cells and/or other immune cells such as dendritic and T cells) may be progressive in mimicking the *in vivo* condition (Chanput *et al*., 2014).

Further studies may be required to fractionate the active crude extracts in an attempt to reduce/remove non-active polar chemical species from the desired non-polar antimycobacterial compounds. This may be achieved by employing a combination of solvent-solvent fractionation and chromatography techniques such as liquid chromatography–mass spectrometry (LC–MS). Despite the drawback of potentially recovering small amounts of the active compounds, purification may also reduce the toxic effects reported (Masoko *et al*., 2010; Eloff *et al*., 2005).

This study primarily investigated the effect of *tkt* and *aroG* gene knockdowns on the Mycobacterium metabolism and susceptibility to chemical inhibition. It would be interesting to also evaluate the effect of the plant extracts on the gene products of the *tkt* and *aroG* gene, being the transketolase and 3-Deoxy-D-Arabino-Heptulosonate-7-Phosphate synthase and compare the results with those of the current study. This may be achieve be employing immunoblotting (western blotting) the assess the expression of the gene products in the presence and absence of ATC and/or extracts. In addition, effects of the extracts on the enzyme kinetics of both transketolase and DAHPS would provide indispensable data to better understand the mechanism of action of the active extracts. To exclusively validate the activity of the extracts, the CRISPRi system need to be introduced into the H37Rv strain of *Mycobacterium tuberculosis*.

8.4 References

Beste, D.J, and McFadden, J. 2010. System-level strategies for studying the metabolism of *Mycobacterium tuberculosis*. *Molecular BioSystems*, **6**: 2363–2372.

Choudhary, E., Thakur, P., Pareek, M. and Agarwal, N. 2015. Gene silencing by CRISPR interference in *Mycobacteria*. *Nature communications,* **6**: Doi: 10.1038/ncomms7267.

Danilchanka, O., Pires, D., Anes, E. and Niederweis, M. 2015. The *Mycobacterium tuberculosis* outer membrane channel protein CpnT confers susceptibility to toxic molecules. *Antimicrobial Agents and Chemotherapy*, **59**: 2328– 2336.

Eloff, J.N., Famakin, J.O. and Katerere, D.R.P. 2005. *Combretum woodii* (Combretaceae) leaf extracts have high activity against Gram-negative and Gram positive bacteria*. African Journal of Biotechnology*, **4(10)**: 1161–1166.

Farha, M.A. and Brown, E.D. 2015. Strategies for target identification of antimicrobial natural products. *Natural Product Reports*, Doi: 10.1039/c5np00127g.

Kolly, G.S., Sala, C., Vocat, A., Cole, S.T. 2014. Assessing essentiality of transketolase in *Mycobacterium tuberculosis* using an inducible protein degradation system, *FEMS Microbiology Letters*, **358(1)**: 30–35.

Madikizela, B. Ndhlala, A.R., Finnie, J.F. and Van Staden, J. 2014. Antimycobacterial, anti-inflammatory and genotoxicity evaluation of plants used for the treatment of tuberculosis and related symptoms in South Africa. *Journal of Ethnopharmacology*, **153(2)**: 386–391.

Mashabela, G.T., De Wet, T.J. and Warner, D.F. 2019. *Mycobacterium tuberculosis* metabolism. *Microbiology Spectrum*, **7(4)**: Doi: 10.1128/microbiolspec.GPP3-0067-2019.

Masoko, P., Picard, J., Howard, R. L,. Mampuru, L. J. and Eloff, J. N. 2010. *In vivo* antifungal effect of Combretum and Terminalia species extracts on cutaneous wound healing in immunosuppressed rats. *Pharmaceutical Biology*, **48(6)**: 621–632.

Maueröder, C., Chaurio, R.A., Dumych, T., Podolska, M., Lootsik, M.D., Culemann, S., Friedrich, R.P., Bilyy, R., Alexiou, C., Schett, G., Berens, C., Herrmann, M. and Munoz, L.E. 2016. A blast without power: cell death induced by the tuberculosis-necrotizing toxin fails to elicit adequate immune responses. *Cell Death Differ*, **23**:1016–1025.

Mazlun, M.H., Sabran, S.F., Mohamed, M., Abu Bakar, M.F. and Abdullah, Z. 2019. Phenolic compounds as promising drug candidates in tuberculosis therapy. *Molecules*, **24(13)**: Doi:10.3390/molecules24132449

Newman, D.J., Cragg, G.M. 2016. Natural products as sources of new drugs from 1981 to 2104. *Journal of Natural Products*, **79**: 629–661.

Ogbourne, S.M., Parsons, P.G. 2014. The value of nature's natural product library for the discovery of new chemical entities: the discovery of *Ingenol mebutate*. *Fitoterapia*, **2014(98)**: 36–44.

Rock, J. M., Hopkins, F. F., Chavez, A., Diallo, M., Chase, M. R., Gerrick, E. R., Pritchard, J. R., Church, G. M., Rubin, E. J., Sassetti, C. M., Schnappinger, D. and Fortune, S. M. 2017. Programmable transcriptional repression in Mycobacteria using an orthogonal CRISPR interference platform. *Nature Microbiology*, **2**: 16274.

Singh, A. K., Carette, X., Potluri, L.-P., Sharp, J. D., Xu, R., Prisic, S. and Husson, R. N. 2016. Investigating essential gene function in *Mycobacterium tuberculosis* using an efficient CRISPR interference system. *Nucleic Acids Research*, **44(18):** e143–e143. doi:10.1093/nar/gkw625.

Warner, D.F. 2015. *Mycobacterium tuberculosis* Metabolism. *Cold Spring Harbor Perspectives in Medicine*, **5**: a021121.

Yuan, T. and Sampson, N.S. 2018. Hit generation in TB drug discovery: From genome to granuloma. *Chemical Reviews*, **118**: 1887–1916.